frontiers | Research Topics

Methods and applications in clinical and translational physiology

Edited by
Claudio de Lucia, Christina Maria Pabelick, Yih-Kuen Jan, Gaetano Santulli and Pierre Denise

Published in
Frontiers in Physiology

FRONTIERS EBOOK COPYRIGHT STATEMENT

The copyright in the text of individual articles in this ebook is the property of their respective authors or their respective institutions or funders. The copyright in graphics and images within each article may be subject to copyright of other parties. In both cases this is subject to a license granted to Frontiers.

The compilation of articles constituting this ebook is the property of Frontiers.

Each article within this ebook, and the ebook itself, are published under the most recent version of the Creative Commons CC-BY licence. The version current at the date of publication of this ebook is CC-BY 4.0. If the CC-BY licence is updated, the licence granted by Frontiers is automatically updated to the new version.

When exercising any right under the CC-BY licence, Frontiers must be attributed as the original publisher of the article or ebook, as applicable.

Authors have the responsibility of ensuring that any graphics or other materials which are the property of others may be included in the CC-BY licence, but this should be checked before relying on the CC-BY licence to reproduce those materials. Any copyright notices relating to those materials must be complied with.

Copyright and source acknowledgement notices may not be removed and must be displayed in any copy, derivative work or partial copy which includes the elements in question.

All copyright, and all rights therein, are protected by national and international copyright laws. The above represents a summary only. For further information please read Frontiers' Conditions for Website Use and Copyright Statement, and the applicable CC-BY licence.

ISSN 1664-8714
ISBN 978-2-83252-043-7
DOI 10.3389/978-2-83252-043-7

About Frontiers

Frontiers is more than just an open access publisher of scholarly articles: it is a pioneering approach to the world of academia, radically improving the way scholarly research is managed. The grand vision of Frontiers is a world where all people have an equal opportunity to seek, share and generate knowledge. Frontiers provides immediate and permanent online open access to all its publications, but this alone is not enough to realize our grand goals.

Frontiers journal series

The Frontiers journal series is a multi-tier and interdisciplinary set of open-access, online journals, promising a paradigm shift from the current review, selection and dissemination processes in academic publishing. All Frontiers journals are driven by researchers for researchers; therefore, they constitute a service to the scholarly community. At the same time, the *Frontiers journal series* operates on a revolutionary invention, the tiered publishing system, initially addressing specific communities of scholars, and gradually climbing up to broader public understanding, thus serving the interests of the lay society, too.

Dedication to quality

Each Frontiers article is a landmark of the highest quality, thanks to genuinely collaborative interactions between authors and review editors, who include some of the world's best academicians. Research must be certified by peers before entering a stream of knowledge that may eventually reach the public - and shape society; therefore, Frontiers only applies the most rigorous and unbiased reviews. Frontiers revolutionizes research publishing by freely delivering the most outstanding research, evaluated with no bias from both the academic and social point of view. By applying the most advanced information technologies, Frontiers is catapulting scholarly publishing into a new generation.

What are Frontiers Research Topics?

Frontiers Research Topics are very popular trademarks of the *Frontiers journals series*: they are collections of at least ten articles, all centered on a particular subject. With their unique mix of varied contributions from Original Research to Review Articles, Frontiers Research Topics unify the most influential researchers, the latest key findings and historical advances in a hot research area.

Find out more on how to host your own Frontiers Research Topic or contribute to one as an author by contacting the Frontiers editorial office: frontiersin.org/about/contact

Methods and applications in clinical and translational physiology

Topic editors

Claudio de Lucia — Local Health Authority Naples 1 Center, Italy
Christina Maria Pabelick — Mayo Clinic, United States
Yih-Kuen Jan — University of Illinois at Urbana-Champaign, United States
Gaetano Santulli — Albert Einstein College of Medicine, United States
Pierre Denise — INSERM U1075 Mobilités Vieillissement, Pathologie, Santé, France

Citation

de Lucia, C., Pabelick, C. M., Jan, Y.-K., Santulli, G., Denise, P., eds. (2023). *Methods and applications in clinical and translational physiology*. Lausanne: Frontiers Media SA. doi: 10.3389/978-2-83252-043-7

Table of contents

frontiers | Frontiers in Physiology

TYPE Editorial
PUBLISHED 15 March 2023
DOI 10.3389/fphys.2023.1169544

Check for updates

OPEN ACCESS

EDITED AND REVIEWED BY
Johannes Van Lieshout,
University of Amsterdam, Netherlands

*CORRESPONDENCE
Gaetano Santulli,
gsantulli001@gmail.com

SPECIALTY SECTION
This article was submitted to Clinical and Translational Physiology, a section of the journal Frontiers in Physiology

RECEIVED 19 February 2023
ACCEPTED 09 March 2023
PUBLISHED 15 March 2023

CITATION
Santulli G, Pabelick CM, Jan Y-K, Denise P and de Lucia C (2023), Editorial: Methods and applications in clinical and translational physiology.
Front. Physiol. 14:1169544.
doi: 10.3389/fphys.2023.1169544

COPYRIGHT
© 2023 Santulli, Pabelick, Jan, Denise and de Lucia. This is an open-access article distributed under the terms of the Creative Commons Attribution License (CC BY). The use, distribution or reproduction in other forums is permitted, provided the original author(s) and the copyright owner(s) are credited and that the original publication in this journal is cited, in accordance with accepted academic practice. No use, distribution or reproduction is permitted which does not comply with these terms.

Editorial: Methods and applications in clinical and translational physiology

Gaetano Santulli[1,2]*, Christina M. Pabelick[3], Yih-Kuen Jan[4], Pierre Denise[5] and Claudio de Lucia[6]

[1]Department of Medicine, Wilf Family Cardiovascular Research Institute, Fleischer Institute for Diabetes and Metabolism (FIDAM), Albert Einstein College of Medicine, New York, NY, United States, [2]Department of Molecular Pharmacology, Einstein-Mount Sinai Diabetes Research Center (ES-DRC), Einstein Institute for Aging Research, Institute for Neuroimmunology and Inflammation (INI), Albert Einstein College of Medicine, New York, NY, United States, [3]Mayo Clinic, Rochester, MN, United States, [4]University of Illinois at Urbana-Champaign, Champaign, IL, United States, [5]Université de Caen Normandie, Inserm, COMETE U1075, CYCERON, CHU de Caen, Normandie University, Caen, France, [6]Geriatric Center Frullone, ASL (Azienda Sanitaria Locale-Local Health Authority) Napoli 1 Centro, Naples, Italy

KEYWORDS

translational science, physiology, technologies, bioengineering, nanotechnology, biomedicine, advanced biomedical applications, applied physiology

Editorial on the Research Topic
Methods and applications in clinical and translational physiology

The present Research Topic, entitled "Methods and Applications in Clinical and Translational Physiology" is part of the *Methods and Applications in Physiology* series. This series essentially aims at emphasizing the latest experimental techniques developed to understand the main fundamental questions in physiology. Therefore, this Research Topic covers the latest advances in technologies that will foster and advance scientific discoveries.

Our Research Topic has collected eight original articles and one review. The opening article is a randomized crossover study designed to determine the effect of hypoxia on metabolism in men with excess weight (Mekjavic et al.). Subjects participating in this study, conducted in Slovenia, undertook two trials, during which they were confined to normoxic vs. hypoxic conditions; the Authors concluded that the greater postprandial blood-glucose response following hypoxic confinement suggests the potential development of insulin resistance (Mekjavic et al.).

Then, two articles describe a novel device to measure pain (Boing-Messing et al.) and a new low-cost force plate to measure balance and postural sway (Lo et al.). The first device, called eEGG, which stands for electronic Egg, has been tested by German scientists and has been shown to have a strong correlation with the hand dynamometer, strongly suggesting that this new device could be used in medical practice (Boing-Messing et al.). Similarly, the force plate, evaluated both in young and elderly subjects was reliable when assessing several parameters related to the center-of-pressure (Lo et al.).

Next, we have a proteomic (Deng et al.) and a metabolomic (Sempore et al.) study. In the first one, aiming at identifying serum biomarkers clinically useful in acute aortic dissection, Deng, Liu, and others combine two established methodologies, namely, "isobaric Tags for Relative and Absolute Quantitation" (*iTRAQ*) and label-free methods, demonstrating that FGL1, MMP9, PI16, and Lumican may serve as potential biomarkers in patients with acute aortic dissection (Deng et al.). In the metabolomic study, Semporé and collaborators provide new insights into the biological modifications that accompany exercise in lower extremity

artery disease, thereby contributing to a better understanding of the pathophysiology underlying walking impairment (Sempore et al.).

In the following study, Mexican researchers demonstrate that females undergoing peritoneal dialysis present higher serum levels of icodextrin metabolites–a specific fraction of dextrin (a starch-derived water-soluble glucose polymer) that has been successfully used as colloid osmotic agent–which may exert an increased colloid-osmotic pressure followed by reduced ultrafiltration volumes and increased blood volume and blood pressure (Paniagua et al.).

Then, we have two studies important in ophthalmology, mathematically proving the potential for mechanical damage to the corneal wound in cataract surgery (Qi et al.) and showing that, compared to gas tamponade, intravitreal silicone oil results in a significantly greater decrease in the thickness of the peripapillary retinal nerve fiber layer in patients with proliferative diabetic retinopathy (Wang et al.).

A systematic review examining the effects of duloxetine in patients with knee osteoarthritis concludes this Research Topic, showing that this treatment may be an effective treatment for improving pain and depressive symptoms in these patients (Zhou et al.).

Author contributions

GS prepared the first draft; all Authors edited the manuscript and approved the final version.

Funding

The Santulli's Lab is supported in part by the National Institutes of Health (NIH): National Heart, Lung, and Blood Institute (NHLBI: R01-HL164772, R01-HL159062, R01-HL146691, T32-HL144456), National Institute of Diabetes and Digestive and Kidney Diseases (NIDDK: R01-DK123259, R01-DK033823) to GS, National Center for Advancing Translational Sciences (NCATS: UL1TR002556-06) to GS, by the Diabetes Action Research and Education Foundation (to GS), and by the Monique Weill-Caulier and Irma T. Hirschl Trusts (to GS).

Conflict of interest

The authors declare that the research was conducted in the absence of any commercial or financial relationships that could be construed as a potential conflict of interest.

Publisher's note

All claims expressed in this article are solely those of the authors and do not necessarily represent those of their affiliated organizations, or those of the publisher, the editors and the reviewers. Any product that may be evaluated in this article, or claim that may be made by its manufacturer, is not guaranteed or endorsed by the publisher.

frontiers in Physiology

ORIGINAL RESEARCH
published: 18 November 2021
doi: 10.3389/fphys.2021.758085

Exercise-Induced Plasma Metabolomic Profiles in Patients With Peripheral Arterial Disease

*Wendsèndaté Yves Semporé[1,2,3], Juan Manuel Chao De La Barca[3,4], Jeanne Hersant[5], Nafi Ouédraogo[6], Téné Marceline Yaméogo[7], Samir Henni[3,5], Pascal Reynier[3,4] and Pierre Abraham[2,3,5]**

[1] Centre MURAZ, National Institute of Public Health, Bobo Dioulasso, Burkina Faso, [2] Sports Medicine Department, University Hospital of Angers, Angers, France, [3] MitoVasc Research Unit, CNRS 6015, INSERM U-1083, University of Angers, Angers, France, [4] Biochemistry and Molecular Biology Laboratory, University Hospital of Angers, Angers, France, [5] Vascular Medicine Department, University Hospital of Angers, Angers, France, [6] Physiology, Nazi Boni University, Bobo Dioulasso, Burkina Faso, [7] Internal Medicine, Nazi Boni University, Bobo Dioulasso, Burkina Faso

OPEN ACCESS

Edited by:
Claudio de Lucia,
Sapienza University of Rome, Italy

Reviewed by:
Atsushi Izawa,
Shinshu University, Japan
Toshiaki Miyamoto,
Hyogo University of Health Sciences, Japan

***Correspondence:**
Pierre Abraham
piabraham@chu-angers.fr

Specialty section:
This article was submitted to Clinical and Translational Physiology, a section of the journal Frontiers in Physiology

Received: 13 August 2021
Accepted: 19 October 2021
Published: 18 November 2021

Citation:
Semporé WY, Chao De La Barca JM, Hersant J, Ouédraogo N, Yaméogo TM, Henni S, Reynier P and Abraham P (2021) Exercise-Induced Plasma Metabolomic Profiles in Patients With Peripheral Arterial Disease. Front. Physiol. 12:758085. doi: 10.3389/fphys.2021.758085

Aim: A better knowledge of the biological consequences in the blood of these exercise-induced ischemic events in lower extremity artery disease (LEAD) may improve the prospects of disease management. We explored the preminus postexercise metabolomic difference in 39 patients with LEAD referred for a treadmill oximetry test [transcutaneous oximetry ($TcPO_2$)].

Methods: Ischemia was estimated through the sum of decrease from rest of oxygen pressure (DROPs) (limb $TcPO_2$ changes minus chest $TcPO_2$ changes) at buttocks, thighs, and calves regions. Targeted metabolomic analyses measuring 188 metabolites were performed on a few microliters blood samples taken at the earlobe at rest and 3 min after exercise.

Results: Maximum walking distance (MWD) was 290 m (120–652 m) and ankle brachial index (ABI) was 0.67 ± 0.17. Supervised paired partial least squares discriminant analysis based on 23,345 models showed good predictive performance for test sets with a median area under the receiver operating characteristic (AUROC) curve value of 0.99 and a p-value of 0.00049. The best discriminant metabolites contributing to the model included a subset of 71 (47%) of the 150 accurately measured metabolites in the plasma, comprising 3 acylcarnitines, 3 amino acids, 5 biogenic amines, 9 sphingomyelin, 7 lysophosphatidylcholines, and 44 phosphatidylcholines. In addition, 16 of these metabolites were found to correlate with one or more severity scores of the LEAD.

Conclusion: Our results provide new insights into the biological changes that accompany exercise in LEAD and contribute to a better understanding of walking impairment pathophysiology in LEAD, highlighting new candidate biomarkers.

Keywords: walking impairment, exercise, treadmill test, transcutaneous oximetry, metabolomic profile

INTRODUCTION

Lower extremity artery disease (LEAD) is a vascular pathology mainly resulting from atherosclerosis that obstructs arteries and compromises vascularization of the muscles in the lower limbs (Serrano Hernando and Martín Conejero, 2007; Krishnan and Collins, 2014). The prevalence of LEAD increases with age. The number of patients with LEAD worldwide is estimated at more than 200 million (Fowkes et al., 2013). In France, the prevalence of LEAD defined by an ankle brachial index (ABI) less than 0.9 is estimated at 16% in the population of 65 years old (Walters et al., 1992; Boccalon et al., 2000; Criqui and Aboyans, 2015; Fowkes et al., 2017). The overall prevalence of peripheral arterial diseases increased by 25% between 2000 and 2010, especially in low- and middle-income countries (Fowkes et al., 2013). In its early stages, LEAD is characterized by chronic and repeated episodes of transient ischemia during walking due to the insufficient delivery of oxygen to meet the oxygen requirements of lower limb exercising muscles. A better knowledge of the biological consequences of these transient exercise-induced ischemic events is fundamental to developing potential future therapeutic improvements.

Transcutaneous oximetry ($TcPO_2$) allows for the evaluation of the severity and diffusion (buttocks, thighs, and calves) of exercise-induced lower limb ischemia (Abraham et al., 2003) and the detection of eventual systemic exercise-induced hypoxemia (Abraham et al., 2018, 2021).

The recent development of omics sciences, in particular metabolomics, permits deep biochemical phenotyping through the detection and quantification of a broad spectrum of metabolites in biological fluids with diagnostic, prognostic, or therapeutic follow-up values. It is increasingly used in the investigation of cardiovascular diseases and has enabled great advances in the knowledge of the biology of ischemia in recent years (Dang et al., 2018; Ismaeel et al., 2019; Schranner et al., 2020).

Previous studies have focused on studying the resting metabolomic profile of patients with LEAD at different stages of the disease (i.e., intermittent claudicants vs. critical limb ischemia) compared with controls. Different metabolomic signatures were found between patients with LEAD and controls with concern to the concentrations of serum amino acids, serum acylcarnitines and hexoses, serum biogenic amines, serum ceramides, serum cholesteryl esters (CEs), sphingomyelins, diglycerides, triglycerides, and phosphatidylcholines (Ismaeel et al., 2019). In another study, Azab et al. (2020) showed the different metabolomic signatures between these different categories of patients with LEAD and control subjects. Ismaeel et al. (2019) also found significant correlations between resting ABI and blood ceramides. Other authors confirmed different resting metabolomic signatures between male patients with LEAD and controls in a comparative metabolomic study on serum low-molecular metabolites and oxidized low-density lipoprotein (oxLDL) (Zagura et al., 2015). To the best of our knowledge, no study investigated the metabolomic signature and its correlation with the severity of exercise-induced ischemia in patients with LEAD.

Our main objective was to determine the metabolomic impact of exercise on blood in a small set of highly selected patients with LEAD by confirming the presence of limb exercise-induced ischemia (with $TcPO_2$) and by excluding factors that interfere with biological results (e.g., exercise-induced hypoxemia, non-vascular limitation). Our secondary objective was to evaluate the correlation between metabolomic changes and clinical indices of LEAD severity at rest and exercise in those patients.

MATERIALS AND METHODS

Participants

We conducted a prospective study from October 2017 to March 2019. The protocol was systematically proposed to all the adult ($\geq$18 years old) patients referred to the Vascular Medicine Department of the University Hospital of Angers for a treadmill exercise $TcPO_2$ with significant walking limitation [self-reported Walking Estimated Limitation Calculated by History (WELCH) score $\leq$ 50] for at least 3 months and no self-reported non-limb limitation. Most patients are referred to us for the diagnosis of the vascular origin of exercise-related pain. Non-inclusion criteria were coagulation disorders or on anticoagulant therapies, self-reported pulmonary, osteoarticular, or cardiac limitation, inability to walk on the treadmill at the goal speed (walking time over 10 m at spontaneous speed $>$ 10 s), and participation in another protocol.

Exclusion criteria were the absence of limitation on the treadmill (walking time $>$ 15min), absence of symptoms in the lower limbs, non-vascular limitation to walking (myocardial ischemia and joint pain), systemic hypoxemia induced by exercise defined as a chest decrease from rest $>$ 5 mm Hg during exercise, absence of significant ischemia on all the limb probes, and analytic or blood sample failure or biological outlier values. These strict inclusion/exclusion criteria were expected to result in many excluded patients but in a highly selected population with proof of limiting limb ischemia and absence of non-limb limitation.

Ethical Approval

This study was approved by the "Ile de France II" personal protection committee on September 8, 2017, under number 00001072. Written informed consent was obtained from each participant before inclusion in this study after a full explanation of the goal and methodology of this study. This study was registered on the clinical trials on September 28, 2017, under number NCT03305198 before first inclusion and performed according to the recommendation of the Declaration of Helsinki.

Measurements

At inclusion, clinical and anthropometric information were measured or fully extracted from the medical records of the patients including age, weight, height, abdominal circumference, history of diseases, and treatments. Claudication was defined as pain in the lower limbs (calves, thighs, and buttocks) occurring when walking and forcing the patient to stop. ABI was defined by the ratio of the systolic pressure in the legs to the systolic pressure in the arms. LEAD was defined as ABI $<$ 0.9. The

maximum walking distance (MWD) and the maximum walking time (MWT) were determined during the treadmill walking test at a constant load of 3.2 kmh^{-1} and a slope of 10%.

Exercise Oximetry

Exercise $TcPO_2$ measurements were performed during a treadmill exercise test under electrocardiographic supervision according to a standardized procedure and set of equipment (PF6000 Perimed® , Stockholm, Sweden, United Kingdom) connected to a computer with the software $AcqTcPO_2$, which automatically calculates in real time the decrease from rest of oxygen pressure (DROP: limb changes minus chest changes) (Abraham et al., 2005).

We used eight probes (one on each calf, one on each thigh, one on each buttock, and two on the chest). The left thoracic probe was considered a default by the computer as the reference probe for the DROP calculation. In the event of measurement anomalies or failure of the left thoracic $TcPO_2$ sensor head, the right thoracic probe was used as a reference probe for the calculation of DROPs. After positioning the probes, we waited between 10 and 20 min for the local temperature of the probes to rise to 44°C and for the transcutaneous pressure values in O_2 to stabilize. The recording of the $TcPO_2$ treadmill exercise test took place in three steps:

- At rest for 2 min, with the patient standing still.
- During exercise: The treadmill speed began at 1 km/h and was progressively increased to a maximum of 3.2 kmh^{-1} in 1 min. This walking speed, with a constant slope of 10%, was maintained until the maximum walking capacity was reached (and not just the appearance of pain) in case of myocardial ischemia (ST depression $>$ 1 mm) or after a maximum of 15 min (absence of limitation).
- Following exercise for 10 min during which the $TcPO_2$ measurement was continuously monitored and the patient remained on his or her feet and the treadmill was at rest.

Throughout the test, patients were asked to report limb and non-limb symptoms. At the end of the test, the minimum DROPs of each of the probes at the lower limbs and the MWD were collected. The presence of ischemia was defined as DROP $<$ −15 mmHg (Abraham et al., 2003; Bouyé et al., 2004). The presence of exercise-induced systemic hypoxemia was defined as a decrease in chest $TcPO_2 > 5$ mmHg (Abraham et al., 2021). For further analysis, the sum of minimal DROPs of the six limb probes was used as an index of LEAD severity.

Biology

Preanalytical Aspects

We performed two blood samples per patient, one at rest before the treadmill test and a second sample at 3 min of rest after exercise. For each sample, 200 µl of blood were collected after an earlobe incision in a glass capillary rinsed with heparin. After homogenization, the glass capillary was immediately centrifuged at 2,000 g for 4 min without brakes and at room temperature. An aliquot of 50–60 µl of the supernatant (plasma) was prepared for each sample in polypropylene tubes and frozen at −20°C before being transferred on ice on the same day to the biochemistry and molecular biology laboratory, where it was stored at −80°C before metabolomic analysis.

Analytical Aspects

We used a targeted metabolomics approach by using a standardized kit developed by the Austrian company (Biocrates Life Sciences, Innsbruck, Austria). This kit (AbsoluteIDQ® p180) benefits from internal standards, quality controls, and dedicated analysis software and has been validated by numerous publications in clinical biology. This kit allows for the quantification of 188 endogenous molecules including free carnitine (C0), 39 acylcarnitines (C), the sum of hexoses (H1), 21 amino acids, 21 biogenic amines, and 105 lipids (refer to **Supplementary Table 1**). Four different classes of lipids are detected by the kits: 14 lysophosphatidylcholines (lysoPC), 38 diacylphosphatidylcholines (PCaa), 38 acyl-alkyl-phosphatidylcholines (PCae), and 15 sphingomyelins (SM). For metabolite identification and quantification, the Q-Trap 5500 Mass spectrometer (AB Sciex LLC, Redwood City, California, United States) coupled with the 1260 Agilent high performance liquid chromatography (HPLC) system and the ECLIPSE XDB-C18 3.5 µm 3.0 mm × 100 mm Column (Agilent Technologies, Santa Clara, California, United States) were used. Flow-injection analysis with tandem mass spectrometry (FIA-MS/MS) was used for quantifying acylcarnitines, glycerophospholipids, sphingolipids, and sugars, whereas liquid chromatography (LC) enabled the separation of amino acids and biogenic amines before detection of LC with tandem mass spectrometry (LC-MS/MS).

All the reagents used in this analysis were of LC-MS grade and purchased from the VWR (Fontenay-sous-Bois, France, United Kingdom) and Merck (Molsheim, France, United Kingdom). Sample preparation and analyses were performed following the Kit User Manual. Each plasma sample was thawed and vortexed thoroughly after thawing and centrifuged at 4°C for 5 min at 5,000 g. A total of 10 µl of each sample were mixed with the isotopically labeled internal standard in a microtiter plate and dried under nitrogen flow (nitrogen evaporator 96 well plate; Stuart SBM 200 D/3, Stuart, Stone, United Kingdom). Metabolites then were derivatized with phenylisothiocyanate (PITC) 5% for 20 min at room temperature and subsequently dried for 30 min under nitrogen flow. For extraction, the first 300 µl extraction solvent (5 mM ammonium acetate in methanol) was added and incubated with shaking at 450 revolutions per min (IKA MS3 digital, Thermo-Fisher Scientific, Illkrich, France, United Kingdom) for 30 min at room temperature followed by filtration by centrifugation (Hettich Zentrifugen Rotina 380R, Bäch, Switzerland, United Kingdom) for 2 min at 500 g. Subsequently, 200 µl were removed from the filtrate, transferred to a fresh microtiter deep-well plate, and diluted with 200 µl water for LC-MS analysis of biogenic amines and amino acids. To the remaining 100 µl from the filtrate, 500 µl of MS running solvent was added for FIA-MS/MS. Both the types of measurement were performed on the QTRAP mass spectrometer applying electrospray ionization (ESI) (AB Sciex API5500Q-TRAP, SCIEX, Villebon-sur-Yvette, France, United Kingdom). The MS was coupled to an HPLC (Agilent Technologies 1200 series, Les Ulis, France, United Kingdom).

In the case of LC-MS, the metabolites were separated by a hyphenated reverse phase column (Agilent, Zorbax Eclipse XDB C18, 3.0 mm × 100 mm, 3.5 μm) preceded by a precolumn (Security Guard, Phenomenex, C18, 4 mm × 3 mm, Phenomenex, Torrance, California, United States) applying a gradient of solvent A (formic acid 0.2% in water) and solvent B (formic acid 0.2% in acetonitrile) over 7.3 min (0.5 min 0% B, 5 min 70% B, 0.3 min 70% B, 2 min 0% B) at a flow rate of 500 μl/min. The oven temperature was 50°C. For LC-MS analysis and for FIA, 10 and 2 μl × 20 μl samples, respectively, were subjected to measurements in the positive and negative modes. The identification and quantification were achieved by multiple reaction monitoring (MRM) standardized by applying spiked-in isotopically labeled standards in the positive and negative modes, respectively. For calibration, a calibrator mixture consisting of seven different concentrations was used. Quality controls derived from lyophilized human plasma samples were included for three different concentration levels. For FIA, an isocratic method was used (100% organic running solvent) with varying flow conditions (0 min, 30 μl/min; 1.6 min 30 μl/min; 2.4 min, 200 μl/min; 2.8 min, 200 μl/min; 3 min 30 μl/min). The MS settings were as follows: scan time 0.5 s; IS voltage for positive mode 5,500 V, for negative mode −4,500 V; source temperature 200°C; with nitrogen as the collision gas medium. The corresponding parameters for LC-MS were set as follows: scan time 0.5 s, source temperature 500°C, with nitrogen as the collision gas medium. All the reagents used in the processing and analysis were of LC-MS grade. Milli-Q Water Ultrapure was used fresh after being prepared by the high-purity water system with Millipore (Milli-Di). The raw data of the Analyst software (AB Sciex, Framingham, Massachusetts, United States) were processed by the MetIDQ software, which is an integral part of the p180 Kit

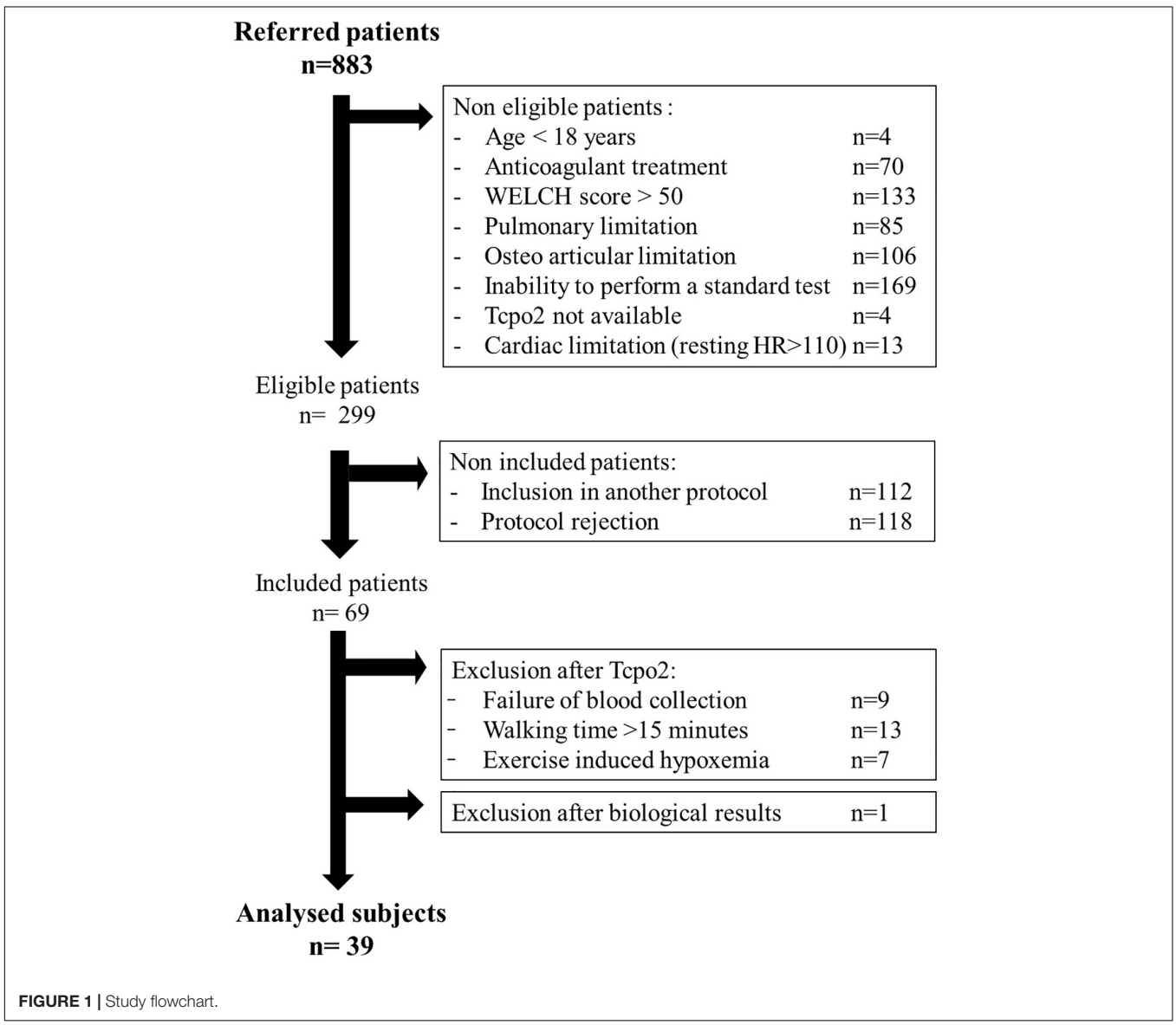

FIGURE 1 | Study flowchart.

(Biocrates Life Sciences AG). This streamlines data analysis by the automated calculation of metabolite concentrations providing quality measurements and quantification.

Statistical Analyses

Comparison between included and excluded subjects (among which patients for whom we failed to collect blood samples) was performed by the Mann–Whitney *U*-test or the unpaired *t*-test and the χ^2-test. After validation of the three levels of quality control used with the kit, the metabolite concentrations were used for statistical analyses only if they were in the quantitation range determined by the calibration curves. Indeed, metabolites with more than 20% of their values outside of the quantitation range (i.e., concentration above the upper limit of quantitation or below the lower limit of quantitation) were not considered. Before removing a given metabolite with more than 20% but less than 40% outside of the quantitation range for statistical analysis, the χ^2-test was performed with the independence between in/out of range and rest/postexercise conditions as the null hypothesis.

The projection-based multivariate analyses were performed on centered and unit variance scaled data. An unsupervised analysis was conducted by using paired principal component analysis (pPCA) to detect similar groups of samples and outliers, i.e., samples displaying an atypical metabolite profile. Paired partial least squares discriminant analysis (pPLS-DA) was performed to discriminate between rest and postexercise samples on the basis of their metabolomic profiles. The data were randomly divided into the training-validation set (30 samples) and test sets (9 samples) from each group. Samples from the training-validation set were randomly split into 20 samples for training the model and 10 samples used for validation of models built with training samples. From the 30,045,015 possible combinations (i.e., models) obtained by choosing 20 samples from a total of 30, we picked 23,345 combinations by sampling the matrix **C** containing all the combinations on its columns every 1,287 columns. This was done to make the process computationally feasible, considering that the probability that two samples allocated to the same set (training or validation) in a given column of **C** was higher if they were in the same set-in neighbor columns [i.e., columns n and (n + 1) differed only in one element] of **C**. The predictive performance of each of the 23,345 pPLS-DA models built with training samples was evaluated by using the area under the receiver operating characteristic (AUROC) curve value and its associated *p*-value. This *p*-value measures the probability for a given model to randomly predict sample allocation (i.e., rest or postexercise metabolomic profile). Since AUROCs and *p*-values cannot be considered to be normally distributed, median values instead of means were used to evaluate pPLS-DA robustness and to decide whether pPLS-DA models satisfactorily separate the two groups. Cutoff values of 0.8 and 0.05 were selected for the median AUROCs and *p*-values, respectively. Training-validation set strategy allows us to select the best models (i.e., models having the highest AUROC) and eventually evaluate their predictive performance on the test set. The global performance of pPLS models built with training sets was considered satisfactory only if the median AUROC value ≥ 0.8 and the median *p*-value ≤ 0.05. In the case of satisfactory global performance, the selection of the discriminant variable (i.e., metabolites) was based on the variable importance for the projection (VIP) and the loading parameters. VIP values summarize the importance of each variable for the pPLS-DA model, whereas the loading values are indicators of the relationship between the **Y** vector containing the class information (i.e., whether rest or postexercise groups) and variables in the **X** matrix (i.e., metabolites). Variables with a VIP value greater than unity are important for group discrimination. Multivariate analysis was performed by using the mixOmics R package (Kim-Anh et al., 2016).

In addition, we performed the Pearson correlation between the clinical criteria of LEAD severity (ABI, DROPs, MWT, and WELCH score) and metabolite exercise-induced changes.

RESULTS

From the referred population, we included 69 patients. Of these, 40 patients were available for a metabolomic determination as shown in **Figure 1**. One patient was excluded after the analysis of blood samples because of outlying results. The general characteristics of 39 analyzed and 30 excluded patients are presented in **Table 1**. All the patients had a symptomatic LEAD and they reported pain during walking. The majority of patients had a history of hypertension and was a current or former smoker. Almost all the patients were under antiplatelet treatment.

TABLE 1 | Characteristics of the patients as shown, studied patients were similar to excluded patients except on walking capacity and ankle brachial index (ABI) estimation.

	Analyzed *n* = 39	Excluded *n* = 30	*p*
Characteristics			
Age (years)	66.1 ± 11.2	67.3 ± 9.3	0.630
Male gender	34 (87.2)	26 (86.7)	0.950
Weight (Kg)	75.3 ± 13.5	74.1 ± 12.5	0.697
Height (m)	1.68 ± 0.08	1.68 ± 0.07	0.711
Body Mass Index (Kgm^{-2})	26.7 ± 4.4	26.4 ± 4.4	0.829
Ankle Brachial Index	0.67 ± 0.19	0.80 ± 0.23	0.014
WELCH score	18 [10–30]	17 [12–31]	0.771
Hemoglobin concentration ($gdcl^{-1}$)	14.7 ± 1.7	15.1 ± 2.0	0.349
Glycemia (gL^{-1})	1.2 ± 0.4	1.3 ± 0.5	0.349
History of			
Hypertension (%)	26 (66.7)	15 (50.0)	0.213
History of lower limb revascularization (%)	20 (51.3)	14 (46.7)	
Diabetes mellitus (%)	5 (12.8)	7 (30.4)	0.253
Ongoing treatments			
Antiplatelet treatment (%)	36 (92.3)	30 (100.0)	0.120
Anti-hypertensive drugs (%)	26 (66.7)	15 (50.0)	0.250
Statins (%)	28 (71.8)	25 (83.3)	0.260
Beta blockers (%)	8 (20.5)	9 (30.0)	0.365
Treadmill test results			
Maximum walking distance (m)	361 [245–527]	1028 [369–1195]	0.001
Sum of minimal DROP values (mmHg)	103 [84–133]	104 [70–135]	0.517

Transcutaneous Oximetry

Transcutaneous oximetry was obtained for all the patients, with various degrees of localized (calf only) or diffuses (calves and thighs and buttocks) ischemia. Typical examples of recording are provided as additional content in **Supplementary Data** (**Figure 2**). The distribution and frequency of exercise-induced ischemia by area (buttocks, thighs, and calves) in the lower limbs during $TcPO_2$ tests are presented in **Figure 3**. The raw results underlying abnormal individual values after $TcPO_2$ tests are presented on a table submitted as **Supplementary Table 2**.

Metabolomic Profiles

The flowchart for metabolomic analyses is presented in **Figure 4**. Among the 188 analyzed metabolites, 150 metabolites were considered accurately measured after validation of the quality controls. These raw data are available in **Supplementary Table 3**. The non-supervised pPCA approach (**Figure 5**) highlighted an outlier. The two samples of this patient were excluded from the metabolomics datasets during subsequent statistical analyses.

Supervised pPLS-DA based on 23,345 models enabled a clear distinction between rest and postexercise samples (**Figure 6**)

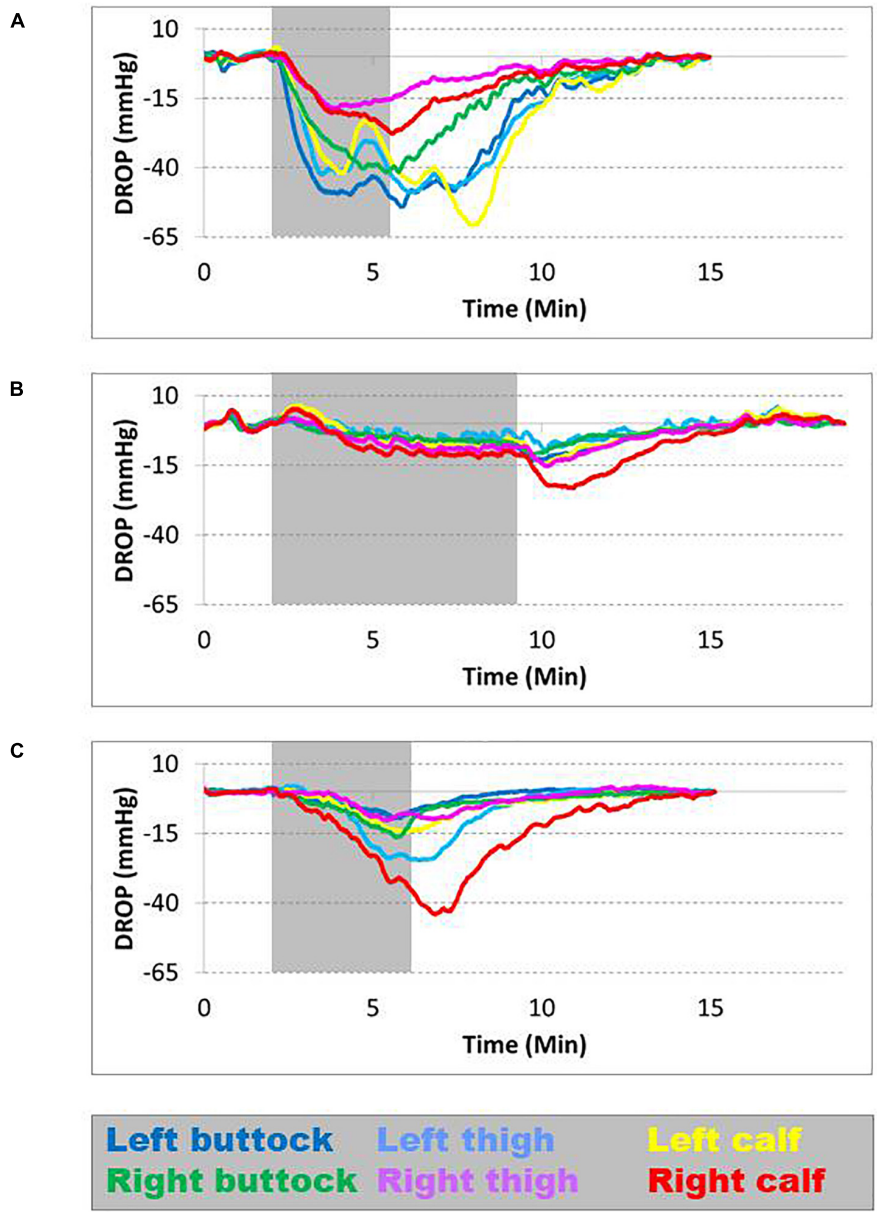

FIGURE 2 | Different types of ischemia found during transcutaneous oximetry ($TcPO_2$); each curve represents a specific probe location and is color coded. The gray area represents the period of walking on the treadmill. The normal limit is −15 mm Hg. **(A)** Is patient 15: During walking, all the curves fall below the threshold, indicating ischemia in both the lower limbs. **(B)** Is patient 48: During walking, only the right calf falls below the threshold, indicating an isolated right calf. **(C)** Is patient 52: During walking, ischemia affects predominantly the right calf and left thigh.

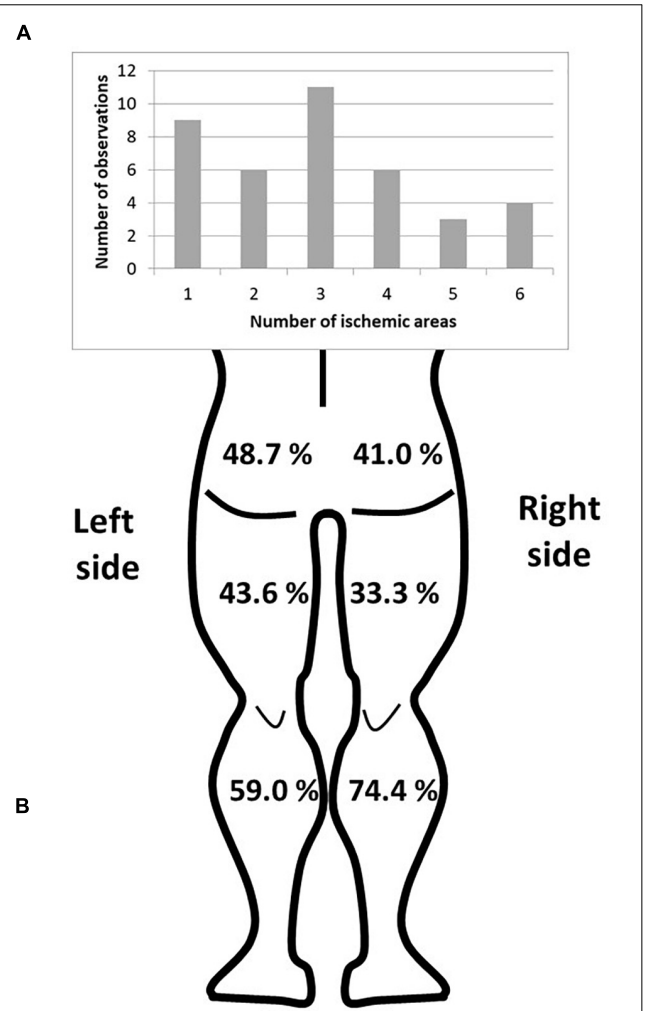

FIGURE 3 | Distribution of the ischemic areas of the lower limbs. **(A)** Number of observations according to the number of ischemic areas. **(B)** Frequency of exercise-induced ischemia by area (buttocks, thighs, and calves) in the lower limbs.

and showed very good predictive performance of training sets on validation sets with a median AUROC value of 0.95 and a *p*-value of 0.00067 (**Figure 7**). Considering this high global predictive performance, the AUROC cutoff was placed at 0.95 (12,941 models) in choosing the best models among all the 23,345 models. Median values for the AUROC test and *p*-values (0.988 and 0.00049, respectively) demonstrated excellent predictive capabilities and low overfitting of the pPLS-DA best models built with the training sets when applied to the test set (**Figure 8**).

The best discriminant metabolites (VIP > 1 and high absolute loading values) were combined in a volcano plot (**Figure 9**). These best discriminant metabolites included a subset of 71 (47%) of the accurately measured metabolites in the plasma, comprising three acylcarnitines (C2, C12, and C16), three amino acids (serine, alanine, and glutamine), five biogenic amines[spermine, putrescine, methionine sulfoxide, acetylornithine, and α-aminoadipate (α-AAA)], nine sphingomyelin, seven lysophosphatidylcholines, and 44 phosphatidylcholines. Four of these metabolites showed postexercise decreased concentrations (spermine, putrescine, serine, and methionine sulfoxide), whereas all the other metabolites had increased concentrations.

A total of 16 of these metabolites, or metabolite ratios, were found to correlate with one or more severity scores (ABI, DROP, MWT, and WELCH scores) of LEAD including kynurenine/tryptophan ratio, hydroxyproline, symmetric dimethyl arginine (SDMA), SDMA/arginine ratio, C5 acylcarnitine, arginine, aspartate, asparagine, lysine, ornithine, proline, putrescine, spermidine, spermine, PC aa C42:6, and the ratio between monounsaturated fatty acid (MUFA) to saturated fatty acid (SFA) or MUFA (PC)/SFA (PC) ratio (**Table 2**). The summarization of the results of the metabolomic analysis is shown in **Figure 4**.

DISCUSSION

While many studies have characterized the exercise-induced metabolomic profiles and have been recently reviewed (Sakaguchi et al., 2019; Morville et al., 2020; Schranner et al., 2020), very few have specifically investigated these profiles in patients with peripheral arterial disease (Ismaeel et al., 2019). At rest in LEAD, there is a known relationship between the metabolomic profile and arterial resistance (Zagura et al., 2015) or the occurrence of early death (Huang et al., 2013). We carried out a comparative study of the metabolomic profile of patients with LEAD by targeting 188 metabolites at rest and after exercise coupled with $TcPO_2$ ischemic evaluation. $TcPO_2$ has considerably improved the knowledge of LEAD pathophysiology. It allows a better assessment of the severity of LEAD by a quantified measurement of the ischemia (buttock, thigh, and leg) during exercise in a standardized treadmill test. $TcPO_2$, therefore, allows us to spatially and temporally quantify exercise-induced ischemia in LEAD (Got, 1998; Abraham et al., 2018). The plasma metabolomic profile of the 150 accurately measured metabolites was sharply affected by exercise in these patients and several metabolites were found significantly correlated with scores of LEAD clinical severity.

Metabolomic Signature Induced by Exercise in Patients With Lower Extremity Artery Disease

Targeted metabolomics has highlighted a metabolic signature that could improve the prediction of cardiovascular events in the elderly (Rizza et al., 2014). In patients with LEAD, different metabolic signatures exist between patients with intermittent claudication and those with critical limb ischemia (Ismaeel et al., 2019). A relationship between the metabolomic profile and arterial resistance (Zagura et al., 2015) or the occurrence of early death (Huang et al., 2013) was previously observed. In this study, the multivariate analysis revealed strong discrimination after and before exercise, the best discriminant metabolites contributing to the model involving 47% (n = 71) of the 150 accurately measured metabolites

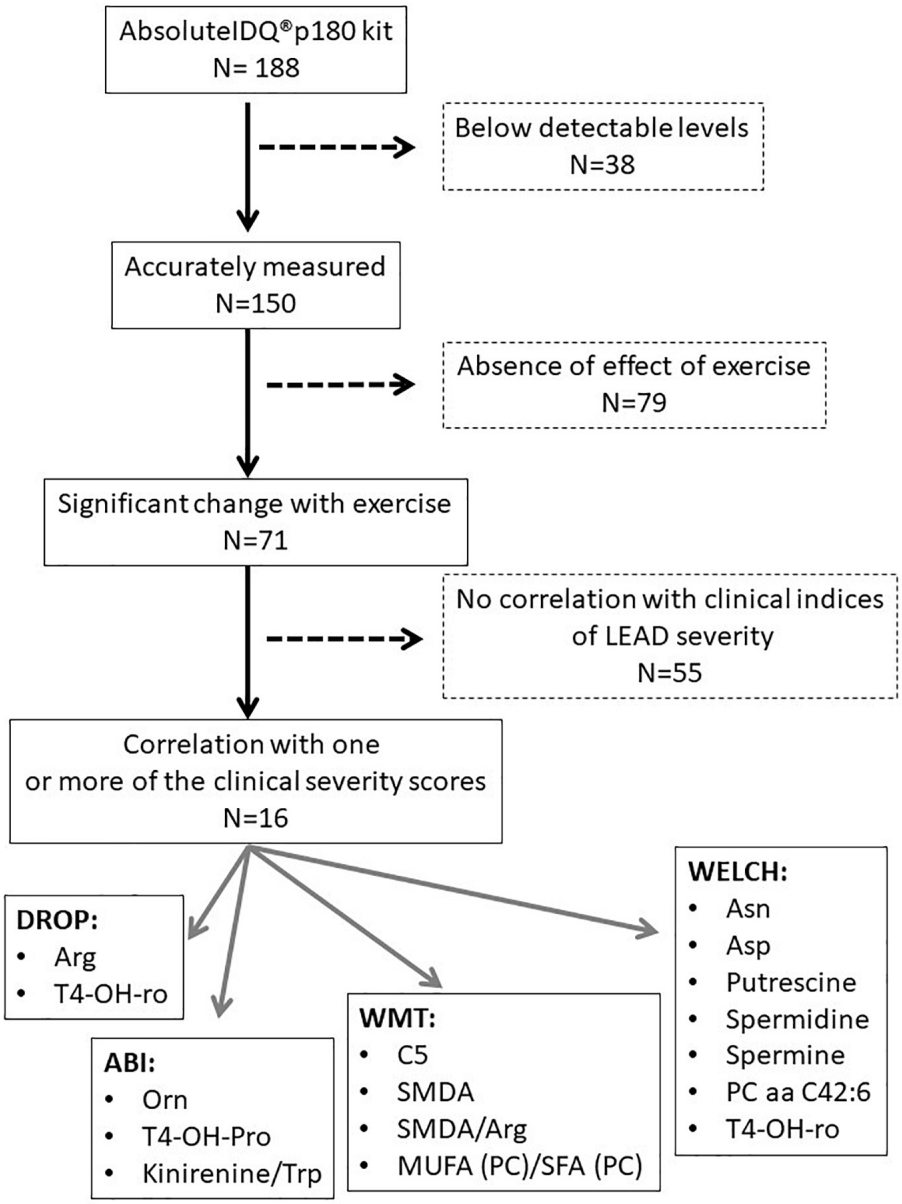

FIGURE 4 | Flowchart of metabolomic analyses.

in the plasma. As far as exercise is a major physiological stress, it is therefore not surprising to find almost half of the metabolites included in the subset of best discriminating metabolites. Four of these metabolites showed postexercise decreased concentrations (spermine, putrescine, serine, and methionine sulfoxide), whereas all the other metabolites (n = 67) showed increased concentrations: alanine, glutamine, acetylornithine, α-AAA, C2, C12, C16, nine sphingomyelins, seven lysophosphatidylcholines, and 44 phosphatidylcholines.

The increase in acylcarnitine plasma concentration during exercise is a well-known phenomenon (Sakaguchi et al., 2019; Morville et al., 2020), which reflects either the increased release of these energetic substrates by the liver and adipose tissue to support exercise or their insufficient mitochondrial consumption by skeletal muscle due to exercise-induced ischemia and anoxia. Critical limb ischemia in patients with LEAD (Ismaeel et al., 2019) showed a decreased concentration of acylcarnitines, showing a possible mismatch between acute ischemic attacks and more moderate stress-induced ischemia in this study.

Glucose, the other major energy substrate, is generally increased after exercise (Sakaguchi et al., 2019), but it was found to be lowered after a walking test in patients with intermittent claudication (Coolen et al., 2008). No variation in the glucose level was revealed by our study that accords with the finding of Ismaeel et al. (2019) that compared patients with LEAD to healthy controls at rest (Ismaeel et al., 2019).

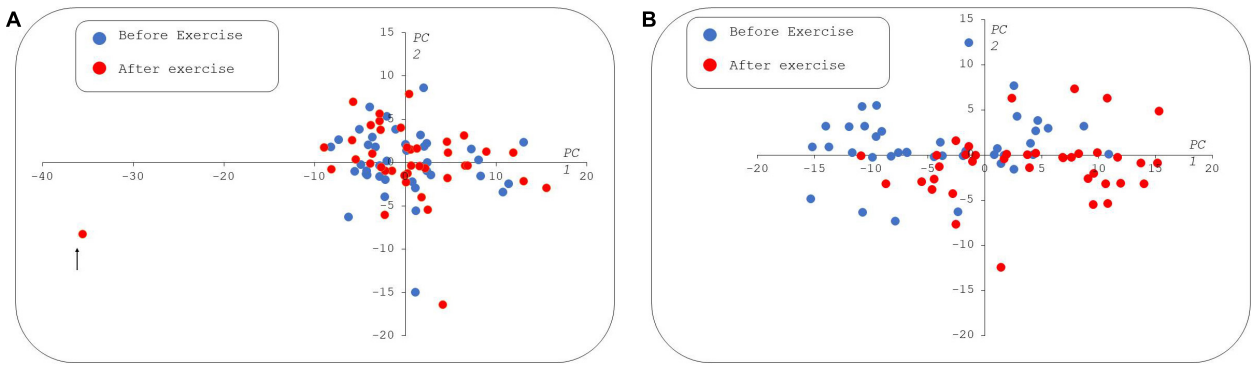

FIGURE 5 | Paired principal component analysis (pPCA) scatter plot of metabolomic data. In the left panel **(A)**, all the samples were used for pPCA, the first principal component (PC1) explains 30% of the total variance and the second (PC2) captures 11%. The sample spotted with a black arrow appears as an outlier in PC1. The right panel **(B)** shows the PCA built without the outlier. In the second pPCA, the first and second PCs explain 43 and 9% of the total variance, respectively. At rest, samples are indicated by blue circles and postexercise samples taken from the same patients as red circles. In both the scatter plots, X and Y axes are dimensionless. PC1, 2: Principal components 1 and 2, respectively.

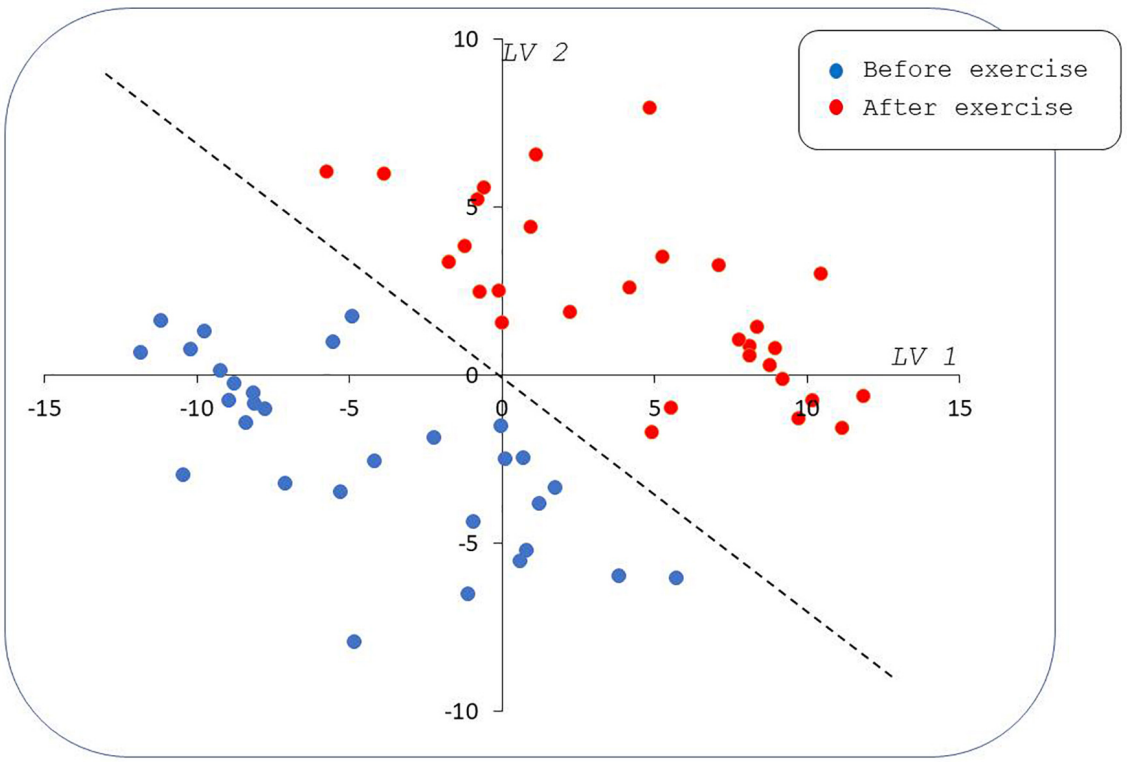

FIGURE 6 | Paired partial least squares discriminant analysis (PLS-DA) scatter plot by using median values for scores of best models. Samples taken from patients before the effort (blue circles) are well separated from samples taken on the same patients after the effort (red circles) in the plane formed by the first and second latent variables (LV1 and LV2). The dashed line represents a frontier between pre- and postexercise samples; this line is a linear combination of LV1 and LV2 indicating an equal contribution of both the latent variables to between-groups discrimination. Note that LV1 and LV2 are dimensionless.

The alteration in amino acid metabolism is also a well-known phenomenon during exercise (Sakaguchi et al., 2019; Kelly et al., 2020). However, the modification of branched amino acids (leucine, isoleucine, and valine), which are amino acids linked to insulin resistance frequently reported in postexercise studies (Kelly et al., 2020), was not observed in patients with LEAD. Serine and glutamine, modified after exercise in our patients, have already been shown to be modified in patients with non-LEAD after exercise (Schranner et al., 2020) and might, therefore, not be specific to LEAD. Alanine was one of the most modified metabolites (VIP > 1.8) in our signature. This amino acid is closely related to lactate, which has not been measured

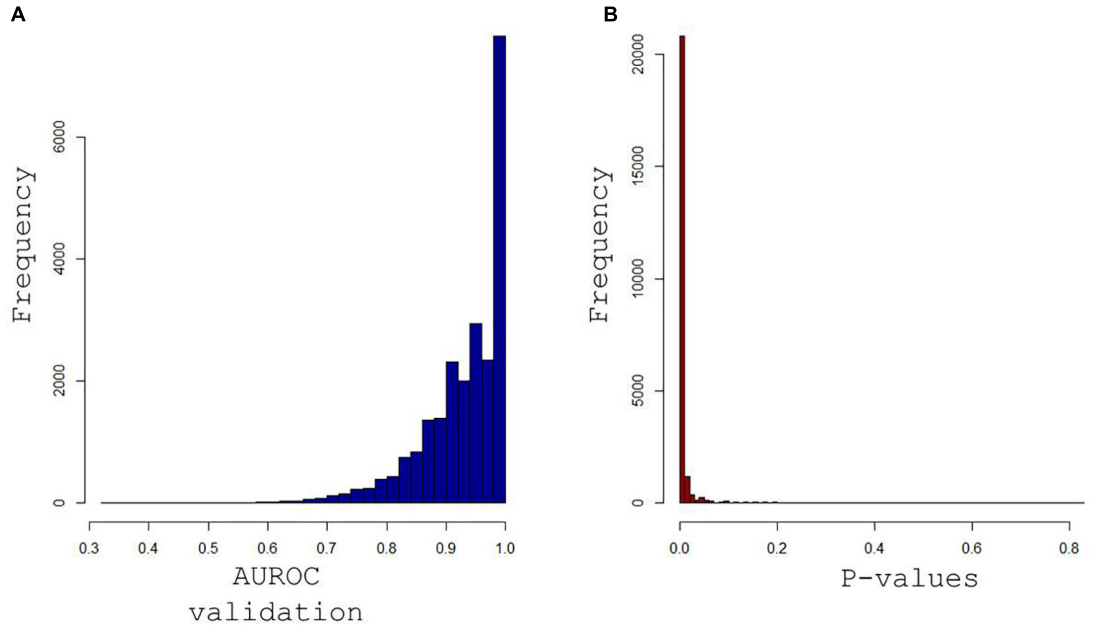

FIGURE 7 | Histograms of the area under receiver operating characteristics (AUROC) curve for validation sets in **(A)** and their associated *p*-values in **(B)** obtained when each of the 23,345 models built with training samples were applied to the remaining validation samples. Median values for the AUROC values and *p*-values (0.95 and 0.00067) demonstrate the excellent predictive capabilities and low overfitting tendency of the paired PLS-DA models.

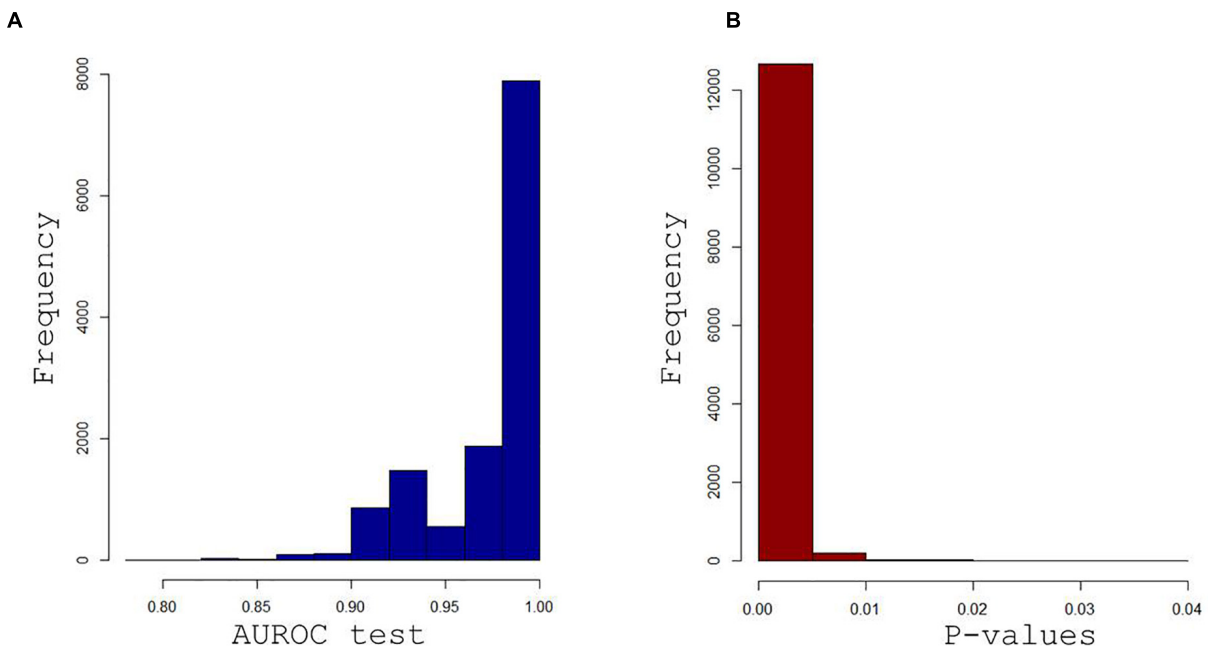

FIGURE 8 | Histograms of the AUROC curve values **(A)** and associated *p*-values **(B)** were obtained when the 12,941 best training-validation models were applied on the test set. Median values for the AUROC values and *p*-values (0.988 and 0.00049) demonstrate the excellent predictive capabilities and low overfitting tendency of the paired PLS-DA best models.

here. Its sharp increase is, therefore, evidence that ischemia is induced in patients by exercise.

Methionine sulfoxide (Met-SO) is a biomarker of oxidative stress that we found to be increased after exercise in patients with LEAD. This variation was not found by the two previous studies performed in patients with LEAD at rest (Ismaeel et al., 2019) and after exercise (Coolen et al., 2008) nor after exercise more generally. This metabolite would, therefore, be

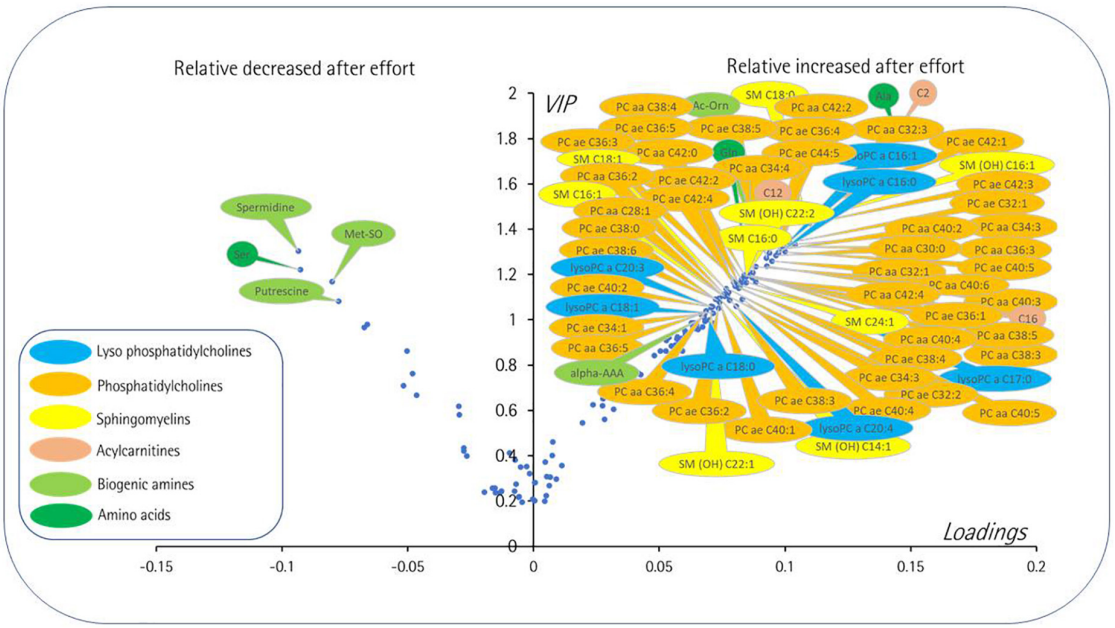

FIGURE 9 | Volcano plot [loadings vs. variable importance for the projection (VIP)] from the 12,941 paired PLS-DA best models comparing at rest and postexercise plasma samples. Only the most important metabolites, i.e., those with VIP ≥ 1, have been labeled. Negative loadings indicate relatively decreased metabolite after exercise compared to the rest situation. The main features are decreased levels after exercise of some polar metabolites including amino acid serine, two polyamines (putrescine and spermidine), and a marker of oxidative stress (methionine sulfoxide). Then again, many lipidic species including diacyl (PC aa) and alkyl-acyl (PC ae) phosphatidylcholines, sphingomyelins (SM), lysophosphatidylcholines (lysoPC), and long chain acylcarnitines (C12 and C16) along with more polar metabolites comprising acetylcarnitine (C2), acetylornithine (Ac-Orn), alpha-aminoadipic acid (alpha-AAA), and amino acids alanine (Ala) and glutamine (Gln). The color coding is as follows: amino acids, dark green; biogenic amines, light green, acylcarnitines, brown; lysophosphatidylcholines, blue; phosphatidylcholines, orange; sphingomyelin, yellow. For phosphatidylcholines, the sum of the length of the two acyl or acyl-alkyl groups is noted after the C and is followed by the number of double bonds. The same notation is used for representing the length and the number of double bonds in the acyl chain of SM and lysoPC.

TABLE 2 | Significant correlations between metabolite concentration changes and clinical criteria of severity.

	ABI	*p*-value	DROPs	*p*-value	MWT	*p*-value	WELCH score	*p*-value
C5	−0.083	0.617	−0.143	0.385	0.373	0.020*	0.280	0.085
Arg	0.115	0.487	−0.354	0.027*	0.123	0.454	−0.098	0.554
Asn	0.164	0.318	−0.200	0.221	0.065	0.695	0.319	0.048*
Asp	−0.095	0.563	−0.072	0.665	0.147	0.372	0.400	0.012*
Lys	−0.354	0.027*	0.243	0.136	0.247	0.129	−0.025	0.878
Orn	−0.356	0.026*	0.192	0.241	0.242	0.138	0.121	0.464
Pro	−0.339	0.035*	0.145	0.377	0.121	0.461	−0.053	0.747
Putrescine	0.168	0.307	−0.270	0.097	−0.085	0.607	0.322	0.046*
SDMA	−0.245	0.133	−0.056	0.734	0.385	0.016*	0.047	0.776
Spermidine	−0.121	0.465	−0.053	0.748	−0.030	0.856	0.365	0.022*
Spermine	−0.027	0.871	−0.095	0.567	−0.025	0.878	0.337	0.036*
t4-OH-Pro	−0.404	0.011*	0.327	0.042*	0.225	0.169	−0.211	0.197
PC aa C42:6	−0.286	0.077	0.110	0.507	−0.016	0.924	−0.385	0.015*
SDMA/Arg	−0.232	0.156	0.033	0.844	0.345	0.032*	0.080	0.630
Kynurenine/Trp	0.406	0.010*	−0.114	0.488	0.000	1.000	0.045	0.786
MUFA (PC)/SFA (PC)	0.086	0.603	−0.037	0.822	0.337	0.036*	0.000	0.998

*$p < 0.05$.
All other metabolites showed no significant correlations and are not reported in the table. Note that no adjustment was performed for the multiple comparisons.

a potential biomarker of exercise-induced oxidative stress in patients with arteriopathy.

To the best of our knowledge, alpha-aminoadipate is a biomarker of insulin resistance (Wang et al., 2013) that has not been associated with LEAD or with exercise in general. Likewise, the variation observed in this study of acetylornithine has not been previously reported. However, ornithine has been shown to be decreased in peripheral artery disease at rest

(Ismaeel et al., 2019). These two metabolites could, therefore, constitute candidate biomarkers of the stress induced by exercise in patients with LEAD.

Little information is available in the literature concerning polyamines (spermine and putrescine), found to be lowered by exercise in this study, in LEAD, or muscular effort in general. An increase in these polyamines has been shown in skeletal muscle in rats during physical exercise (Turchanowa et al., 2000). In contrast to this study, putrescine has been shown to be increased and spermine unmodified at rest in patients with peripheral artery disease (Ismaeel et al., 2019), suggesting a possible involvement of these regulatory molecules in response to the ischemic stress.

A deep remodeling of phospholipids was observed after exercise in patients with LEAD with increased concentrations of 44 phosphatidylcholines, seven lysophosphatidylcholines, and nine sphingomyelins. This probably corresponds to the mobilization of lipoproteins released in the blood to provide energy substrates. This contrasts with the findings of Ismaeel et al. (2019) showing instead that these three phospholipids were not altered at rest in patients with intermittent claudication, but were lowered during episodes of acute lower limb ischemia. Surprisingly, there is very little information available on the effects of exercise on the plasma concentrations of these three phospholipids, and it is difficult to judge the specificity or non-specificity of this phenomenon.

Metabolites Specifically Related to Ischemia Scores

A total of 16 of these metabolite concentrations was found to correlate with one or more severity scores (ABI, DROP, MWT, and WELCH scores) of the LEAD, including kynurenine/tryptophan ratio, hydroxyproline, SDMA, SDMA/arginine ratio, C5 acylcarnitine, arginine, aspartate, asparagine, lysine, ornithine, proline, putrescine, spermine, spermidine, PC aa C42:6, and the ratio between MUFA to SFA or MUFA (PC)/SFA (PC) ratio.

A large group of these metabolites (SDMA, arginine, ornithine, proline, putrescine, spermine, spermidine, aspartate, asparagine, and lysine) is clearly more or less directly related to the nitric oxide (NO) metabolism, mediating vasodilatation. The correlation of these NO-related metabolites with ischemia is, therefore, not surprising in the situation explored. It should be noted that these metabolites are also often reported as biomarkers of pain, which characterizes the effect of exercise in patients with LEAD. The kynurenine/tryptophan pathway is also involved in vasodilation, pain, and inflammation (Wang et al., 2010).

Hydroxyproline is a metabolite released by the degradation of collagen and marker of tissue damage. Its correlation with the degree of ischemia is, therefore, fully understandable. It is difficult to comment on the correlation of C5 acylcarnitine and PC aa C42:6 with ischemia in the absence of knowledge on the functional specificity of these two lipids compared to their other family members. The MUFA (PC)/SFA (PC) ratio of monounsaturated to saturated glycerophosphocholines is an indicator of fatty acid desaturase activity and may be related to the energetic crisis due to anoxia.

Limitations

The relatively small sample size may appear as a limitation but in our opinion it is a force of this study to attain a highly selected group with proof of exercise-induced ischemia and absence of non-vascular limitation among which exercise-induced hypoxemia is observed in almost 15% of patients complaining claudication (Abraham et al., 2021). Another limit is the number of metabolites explored by our targeted metabolomics approach. However, the standardized and quantitative nature of this approach provided results close to the quality of clinical biology. The use of capillary samples may appear a limitation but is consistent with the volumes needed for metabolomic analysis with the advantage of being minimally invasive. Last, no control group was studied, but patients were their own control (comparison between postexercise and pre-exercise values). Future studies might be needed to investigate the relationship of biomarkers with new indices of clinical severity of exercise-induced ischemia, such as near-IR spectroscopy, contrast ultrasound, MRI, or muscle scintigraphy (Lindner et al., 2008; Potthast et al., 2009; Pande et al., 2011; Boezeman et al., 2016; Cornelis et al., 2021).

CONCLUSION

In the context in which very few metabolomic studies have been carried out in patients with LEAD and even fewer after exercise, this study provides a series of new candidate biomarkers in this pathology. A total of 71 blood metabolites has been shown to be altered by exercise in these patients including metabolites well known to be altered during exercise in general (mainly acylcarnitines and amino acids), and others that were never reported in this context (methionine sulfoxide, α-AAA, acetylornithine, spermine, putrescine, and phospholipid remodeling). A total of 16 metabolites was found to be specifically related to one or more of the indices of clinical severity, two of which correlated to ischemia measured by $TcPO_2$. Not surprisingly, a large part of these metabolites is more or less related to the metabolism of NO, which is a major player in vascular response and pain crisis induced by ischemia. Further correlated metabolites reflect the tissue damage (hydroxyproline) and the energy crisis (phospholipids) induced by ischemia. Further studies of these candidate biomarkers are needed to identify the biomarker or the set of biomarkers that may be the most useful in assessing the severity of vascular damage in patients with LEAD.

DATA AVAILABILITY STATEMENT

The raw data supporting the conclusions of this article will be made available by the authors, without undue reservation.

ETHICS STATEMENT

The studies involving human participants were reviewed and approved by the Comité de Protection des Personnes Ile de France II. The ethics committee waived the requirement of written informed consent for participation.

AUTHOR CONTRIBUTIONS

WS, JH, SH, and PA performed the material preparation and data collection. WS, JC, PR, and PA performed the data analysis. PA, JC, and PR conducted the data interpretation. WS wrote the first draft of the manuscript. All the authors contributed to the study conception and design, commented on previous versions of the manuscript, read, and approved the final manuscript.

FUNDING

The project was partly supported by "Appel d'offre Interne" of the University Hospital in Angers.

ACKNOWLEDGMENTS

We would like to thank Dr. Yannick Bigou and Marine Mauboussin for technical support and to acknowledge the help of medical students of the Vascular Medicine Department of Angers Hospital and Lydie Tessier and Stéphanie Chupin for their technical assistance in metabolomics.

SUPPLEMENTARY MATERIAL

The Supplementary Material for this article can be found online at: https://www.frontiersin.org/articles/10.3389/fphys.2021.758085/full#supplementary-material

Supplementary Table 1 | List of metabolites as provided by the Austrian company Biocrates Life Sciences.

Supplementary Table 2 | The raw results underlying abnormal individual values after $TcPO_2$ tests.

Supplementary Table 3 | Raw data of 150 accurately measured after validation of the quality controls.

REFERENCES

Abraham, P., Colas-Ribas, C., Signolet, I., Ammi, M., Feuilloy, M., Picquet, J., et al. (2018). Transcutaneous exercise oximetry for patients with claudication–a retrospective review of approximately 5,000 consecutive tests over 15 years. *Circ. J.* 82, 1161–1167. doi: 10.1253/circj.CJ-17-0948

Abraham, P., Picquet, J., Bouyé, P., L'Hoste, P., Enon, B., Vielle, B., et al. (2005). Transcutaneous oxygen pressure measurements (tcpO2) at ankle during exercise in arterial claudication. *Int. Angiol.* 24, 80–88.

Abraham, P., Picquet, J., Vielle, B., Sigaudo-Roussel, D., Paisant-Thouveny, F., Enon, B., et al. (2003). Transcutaneous oxygen pressure measurements on the buttocks during exercise to detect proximal arterial ischemia: comparison with arteriography. *Circulation* 107, 1896–1900. doi: 10.1161/01.CIR.0000060500.60646.E0

Abraham, P., Ramondou, P., Hersant, J., Sempore, W. Y., Feuilloy, M., and Henni, S. (2021). Investigation of arterial claudication with transcutaneous oxygen pressure at exercise: interests and limits. *Trends Cardiovasc. Med.* 31, 218–223. doi: 10.1016/j.tcm.2020.03.003

Azab, S. M., Zamzam, A., Syed, M. H., Abdin, R., Qadura, M., and Britz-Mckibbin, P. (2020). Serum metabolic signatures of chronic limb-threatening ischemia in patients with peripheral artery disease. *J. Clin. Med.* 9, 1–24. doi: 10.3390/jcm9061877

Boccalon, H., Lehert, P., and Mosnier, M. (2000). Assessment of the prevalence of atherosclerotic lower limb arteriopathy in France as a systolic index in a vascular risk population. *J. Mal. Vasc.* 25, 38–46.

Boezeman, R. P. E., Moll, F. L., Ünlü, Ç, and de Vries, J. P. P. M. (2016). Systematic review of clinical applications of monitoring muscle tissue oxygenation with near-infrared spectroscopy in vascular disease. *Microvasc. Res.* 104, 11–22. doi: 10.1016/j.mvr.2015.11.004

Bouyé, P., Picquet, J., Jaquinandi, V., Enon, B., Leftheriotis, G., Saumet, J. L., et al. (2004). Reproducibility of proximal and distal transcutaneous oxygen pressure measurements during exercise in stage 2 arterial claudication. *Int. Angiol.* 23, 114–121.

Coolen, S. A., Daykin, C. A., van Duynhoven, J. P. M., van Dorsten, F. A., Wulfert, F., Mathot, J., et al. (2008). Measurement of ischaemia-reperfusion in patients with intermittent claudication using NMR-based metabonomics. *NMR Biomed.* 21, 686–695. doi: 10.1002/nbm.1242

Cornelis, N., Chatzinikolaou, P., Buys, R., Fourneau, I., Claes, J., and Cornelissen, V. (2021). The use of near infrared spectroscopy to evaluate the effect of exercise on peripheral muscle oxygenation in patients with lower extremity artery disease: a systematic review. *Eur. J. Vasc. Endovasc. Surg.* 61, 837–847. doi: 10.1016/j.ejvs.2021.02.008

Criqui, M. H., and Aboyans, V. (2015). Epidemiology of peripheral artery disease. *Circ. Res.* 116, 1509–1526. doi: 10.1161/CIRCRESAHA.116.303849

Dang, V. T., Huang, A., and Werstuck, G. H. (2018). Untargeted metabolomics in the discovery of novel biomarkers and therapeutic targets for atherosclerotic cardiovascular diseases. *Cardiovasc. Hematol. Disord. Targets* 18, 166–175. doi: 10.2174/1871529x18666180420170108

Fowkes, F. G. R., Aboyans, V., Fowkes, F. J. I., McDermott, M. M., Sampson, U. K. A., and Criqui, M. H. (2017). Peripheral artery disease: epidemiology and global perspectives. *Nat. Rev. Cardiol.* 14, 156–170. doi: 10.1038/nrcardio.2016.179

Fowkes, F. G. R., Rudan, D., Rudan, I., Aboyans, V., Denenberg, J. O., McDermott, M. M., et al. (2013). Comparison of global estimates of prevalence and risk factors for peripheral artery disease in 2000 and 2010: a systematic review and analysis. *Lancet* 382, 1329–1340.

Got, I. (1998). Transcutaneous oxygen pressure (TcPO2): advantages and limitations. *Diabetes Metab.* 24, 379–384.

Huang, C. C., McDermott, M. M., Liu, K., Kuo, C. H., Wang, S. Y., Tao, H., et al. (2013). Plasma metabolomic profiles predict near-term death among individuals with lower extremity peripheral arterial disease. *J. Vasc. Surg.* 58, 989–996.e1. doi: 10.1016/j.jvs.2013.04.022

Ismaeel, A., Franco, M. E., Lavado, R., Papoutsi, E., Casale, G. P., Fuglestad, M., et al. (2019). Altered metabolomic profile in patients with peripheral artery disease. *J. Clin. Med.* 8:1463. doi: 10.3390/jcm8091463

Kelly, R. S., Kelly, M. P., and Kelly, P. (2020). Metabolomics, physical activity, exercise and health: a review of the current evidence. *Biochim. Biophys. Acta Mol. Basis Dis.* 1866:165936. doi: 10.1016/j.bbadis.2020.165936

Krishnan, P., and Collins, T. (2014). Peripheral artery disease. *Interv. Cardiol. Clin.* 3, ix–x. doi: 10.1016/j.iccl.2014.07.006

Kim-Anh, L. C., Florian, R., Ignacio, G., and Sebastien, D. (2016). m*ixOmics: Omics Data Integration Project. R Package Version 6.1.1.* Available online at: https://CRAN.R-project.org/package=mixOmics

Lindner, J. R., Womack, L., Barrett, E. J., Weltman, J., Price, W., Harthun, N. L., et al. (2008). Limb stress-rest perfusion imaging with contrast ultrasound for the assessment of peripheral arterial disease severity. *JACC Cardiovasc. Imaging* 1, 343–350. doi: 10.1016/j.jcmg.2008.04.001

Morville, T., Sahl, R. E., Moritz, T., Helge, J. W., and Clemmensen, C. (2020). Plasma metabolome profiling of resistance exercise and endurance exercise in humans. *Cell Rep.* 29:108554. doi: 10.1016/j.celrep.2020.108554

Pande, R. L., Park, M. A., Perlstein, T. S., Desai, A. S., Doyle, J., Navarrete, N., et al. (2011). Impaired skeletal muscle glucose uptake by [18F] fluorodeoxyglucose-positron emission tomography in patients with peripheral artery disease and intermittent claudication. *Arterioscler. Thromb. Vasc. Biol.* 31, 190–196. doi: 10.1161/ATVBAHA.110.217687

Potthast, S., Schulte, A., Kos, S., Aschwanden, M., and Bilecen, D. (2009). Blood oxygenation level-dependent MRI of the skeletal muscle during ischemia in patients with peripheral arterial occlusive disease. *Rofo* 181, 1157–1161. doi: 10.1055/s-0028-1109786

Rizza, S., Copetti, M., Rossi, C., Cianfarani, M. A., Zucchelli, M., Luzi, A., et al. (2014). Metabolomics signature improves the prediction of cardiovascular events in elderly subjects. *Atherosclerosis* 232, 260–264. doi: 10.1016/j.atherosclerosis.2013.10.029

Sakaguchi, C. A., Nieman, D. C., Signini, E. F., Abreu, R. M., and Catai, A. M. (2019). Metabolomics-based studies assessing exercise-induced alterations of the human metabolome: a systematic review. *Metabolites* 9:164. doi: 10.3390/metabo9080164

Schranner, D., Kastenmüller, G., Schönfelder, M., Römisch-Margl, W., and Wackerhage, H. (2020). Metabolite concentration changes in humans after a bout of exercise: a systematic review of exercise metabolomics studies. *Sport. Med. Open* 6, 1–17. doi: 10.1186/s40798-020-0238-4

Serrano Hernando, F. J., and Martín Conejero, A. (2007). Peripheral artery disease: pathophysiology, diagnosis and treatment. *Rev. Esp. Cardiol.* 60, 969–982. doi: 10.1157/13109651

Turchanowa, L., Rogozkin, V. A., Milovic, V., Feldkoren, B. I., Caspary, W. F., and Stein, J. (2000). Influence of physical exercise on polyamine synthesis in the rat skeletal muscle. *Eur. J. Clin. Invest.* 30, 72–78. doi: 10.1046/j.1365-2362.2000.00586.x

Walters, D. P., Gatling, W., Mullee, M. A., and Hill, R. D. (1992). The prevalence, detection, and epidemiological correlates of peripheral vascular disease: a comparison of diabetic and non-diabetic subjects in an english community. *Diabet. Med.* 9, 710–715. doi: 10.1111/j.1464-5491.1992.tb01878.x

Wang, T. J., Ngo, D., Psychogios, N., Dejam, A., Larson, M. G., Vasan, R. S., et al. (2013). 2-Aminoadipic acid is a biomarker for diabetes risk. *J. Clin. Invest.* 123, 4309–4317. doi: 10.1172/JCI64801

Wang, Y., Liu, H., McKenzie, G., Witting, P. K., Stasch, J. P., Hahn, M., et al. (2010). Kynurenine is an endothelium-derived relaxing factor produced during inflammation. *Nat. Med.* 16:607. doi: 10.1038/nm.2092

Zagura, M., Kals, J., Kilk, K., Serg, M., Kampus, P., Eha, J., et al. (2015). Metabolomic signature of arterial stiffness in male patients with peripheral arterial disease. *Hypertens. Res.* 38, 840–846. doi: 10.1038/hr.2015.71

Conflict of Interest: The authors declare that the research was conducted in the absence of any commercial or financial relationships that could be construed as a potential conflict of interest.

Publisher's Note: All claims expressed in this article are solely those of the authors and do not necessarily represent those of their affiliated organizations, or those of the publisher, the editors and the reviewers. Any product that may be evaluated in this article, or claim that may be made by its manufacturer, is not guaranteed or endorsed by the publisher.

Copyright © 2021 Semporé, Chao De La Barca, Hersant, Ouédraogo, Yaméogo, Henni, Reynier and Abraham. This is an open-access article distributed under the terms of the Creative Commons Attribution License (CC BY). The use, distribution or reproduction in other forums is permitted, provided the original author(s) and the copyright owner(s) are credited and that the original publication in this journal is cited, in accordance with accepted academic practice. No use, distribution or reproduction is permitted which does not comply with these terms.

frontiers in Physiology

ORIGINAL RESEARCH
published: 12 January 2022
doi: 10.3389/fphys.2021.801833

Energy Intake of Men With Excess Weight During Normobaric Hypoxic Confinement

Igor B. Mekjavic[1], Mojca Amon[1], Elizabeth J. Simpson[2], Roger Kölegård[3], Ola Eiken[3] and Ian A. Macdonald[2]*

[1] Department of Automation, Biocybernetics and Robotics, Jozef Stefan Institute, Ljubljana, Slovenia, [2] Metabolic and Molecular Physiology Group, Faculty of Medicine and Health Sciences University of Nottingham Queen's Medical Centre, Nottingham, United Kingdom, [3] Division of Environmental Physiology, School of Chemistry, Biotechnology and Health, KTH Royal Institute of Technology, Stockholm, Sweden

Due to the observations of weight loss at high altitude, normobaric hypoxia has been considered as a method of weight loss in obese individuals. With this regard, the aim of the present study was to determine the effect of hypoxia *per se* on metabolism in men with excess weight. Eight men living with excess weight (125.0 ± 17.7 kg; 30.5 ± 11.1 years, BMI: 37.6 ± 6.2 kg·m^{-2}) participated in a randomized cross-over study comprising two 10-day confinements: normobaric (altitude of facility ≃ 940 m) normoxia (NORMOXIA; P_IO_2 = 133 mmHg), and normobaric hypoxia (HYPOXIA). The P_IO_2 in the latter was reduced from 105 (simulated altitude of 2,800 m) to 98 mmHg (simulated altitude of 3,400 m over 10 days. Before, and at the end of each confinement, participants completed a meal tolerance test (MTT). Resting energy expenditure (REE), circulating glucose, GLP-1, insulin, catecholamines, ghrelin, peptide-YY (PYY), leptin, gastro-intestinal blood flow, and appetite sensations were measured in fasted and postprandial states. Fasting REE increased after HYPOXIA (+358.0 ± 49.3 kcal·day^{-1}, $p = 0.03$), but not after NORMOXIA (−33.1 ± 17.6 kcal·day^{-1}). Postprandial REE was also significantly increased after HYPOXIA ($p \leq 0.05$), as was the level of PYY. Furthermore, a tendency for decreased energy intake was concomitant with a significant body weight reduction after HYPOXIA (−0.7 ± 0.2 kg) compared to NORMOXIA (+1.0 ± 0.2 kg). The HYPOXIA trial increased the metabolic requirements, with a tendency toward decreased energy intake concomitant with increased PYY levels supporting the notion of a hypoxia-induced appetite inhibition, that could potentially lead to body weight reduction. The greater postprandial blood-glucose response following hypoxic confinement, suggests the potential development of insulin resistance.

Keywords: obesity, hypoxia, altitude, weight loss, metabolism

OPEN ACCESS

Edited by:
Pierre Denise, Institut National de la Santé et de la Recherche Médicale (INSERM), U1075 Université de Caen Normandie—Pôle des Formations et de Recherche en Santé, France

Reviewed by:
Jamie Matu, Leeds Beckett University, United Kingdom
Mark Hopkins, University of Leeds, United Kingdom

****Correspondence:***
Igor B. Mekjavic
igor.mekjavic@ijs.si

Specialty section:
This article was submitted to Clinical and Translational Physiology, a section of the journal Frontiers in Physiology

Received: *25 October 2021*
Accepted: *16 December 2021*
Published: *12 January 2022*

Citation:
Mekjavic IB, Amon M, Simpson EJ, Kölegård R, Eiken O and Macdonald IA (2022) Energy Intake of Men With Excess Weight During Normobaric Hypoxic Confinement. Front. Physiol. 12:801833. doi: 10.3389/fphys.2021.801833

Abbreviations: BMI, Body mass index; CSS, Composite satiety score; ECG, Electrocardiogram; ELISA, Enzyme-linked immunosorbent assay; EPO, Erythropoietin; F_IO_2, Fraction of inspired oxygen; HOMA, Homeostatic food consumption; HOMA IR, Insulin resistance; HOMA ß, cell function; HR, Heart rate; MTT, Meal tolerance test; PFC, Prospective food consumption; P_IO_2, Partial pressure of inspired oxygen; PYY, Peptide YY; REE, Resting energy expenditure; RH, Relative humidity; RIA, Radio-immunoassay; S_pO_2, Capillary oxyhaemoglobin saturation; VAS, Visual analog scale; $\dot{V}O_2$, Oxygen uptake; $\dot{V}CO_2$, Carbon dioxide production.

NEW FINDINGS

- Prolongued exposure of humans to high altitude has been observed to cause weight loss, and the etiology of this hypoxia-induced loss of body mass remains relatively unresolved. Previous observations of this high altitude anorexia phenomenon in climbers may have been confounded by increased physical activity, insufficient food availability and environmental cold.
- A controlled 10-day normobaric hypoxic confinement of men with excess weight revealed a significant appetite suppression with a concomitant loss of body mass when compared to similar confinement in normobaric normoxia.

INTRODUCTION

Obesity has become a global epidemic. Considering the morbidity, mortality, social and economic burdens related to this malady, it is obvious that effective prevention strategies and treatments are needed. Once body mass index (BMI) exceeds 30 $kg.m^{-2}$, mortality rate from all causes, especially cardiovascular disease, increases by 50–100% (Poirier and Després, 2001). In addition to reduced energy intake, the beneficial effects of physical activity in preventing or alleviating chronic diseases and increasing physiological and psychological well-being are well documented (Hudon et al., 2008). However, since obesity also increases cardiovascular risk, the prescription of exercise must be conducted with care. Particularly in obese individuals, exercise limitation can profoundly restrict daily activities and thus impair quality of life. The American College of Sports Medicine (Jakicic et al., 2001) recommends that obese individuals should exercise at a moderate intensity (55-69% of maximum heart rate), which can be beneficial for the management of their body weight loss. However, maintenance of such exercise intensity may be difficult for them, thus new, innovative protocols have to be established in order to promote the quality of life in obese individuals.

As a prelude to studies investigating the effect of hypoxic exercise on metabolism, as a novel weight management intervention, we initiated a series of studies to examine resting metabolism during 10-day hypoxic confinement. These initial studies were designed to reveal the effect of hypoxia *per se* on metabolism, without any confounding effects of exercise. Interest in this area arises from anecdotal evidence of loss of weight at altitude, or »high altitude anorexia«, and results of controlled studies reporting hypoxia-induced alterations in metabolism (Milledge, 1972; Haufe et al., 2008; Wiesner et al., 2010).

The observation that high altitude exposure leads to considerable weight loss in alpinists (Pugh, 1954; Milledge, 1972), has led to the suggestion that it might be beneficial to incorporate hypoxic training in weight management programs for obese individuals (Mekjavic et al., 2016). It is known that hypoxia stimulates the sympathetic nervous system and field studies have commonly reported weight loss during exposures to high altitude (Gill and Pugh, 1964; Surks et al., 1966; Consolazio et al., 1968; Krzywicki et al., 1969). From these studies, it is not possible to discern whether weight reduction is due to the increased energy expended during hard physical work, non-shivering and shivering thermogenesis in the cold environment, limited availability or palatability of food, dehydration, malabsorption, acute mountain sickness, or a combination of these factors (Boyer and Blume, 1984). Rose et al. (1988) suggested that hypoxia *per se* might be sufficient cause for the weight loss and decreased food consumption reported by mountain expeditions at high altitude. Netzer et al. (2008) reported an average reduction of 1.14 kg in body weight following an 8-wk exercise program conducted under normobaric hypoxic conditions (inspired fraction of O_2, $F_IO_2 = 0.15$) in obese individuals, but the loss of fat mass was not defined. Moreover, loss of appetite was reported after 31-days of hypobaric hypoxic exposure (Westerterp-Plantenga et al., 1999). Similarly, Wasse et al. (2012) reported a suppression of hunger and food intake after only a 7-h exposure to normobaric hypoxia, comprising a 60-min bout of exercise.

Previously (Mekjavic et al., 2016) we reported a significant increase in fat mass during a 10-d normoxic confinement of normal weight individuals, with a tendency, albeit not significant, toward a decrease in fat mass during hypoxic confinement. Adipose tissue is no longer considered as only an energy storage site, but recent studies also emphasize the importance of adipose tissue as a highly active endocrine organ secreting a range of hormones involved in energy metabolism (Meier and Gressner, 2004). Furthermore, gastrointestinal hormones have important roles in energy homeostasis, glucose and lipid metabolism, reproduction, cardiovascular function, and immunity. They directly influence other organ systems, including the brain, liver, and skeletal muscle, and are significantly regulated by nutritional status (Meier and Gressner, 2004). In addition to adiponectin and resistin, adipose tissue also produces leptin—a satiety hormone. Leptin acts on the central nervous system, in particular the hypothalamus, suppressing food intake and stimulating energy expenditure (Webber and Macdonald, 2000).

Our previous study with normal weight individuals demonstrated that a 10-day exposure to normobaric hypoxia without the confounding effect of strenuous physical exercise resulted in decreased food intake (Mekjavic et al., 2016). The aim of the present study was to assess whether hypoxia might initiate similar significant weight loss in men with excess weight, and whether this loss of mass would be predominantly from the fat tissue compartment.

MATERIALS AND METHODS

Study Population

Eight males with excess weight, all low altitude (351.6 ± 103.7 m) residents, participated in two 10-day trials. Inclusion criteria included total body fat>30% and/or body mass index (BMI) > 27.5 $kg{\cdot}m^{-2}$. Their (mean ± SD) age, mass, percent total body fat, and body mass index (BMI) were 30.5 ± 11.1 years, 125.0 ± 17.7 kg, 30.8 ± 6.1%, and 37.6 ± 6.2 $kg{\cdot}m^{-2}$, respectively. Participant exclusion criteria included a history of physician-diagnosed medical problems, recent prolonged exposure to normobaric or hypobaric hypoxia, or recent weight

loss, participation in any dietary manipulations in the past 6 months, and use of any medications or drugs. All participants gave their written informed consent to participate in the study. The study protocol was approved by the National Committee for Medical Ethics at the Ministry of Health of the Republic of Slovenia (approval no. 108/08/09) and conformed to the Declaration of Helsinki.

Experimental Procedure

The study was conducted at the Olympic Sport Centre Planica (Rateče, Slovenia) situated at an altitude of 940 m. We replicated the protocol used previously with normal weight participants (Mekjavic et al., 2016). Participants undertook two trials, during which they were confined to one floor of the facility. In one trial, the ambient conditions were normoxic (NORMOXIA trial), and in the other they were rendered hypoxic (HYPOXIA trial). The study was designed as a randomized cross-over study. Participants were assigned to two groups: initially one group (N = 4) was confined to a normobaric normoxic environment (NORMOXIA, F_IO_2 = 0.2093) for 10 days and the other (N = 4) to a controlled normobaric hypoxic environment (HYPOXIA) for the same period. During the HYPOXIA trial, the 10-day exposure to a simulated altitude commenced at 2,800 m (P_IO_2 = 105 mmHg) on days 1 and 2, and continued with a daily increase of 200 m, until a simulated altitude of 3,400 m (P_IO_2 = 98 mmHg) was attained. The subjects remained at the simulated altitude of 3,400 m for the remaining 4 days. In both trials, the participants arrived at the facility 3 days prior to the onset of the 10-day confinement. During these 3 days, they were familiarized with the experimental protocol and equipment, and baseline measurements were obtained. Upon completion of the 10-day confinements, participants remained at the facility for an additional 3 days for the post-confinement tests.

After a 3-week wash-out period the participants returned to the Olympic Sport Centre Planica, and the conditions for the participants were crossed-over. During both the NORMOXIA and HYPOXIA trials, participants were confined to the living quarters (each group had at their disposal 3 double sleeping rooms and one living/dining room; total area of $\sim$ 110 m^2).

In the HYPOXIA trial, the reduction in FO_2 was achieved with an oxygen dilution system (B-cat, the Netherlands), based on the Vacuum-Pressure Swing Adsorption principle. The oxygen levels in each room were monitored and recorded at 15-min intervals throughout the 10-day period. In the event that the FO_2 in any given room decreased below the pre-set value, delivery of the hypoxic gas mixture to that room was stopped. In the event that the FO_2 dropped by more than 0.005 of the pre-set value, the control system activated a fan, which delivered external ambient air into that room. As a consequence of the fan being activated, the FO_2 in the room would increase rapidly to the desired level. Once the FO_2 attained the pre-set value, the fan was de-activated. Moreover, each participant was requested to either wear, or have in close proximity, a personal clip-on type of environmental oxygen analyzer (Rae PGM-1100, California, United States) with an audible alarm that was activated in the event that the oxygen level decreased below the pre-set level.

Prior to the onset of the study, participants completed questionnaires regarding their current and past health status, habitual physical activity levels, dietary habits, and food preferences. During the 3-day period prior to each confinement, participants were requested to record their 3-day dietary intake in a food diary. During the 10-day period, participants' physical activity was restricted to slow walks in the living area. Nutritional choices and energy intake were documented in daily nutritional diaries during both trials. The food menu comprised typical national foods, freely available, and an effort was made to accommodate individual food preferences. The participants received the same food menu during each 10-day exposure, but without any restriction regarding the quantity consumed; they ate and drank *ad libitum*. The study was conducted at the Olympic Sport Centre Hotel, and the food was prepared by the kitchen staff. Since all meals were prepared according to preset recipes, the meals on a particular day of the study were identical in both normoxic and hypoxic campaigns. The menus were constructed using the application Open Platform for Clinical Nutrition (OPKP)[1] developed by the Jozef Stefan Institute (Ljubljana, Slovenia). Each day subjects were provided with five meals (breakfast, morning snack, lunch, afternoon snack, dinner). Meals were served at the same time of day. The daily energy intake was recorded and analyzed with the dietary assessment program (OPKP, Jozef Stefan Institute, Ljubljana, Slovenia). Physical activity was monitored continuously with heart-rate (HR) monitors. Participants' well-being was monitored by medical personnel. All participants had personal pulse oximeters (Nonin, Medicals 3100 WristOx, Minnesota, United States) monitoring capillary oxyhaemoglobin saturation (SpO_2) and HR. Symptoms of mountain sickness and individual mood and appetite were monitored daily with the Lake Louise Acute Mountain Sickness Score (LLS, Hackett and Oelz, 1992) and Visual Analog Scales (VAS, Sepple and Read, 1989) for Mood and Appetite, respectively. Metabolic measurements were conducted at the same time of day for each subject (COSMED, Quark PFT, Rome, Italy). The metabolic assessments were conducted in a normoxic environment, 1 day prior to the onset of each 10-day confinement (pre-tests), and on day 10 of the confinement period (post-tests) in either hypoxic or normoxic environments.

Anthropometry

Body composition was analyzed before and after each 10-day confinement with Dual-Emission X-ray absorptiometry (Discovery, Hologic, Inc., Bedford United States). Measurements were made of total body fat mass and regional fat mass (abdominal, right thigh, left thigh) and fat-free mass. Body weight and height were measured with a weighing scale and a stadiometer, respectively (Seca 703, Seca, Hamburg, Germany).

Metabolic Test

Prior to, and on the final day of each 10-day confinement, participants completed a meal tolerance test (MTT) to assess their fasting metabolic status and the postprandial metabolic responses. For 3 days before the pre-confinement metabolic

[1] www.oplp.wi

experiments, participants refrained from any strenuous activity and were limited in their caffeine (daily maximum caffeine content: 150 mg) and alcohol (daily maximum alcohol content: 8 g or 10 ml) consumption. The dietary intake diaries obtained prior to each MTT revealed that the macronutrient composition was similar for the NORMOXIA and HYPOXIA trials. The last meal prior to the MTT was the evening meal the day before the test. For each participant, the composition of the last meal prior to the 12-h fast was the same for each MTT test. For the MTT, participants consumed a standardized mixed nutrient liquid test meal (Ensure, Nutrition shake, vanilla flavor; Abbott) based on their individual body weight (5 ml·kg^{-1}, 1.5 kcal·ml^{-1}) determined on the day of the experiment. Additionally, ^{13}C-labeled glucose (9.2 mg·kg^{-1}) was added to the test meal as an indicator of gastric emptying and glucose uptake and use (expired $^{13}CO_2$ was measured). The average meal volume was 612.9 ± 100.9 ml and contained 123.8 ± 20.4 g of carbohydrate, 38.3 ± 6.3 g of proteins, and 30.2 ± 4.9 g of fat, plus significant amounts of vitamins and minerals. Participants were asked to consume the entire meal portion provided.

Blood Sampling

Blood samples (6 ml) were drawn at regular intervals through a catheter (Baxter Health Care, Valencia, CA) inserted into a dorsal hand vein at the beginning of the experiment. The subject's catheterized hand was placed in a hot box (air temperature 55−60°C) to maintain a constant high hand skin temperature and provide arterialized venous blood. Arterialized venous blood samples were collected in the fasted state prior to the test meal (15 min and approximately 10 s before the meal), and at regular intervals during the 2 h following the ingestion of the test meal, to monitor blood glucose (every 10 min), and to analyze the responses of glucagon-like peptide (GLP-1), serum insulin, peptide YY (PYY) and total ghrelin (every 15 min). Catecholamine (noradrenaline and adrenaline) responses were additionally measured in the fasting state and postprandially. The level of leptin was also measured in the fasted state before and after each trial.

Blood glucose level was analyzed immediately after each arterialized venous blood sample was taken (HemoCue, HMC-201-PROMO, Sweden). For subsequent hormone analyses, all blood samples were either immediately (or after 10 min, in the case of the insulin tube to allow clotting) centrifuged at 3,000 rpm for 10 min (at a temperature of 4°C), and aliquots were kept on ice until the end of the MTT test and stored at −20°C for 1 day, and thereafter at −70°C until further analyses. The analysis of all plasma samples was conducted in duplicate using the assays described below.

Serum insulin concentrations were determined using radio-immunoassay (RIA) (Insulin Coat-A-Count, Diagnostic Products Corp., Los Angeles, United States); GLP-1 concentrations (comprising GLP-1 7-36 amide and 7-37) using Enzyme-Linked ImmunoSorbent Assay (ELISA) (Merck Millipore, Missouri, United States); PYY using RIA for total PYY (Merck Millipore, Missouri, United States) which recognized both PYY1-36 and PYY3-36 in EDTA plasma plus aprotinin; ghrelin was determined using RIA for total ghrelin (Merck Millipore, Missouri, United States) and leptin was determined using a human leptin RIA (Merck Millipore, Missouri, United States). Catecholamines were measured using extraction of the adrenaline and noradrenaline from the plasma (which had been treated with EGTA/glutathione (Sigma-Aldrich, Dorset, United Kingdom) as a preservative) followed by high performance liquid chromatography (HPLC) with electrochemical detection (Forster and Macdonald, 1998).

Labeled glucose artificially enriched with (U-^{13}C) glucose (^{13}C/C > 99%; Isotec, Miamisburg, OH, United States) was dissolved in each participant's liquid meal so that the appearance of $^{13}CO_2$ in the expired air could be used as a marker of the combination of gastric emptying, uptake and oxidation of the test meal. This breath testing is based on the principle that an ingested substrate is metabolized, and a measurable metabolite is then expelled by the respiratory system. Therefore, breath samples were collected simultaneously with the blood samples before and after the meal (at -15, 0, 15, 30, 45, 60, 75, 90, 105, and 120 min) using a breath-sampling bag (500 ml) with a one-way valve for capture of normal exhaled air. To allow analysis of ^{13}C/^{12}C in expired CO_2, 20 ml samples of expired gasses were collected from the breath-sampling bag via a catheter (Baxter Health Care, Valencia, CA) into evacuated tubes (Vacutainers; Becton Dickinson, Franklin Lakes, NJ) and stored until further analysis. All samples were subsequently analyzed in triplicate with mass spectrometry (Prism, VG, Manchester, United Kingdom) and ^{13}C abundance was calculated for all time points. The incremental postprandial response (i.e., the ^{13}C enrichment curve) was integrated and presented as an area under the curve (AUC).

Assessment of Metabolic Rate During Rest

One hour after participants completed their morning personal hygiene and morning body weighing, they relaxed and rested supine for 3 h during the metabolic test. The metabolic tests were conducted at the same time of the day for each participant (between 07:00 a.m. and 01:00 p.m.); the environmental conditions were kept constant: the mean ambient temperature, relative humidity and barometric pressure were 24 ± 0.8°C, 37.4 ± 4.6% and 682 ± 4 mmHg, respectively. The conditions of the laboratory were thermally comfortable. Resting energy expenditure (REE) was measured using indirect respiratory calorimetry with an open-circuit spirometer canopy system (Quark RMR, Cosmed, Italy). A transparent ventilated hood system was placed over the participant's head with a hose connecting the hood to the gas analysis system. The flow of ambient air through the hood was controlled by a pump. The analyzer was calibrated in a normoxic environment for all the tests. Reference gas standards were used to calibrate the system, and all measurements were automatically corrected for environmental temperature, pressure, and humidity. The post-tests in the HYPOXIA trial were performed in a hypoxic environment. During the hypoxic post-tests the metabolic analyzer was calibrated in a normoxic environment, but fasting and post-prandial REE were monitored in the hypoxic environment of the room. Since the hardware and software of the metabolic analyzer (Quark RMR, Cosmed, Italy) was not capable of conducting on-line calculations of REE in a normobaric hypoxic environment, the values of REE in

the hypoxic environment were derived manually from the measurements of the FO_2 entering and exiting the canopy placed on the subject's head, and the air flow through the canopy. Basal measurements of $\dot{V}O_2$ and CO_2 production ($\dot{V}CO_2$) were conducted at 15-min intervals with the individuals awake, before the standard meal and at time-points 15, 45, 75, 105 min, postprandially. To disregard the artifacts that occur during the first few minutes of measurement, when the canopy is placed over a subject's head and the measurement initiated, the calculation of REE was made on the values measured after the first 2 min of the test.

Additionally, HR (Polar, RS400, Finland), arterial pressure (aneroid sphygmomanometer, Welch Allyn, Inc., United States), SpO_2 (Nonin Medicals 3100 WristOx, Minnesota, United States) were recorded at 15-min intervals.

Appetite Sensation

Subjective perceptions of hunger, fullness, desire to eat, thirst and prospective food consumption were assessed using a validated visual analog scale (VAS; Stubbs et al., 2000). The VAS scale was a 100 mm line, anchored to the left with "sensation not felt at all" and to the right with "sensation felt the greatest" and subjects were asked to place a vertical line in relation to their feeling at that particular point in time, these scores were then summed to form the Composite Satiety Score (CSS) according to the following equation (the higher the score, the higher the level of subjective satiety).

$$\text{CSS} = [\text{Full} + (100 - \text{Desire}) + (100 - \text{Hunger}) + (100 - \text{PFC})]/4$$

where,

PFC = prospective food consumption.

Intestinal Blood Flow

Blood flow was measured in the proximal portion of the superior mesenteric artery (SMA), 2–5 cm distally to its origin in the aorta. Flow was estimated by measurements of vessel-lumen diameter and mean flow-velocity, using ultrasonographic/Doppler techniques (Philips CX50, Bothel, Washington). Flow velocity was measured using a 3–12 MHz linear array Doppler transducer that was kept aligned with the vessel; the angle correction of the transducer was maintained at less than 60° and its sample volume was adjusted to cover more than 75 % of the vessel lumen. The diameter of the SMA was measured in B-mode image during end-diastole (determined from the ECG), as wall-to-wall distance in the sagittal section. Assuming that the artery had a circular cross-section, flow was subsequently calculated by multiplying vessel cross-sectional area by the mean flow-velocity. Each flow determination was the average of measurements from 3 to 4 consecutive heart beats, repeated 2–3 times, i.e., the average of data from 6 to 12 beats. The same sonographer performed all measurements.

Calculations and Statistical Methods

Mass spectrometer analysis of breath samples provided a delta value (δ), which was used to calculate abundance (atom %) at each time point using standard methods (Pouteau et al., 1998).

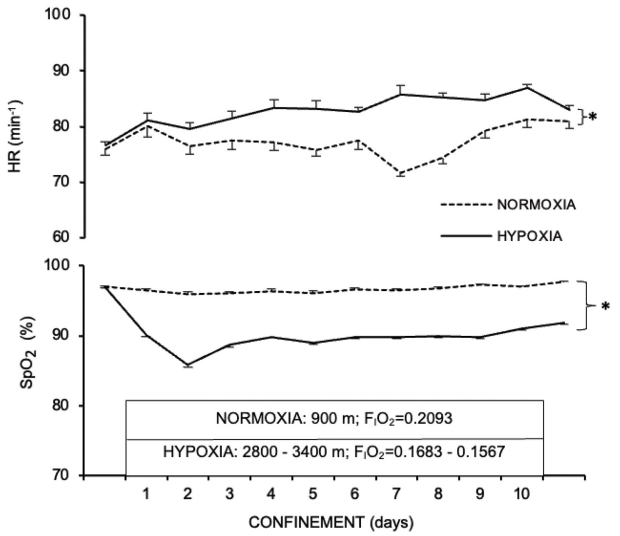

FIGURE 1 | Nocturnal heart rate (HR, min^{-1}) and capillary oxyhaemoglobin saturation (SpO_2, %) before (PRE), during, and at the end (POST) of the NORMOXIA and HYPOXIA trials. Values are mean ± SEM, $n = 8$. *Significant differences between NORMOXIC and HYPOXIC confinement; $p < 0.05$.

Enrichment of breath samples was then obtained by standardizing postprandial values to those at baseline.

The homeostatic model assessment (HOMA) method was used to quantify insulin resistance and β-cell function (Matthews et al., 1985). The non-linear model of two types of HOMA scores were used:

HOMA IR = insulin resistance = (fasting insulin in $mU{\cdot}l^{-1}$) × (fasting plasma glucose in $mmol{\cdot}l^{-1}$) / 22.5
HOMA β = β-cell function [%] = 20 × (fasting insulin in $mU{\cdot}l^{-1}$) / [(fasting glucose in $mmol{\cdot}l^{-1}$)—3.5]

A 2-way ANOVA (NORMOXIA-HYPOXIA, Pre-Post) with repeated measures was used to define the effect of the 10-day confinements on the measured variables. A Tukey *post hoc* test was used to assign the specific differences in the analysis of variance. Additionally, some data were presented as calculated area under curve (AUC) and compared with the same type of ANOVA. Values are mean ± SD unless indicated otherwise. The significance level was set at 0.05.

RESULTS

The average nocturnal capillary oxyhaemoglobin saturation (SpO_2) during the course of the 10-day confinement was lower ($p < 0.001$) in HYPOXIA (90.3 ± 0.2%) than in NORMOXIA (97.4 ± 0.1 %). In contrast, heart rate (HR) was higher ($p = 0.04$) in HYPOXIA (82.7 ± 0.8 min^{-1}) than NORMOXIA (78.8 ± 1.0 min^{-1}, **Figure 1**). Furthermore, arterial pressures were similar before and after both the NORMOXIC (Pre: systolic arterial pressure, SAP = 144 ± 15 mmHg, diastolic arterial pressure, DAP = 88 ± 10 mmHg; Post:

SAP = 138 ± 18 mmHg, DAP = 87 ± 12 mmHg), and HYPOXIC (Pre: SAP = 145 ± 14 mmHg, DAP = 89 ± 11 mmHg; Post: SAP = 137 ± 9 mmHg, DAP = 87 ± 10 mmHg) confinements. No symptoms of mountain sickness (Lake Louise Score) were detected during the HYPOXIC confinement.

The changes in body weight were different ($p = 0.02$; **Table 1**) between the two 10-day confinements. In particular, body weight decreased by 0.7 ± 0.2 kg in HYPOXIA, whereas it increased by 1.0 ± 0.2 kg in NORMOXIA; a difference of 1.7 kg between the two interventions. Neither the HYPOXIC nor the NORMOXIC confinement affected the total or regional body fat mass (**Table 1**).

REE in the fasted state was elevated after HYPOXIC confinement (358 ± 49 kcal·day^{-1}, $p = 0.03$); after NORMOXIC confinement fasting REE remained at similar levels (-33 ± 18 kcal·day^{-1}). Furthermore, after HYPOXIC confinement postprandial REE increased ($p = 0.05$) while no differences were observed after NORMOXIC confinement (**Figure 2**).

The mean energy intake was not significantly different during the NORMOXIC and HYPOXIC confinements, although there was a tendency for it to be lower in HYPOXIA (p = 0.08). Specifically, energy intake was 3,497 ± 189 kcal·day^{-1} in NORMOXIA and 3,264 ± 164 kcal·day^{-1} in HYPOXIA.

The hormone and metabolite concentrations before and after the NORMOXIA and HYPOXIA confinements in the fasted and postprandial states are presented in **Table 2**. The hemoglobin level was unaffected by the HYPOXIC confinement, whereas it decreased after the NORMOXIC confinement. Cholesterol, triglycerides high-density lipoprotein (HDL) and low-density lipoprotein (LDL) levels were unaffected by both confinements. Fasting PYY was significantly decreased both by the NORMOXIC and HYPOXIC confinement, whereas there was a tendency of GLP-1 to be higher after than before each confinement. In the fasted state, all other blood variables remained unaltered by the NORMOXIC as well as the HYPOXIC confinement.

The blood glucose level increased after each MTT. The postprandial blood glucose response was higher after the HYPOXIA confinement than after the NORMOXIA confinement ($p < 0.001$, **Figure 3**). Insulin levels also increased after the test meals, but no significant increases in insulin in the post-HYPOXIC confinement were observed (**Figure 3**). No significant differences ($p = 0.8$) were observed in the postprandial GLP-1 increases in either NORMOXIA or HYPOXIA. Moreover, there were no significant changes in postprandial adrenaline level, while noradrenaline levels increased ($p < 0.001$) after the meal in both the NORMOXIC and HYPOXIC trials. Postprandial total ghrelin levels decreased after the meal (**Table 2**, $p < 0.001$), there being no difference between the NORMOXIA and HYPOXIA ($p = 0.16$). PYY values (**Table 2**) were increased after the meal ($p < 0.001$), with higher responses after the HYPOXIC confinement ($p = 0.01$).

The increments in flow and diameter of the SMA in response to the MTT were similar before and after both the NORMOXIC and HYPOXIC confinements (**Figure 4**).

Moreover, there were no differences in subjective satiety, presented as CSS, in the fasted state before compared to after NORMOXIC or HYPOXIC confinement. Similarly, there were no differences ($p = 0.51$) postprandially in subjective satiety before compared to after the NORMOXIC or HYPOXIC confinement.

DISCUSSION

The main observation of the present study is that of a significant loss in body mass in men with excess weight after a continuous 10-day normobaric hypoxic confinement, compared to an increase in body mass during a normoxic confinement of similar duration. Previous observations of high altitude anorexia in climbers may have been confounded by increased physical activity, insufficient food availability and environmental cold. The present study confirms that hypoxia may lead to body weight reduction in the absence of these cofounders, predominantly due to an increase in REE.

High Altitude Anorexia

Our observation is in agreement with many field studies that have reported remarkable weight loss at altitudes higher than 4,000 m (Westerterp et al., 1992, 1994; Pulfrey and Jones, 1996; Reynolds et al., 1999; Westerterp, 2001; Louis and Punjabi, 2009; Kayser and Verges, 2013; Wandrag et al., 2017). In such field studies, it is difficult to exclude the contribution of cold, physical activity, food availability and palatability, commonly present at high altitude, from the effects of hypoxia *per se*. In the present study, we investigated the responses to 10-days of continuous hypoxia. Gunga et al. (2003) investigated the effect of 3 weeks at moderate altitude (1,700 m) in male subjects with metabolic syndrome (age: 54 years; BMI: 30.3 kg.m^{-2}; with hypertension, hyperlipidemia, diabetes mellitus and/or coronary heart disease). They reported a body weight decrease of 0.9 kg at day 19 at altitude, and a further reduction of 0.7 kg in body weight 6–7 weeks after the altitude exposure. This weight loss was due to a reduction in body fat, whereas no change was observed in lean body mass. However, during the altitude exposure the subjects with metabolic syndrome were active, participating in activities such as mountain hiking between 1,500 and 2,500 m and swimming. Therefore, and because there was no control group, it is not possible to conclude the extent to which the hypoxia *per se* or the physical activity contributed to the weight change. In addition, in the study of Gunga et al. (2003) energy intake was analyzed retrospectively from the questionnaires filled out by participants and from this an average total energy intake of approximately 1,900 kcal·day^{-1} was derived; whilst REE was not measured. This value of 1,900 kcal·day^{-1} was likely a substantial underestimation, as the subjects weight of 92.9 kg would require at least 2,222 kcal·day^{-1} to maintain body weight with a low level of physical activity (derived using the Harris-Benedict equation, revised by Roza and Shizgal, 1984), and substantially more if the level of physical activity was higher. Alternatively, the estimate of a 1,900 kcal·day^{-1} energy intake was correct, in which case the body weight loss is attributable to low energy intake rather than a hypoxia-induced change in metabolism. Similarly, Lippl et al. (2010) observed body weight loss in obese individuals after 14 days at altitude, and concluded that, whatever the cause, it seemed clear that increases in REE contributed to the weight loss.

TABLE 1 | Anthropometric variables before (PRE), and at the end (POST) of the 10-day NORMOXIC and HYPOXIC trials.

	Normoxia Pre	Post	Hypoxia Pre	Post
Body weight (kg)	125.0 ± 17.7	126.0 ± 19.3	123.9 ± 18.0	123.1 ± 19.0
BMI (kg.m^{-2})	37.6 ± 6.2	37.9 ± 6.7	37.3 ± 6.3	37.1 ± 6.6
Lean mass (kg)	77.2 ± 6.9	76.9 ± 8.3	75.7 ± 7.5	74.5 ± 7.1
Total fat mass (%)	30.8 ± 6.1	31.6 ± 5.3	32.1 ± 6.7	31.8 ± 6.1
Abdominal fat (%)	35.1 ± 5.4	36.0 ± 5.2	36.5 ± 5.7	36.2 ± 6.0
Right thigh fat (%)	29.0 ± 6.3	30.3 ± 5.5	30.0 ± 5.9	30.6 ± 6.2
Left thigh fat (%)	28.1 ± 6.3	29.9 ± 5.7	28.4 ± 5.8	30.9 ± 8.0

Values are mean ± SD.

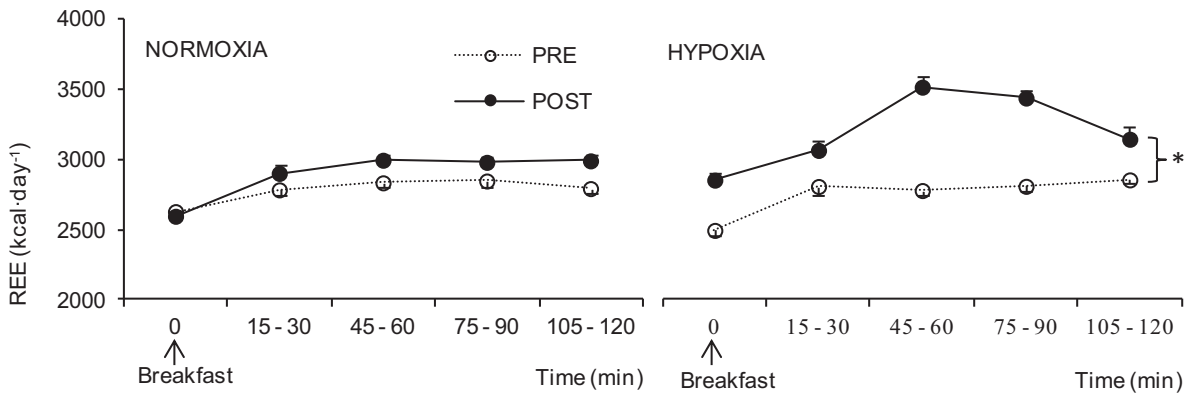

FIGURE 2 | Postprandial resting energy expenditure (REE) before (PRE), and at the end (POST) of the NORMOXIA and HYPOXIA trials. Values are mean ± SEM, $n = 8$. *Significant differences between PRE and POST confinement; $p < 0.05$.

However, in the absence of any control groups or control trials in the aforementioned studies, it is not possible to conclude the extent to which either the hypoxia *per se* or the physical activity contributed to the weight change.

While there were some early indications of unchanged REE at altitude (Stickney and Van Liere, 1953; Chiodi, 1957; Durnin and Brockway, 1959), many investigators have observed an elevated REE at altitude, most likely due to an increased activity-induced energy expenditure in climbing subjects (Picon-Reategui, 1961; Grover, 1963; Gill and Pugh, 1964; Klausen, 1966; Hannon and Sudman, 1973; Butterfield et al., 1992; Pulfrey and Jones, 1996). In most field studies metabolic activity was measured before and after the expeditions, either near to sea level, or from average daily metabolic activity determined from the activity level in the field, and the resting metabolic rate for climbers at altitude was assumed to be the same as at sea level (Westerterp et al., 1992, 1994). However, high altitude anorexia was reported also in hypobaric laboratory studies (Westerterp et al., 2000) and there are also indications of similar effects of normobaric hypoxia. Netzer et al. (2008) reported significant body weight loss after normobaric hypoxic training, but the mechanism of this weight loss remains unresolved. To our knowledge there are as yet no data regarding REE levels during prolonged normobaric hypoxic confinement in the absence of changes in environmental temperature, physical activity and diet. Matu et al. (2017) reported a significantly higher REE during a 5-h exposure to a simulated altitude (normobaric hypoxia) of 4,300 (2,242 ± 269 kJ) compared to sea level (1,826 ± 230 kJ) and a simulated altitude of 2,150 m (1,924 ± 217 kJ). The difference in REE between sea level and 2,150 m simulated altitude was not significant. In the present study, the significantly higher metabolic needs (elevated REE values) after 10-day normobaric HYPOXIA in men with excess weight could be responsible for the observed body weight loss. Despite similar (but not identical) effects of hypobaric and normobaric hypoxic exposures (Richard and Koehle, 2012), the ventilatory response appears to be even more pronounced in normobaric hypoxia (Evetts et al., 2005). In part, the energy cost of such hyperpnea could explain the observed higher REE in HYPOXIA. Our observation is in agreement with studies reporting a 15–26% elevation of REE in patients with chronic obstructive pulmonary diseases (COPD; Vasconcelos et al., 2002; Sergi et al., 2006). Recently, Ramires et al. (2012) have suggested that the increased REE in COPD patients is due to hypermetabolism, greater respiratory muscle effort, higher O_2 requirements and inflammation.

Insulin Sensitivity

The endocrine factors that may have contributed to the observed changes in body weight remain unclear. Although improved short-term glycemic control has been reported after acute hypoxia and after hypoxia combined with exercise (Mackenzie et al., 2011), we observed significantly increased glucose levels after the HYPOXIA trial. The mechanism could be a tendency for insulin resistance. Markedly reduced insulin sensitivity in

TABLE 2 | Hematological variables in fasted state after the meal before (PRE) and at the end (POST) of the NORMOXIC and HYPOXIC trials.

Hematological variables	Normoxia				Hypoxia			
	Pre		Post		Pre		Post	
	Fasted	Postprandial state	Fasted	Postprandial state	Fasted	Postprandial state	Fasted	Postprandial state
Hemoglobin ($g \cdot dL^{-1}$)	154.1 ± 12.3	–	147.6 ± 13.8†	–	154.8 ± 13.6	–	156.0 ± 11.2*	–
Cholesterol ($mg \cdot L^{-1}$)	4.9 ± 1.1	–	4.4 ± 1.1	–	4.9 ± 1.1	–	4.2 ± 1.0	–
Triglyceride ($mg \cdot dL^{-1}$)	2.3 ± 1.4	–	1.9 ± 1.4	–	2.4 ± 1.4	–	2.1 ± 1.3	–
HDL ($mg \cdot dL^{-1}$)	1.1 ± 0.6	–	0.9 ± 0.3	–	1.1 ± 0.7	–	0.9 ± 0.3	–
LDL ($mg \cdot dl^{-1}$)	2.9 ± 0.7	–	2.7 ± 0.7	–	2.9 ± 0.7	–	2.5 ± 0.7	–
Blood glucose ($mmol \cdot L^{-1}$)	4.7 ± 0.5	7.5 ± 0.6$^{\#}$	4.7 ± 0.7	7.5 ± 0.7#	4.4 ± 0.6	7.1 ± 0.8$^{\#}$	4.4 ± 0.5	7.7 ± 0.7#*
Insulin ($pmol \cdot L^{-1}$)	19.0 ± 18.9	150.3 ± 61.7$^{\#}$	17.6 ± 13.8†	195.1 60.3$^{\#}$	14.6 ± 11.0	171.7 ± 54.1$^{\#}$	15.5 ± 10.8	188.5 ± 42.3$^{\#}$
HOMA-IR	0.7 ± 0.8	–	0.6 ± 0.5	–	0.5 ± 0.4	–	0.6 ± 0.4	–
GLP-1 (pM)	2.1 ± 1.0	3.2 ± 1.3$^{\#}$	2.4 ± 1.6	3.2 ± 1.2$^{\#}$	1.9 ± 0.9	3.4 ± 2.2$^{\#}$	2.2 ± 0.9	3.3 ± 1.2$^{\#}$
Adrenaline ($nmol \cdot L^{-1}$)	0.2 ± 0.1	0.1 ± 0.1$^{\#}$	0.2 ± 0.1	0.1 ± 0.1#	0.2 ± 0.1	0.1 ± 0.1#	0.1 ± 0.1	0.1 ± 0.1#
Noradrenaline ($nmol \cdot L^{-1}$)	1.2 ± 0.3	1.5 ± 0.5	1.3 ± 0.7	1.4 ± 0.6	1.1 ± 0.3	1.3 ± 0.2	1.3 ± 0.5	1.5 ± 0.4
Ghrelin ($pg \cdot ml^{-1}$)	925.6 ± 333.4	833.1 ± 245.1$^{\#}$	945.8 ± 367.8	826.5 ± 278.3$^{\#}$	965.1 ± 394.2	873.2 ± 273.4$^{\#}$	940.0 ± 216.9	840.4 ± 176.0$^{\#}$
Leptin ($ng \cdot ml^{-1}$)	18.6 ± 9.4	–	21.1 ± 11.6	–	17.1 ± 10.0	–	18.5 ± 9.9	–
PYY ($pg \cdot ml^{-1}$)	105.9 ± 40.3	136.1 ± 36.2$^{\#}$	97.2 ± 24.8†	129.9 ± 25.7$^{\#}$	103.0 ± 22.7	137.4 ± 49.6$^{\#}$	91.9 ± 17.8†	129.8 ± 48.2$^{\#}$

Values are mean ± SD.

HDL, high-density lipoprotein; LDL, low-density lipoprotein; HOMA-IR, homeostasis model assessment–insulin resistance, GLP-1, glucagon-like peptide-1; PYY, peptide YY_{3-36}.

*$^{\#}$Significant ($p \leq 0.05$) differences postprandialy; †significant ($p \leq 0.05$) differences between NORMOXIA and HYPOXIA in the same state; *significant ($p \leq 0.05$) differences between pre and post in the same confinement.*

healthy men and women at high altitude has been already attributed to the hypoxic stimulus (Larsen et al., 1997; Braun et al., 2001). In addition, similar responses have been observed in lean and obese mice by Reinke et al. (2011), who reported insulin resistance concomitant with significant increases in leptin, and severe systemic inflammation following two hypoxic regimens (intermittent and sustained hypoxia).

Moreover, the present subjects had excess weight and adipose tissue is recognized as a source of pro-inflammatory cytokines that are linked to insulin resistance in muscle and liver (Guzik et al., 2006). There are some suggestions that this pro-inflammatory state is due, in part, to chronic hypoxia induced in the adipose tissue of obese individuals, giving rise to a cascade of biochemical events leading to the release of the proinflammatory/insulin resistance mediating cytokines (Trayhurn and Wood, 2004). Thus, it is possible that normobaric hypoxia may exacerbate this effect of the cytokines, which may lead to increased insulin resistance, but further research is needed to evaluate this.

Appetite Hormones

Body weight reduction may be a result of an imbalance in the communication between the gastrointestinal tract and nervous system required for gut-brain signaling of the food intake control (Konturek et al., 2004; Hussain and Bloom, 2013). Moreover, disturbed body weight regulation at high altitude can be caused by appetite change or altered requirements, or a combination of both. In the present study there were no significant changes in energy intake after the NORMOXIA trial, but a tendency toward decreased intake after the HYPOXIA trial.

Present observations are in agreement with those of Westerterp et al. (1992, 1994) who reported decreased body weight mainly due to decreased appetite and an associated decrease of caloric intake at simulated high altitude (hypobaric hypoxia). It has been proposed that gut hormones may be a useful target for anti-obesity therapy (Murphy and Bloom, 2004; Cummings and Overduin, 2007; Hussain and Bloom, 2013). For example, PYY is thought to have a critical role in energy intake inhibition (Batterham et al., 2002). PYY is released into the circulation proportional to food intake within 1-h post-feeding (Adrian et al., 1985). Wasse et al. (2012) investigated the acute effects of normobaric hypoxia on PYY and acylated ghrelin (appetite stimulator). They reported a suppression of energy intake after 7 h of normobaric hypoxia (F_IO_2 = 12.7, simulated altitude 4,000 m), a suppression of acylated ghrelin concentrations and a tendency for suppressed PYY. Although we observed the anticipated decrease in total ghrelin postprandially, there were no differences in its level

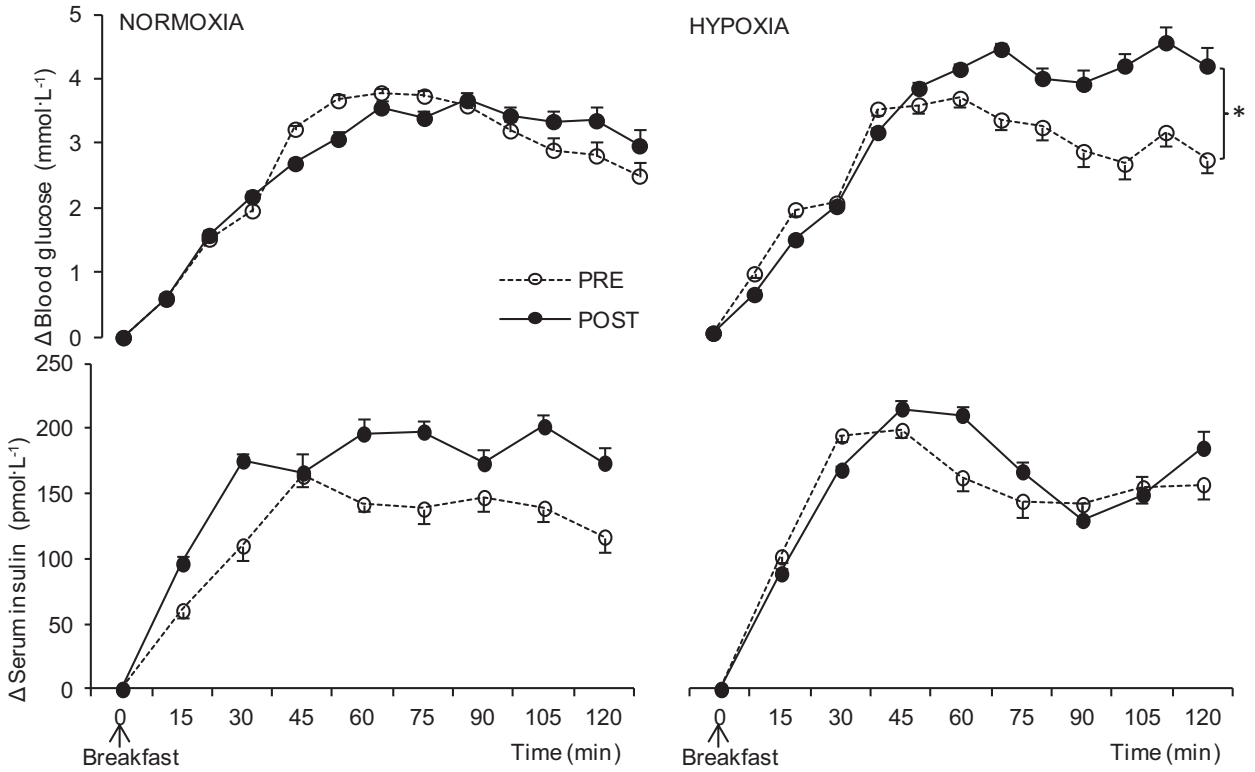

FIGURE 3 | Postprandial delta blood glucose and serum insulin before (PRE), and at the end (POST) of the 10-day normoxic (NORMOXIA) and hypoxic (HYPOXIA) confinements. Values are mean ± SEM, $n = 8$. *Significant differences between PRE and POST confinement; $p < 0.05$.

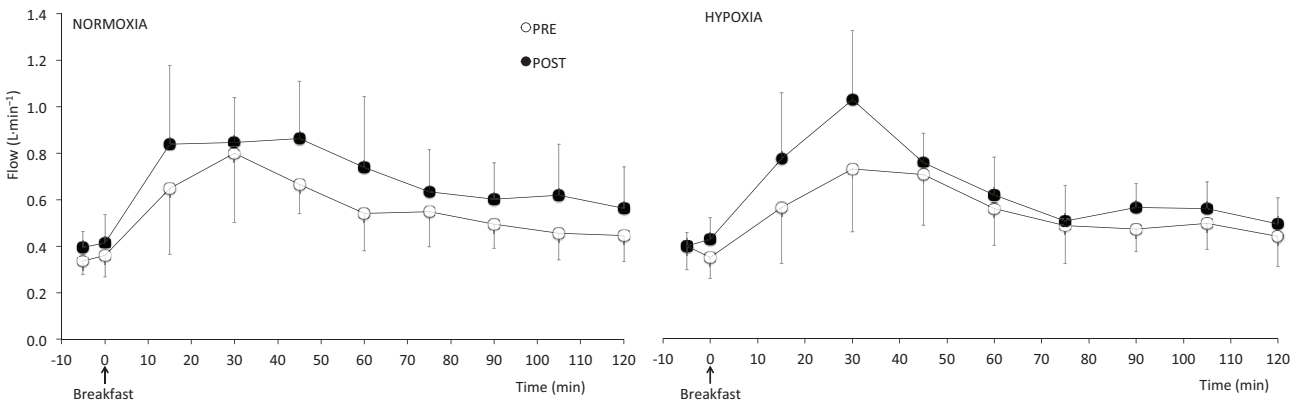

FIGURE 4 | Postprandial blood flow of the superior mesenteric artery before (PRE) and at the end (POST) of the 10-day normoxic (NORMOXIA) and hypoxic (HYPOXIA) confinements. Values are mean ± SEM, $n = 8$.

and response between the 10-day NORMOXIA and HYPOXIA trials, thus not lending support to an exacerbated ghrelin-induced suppression of appetite during hypoxic exposure, as suggested by Wasse et al. (2012). Our finding of an increase in postprandial PYY after prolonged HYPOXIA concomitant with a reduction of spontaneous energy intake could support the notion of a potentially beneficial role of hypoxia in obesity prevention.

Leptin levels provide feedback regarding adipose tissue mass to central regions and regulate food intake. Although the observed levels of leptin in the subjects participating in the present study are in agreement with the higher levels normally observed in obese individuals (Rosická et al., 2003) compared to non-obese, there were no significant changes in leptin levels as a consequence of either the NORMOXIC or HYPOXIC confinement.

Mesenteric Artery Flow

A suppressed total ghrelin level after 7 h of normobaric hypoxia has been associated with impaired gut blood flow at high altitude (Wasse et al., 2012). Namely, a decreased flow in the SMA after acute hypobaric hypoxia (2 h, equivalent to 4,800 m) compared with flow in normoxia was reported earlier by Loshbaugh et al. (2006). They hypothesized that, if reduction in blood flow was maintained during prolonged exposure, it might be responsible for reduced appetite and weight loss at altitude. In contrast, Kalson et al. (2010) reported decreased energy intake and increased resting blood flow in the gastrointestinal tract during acute exposure to high altitude hypoxia (2 nights acclimatization at 3,300 m; measurements were made 24 h after exposure to 4,329 m). Furthermore, in their study the increased mesenteric artery flow response following food ingestion was maintained. They concluded that reduced blood flow is unlikely to cause gastrointestinal responses (increase in gut hormones) and reduced appetite at high altitude. However, the proposed vascular mechanism of potential changes in acylated ghrelin or PYY (Wasse et al., 2012) during longer exposure to hypoxia was not clear. Our observations of unchanged flow response in the mesenteric artery after 10-day HYPOXIA measured in hypoxic conditions supports the suggestion of Kalson et al. (2010), that impaired gut blood flow does not contribute to high altitude anorexia after several days. Further research is needed regarding neurohormonal and vascular satiety signaling, which in the present study did not reach significant differences, but may nevertheless contribute to reduced appetite.

Weight Loss

The present study is in agreement with those suggesting that controlled hypoxia might be incorporated in weight loss protocols (Netzer et al., 2008; Wasse et al., 2012). Previous altitude studies have indicated that the decrease in weight is mainly attributable to a loss of fat (Rose et al., 1988; Armellini et al., 1997; Westerterp-Plantenga et al., 1999; Gunga et al., 2003). For example, Fusch et al. (1996) reported that 70% of the weight loss after 2 months at high altitude (4,900 m) was due to body fat loss. Similarly, Boyer and Blume (1984) reported that 33% of the weight loss after 10 days at 6,000 m was due to loss of fat content. Ge et al. (2010) reported reduced waist circumference after a month at an altitude of 4,638 m. In addition, the degree of weight loss positively correlated with the baseline body weight, suggesting that more body weight will be lost during a stay at high altitude, if the initial body weight is higher. In our study, the changes in body composition were too small to define whether body weight loss was due to loss of fat or lean body mass (**Table 1**), or whether, and to what extent dehydration contributed to the weight loss. Similarly, the previously reported loss of body weight after normobaric hypoxic training in obese individuals (Netzer et al., 2008) was not defined as regards the share of the loss being contributed by fat, lean body and water. Specifically, Netzer et al. (2008) reported alterations in fat metabolism. Namely, there was a tendency for triglycerides, low density lipoproteines (LDL), cholesterol to be reduced while high density cholesterol (HDL) remained stable, however, as in our study, none of these changes reached the level of statistical significance (**Table 2**).

SUMMARY

A limitation of the present study is the small sample size. Nevertheless, the results point to some potential benefits of normobaric hypoxic confinement, which warrant further investigation. Normobaric hypoxic confinement (HYPOXIA) in the present study resulted in significantly increased levels of REE, suggesting a potential value of hypoxia in achieving weight loss in obese individuals. The observed tendency for decreased energy intake during hypoxia combined with the enhancement of PYY secretion under hypoxic conditions may be one of the potential mechanisms for the hypoxia induced body weight loss (Karra et al., 2009; Hussain and Bloom, 2013). An optimal weight loss regimen should also involve physical activity to control glucose regulation, especially if it is compromised by hypoxia, but this needs to be explored further.

DATA AVAILABILITY STATEMENT

The raw data supporting the conclusions of this article will be made available by the authors, without undue reservation.

ETHICS STATEMENT

The studies involving human participants were reviewed and approved by the Komisija za medicinsko etiko, Ministrstvo za zdravje. The patients/participants provided their written informed consent to participate in this study.

AUTHOR CONTRIBUTIONS

IBM, OE, and IAM conceived and designed the study. Together with MA, ES, and RK conducted the studies, analyzed, and interpreted the results. IBM and MA drafted the manuscript. ES, RK, OE, and IAM critically revised the manuscript. All authors approved the final version of the manuscript and agreed to be accountable for all aspects of the work in ensuring that questions related to the accuracy or integrity of any part of the work are appropriately investigated and resolved. All persons designated as authors qualify for authorship, and all those who qualify for authorship are listed.

FUNDING

This study was supported, in part, by a grant from the Slovene Research Agency (ARRS Programme Grant No. P2-0076) to IBM. MA was recipient of a postgraduate scholarship from the Slovene Technological Agency; the scholarship was financed, in part, by the European Union "European Social Fund."

ACKNOWLEDGMENTS

We would like to thank all the subjects for their diligence and positive attitude during this study. We express our appreciation to the laboratory research group and research technicians of University of Nottingham whose collaboration made this enormous biochemical laboratory work possible and especially to Sally Cordon for her help. We thank to Miro Vrhovec for outstanding technical assistance.

REFERENCES

Adrian, T. E., Ferri, G. L., Bacarese-Hamilton, A. J., Fuessl, H. S., Polak, J. M., and Bloom, S. R. (1985). Human distribution and release of a putative new gut hormone, peptide YY. *Gastroenterology* 89, 1070–1077. doi: 10.1016/0016-5085(85)90211-2

Armellini, F., Zamboni, M., Robbi, R., Todesco, T., Bissoli, L., Mino, A., et al. (1997). The effects of high altitude trekking on body composition and resting metabolic rate. *Horm. Metab. Res.* 1997, 458–461. doi: 10.1055/s-2007-979077

Batterham, R. L., Cowley, M. A., Small, C. J., Herzog, H., Cohen, M. A., Dakin, C. L., et al. (2002). Gut hormone PYY(3-36) physiologically inhibits food intake. *Nature* 418, 650–654. doi: 10.1152/ajpregu.00674.2005

Boyer, S. J., and Blume, F. D. (1984). Weight loss and changes in body composition at high altitude. *J. Appl. Physiol.* 57, 1580–1585. doi: 10.1152/jappl.1984.57.5.1580

Braun, B., Rock, P. B., Zamudio, S., Wolfel, G. E., Mazzeo, R. S., Muza, S. R., et al. (2001). Women at altitude: short-term exposure to hypoxia and/or alpha(1)-adrenergic blockade reduces insulin sensitivity. *J. Appl. Physiol.* 91, 623–631. doi: 10.1152/jappl.2001.91.2.623

Butterfield, G. E., Gates, J., Fleming, S., Brooks, G. A., Sutton, J. R., and Reeves, J. T. (1992). Increased energy intake minimizes weight loss in men at high altitude. *J. Appl. Physiol.* 72, 1741–1748. doi: 10.1152/jappl.1992.72.5.1741

Chiodi, H. (1957). Respiratory adaptations to chronic high altitude hypoxia. *J. Appl. Physiol.* 10, 81–87. doi: 10.1152/jappl.1957.10.1.81

Consolazio, C. F., Matoush, L. O., Johnson, H. L., Krzywicki, H. J., Isaac, G. J., and Witt, N. F. (1968). Metabolic aspects of calorie restriction: hypohydration effects on body weight and blood parameters. *Am. J. Clin. Nutr.* 21, 793–802. doi: 10.1093/ajcn/21.8.793

Cummings, D. E., and Overduin, J. (2007). Gastrointestinal regulation of food intake. *J. Clin. Invest.* 117, 13–23. doi: 10.1172/JCI30227

Durnin, J. V., and Brockway, J. M. (1959). Determination of the total daily energy expenditure in man by indirect calorimetry: assessment of the accuracy of a modern technique. *Br. J. Nutr.* 13, 41–53. doi: 10.1079/bjn19590007

Evetts, G., Hartley, A., Keane, S., Keegan, J., Simpson, A., Taylor, A., et al. (2005). "A comparison of acute hypoxia induced by low concentrations of oxygen at ground level, 10,000 feet and by air at 25,000 feet. Implications for military aircrew training," in *Proceedings of the SAFE Europe2005 Symposium*, (Henlow: Kings College Aerospace Medicine Group).

Forster, C. D., and Macdonald, I. A. (1998). The assay of cathecolamine content of small volumes of human plasma. *Biomed. Chromatogr.* 12, 209–215. doi: 10.1002/(sici)1099-0801(199905)13:3<209::aid-bmc820>3.0.co;2-z

Fusch, C., Gfrörer, W., Koch, C., Thomas, A., Grünert, A., and Moeller, H. (1996). Water turnover and body composition during long-term exposure to high altitude (4,900-7,600 m). *J. Appl. Physiol.* 80, 1118–1125. doi: 10.1152/jappl.1996.80.4.1118

Ge, R. L., Wood, H., Yang, H. H., Liu, Y. N., Wang, X. J., and Babb, T. (2010). The body weight loss during acute exposure to high-altitude hypoxia in sea level residents. *Sheng Li Xue Bao* 62, 541–546.

Gill, M. B., and Pugh, L. G. (1964). Basal metabolism and respiration in men living at 5.800 m (19.000 ft). *J. Appl. Physiol.* 19, 949–954. doi: 10.1152/jappl.1964.19.5.949

Grover, R. F. (1963). Basal oxygen uptake of man at high altitude. *J. Appl. Physiol.* 18, 909–912. doi: 10.1152/jappl.1963.18.5.909

Gunga, H. C., Fries, D., Humpeler, E., Kirsch, K., Boldt, L. E., Koralewski, E., et al. (2003). Austrian Moderate Altitude Study (AMAS 2000) - fluid shifts, erythropoiesis, and angiogenesis in patients with metabolic syndrome at moderate altitude (congruent with 1700 m). *Eur. J. Appl. Physiol.* 88, 497–505. doi: 10.1007/s00421-002-0734-x

Guzik, T. J., Mangalat, D., and Korbut, R. (2006). Adipocytokines - novel link between inflammation and vascular function? *J. Physiol. Pharmacol.* 57, 505–528.

Hackett, P. H., and Oelz, O. (1992). "The Lake Louise Consensus on the definition and quantification of altitude illness," in *Hypoxia and Mountain Medicine*, eds J. R. Sutton, C. S. Houston, and G. Coates (Burlington, VT: Queen City Press), 327–330.

Hannon, J. P., and Sudman, D. M. (1973). Basal metabolic and cardiovascular function of women during altitude acclimatization. *J. Appl. Physiol.* 34, 471–477. doi: 10.1152/jappl.1973.34.4.471

Haufe, S., Wiesner, S., Engeli, S., Luft, F. C., and Jordan, J. (2008). Influences of normobaric hypoxia training on metabolic risk markers in human subjects. *Med. Sci. Sports Exerc.* 40, 1939–1944. doi: 10.1249/MSS.0b013e31817f1988

Hudon, C., Soubhi, H., and Fortin, M. (2008). Relationship between multimorbidity and physical activity: secondary analysis from the Quebec health survey. *BMC Public Health* 8:304. doi: 10.1186/1471-2458-8-304

Hussain, S. S., and Bloom, S. R. (2013). The regulation of food intake by the gut-brain axis: implications for obesity. *Int. J. Obesity* 37, 625–633. doi: 10.1038/ijo.2012.93

Jakicic, J., Clark, K., Coleman, E., Donnelly, J., Foreyt, J., Melanson, E., et al. (2001). Appropriate intervention strategies for weight loss and prevention of weight regain for adults. *Med. Sci. Sports Exerc.* 33, 2145–2156. doi: 10.1097/00005768-200112000-00026

Kalson, N. S., Hext, F., Davies, A. J., Chan, C. W., Wright, A. D., and Imray, C. H. (2010). Do changes in gastro-intestinal blood flow explain high altitude anorexia? *Eur. J. Clin. Invest.* 40, 735–741. doi: 10.1111/j.1365-2362.2010.02324.x

Karra, E., Chandarana, K., and Batterham, R. I. (2009). The role of peptide YY in apetite regulation and obesity. *J. Physiol.* 587, 19–25. doi: 10.1113/jphysiol.2008.164269

Kayser, B., and Verges, S. (2013). Hypoxia, energy balance and obesity: from pathophysiological mechanisms to new treatment strategies. *Obes. Rev.* 14, 579–592. doi: 10.1111/obr.12034

Klausen, K. (1966). Man's acclimatization to altitude during the first week at 3.800 m. *Schweiz Z. Sportmed.* 1966, 246–253.

Konturek, S. J., Konturek, J. W., Pawlik, T., and Brzozowski, T. (2004). Brain-gut axis and its role in the control of food intake. *J. Physiol. Pharmacol.* 55, 137–154.

Krzywicki, H. J., Consolazio, C. F., Matoush, L. O., Johnson, H. L., and Barnhart, R. A. (1969). Body composition changes during exposure to altitude. *Fed. Proc.* 28, 1190–1194.

Larsen, J. J., Hansen, J. M., Olsen, N. V., Galbo, H., and Dela, F. (1997). The effect of altitude hypoxia on glucose homeostasis in men. *J. Physiol.* 504, 241–249. doi: 10.1111/j.1469-7793.1997.241bf.x

Lippl, F. J., Neubauer, S., Schipfer, S., Lichter, N., Tufman, A., Otto, B., et al. (2010). Hypobaric hypoxia causes body weight reduction in obese subjects. *Obesity (Silver Spring)* 18, 675–681. doi: 10.1038/oby.2009.509

Loshbaugh, J. E., Loeppky, J. A., and Greene, E. R. (2006). Effects of acute hypobaric hypoxia on resting and postprandial superior mesenteric artery blood flow. *High Alt. Med. Biol.* 7, 47–53. doi: 10.1089/ham.2006.7.47

Louis, M., and Punjabi, N. M. (2009). Effects of acute intermittent hypoxia on glucose metabolism in awake healthy volunteers. *J. Appl. Physiol.* 106, 1538–1544. doi: 10.1152/japplphysiol.91523.2008

Mackenzie, R., Maxwell, N., Castle, P., Brickley, G., and Watt, P. (2011). Acute hypoxia and exercise improve insulin sensitivity (S(I) (2*)) in individuals with type 2 diabetes. *Diabetes Metab. Res. Rev.* 27, 94–101. doi: 10.2165/00007256-200838010-00001

Matthews, D. R., Hosker, J. P., Rudenski, A. S., Naylor, B. A., Treacher, D. F., and Turner, R. C. (1985). Homeostasis model assessment: insulin resistance and

beta-cell function from fasting plasma glucose and insulin concentrations in man. *Diabetologia* 28, 412–419. doi: 10.1007/BF00280883

Matu, J., Deighton, K., Ispoglou, T., and Duckworth, L. (2017). The effect of moderate versus severe simulated altitude on apetite, gut hormones, energy intake and substrate oxidation in men. *Appetite* 113, 284–292. doi: 10.1016/j.appet.2017.02.041

Meier, U., and Gressner, A. M. (2004). Endocrine regulation of energy metabolism: review of pathobiochemical and clinical chemical aspects of leptin, ghrelin, adiponectin, and resistin. *Clin. Chem.* 50, 1511–1525. doi: 10.1373/clinchem.2004.032482

Mekjavic, I. B., Amon, M., Kolegard, R., Stylianos, N., Kounalakis, S. N., Simpson, L., et al. (2016). The effect of normobaric hypoxic confinement on metabolism, gut hormones, and body composition. *Front. Physiol.* 7:202. doi: 10.3389/fphys.2016.00202

Milledge, J. S. (1972). Arterial oxygen desaturation and intestinal absorption of xylose. *Br. Med. J.* 2, 557–558. doi: 10.1136/bmj.3.5826.557

Murphy, K. G., and Bloom, S. R. (2004). Gut hormones in the control of appetite. *Exp. Physiol.* 89, 507–516. doi: 10.1113/expphysiol.2004.027789

Netzer, N. C., Chytra, R., and Küpper, T. (2008). Low intense physical exercise in normobaric hypoxia leads to more weight loss in obese people than low intense physical exercise in normobaric sham hypoxia. *Sleep Breath* 12, 129–134. doi: 10.1007/s11325-007-0149-3

Picon-Reategui, E. (1961). Basal metabolic rate and body composition at high altitudes. *J. Appl. Physiol.* 16, 431–434. doi: 10.1152/jappl.1961.16.3.431

Poirier, P., and Després, J. P. (2001). Exercise in weight management of obesity. *Cardiol. Clin.* 19, 459–479.

Pouteau, E., Maugere, P., Darmaun, D., Marchini, J. S., Piloquet, H., Dumon, H., et al. (1998). Role of glucose and glutamine synthesis in the differential recovery of 13CO2 from infused (2-13C) versus (1-13C) acetate. *Metabolism* 47, 549–554. doi: 10.1016/s0026-0495(98)90238-4

Pugh, L. G. C. (1954). Himalayan rations with special reference to the 1953 expedition to Mount Everest. *Proc. Nutr. Soc.* 13, 60–69. doi: 10.1079/pns19540017

Pulfrey, S. M., and Jones, P. J. (1996). Energy expenditure and requirement while climbing above 6,000 m. *J. Appl. Physiol.* 81, 1306–1311. doi: 10.1152/jappl.1996.81.3.1306

Ramires, B. R., de Oliveira, E. P., Pimentel, G. D., Portero-McLellan, K. C., Nakato, D. M., Faganello, M. M., et al. (2012). Resting energy expenditure and carbohydrate oxidation are higher in elderly patients with COPD: a case control study. *Nutr. J.* 11:37. doi: 10.1186/1475-2891-11-37

Reinke, C., Bevans-Fonti, S., Drager, L. F., Shin, M. K., and Polotsky, V. Y. (2011). Effects of different acute hypoxic regimens on tissue oxygen profiles and metabolic outcomes. *J. Appl. Physiol.* 111, 881–890. doi: 10.1152/japplphysiol.00492.2011

Reynolds, R. D., Lickteig, J. A., Deuster, P. A., Howard, M. P., Conway, J. M., Pietersma, A., et al. (1999). Energy metabolism increases and regional body fat decreases while regional muscle mass is spared in humans climbing Mt. Everest. *J. Nutr.* 129, 1307–1314. doi: 10.1093/jn/129.7.1307

Richard, N. A., and Koehle, M. S. (2012). Differences in cardio-ventilatory responses to hypobaric and normobaric hypoxia: a review. *Aviat. Space Environ. Med.* 83, 677–684. doi: 10.3357/asem.3182.2012

Rose, M. S., Houston, C. S., Fulco, C. S., Coates, G., Sutton, J. R., and Cymerman, A. (1988). Operation Everest. II: nutrition and body composition. *J. Appl. Physiol.* 65, 2545–2551. doi: 10.1152/jappl.1988.65.6.2545

Rosická, M., Krsek, M., Matoulek, M., Jarkovská, Z., Marek, J., Justová, V., et al. (2003). Serum ghrelin levels in obese patients: the relationship to serum leptin levels and soluble leptin receptors levels. *Physiol. Res.* 52, 61–66.

Roza, A. M., and Shizgal, H. M. (1984). The Harris Benedict equation reevaluated: resting energy requirements and the body cell mass. *Am. J. Clin. Nutr.* 40, 168–182. doi: 10.1093/ajcn/40.1.168

Sepple, C. P., and Read, N. W. (1989). Gastrointestinal correlates of the development of hunger in man. *Appetite* 13, 183–191. doi: 10.1016/0195-6663(89)90011-1

Sergi, G., Coin, A., Marin, S., Vianello, A., Manzan, A., Peruzza, S., et al. (2006). Body composition and resting energy expenditure in elderly male patients with chronic obstructive pulmonary disease. *Respir. Med.* 100, 1918–1924. doi: 10.1016/j.rmed.2006.03.008

Stickney, J. C., and Van Liere, E. J. (1953). Acclimatization to low oxygen tension. *Physiol. Rev.* 33, 13–34. doi: 10.1152/physrev.1953.33.1.13

Stubbs, R. J., Hughes, D. A., Johnstone, A. M., Rowley, E., Reid, C., Elia, M., et al. (2000). The use of visual analogue scales to assess motivation to eat in human subjects: a review of their reliability and validity with an evaluation of new hand-held computerized systems for temporal tracking of appetite ratings. *Br. J. Nutr.* 84, 405–415. doi: 10.1017/S0007114500001719

Surks, M. I., Chinn, K. S., and Matoush, L. R. (1966). Alterations in body composition in man after acute exposure to high altitude. *J. Appl. Physiol.* 21, 1741–1746. doi: 10.1152/jappl.1966.21.6.1741

Trayhurn, P., and Wood, I. S. (2004). Adipokines: inflammation and the pleiotropic role of white adipose tissue. *Br. J. Nutr.* 92, 347–355. doi: 10.1017/S0007114508971282

Vasconcelos, F. C., Mota, E., da, S., Lopes, M. F., de, L., Fernandes, S., et al. (2002). Medeiros, Zilanda Lameira de. Terapia nutricional na doença pulmonar obstrutiva crônica associada à desnutrição protéico-calórica: artigo de revisão. *Rev. Para. Med.* 16, 47–52.

Wandrag, L., Siervo, M., Riley, H. L., Khosravi, M., Fernandez, B. O., Leckstrom, C. A., et al. (2017). Does hypoxia play a role in the development of sarcopenia in humans? Mechanistic insights from the Caldwell Xtreme Everest Expedition. *Redox Biol.* 13, 60–68. doi: 10.1016/j.redox.2017.05.004

Wasse, L. K., Sunderland, C., King, J. A., Batterham, R. L., and Stensel, D. J. (2012). The influence of rest and exercise at a simulated altitude of 4000 m on appetite, energy intake and plasma concentrations of acylated ghrelin and peptide YY. *J. Appl. Physiol.* 112, 552–559. doi: 10.1152/japplphysiol.00090.2011

Webber, J., and Macdonald, I. A. (2000). Signalling in body-weight homeostasis: neuroendocrine efferent signals. *Proc. Nutr. Soc.* 59, 397–404. doi: 10.1017/S0029665100000446

Westerterp, K. R. (2001). Energy and water balance at high altitude. *News Physiol. Sci.* 16, 134–137. doi: 10.1152/physiologyonline.2001.16.3.134

Westerterp, K. R., Kayser, B., Brouns, F., Herry, J. P., and Saris, W. H. (1992). Energy expenditure climbing Mt. Everest. *J. Appl. Physiol.* 73, 1815–1819. doi: 10.1152/jappl.1992.73.5.1815

Westerterp, K. R., Kayser, B., Wouters, L., Le Trong, J. L., and Richalet, J. P. (1994). Energy balance at high altitude of 6,542 m. *J. Appl. Physiol.* 77, 862–866. doi: 10.1152/jappl.1994.77.2.862

Westerterp, K. R., Meijer, E. P., Rubbens, M., Robach, P., and Richalet, J. P. (2000). Operation Everest III: energy and water balance. *Pflugers Arch.* 439, 483–488. doi: 10.1007/s004249900203

Westerterp-Plantenga, M. S., Westerterp, K. R., Rubbens, M., Verwegen, C. R., Richalet, J. P., and Gardette, B. (1999). Appetite at "high altitude" [Operation Everest III (Comex-.'97)]: a simulated ascent of Mount Everest. *J. Appl. Physiol.* 87, 391–399. doi: 10.1152/jappl.1999.87.1.391

Wiesner, S., Haufe, S., Engeli, S., Mutschler, H., Haas, U., Luft, F. C., et al. (2010). Influences of normobaric hypoxia training on physical fitness and metabolic risk markers in overweight to obese subjects. *Obesity* 18, 116–120. doi: 10.1038/oby.2009.193

Conflict of Interest: The authors declare that the research was conducted in the absence of any commercial or financial relationships that could be construed as a potential conflict of interest.

Publisher's Note: All claims expressed in this article are solely those of the authors and do not necessarily represent those of their affiliated organizations, or those of the publisher, the editors and the reviewers. Any product that may be evaluated in this article, or claim that may be made by its manufacturer, is not guaranteed or endorsed by the publisher.

Copyright © 2022 Mekjavic, Amon, Simpson, Kölegård, Eiken and Macdonald. This is an open-access article distributed under the terms of the Creative Commons Attribution License (CC BY). The use, distribution or reproduction in other forums is permitted, provided the original author(s) and the copyright owner(s) are credited and that the original publication in this journal is cited, in accordance with accepted academic practice. No use, distribution or reproduction is permitted which does not comply with these terms.

frontiers in Physiology

ORIGINAL RESEARCH
published: 28 March 2022
doi: 10.3389/fphys.2022.832172

The eEgg: Evaluation of a New Device to Measure Pain

Dshamilja M. Böing-Meßing[1], Fabian Tomschi[1], Thomas Cegla[2] and Thomas Hilberg[1]**

[1]Department of Sports Medicine, University of Wuppertal, Wuppertal, Germany, [2]Department of Pain Medicine, Helios Klinikum Wuppertal, Wuppertal, Germany

Aim: The aim of this study was to evaluate whether pain stimuli can be measured validly and reliably by the eEgg (electronic Egg), a new device to measure pain intensity, in comparison to the hand dynamometer.

Methods: This study consists of screening and diagnostic tests conforming to the standard criterion of handgrip strength measurement. Fifty healthy participants (25 women, 25 men; age, 39.1 ± 13.7 years) participated in this study. The approach of intermodal comparison was used to transfer different degrees of pain sensations into measurable handgrip strength values. This included an intensity comparison of 10-100% of the subjective maximum handgrip strength and an application of thermal stimuli of 34-48°C. The eEgg was compared to the numeric rating scale (NRS) as a categorization method regarding the subjective assessment of pain. An online questionnaire was distributed to test the evaluation of the product's features.

Results: Regarding the experiment's validity, the handgrip strength values showed significant ($p < 0.05$) positive correlations between the eEgg and the hand dynamometer (intensities: r=0.328 to r=0.550; thermal stimuli: r=0.353 to r=0.614). The reliability results showed good to very good correlations ($p < 0.05$) in the calculated ICC (intraclass correlation coefficient) values between the individual measurement devices: eEgg intensities: ICC=0.621 to 0.851; thermal stimuli: ICC=0.487 to 0.776 and hand dynamometer intensities: ICC= 0.789 to 0.974; thermal stimuli: ICC=0.716 to 0.910.

Conclusion: The new eEgg device shows strong correlations with the hand dynamometer. The central limitation focuses on the obligatory use of an arbitrary unit (AU) for the eEgg. The results of the study indicate that this device can be used in medical and therapeutic practice in the future.

Keywords: handgrip, pain, intermodal comparison, dynamometer, clinical applicability, cross-modality matching

OPEN ACCESS

Edited by:
Claudio Lucia,
Scientific Clinical Institute Maugeri, Italy

Reviewed by:
Alfonso Javier Ibáñez-Vera,
University of Jaén, Spain
Gorm Henrik Fogh Rasmussen,
Aalborg University, Denmark

****Correspondence:***
Dshamilja M. Böing-Meßing
dshamilja.boeing-messing-hk@uni-wuppertal.de
Thomas Hilberg
hilberg@uni-wuppertal.de

Specialty section:
This article was submitted to Physio-logging, a section of the journal Frontiers in Physiology

Received: *14 December 2021*
Accepted: *07 March 2022*
Published: *28 March 2022*

Citation:
Böing-Meßing DM, Tomschi F, Cegla T and Hilberg T (2022) The eEgg: Evaluation of a New Device to Measure Pain. Front. Physiol. 13:832172. doi: 10.3389/fphys.2022.832172

INTRODUCTION

The measurement of pain is essential for pain management, which is of major importance for research on and therapy of acute and chronic pain. Especially the transfer of the highly individual pain perception to numerical values presents a measurement difficulty in clinical practice and the measurement of pain intensity and pain perception is a particular challenge (Fillingim et al., 2016; Manworren and Stinson, 2016; Darbari and Brandow, 2017). Most methods for pain measurement are relying on its subjective

evaluation, e.g., the numeric rating scale (NRS) or the visual rating scale (VAS) (Bijur et al., 2003; Williamson and Hoggart, 2005). Further methods, such as pressure pain or heat thresholds, can be used by applying experimental pain stimuli to measure pain sensitivity. In the case of pressure pain thresholds, mechanical stimuli are usually applied *via* pressure algometers by which pressure is applied to a certain body site of the individual with increasing pressure. The individual then states verbally when the pressure exerted becomes painful for the first time. Thus, pain thresholds can be determined, and the pressure applied can be read out in Newton and pain can be measured in a semi-objective manner (Hansen, 1997; Krüger et al., 2021; Luedi et al., 2021). Another method that can be used to evaluate pain is to ask the individual to translate his/her current pain state into another sensory modality, e.g., handgrip strength (Rowbotham, 2001). This method of pain assessment is founded on the theory of intermodal comparison. This theory describes by which means the intensity of pain (usually point prevalence) can be translated into another sensory modality. Subjectively perceived pain is thereby expressed *via* the hand force exerted on a separate device, e.g., the hand dynamometer (HD) (Schandry and Beltz, 2016). Thus, the subjectively experienced pain can be read out in Newton and the individual's pain is measured semi-objectively. This principle is also known as cross-modality matching (Seidel et al., 1988). Hence, diverse types of pain can be evaluated using the intermodal comparison, e.g., headache, post-operative pain etc., making this method usable in different contexts. The HD is the standard device for the measurement of handgrip strength showing high reliability and validity (Güclüöver et al., 2015; Paramasivan et al., 2019). The HD was also used in previous research that employed the intermodal comparison principle to evaluate pain (Gracely et al., 1978).

Based on these considerations new devices are to be developed to evaluate the individual's current pain state by asking the individuals to express their current pain state *via* pressing an external device. To the best of our knowledge, the above-mentioned procedure is today only employed by using a HD. The HD was developed to measure handgrip strength and not for the purpose of the intermodal comparison. Hence, the pain measurement device "eEgg" was developed to make use of this procedure and to allow a semi-objective measurement of pain. The eEgg is presented in the study presented herein for the first time and the study aimed to evaluate whether experimental pain stimuli can be measured validly and reliably using the eEgg. Based on these considerations, the following hypotheses were stated: 1) the eEgg is a reliable and valid device to measure experimental pain stimuli of different intensities. 2) The eEgg and the NRS are comparable according to semi-objective and subjective criteria regarding experimental pain stimuli. 3) The eEgg is a feasible and well accepted tool to measure pain in practical use.

METHODS

Ethics

The study and the used protocols were approved by the ethics committee of the University of Wuppertal at the 16th of May 2019. These protocols are in line with the Declaration of Helsinki. Participants gave written informed consent to participate in the study and were verbally instructed about the procedures conducted in this study.

TABLE 1 | Anthropometric data of the participants. Data are presented as means ± standard deviation (Range).

Variables mean ± SD (min-max)		
Sex	male (N = 25)	female (N = 25)
Age [years]	39.8 ± 13.9 (23–61)	38.4 ± 13.8 (23–62)
Height [cm]	181.8 ± 8.0 (165–196)	169.2 ± 5.0 (162–183)
Weight [kg]	80.8 ± 10.5 (60–97)	72.0 ± 14.1 (57–103)

Participants

The sample size was calculated a priori *via* G*Power (Version 3.1.9.4) for an assumed moderate correlation between the eEgg and the HD and an alpha-error probability of 0.05 and a power of 0.80 was assumed. This resulted in a sample size of at least 46 subjects. Considering possible dropouts, 50 healthy volunteers participated in the study (**Table 1**). No participants were excluded from the study. The age distribution was as follows: 20–28 (N = 16/7♂ 9♀), 29–38 (N = 11/6♂ 5♀), 39–48 (N = 8/4♂ 4♀), and 49–65 (N = 15/8♂ 7♀). All participants completed the first experimental test and the online questionnaire. Yet, one participant did not conduct the second experimental test due to personal reasons and two other participants did not finish the online questionnaire.

Participants were considered eligible for inclusion if they were aged between 18 and 65 years. Participants were excluded if they suffered from any known neurological condition (e.g., multiple sclerosis), or disease that could limit hand function (e.g., carpal tunnel syndrome), reported any acute or chronic pain, or used pain medication regularly. In- and exclusion criteria regarding pain were assessed by the German PainDETECT© questionnaire (Freynhagen et al., 2006).

Study Design

The aim of the present study was to test the reliability (*via* a test-restest design) and validity (*via* the correlation to the HD as a standard) of the eEgg. Participants were asked to transfer the perceived pain sensation into handgrip strength applied to the eEgg and the HD, respectively. It was further elaborated, whether the semi-objective results of the eEgg can be compared with the subjective data from the NRS. Lastly, the acceptance and the evaluation of the product´s characteristics of the eEgg (e.g., egg size, egg hardness, and egg color) were assessed subsequently using an online questionnaire.

To do so, the study design consisted of three parts. In the first experimental test (see **Figure 1A**) the participants were asked to express 10–100% of their maximum handgrip strength in intervals in steps of 10% in a randomized order for both devices, i.e., with the eEgg (**Figures 2A,B**) and the lite hydraulic hand dynamometer 12-0241 (Baseline® USA; **Figure 2C**). Reference benchmarks were provided verbally with 100% of the handgrip strength being considered to be the

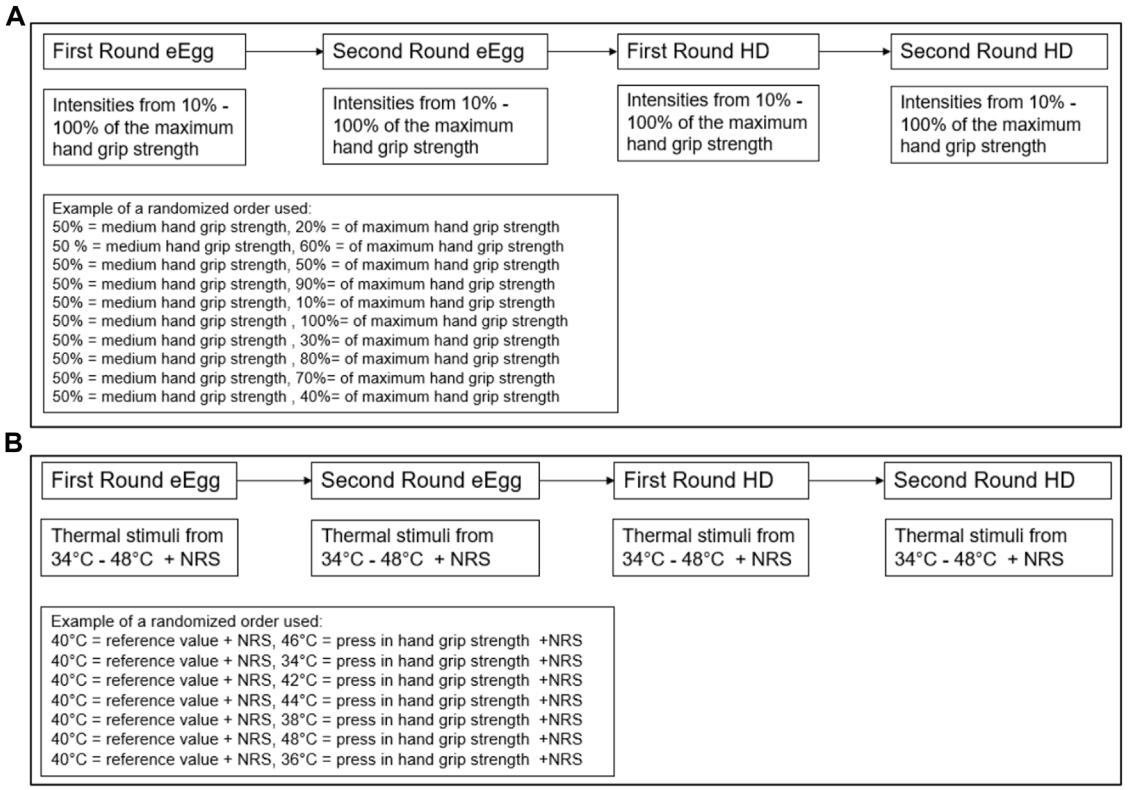

FIGURE 1 | Study design of the first **(A)** and second **(B)** experimental tests. The order of the devices used (eEgg or hand dynamometer) was randomized. *eEgg, electronic egg; HD, hand dynamometer.*

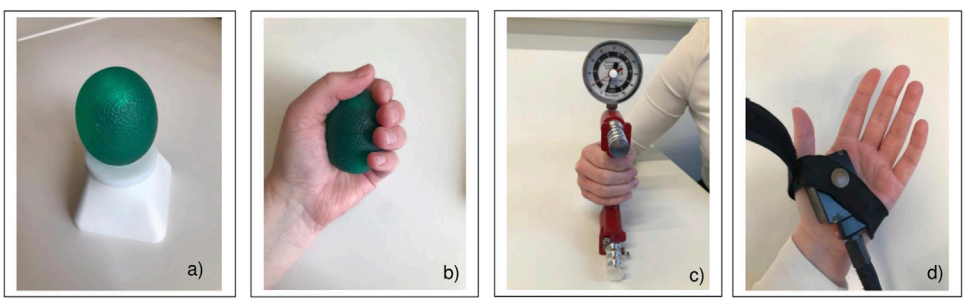

FIGURE 2 | (A) The eEgg (electronic egg) in its docking station. **(B)** The position of the eEgg during its application with pressure sensors inside. **(C)** The hand dynamometer and its position during its application. **(D)** The application of the thermal stimuli using the Thermo Sensory Analyzer positioned at the lower part of the palm.

maximum handgrip force that could possibly be applied to the eEgg and HD, respectively. Further, 50% of the handgrip strength was considered to resemble a firm handshake, and 0% was instructed as not pressing the devices but only holding them. The participants pressed a reference value of 50% every time before a new intensity was pressed. This test was conducted two times (first and second round) in a test-retest-design.

In the second experimental test (see **Figure 1B**), thermal stimuli of 34–48°C were applied. The participants expressed the perceived heat intensity as handgrip strength for each trial twice (first and second round) in a test-retest-design. Additionally, they indicated their sensation of pain resulting from the heat stimuli *via* a NRS. The participants pressed a reference value (40°C) every time before reacting to the next heat stimulus and between every thermal stimulus.

The order of the devices used in the first and second experimental tests was randomized. Randomization was conducted using a randomization generator (https://www.random.org/lists). The subjects were randomly assigned to the different groups. In the third part of this study, participants were

asked to fill out an online questionnaire to evaluate the eEgg characteristics, which can be found in **Supplementary Material S4**.

Material/Measurement

The eEgg (see **Figures 2A,B**) employs contact sensors to measure the pressure on the surface material. The three-dimensional pressure forces are recorded by several sensors, which are located in a sensor sleeve. This sensor sleeve has an elongated shape and is located in the centre of the eEgg. The sensors provide signals that are then bundled into a sum signal. This sum signal consists of all the average values of the individual sensors. The data from the sum signal are then transferred to device-related software (eEGG_V1.4) *via* Bluetooth and displayed in an Excel file. Via their graphic representation, the values of the respective manual pressure measurement of each run can be read out.

The values expressed by the eEgg do not possess a known physical measurement unit and the values are expressed in an arbitrary numerical unit (AU) based on a positive metric scale with higher values indicting higher applied pressure. The measured pressure is related to the individual base pressure. This basic pressure is created by the effect of the material on the sensors and the position of the eEgg in the hand. Meaning that different basic pressures can have an effect on the eEgg for each measurement (Bromm and Rottmann, 2018). Yet, this is later subtracted from the pressed values in the evaluation by the software.

In the second experimental test, thermal stimuli were applied to the heel of the hand (see **Figure 2D**) to induce a heat sensation using the Thermo Sensory Analyzer 2001-I (TSA, Medoc, Ramat Yishai, Israel). The baseline temperature was set to 32°C and lasted for 15 s and the temperature was increased by 1°C/s up to the final temperatures, e.g., 48°C, which lasted for 8 s.

After each trial, the pain perception was assessed using the NRS, which ranges from 0 (no pain)–100 (max. pain). The NRS represents a validated pain assessment tool (Williamson and Hoggart, 2005; Hjermstad et al., 2011; Alghadir et al., 2018).

Furthermore as the third part, the study design included an online questionnaire with 29 questions which were specifically designed to evaluate the acceptance and usability of the eEgg. The questions were formulated regarding the acceptance and the evaluation of the product´s features of the eEgg in practical use. Besides, questions concerning the comparison between the eEgg and the HD and regarding the future use of the eEgg were asked. The duration of the processing the questionnaire was approximately 10–15 min. The answers were designed in a Likert scale: 1 = *strongly disagree*; 2 = *disagree*; 3 = *neither agree or disagree*; 4 = *agree;* and 5 = *strongly agree* (see **Supplementary Material S4**).

Statistical Analysis

For statistical analysis, SPSS for Windows (Version 27.0; SPSS Inc., Chicago, IL, USA) was used. The Shapiro–Wilk test was used to test the normal distribution indicating mainly non-normal distributed data. Therefore, non-parametric tests were employed to conduct the statistical calculations.

Reliability was assessed in the first and second experimental test during the test-retest procedure by examining the intraclass correlation (ICC) values for the eEgg and HD, respectively. The ICC was interpreted according to Koo and Li, 2016. The ICC can be interpreted as: <0.50 "poor", 0.50–0.75 "fair", 0.75–0.90 "good," and 0.90–1.0 "excellent" (Koo and Li, 2016). Further, the standard error of measurement (SEM) was calculated using the following formula: $SEM = SD\sqrt{1-r}$ (Eliasziw et al., 1994).

The validity was determined by calculating the correlation coefficient between the eEgg and the HD in the first and second experimental test according to the rank correlation by Spearman. The correlation coefficient was interpreted according to (Cohen et al., 1988) (r = 0.10: low or weak correlation; r = 0.30: medium or moderate correlation; r = 0.50: large or strong correlation).

Handgrip strength values measured with the eEgg and HD, as well as NRS values, in response to thermal stimuli of the second experimental test are presented as means (± standard deviation). NRS values resulting from the thermal stimuli in the second experimental test were compared using the Mann-Whitney-U test. Handgrip values of the eEgg and HD of adjacent temperatures were compared using the Wilcoxon test within one device. Differences were considered to be significant with a *p*-value of <0.05. The program Limesurvey was used for the online questionnaire and the results are presented as percentages.

RESULTS

Results of the First Experimental Test—Intensity

With respect to the first reliability testing, data of the first and second run of the test-retest procedure of the eEgg are illustrated in **Figure 3A** and data of the eEgg and HD are presented in **Supplementary Material S1**. ICC values of the HD are higher than the eEgg's ICC values regarding the different intensities (see **Table 2** left). The ICC values of the HD range from 0.789 to 0.974, whereas the ICC values of the eEgg range from 0.621 to 0.851. The SEM values of the eEgg ranged from 129.0 to 308.7 and of the HD from 2.0 to 3.0 (see **Table 2** left).

Regarding validity testing, the values of the eEgg and the values of the HD show a positive correlation (range: r = 0.328 - r = 0.550) with respect to the different intensities representing a medium to strong effect when comparing the handgrip strength values from the intensity run of the eEgg and of the HD (see **Table 3**).

The results of the first experimental test show a similar increase of mean values of both the HD and the eEgg. The average maximum handgrip strength measured by the eEgg (AU) resulted in a mean of 1969.0 (±575.7). The average maximum handgrip strength of the HD (kg) resulted in a mean of 36.1 (±12.3). The handgrip strength values increased with growing intensities (see **Figure 4A** and **Supplementary Material S1** for data presentation).

Results of the Second Experimental Test - Temperature

Regarding the second reliability testing, data of the first and second run of the test-retest procedure of the eEgg are illustrated in **Figure 3B** and data of the eEgg and HD are presented in **Supplementary Material S2**. The ICC values at different

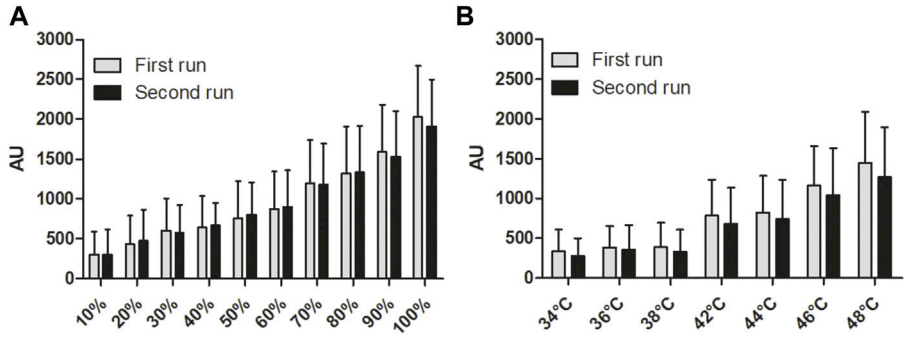

FIGURE 3 | Test-retest results of the eEgg. Handgrip strength values from the eEgg (AU) according to **(A)** different intensities and **(B)** different temperatures of the first and second run, respectively. Data are presented as mean values ± standard deviation. *eEgg, electronic egg.*

TABLE 2 | Test-retest-reliability—ICC and SEM values: average measurements, intensity and thermal stimuli.

Intensity	First Experimental Test–Intensity						Second Experimental Test–Temperature (°C)						
	eEgg			HD			Temperature	eEgg			HD		
	ICC	p	SEM	ICC	p	SEM		ICC	p	SEM	ICC	p	SEM
10%	0.777	<0.001	129.0	0.857	<0.001	2.1	34°C	0.532	0.004	142.5	0.834	<0.001	1.6
20%	0.748	<0.001	168.0	0.789	<0.001	2.6	36°C	0.667	<0.001	144.4	0.716	<0.001	2.2
30%	0.772	<0.001	163.9	0.902	<0.001	2.1	38°C	0.487	0.011	170.3	0.854	<0.001	1.5
40%	0.773	<0.001	166.9	0.877	<0.001	2.3	42°C	0.752	<0.001	204.0	0.820	<0.001	2.6
50%	0.721	<0.001	203.6	0.899	<0.001	2.4	44°C	0.725	<0.001	222.2	0.910	<0.001	2.3
60%	0.778	<0.001	196.0	0.875	<0.001	2.8	46°C	0.728	<0.001	252.2	0.854	<0.001	2.9
70%	0.741	<0.001	240.8	0.904	<0.001	2.4	48°C	0.776	<0.001	273.7	0.827	<0.001	3.7
80%	0.621	0.001	308.7	0.926	<0.001	2.9	—	—	—	—	—	—	—
90%	0.751	<0.001	260.1	0.927	<0.001	3.0	—	—	—	—	—	—	—
100%	0.851	<0.001	222.2	0.974	<0.001	2.0	—	—	—	—	—	—	—

HD, hand dynamometer; ICC, intraclass coefficient; SEM, standard error of measurement; p*-values are considered significant with* $p < 0.05$.

TABLE 3 | Correlation values of the handgrip strength values of the eEgg and the hand dynamometer.

Correlations Between eEgg and Hand Dynamometer					
First experimental test—intensity			Second experimental test - temperature		
Intensity	r	p	Temperature	r	p
10%	0.550	<0.001	34°C	0.478	<0.001
20%	0.328	0.020	36°C	0.353	0.013
30%	0.454	<0.001	38°C	0.557	<0.001
40%	0.494	<0.001	42°C	0.571	<0.001
50%	0.398	0.004	44°C	0.460	<0.001
60%	0.452	<0.001	46°C	0.449	0.001
70%	0.470	<0.001	48°C	0.614	<0.001
80%	0.372	0.008	—	—	—
90%	0.396	0.004	—	—	—
100%	0.368	0.008	—	—	—

r = correlations coefficient according to Spearman; p*-values are considered significant with* $p < 0.05$.

temperatures using the eEgg show a range from 0.487 to 0.776. The ICC values using the HD range from 0.716 to 0.910 (see **Table 2** right). In the second experimental test, the SEM values of the eEgg ranged from 142.5 to 273.7 and of the HD from 1.5 to 3.7 (see **Table 2** right).

With respect to validity testing, the correlations of the handgrip strength values between the eEgg and the HD after thermal stimuli show significant positive correlations ranging from r = 0.353 to r = 0.614 indicating a medium to strong correlation (see **Table 3**).

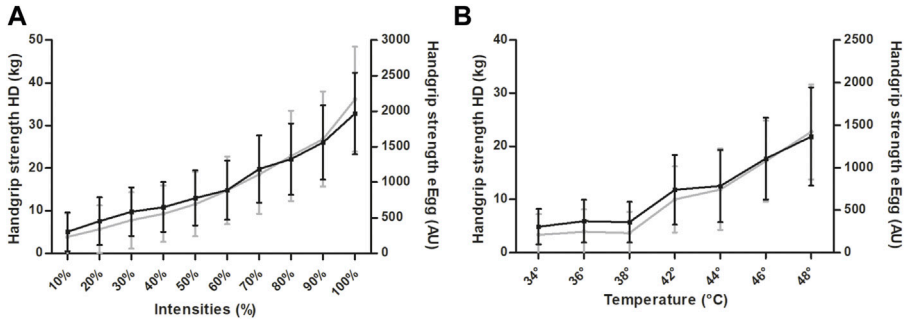

FIGURE 4 | Mean comparison of the handgrip strength values of the eEgg and the hand dynamometer (HD). **(A)** In response to intensities ranging from 10 to 100% of the maximum handgrip strength. **(B)** In response to thermal stimuli ranging from 34 to 48°C. Data are presented as mean ± standard deviation. Grey colour indicates hand dynamometer (HD); Black colour indicates eEgg. *eEgg, electronic egg.*

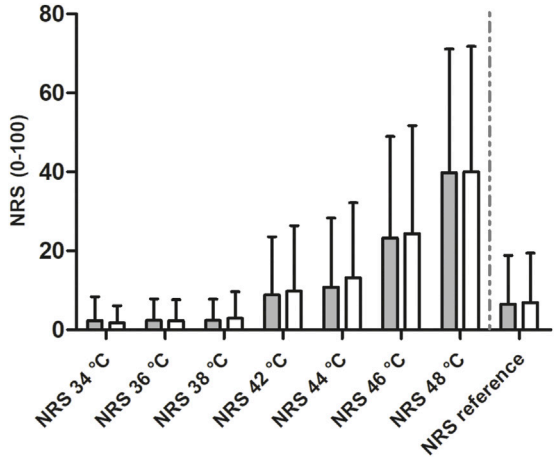

FIGURE 5 | Comparison of the NRS values resulting from thermal stimuli during the second experimental test employing the hand dynamometer (grey filling) and the eEgg (white filling), respectively. Data are presented as means ± standard deviation. No significant difference is observed between the NRS values. *NRS, Numerical Rating Scale; eEgg, electronic egg.*

The pain perception assessed by applying heat stimuli showed that the handgrip strength values of both devices follow the same trend and increased similarly (see **Figure 4B** and **Supplementary Material S2** for data presentation). Statistical analyses revealed that significant differences in the handgrip strengths between adjacent temperatures were observed between 34 and 36°C, 38 and 42°C, 44 and 46°C, as well as 46 and 48°C in the eEgg and between 34 and 36°C, 38 and 42°C, 42 and 44°C, 44 and 46°C, as well as 46 and 48°C in the HD.

When comparing the NRS values resulting from the heat stimuli in the run using the eEgg and the HD, respectively, results show that the NRS values do not differ between both runs, with $p > 0.05$ for all temperatures (see **Figure 5** and **Supplementary Material S3** for data presentation).

Results of the Online Questionnaire

The participants rated their first and final impression of the eEgg in grades from 1 (best) to 6 (worst). The average grade overall was two. Further results are presented in **Table 4**.

DISCUSSION

The hypotheses stated in the context of this study were threefold and summarizing the results regarding these hypotheses can be stated as follows: 1) it can be concluded that the eEgg presents different handgrip strengths, indicated as different percentages of the maximum handgrip strength and indicated as handgrip strength in response to different experimental heat stimuli, in a reliable manner with fair to good ICC values. With respect to validity testing, the study results show that the eEgg shows medium to large correlations with the HD. 2) it can be concluded that NRS responses, as a subjective measure, and handgrip responses using the eEgg, as a semi-objective measure, is similar. 3) it was shown that the eEgg is perceived as a pleasant and feasible device to measure pain in a semi-objective manner.

More specifically, a test-retest reliability in a fair to good correlation state was observed for the eEgg regarding the first experimental test regarding intensity and a fair to good correlation in the second experimental test regarding temperature. Both results indicate that the eEgg is reliable in a wide spectrum of handgrip intensities (10–100% of maximum handgrip strength) and, more importantly, in wide spectrum of experimental pain stimuli (34–48°C). Therefore, the eEgg seems to be a tool that is able to document differently intensive subjective pain states in a semi-objective manner. However, the handgrip strength values of the eEgg show overall lower ICC values than the ones obtained by the HD which is considered to be the gold standard for handgrip measurements, also in the context of intermodal comparisons (Gracely et al., 1978). The reliability of the values of the HD used in this study are in line with previous studies (Allen and Barnett, 2011; Güçlüöver et al., 2015; Paramasivan et al., 2019).

TABLE 4 | Selected results of the online questionnaire N = 48.

	1 = strongly Disagree (%)	2 = disagree (%)	3 = neither Agree or Disagree (%)	4 = agree (%)	5 = strongly Agree (%)
HD more comfortable	58.3	31.3	4.2	4.2	2.1
eEgg measures imprecisely	47.9	29.2	10.4	10.4	2.1
eEgg measures more precisely	0.0	4.2	18.8	39.6	37.5
Material comfortable	6.3	0.0	14.6	41.7	37.5
Position comfortable	4.2	4.2	14.6	35.4	41.7
Shape comfortable	2.1	2.1	4.2	37.5	54.2
Handling comfortable	2.1	2.1	12.5	41.7	41.7
Preference eEgg	2.1	8.3	12.5	39.6	37.5
NRS easier to express	35.4	33.3	18.8	10.4	2.1
eEgg easier to express	2.1	8.3	25.0	43.8	20.8
Future use	4.2	4.2	27.1	45.8	18.8

NRS, numerical rating scale; HD, hand dynamometer.

Further, this study demonstrated that the eEgg measures hand pressure intensities and thermal stimuli intensities in a valid manner compared to the HD as the gold standard. With respect to the first and second experimental tests the handgrip strengths measured correlated positively when using the eEgg and the HD indicating medium to large correlations in the first and second experimental tests. More specifically, this correlation was observed in the entire spectrum used in this study. I.e., significant positive correlations were observed for all intensity tests (10–100% of maximum handgrip strength) and for all temperatures, except for one temperature (36°C). This observation might be attributed to the impact of the ambient and human body temperature on pain sensation might have been an influencing factor (Strigo et al., 2000; Gekle and Singer, 2010; Obermeyer et al., 2017). The handgrip strength values (369.7 AU) pressed at 36°C are slightly higher than the handgrip strength values (357.1 AU) pressed at 38°C, though they are not significantly different. The handgrip strength values of the higher temperature ranges are more clearly distinguishable from each other. The thermal stimuli higher than 42°C were more clearly distinguishable by the participants no matter what device was used as adjacent temperatures showed significant differences. The temperatures of 34, 36, and 38°C are similar to the human body temperature and it is most likely difficult to feel the difference between the respective temperatures. Yet, significant differences in handgrip pressure were observed between the adjacent temperatures 34 and 36°C employing the eEgg indicating a good sensitivity. Yet, no such difference was observed between 36 and 38°C. This result was observed for the HD as well. Each individual possesses a different basic body temperature due to their gender, age, weight, and demographic conditions (Obermeyer et al., 2017). These results underline the difficulty of differentiating the values close to the body temperature by handgrip strength and might be one reason for the lack of a significant correlation between the eEgg and the HD observed at 36°C.

The NRS values represent a subjective pain rating by the individual (Bijur et al., 2003; Alghadir et al., 2018). NRS values recorded in the second experimental test demonstrated an increase with increasing temperatures, which was to be expected. This increase is also observed in the semi-objective values expressed by the Egg and it can be observed that higher subjective pain ratings *via* NRS go along with higher semi-objective values using the eEgg, as well as the HD. For the measurement of pain, the self-report by the patient is of crucial importance. Therefore, the NRS, and also the VAS, are the pain measurement tools, which are usually used in clinical practice (Haefeli and Elfering, 2006; Gélinas, 2016). In addition, in the context of sport sciences, various scales, above all the rate of perceived excretion (RPE) scale, are used to subjectively scale exertion, breathlessness, and fatigue usually during a standardized ergometer test (Williams, 2017). Moreover, various pain scales are also used to evaluate bodily and muscular pain (O'connor et al., 2000). One example is the CR 10 scale, which was initially developed to measure exertion as well as pain, e.g., muscular and/or exertional pain (Borg, 1998). The eEgg presents a new way to measure pain providing numerical readouts, which might also be used in the context of sports science and sport medicine.

In this study, participants of broad age range were included, and the age distribution might be biased towards the younger and older individuals. Yet, the influence of age on pain perception is mostly recognized when obtaining pain thresholds with higher pain thresholds observed in older people, which was not done in this study (Lautenbacher et al., 2017). Participants had to rate their perceived pain sensation on the NRS and employing the respective devices.

The results of the online questionnaire illustrate the participants' impression of the more precise and more comfortable use of the eEgg in comparison to the HD, which can be used to employ the principle of the intermodal comparison (Gracely et al., 1978). Influencing factors might be the soft surface material and the overall larger contact area of the hand with the eEgg. In contrast to the HD, the flexible material of the eEgg provides a pleasant feedback feeling. This could have led to a better-perceived assessment ability of the participants' handgrip strength.

Using the eEgg with a connected mobile application presents one development goal which might improve pain management in clinical settings in the future as more and more

measurement tools can be employed with apps and possess multiple digital features. Recent studies highlight the potential of these mobile digital apps for more accurate pain management (Zhao et al., 2019; Zheng et al., 2020). Due to the already existing digital data transmission *via* Bluetooth, the eEgg has the prerequisite to be connected to compatible apps and devices in the future.

Limitations

Pain is a subjective sensation that cannot be measured objectively. Therefore, the measurements made underly some kind of subjective variance that cannot be excluded. Yet, the eEgg provides numerical values that can be read out by clinicians and used to interpret the patient's pain providing a semi-objective evaluation. However, the major limitation of the eEgg is the missing standardised unit. Instead, an arbitrary unit is employed. Due to the fact that this is the first study presenting results of the eEgg, the obtained results cannot be compared to other studies or data. But, the development and calibration of a standardised measurement unit would allow a more decisive statistical analysis and an even more precise comparison between the eEgg and other devices, such as the HD, and the results presented herein present a starting point for future research and development.

CONCLUSION

The evaluation of the eEgg regarding reliability and validity shows that the eEgg is a reliable device to measure pain in a semi-objective manner with fair to good ICC values. Yet, the ICC values of the test-restest reliability testing are lower when using the eEgg compared to the HD. Validity testing by comparing the eEgg to the HD revealed medium to large correlations in both experimental tests conducted. It needs to be mentioned that the eEgg employs an arbitrary unit and the inclusion of a physical unit is suggested. The handling of the eEgg is perceived as more pleasant by the participants compared to the HD. The eEgg can be considered as an usable device for the measurement of pain that can be employed in further clinical and therapeutic settings.

DATA AVAILABILITY STATEMENT

The data that support the findings of this study are available from the corresponding author, DB-M, upon reasonable request.

ETHICS STATEMENT

The studies involving human participants were reviewed and approved by Ethics Committee of the University of Wuppertal. The participants provided their written informed consent to participate in this study.

AUTHOR CONTRIBUTIONS

The contributions of the authors were as follows: DB-M and TH had the original idea for the study. DB-M recruited the subjects and conducted the survey. TH, FT and TC supported DB-M in the data analysis. DB-M, FT, and TH wrote the manuscript. TC critically reviewed the manuscript. TH supervised the project.

FUNDING

The study was supported by the Department of Sports Medicine, University of Wuppertal.

SUPPLEMENTARY MATERIAL

The Supplementary Material for this article can be found online at: https://www.frontiersin.org/articles/10.3389/fphys.2022.832172/full#supplementary-material

REFERENCES

Alghadir, A., Anwer, S., Iqbal, A., and Iqbal, Z. (2018). Test–retest Reliability, Validity, and Minimum Detectable Change of Visual Analog, Numerical Rating, and Verbal Rating Scales for Measurement of Osteoarthritic Knee Pain. *Jpr* Vol. 11, 851–856. doi:10.2147/JPR.S158847

Allen, D., and Barnett, F. (2011). Reliability and Validity of an Electronic Dynamometer for Measuring Grip Strength. *Int. J. Ther. Rehabil.* 18, 258–264. doi:10.12968/ijtr.2011.18.5.258

Banzer, W., and Bürklein, M. (2004). "Funktionsdiagnostik des Bewegungssystems in der Sportmedizin," in *Funktionsdiagnostik des Bewegungssystems in der Sportmedizin*. Editors W. Banzer, K. Pfeifer, and L. Vogt (Springer-Verlag Berlin Heidelberg). doi:10.1007/978-3-642-18626-4

Bijur, P. E., Latimer, C. T., and Gallagher, E. J. (2003). Validation of a Verbally Administered Numerical Rating Scale of Acute Pain for Use in the Emergency Department. *Acad. Emerg. Med* 10 (4), 390–392. doi:10.1111/j.1553-2712.2003.tb01355.x

Borg, G. (1998). Borg's Perceived Exertion and Pain Scales. *Hum. kinetics*.

Bromm, B., and Rottmann, F. (2018). *Schmerzmessung mit Hilfe des eEGGs*.

Cohen, J., and Hillsdale, N. J. (1988). *Statistical Power Analysis for the Behavioral Sciences*. 2nd ed. L. Erlbaum Associates. doi:10.1016/C2013-0-10517-X

Darbari, D. S., and Brandow, A. M. (2017). Pain-measurement Tools in Sickle Cell Disease: where Are We Now? *Hematol. Am. Soc. Hematol. Edu. Program* 2017 (1), 534–541. doi:10.1182/asheducation-2017.1.534

Eliasziw, M., Young, S. L., Woodbury, M. G., and Fryday-Field, K. (1994). Statistical Methodology for the Concurrent Assessment of Interrater and Intrarater Reliability: Using Goniometric Measurements as an Example. *Phys. Ther.* 74 (8), 777–788. doi:10.1093/ptj/74.8.777

Fillingim, R. B., Loeser, J. D., Baron, R., and Edwards, R. R. (2016). Assessment of Chronic Pain: Domains, Methods, and Mechanisms. *The J. pain* 17 (9 Suppl. l), T10–T20. doi:10.1016/j.jpain.2015.08.010

Freynhagen, R., Baron, R., Gockel, U., and Tölle, T. R. (2006). painDETECT: a New Screening Questionnaire to Identify Neuropathic Components in Patients with Back Pain. *Curr. Med. Res. Opin.* 22 (10), 1911–1920. doi:10.1185/030079906X132488

Gekle, M., and Singer, D. (2010). "Temperaturregulation und Wärmehaushalt," in *Physiologie. Georg Thieme Verlag 8*. Editors H. C. Pape, A. Kurtz, and S. Silbernagl (unveränderte Auflage.

Gélinas, C. (2016). Pain Assessment in the Critically Ill Adult: Recent Evidence and New Trends. *Intensive Crit. Care Nurs.* 34, 1–11. doi:10.1016/j.iccn.2016.03.001

Gracely, R. H., McGrath, P., and Dubner, R. (1978). Validity and Sensitivity of Ratio Scales of Sensory and Affective Verbal Pain Descriptors: Manipulation of Affect by Diazepam. *Pain* 5 (1), 19–29. doi:10.1016/0304-3959(78)90021-0

Güçlüöver, A., Kutlu, M., Ciğerci, A. E., Esen, H. T., Demirkan, E., and Erdoğdu, M. (2015). Determination the Validity of the New Developed Sport Experts® Hand Grip Dynamometer, Measuring Continuity of Force, and Comparison with Current Takei and Baseline® Dynamometers. *The J. Sports Med. Phys. fitness* 55 (11), 1318–1321. PMID: 25289714Haefeli,.

Haefeli, M., and Elfering, A. (2006). Pain Assessment. *Eur. Spine J.* 15 (1), S17–S24.

Hansen, B. (1997). Through a Glass Darkly: Using Behavior to Assess Pain. *Semin. Vet. Med. Surg. Small Anim.* 12 (No. 2), 61–74. doi:10.1016/s1096-2867(97)80003-5

Hjermstad, M. J., Fayers, P. M., Haugen, D. F., Caraceni, A., Hanks, G. W., Loge, J. H., et al. (2011). Studies Comparing Numerical Rating Scales, Verbal Rating Scales, and Visual Analogue Scales for Assessment of Pain Intensity in Adults: a Systematic Literature Review. *J. Pain Symptom Manage.* 41 (6), 1073–1093. doi:10.1016/j.jpainsymman.2010.08.016

Koo, T. K., and Li, M. Y. (2016). A Guideline of Selecting and Reporting Intraclass Correlation Coefficients for Reliability Research. *J. chiropractic Med.* 15 (2), 155–163. doi:10.1016/j.jcm.2016.02.012

Krüger, S., Herzig, M., and Hilberg, T. (2021). Changes in Pain Profile of Patients with Haemophilia during 1-year Follow-up. *Haemophilia* 27 (5), 783–792.

Lautenbacher, S., Peters, J. H., Heesen, M., Scheel, J., and Kunz, M. (2017). Age Changes in Pain Perception: a Systematic-Review and Meta-Analysis of Age Effects on Pain and Tolerance Thresholds. *Neurosci. Biobehavioral Rev.* 75, 104–113. doi:10.1016/j.neubiorev.2017.01.039

Luedi, M. M., Schober, P., Hammoud, B., Andereggen, L., Hoenemann, C., and Doll, D. (2021). Preoperative Pressure Pain Threshold Is Associated with Postoperative Pain in Short-Stay Anorectal Surgery: a Prospective Observational Study. *Anesth. analgesia* 132 (3), 656–662. doi:10.1213/ane.0000000000005072

Manworren, R. C. B., and Stinson, J. (2016). Pediatric Pain Measurement, Assessment, and Evaluation. *Semin. Pediatr. Neurol.* 23 (3), 189–200. doi:10.1016/j.spen.2016.10.001

Nilges, P. (2006). "Klinische Schmerzmessung," in *Praktische Schmerztherapie*. Editors R. Baron and M. Strumpf (Springer-Verlag Berlin Heidelberg).

O'connor, P. J., Murphy, R. M., Courson, R. W., and Ferrara, M. S. (2000). Pain Assessment in Journal of Athletic Training Articles 1992-1998: Implications for Improving Research and Practice. *J. Athl Train.* 35 (2), 151–154.

Obermeyer, Z., Samra, J. K., and Mullainathan, S. (2017). Individual Differences in normal Body Temperature: Longitudinal Big Data Analysis of Patient Records. *BMJ* 359, j5468. Dec 13. doi:10.1136/bmj.j5468

Paramasivan, M., Kiruthigadevi, S., and Amal, K. F. (2019). Test-retest Reliability of Electronic Hand Dynamometer in Healthy Adults. *Int. J. Adv. Res.* 7, 325–331. doi:10.21474/IJAR01/9042

Rowbotham, M. C. (2001). What Is a 'clinically Meaningful' Reduction in Pain? *Pain* 94 (2), 131–132. doi:10.1016/s0304-3959(01)00371-2

Schandry, R., and Beltz, J. (2016). *Biologische Psychologie*. Weinheim Basel: Beltz.

Seidel, H., Harazin, B., Pavlas, K., Sroka, C., Richter, J., Blüthner, R., et al. (1988). Isolated and Combined Effects of Prolonged Exposures to Noise and Whole-Body Vibration on Hearing, Vision and Strain. *Int. Arch. Occup. Environ. Heath* 61, 95–106. doi:10.1007/bf00381613

Strigo, I. A., Carli, F., and Bushnell, M. C. (2000). Effect of Ambient Temperature on Human Pain and Temperature Perception. *Anesthesiology* 92 (3), 699–707. doi:10.1097/00000542-200003000-00014

Williams, N. (2017). The Borg Rating of Perceived Exertion (RPE) Scale. *Occup. Med.* 67 (5), 404–405. doi:10.1093/occmed/kqx063

Williamson, A., and Hoggart, B. (2005). Pain: a Review of Three Commonly Used Pain Rating Scales. *J. Clin. Nurs.* 14 (7), 798–804. doi:10.1111/j.1365-2702.2005.01121.x

Zhao, P., Yoo, I., Lancey, R., and Varghese, E. (2019). Mobile Applications for Pain Management: an App Analysis for Clinical Usage. *BMC Med. Inform. Decis. Mak* 19 (1), 106. doi:10.1186/s12911-019-0827-7

Zheng, C., Chen, X., Weng, L., Guo, L., Xu, H., Lin, M., et al. (2020). Benefits of Mobile Apps for Cancer Pain Management: Systematic Review. *JMIR Mhealth Uhealth* 8 (1), e17055. doi:10.2196/17055

Conflict of Interest: The authors declare that the research was conducted in the absence of any commercial or financial relationships that could be construed as a potential conflict of interest.

Publisher's Note: All claims expressed in this article are solely those of the authors and do not necessarily represent those of their affiliated organizations, or those of the publisher, the editors and the reviewers. Any product that may be evaluated in this article, or claim that may be made by its manufacturer, is not guaranteed or endorsed by the publisher.

Copyright © 2022 Böing-Meßing, Tomschi, Cegla and Hilberg. This is an open-access article distributed under the terms of the Creative Commons Attribution License (CC BY). The use, distribution or reproduction in other forums is permitted, provided the original author(s) and the copyright owner(s) are credited and that the original publication in this journal is cited, in accordance with accepted academic practice. No use, distribution or reproduction is permitted which does not comply with these terms.

frontiers | Frontiers in Physiology

ORIGINAL RESEARCH
published: 08 April 2022
doi: 10.3389/fphys.2022.834214

Estimations of Critical Clear Corneal Incisions Required for Lens Insertion in Cataract Surgery: A Mathematical Aspect

Nan Qi[1], David Lockington[2], Lei Wang[3], Kanna Ramaesh[2] and Xiaoyu Luo[4]*

[1]Institute of Marine Science and Technology, Shandong University, Qingdao, China, [2]Tennent Institute of Ophthalmology, Gartnavel General Hospital, Glasgow, United Kingdom, [3]Beijing National Center for Applied Mathematics, Academy for Multidisciplinary Studies, Capital Normal University Beijing, Beijing, China, [4]School of Mathematics and Statistics, University of Glasgow, Glasgow, United Kingdom

In a routine cataract operation cornea tissue may be damaged when an intra-ocular lens (IOL) injector of diameter between 1.467 and 2.011 mm is inserted through an empirically designed 2.2 mm corneal incision. We aimed to model and estimate the minimal length of the incision required to avoid wound tear. It was assumed that the damage was caused by tissue fracture at the tips of the incision, and this fracture could be studied using damage and fracture mechanics. The criterion of the damage was caused by a tear governed by the critical energy release rate (ERR) G_c, which is tissue dependent. Analytical and numerical studies were both conducted indicating the possibility of a safe and effective incision in cataract surgery. Six commonly used IOL injection systems were examined. Our results suggested that the recommended 2.2 mm incision cannot be treated as a universal threshold. Quicker IOL insertion may reduce wound damage. It was also recommended to advance IOL injector *via* its minor axis, and to cut the tear preferably along the circumferential direction due to tissue orthotropy. This study provides useful information and a deeper insight into the potential for mechanical damage to the corneal wound in cataract surgery.

Keywords: intra-ocular lens (IOL) injection system, tissue damage, energy release rate, linear fracture mechanics, finite element analysis

OPEN ACCESS

Edited by:
Yih-Kuen Jan, University of Illinois at Urbana-Champaign, United States

Reviewed by:
Ben-Yi Liau, Hungkuang University, Taiwan
Pu-Chun Mo, National Cheng Kung University, Taiwan
Shizuya Saika, Wakayama Medical University Hospital, Japan

****Correspondence:***
Nan Qi
Nan.Qi@sdu.edu.cn

Specialty section:
This article was submitted to Clinical and Translational Physiology, a section of the journal Frontiers in Physiology

Received: *13 December 2021*
Accepted: *16 March 2022*
Published: *08 April 2022*

Citation:
Qi N, Lockington D, Wang L, Ramaesh K and Luo X (2022) Estimations of Critical Clear Corneal Incisions Required for Lens Insertion in Cataract Surgery: A Mathematical Aspect. Front. Physiol. 13:834214. doi: 10.3389/fphys.2022.834214

1 INTRODUCTION

Advances in ocular surgical techniques have resulted in significant reductions in the dimensions of the surgical incisions required to extract the cataractous lens and replace it with an intra-ocular lens (IOL). These smaller wound developments have clinically contributed to safer surgery, with quicker procedures, faster recovery and minimal surgically induced astigmatism (Al Mahmood et al., 2014; Bernhisel and Pettey, 2020). The advent of foldable IOLs further encouraged smaller wound sizes. The most common size of IOL optic is a 6 mm diameter circle, with two legs (haptics) resulting in an approximate IOL length of 12 mm (Randleman and Lockwood, 2016). To deliver these foldable IOLs into eyes in a micro-incisional cataract surgery, an appropriate injector system (manual or pre-loaded) is required to permit safe insertion through a corneal wound (generally around 2.2 mm in length) (Nanavaty and Kubrak-Kisza, 2017; Kim et al., 2014; He et al., 2021; Zhang et al., 2022).

The manufacturers of these micro-incisional injector systems often claim that their device fits through a 2.2 mm incision, however, it is clinically common to experience significant tissue resistance during IOL delivery. To address this resistance, the surgeon has two options: either to twist and force the IOL through the wound (so called "wound-assisted"), or surgically widen it with a surgical keratome blade. Corneal incisions for intra-ocular surgery have long been associated with varying degrees of surgically induced astigmatism, so smaller incisions are preferable (Shepherd, 1989; Kim et al., 2014). However, the surgeon is trying to balance this against the potential for causing irregular forced tissue damage.

Previous studies have compared and investigated the relationship between various types of IOLs, injector systems, insertion techniques, insertion speeds and incision sizes (Ouchi, 2012; Kim et al., 2014; El Massry et al., 2016; Nanavaty and Kubrak-Kisza, 2017). Smaller incision sites may be more prone to corneal trauma, including microtears and tissue stretching (Matossian et al., 2015; Oshika and Wolfe, 2019). The internal wound stretch (the maximum post-IOL implantation wound size and percentage stretch) between 5 preloaded IOL systems and the implications on wound integrity have been previously investigated in porcine eyes (Nanavaty and Kubrak-Kisza, 2017).

Reliable wound construction is essential. If the corneal incision is inadequate in length and subjected to further stretching by surgical instrumentation or during forced insertion of the IOL, it is less likely to maintain its integrity, leak aqueous and be a potential reason for post-operative infection (El Massry et al., 2016). We wondered if a forced wound stretch is more likely to be incompetent due to tissue damage/fracture compared to a surgically sharp blade extended wound. We wished to identify the key factors affecting the wound stretch in order to make recommendations as to the optimum wound size for IOL insertion *via* commonly used IOL injectors.

In this study, a simplified analytical model is provided to investigate this clinical scenario, and its theory based on the concept of energy release rate in fracture mechanics is described, followed by a numerical finite element simulation, conducted in **Section 2**. In **Section 3**, results are presented with the dimensions of commonly used IOL injectors and followed by discussions and conclusions.

2 METHODS

2.1 Energy Release Rate

To find an optimal incision size that is adequate in length to avoid tissue stretching along the incision line due to injection and as small as possible to reduce its impact on wound integrity, the priority is to correlate the tissue failure with IOL injector options.

To describe material failure in damage and fracture mechanics, one very commonly used mathematical theory is based on calculating the energy release rate (ERR), G, which was developed by, among others, Griffith (Griffith, 1921) and extended by Irwin and Wells (Irwin and Wells, 1965). It is the energy per unit length released from the system by extending the tear surface by an infinitesimal length da in plane problem, i.e., $G = -\mathrm{d}\Pi/\mathrm{d}a$, where Π is the mechanical energy. The concept of ERR stems from the energy balance principle during an infinitesimal quasi-static tear extension. The total potential energy of a sample of tissue with a tear under deformation can be expressed as

$$E = \Pi + G_c a, \tag{1}$$

where the mechanical energy $\Pi = \Psi - W$, Ψ is the total strain energy and W is work done by loads. G_c, as a material parameter, is the critical energy required to break all atomic bonds per unit length in a two dimensional (2D) problem as studied here and a is the total tear length. The minimal potential energy principle requires that

$$\frac{\mathrm{d}E}{\mathrm{d}a} = \frac{\mathrm{d}\Pi}{\mathrm{d}a} + G_c < 0, \tag{2}$$

which is equivalent to

$$G > G_c. \tag{3}$$

This is the criterion to determine if the tear may propagate (i.e., it is energetically feasible); otherwise, it is stationary.

2.2 Model Set-Up

By assuming the cornea be a simple linear material and ignoring its curvature, we considered a 2D infinite plate containing a pre-existing incision of length 2a, the incision size was assumed to be relatively small compared to the cornea studied.

By applying an IOL injector through the incision, the line incision opened and expanded to a diamond shape, as shown in **Figure 1**. This was a basic fracture mode called Mode I or Opening Mode, i.e., the two crack surfaces experienced a jump only in u_y, that is, they moved away symmetrically with respect to the undeformed crack plane.

It can be shown that the general displacement solution of the upper crack surface for the Mode I problems is given by (Westergaard, 1933; Sun et al., 2012) (see detailed derivations *via* Westergaard function in **Supplementary Material**)

$$u_y = \frac{\kappa + 1}{4\mu} \frac{K_I}{\sqrt{\pi a}} \sqrt{a^2 - x^2}, \tag{4}$$

where $\mu = \frac{E}{2(1+\nu)}$ is the shear modulus, E and ν are the Young's modulus and the Poisson's ratio of cornea, $\kappa = (3 - \nu)/(1 + \nu)$ in a plane stress problem. K_I is the stress intensity factor, which describes the state of stress at the edges, and depends on different boundary conditions.

To permit one injector to apply through, the displacement of the crack surface at $x = 0$ was at least the same size of half the injector's smallest diameter, i.e., half of its minor axis b/2. Thus,

$$\frac{2K_I}{E}\sqrt{\frac{\pi}{a}} = \frac{b}{2}. \tag{5}$$

Using the relationship between ERR and the stress intensity factor $G = \frac{K_I^2}{E}$ and the criterion to keep a stationary tear in **Eq. 3**, the critical incision length $2a_c$ could then be obtained by

$$2a_c = \frac{\pi E b^2}{8G_c} \tag{6}$$

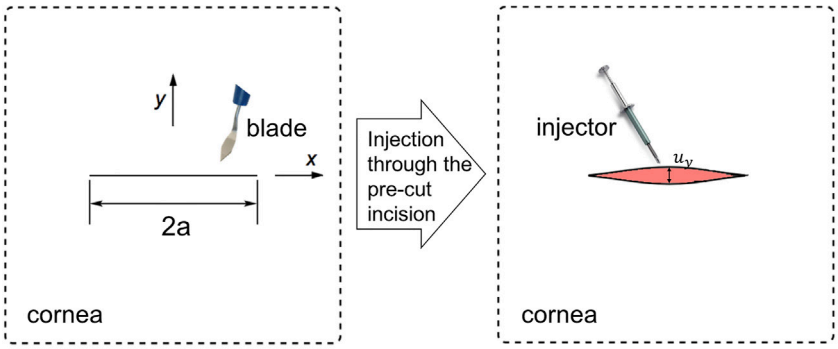

FIGURE 1 | In a 2D infinitely large cornea tissue piece, a incision cut by a blade of length 2*a* was subjected to a injector, which expanded the tissue to an Mode I opening.

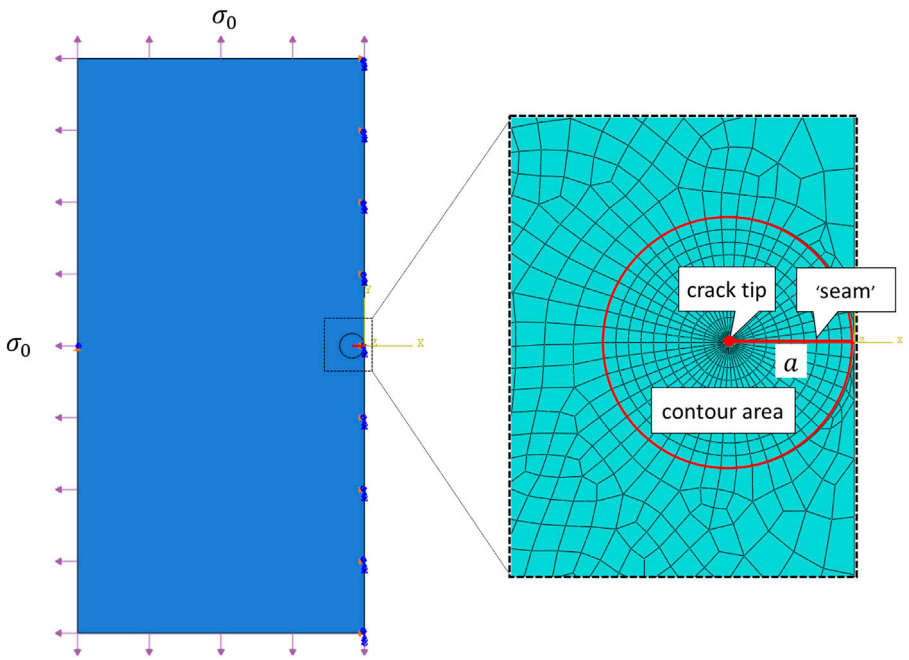

FIGURE 2 | Sketch of a large 2D plate with a transverse tear of length 2*a* under a uniformly distributed stress σ_0 at each edge. Note that only left half of the problem was conducted in the FE simulation. The insert shows the designed FE mesh generation, where the crack tip was surrounded by a sweeping contour area for ERR calculation.

It was clear to see that the allowed incision length was proportional to the injector size, decreases linearly with critical ERR, and increased linearly with the Young's modulus.

2.3 Finite Element Analysis

Consider a large square sample (60 mm × 60 mm[1]) with a 2*a* mm crack in the middle, a classical Mode I boundary condition, i.e., a uniformly distributed stress σ_0 at each edge, was applied. And the amount of stress being applied was adjusted so that the displacement of the crack surface in the middle is $b/2$. From analytical derivation $\sigma_0 = \frac{Eb}{2a}$ and details analytical derivation could be found *via* **Supplementary Equation S8** in Supplementary Material. Only left half of this symmetric problem was simulated in the finite element (FE) simulation and depicted in **Figure 2**. The right edge was fixed in x direction to secure symmetry, the central point on the left edge was all fixed to avoid rigid body motion.

The finite element simulations were performed using the commercially available finite element package Abaqus, 2013,

[1]This size is insignificant to results and was chosen to be large enough compared to tear dimension.

TABLE 1 | Material parameters for healthy porcine corneas at different strain rates (Tonsomboon et al., 2014).

Strain rate ($mm \cdot min^{-1}$)	E (MPa)	G_c (kJ/m^2)
3 (slow)	9.59	3.39
30 (medium)	10.29	4.40
300 (fast)	9.82	5.40

TABLE 2 | Critical incision lengths for six IOL injection systems at various incision speeds. The critical length larger than recommended 2.2 mm are shown in bold.

IOL injector	Minor axis b (mm)	Injection speed	Critical length $2a_c$ (mm)
U	1.467	Fast	1.537
		Medium	1.976
		Slow	**2.391**
E	1.671	Fast	1.994
		Medium	**2.564**
		Slow	**3.102**
R	1.734	Fast	2.147
		Medium	**2.761**
		Slow	**3.340**
iT	1.829	Fast	**2.389**
		Medium	**3.072**
		Slow	**3.716**
iS	1.834	Fast	**2.402**
		Medium	**3.089**
		Slow	**3.737**
CT	1.847	Fast	**2.436**
		Medium	**3.133**
		Slow	**3.790**

and was conducted on Intel(R) Core(TM) i7-10700 CPU at2.90 GHz machine with 32.0 GB RAM. The crack was firstly represented by a partition and created by defining a "seam", where nodes on elements on each side of the crack could be separated. ERR, as a contour energy integral, was calculated for layers of elements in rings, this required a spider web-like mesh generated around the crack tip. Sweeping strategy was selected and triangular element was wrapped around the crack tip. In particular, each ring of elements along the crack corresponded to a contour integral. For a typical simulation, we used a total of 23,881 nodes and 7,870 elements (CPS4R: Bilinear elements using reduced integration with hourglass control), and as shown in **Figure 2**, 10 contours were generated for ERR evaluations. One simulations took about 3–5 min with a reasonable initialization. The grid size was chosen following a grid independence test (simulations were run for increasingly refined grids until the results converged).

In FE simulations, Abaqus scripts were developed in Linux shell, so as to easily, automatically and robustly alternating the values of crack length a and communicating to its corresponding distributed stress σ_0. This powerful tool allowed us to combine the functionality of the Graphical User Interface (GUI) of Abaqus and the power of the programming language *Python*.

TABLE 3 | The sizes of all IOLs in axial and profile views (Nanavaty and Kubrak-Kisza, 2017). The minor axis length (in bold) were selected for calculations.

IOL injector		
U	2.011	**1.467**
E	1.902	**1.671**
R	1.739	**1.734**
iT	**1.829**	1.847
iS	**1.834**	1.870
CT	**1.847**	1.852

3 RESULTS

3.1 Analytical Results

Assuming that the cornea was isotropic, typical strain rate-dependent material parameters of E and G_c from porcine cornea (Tonsomboon et al., 2014) were listed in **Table 1**. Six preloaded IOL delivery system with different diameters were compared and listed in **Table 2**. These company products (Nanavaty and Kubrak-Kisza, 2017; Zhang et al., 2022) are Ultrasert (U) (Alcon Laboratories, Inc.), Eyecee (E) (Bausch & Lomb, Inc.), iSert (iS) (Hoya Surgical Optics, Inc.), CT Lucia (CT) (Carl Zeiss Meditec AG), iTec (iT) (Abbott Medical Optics, Inc.) and Rayone (R) (Rayner Intraocular Lenses Ltd.), respectively. All IOLs have a straw-like bevel face at the tip of its nozzle to aid delivery and their sizes in both axial and profile views are detailed in **Table 3**. The majority of injectors have a circular cross-section (e.g., R injector had major axis length of 1.739 mm and minor axis of 1.734 mm). Injectors U and E had a noticeable elliptical major-minor axial ratio of 1.37 and 1.14.

By applying **Eq. 6**, the corresponding energy release rate G against incision length $2a$ for two representative injection systems CT and U, i.e., with largest and smallest injector sizes, was depicted in **Figure 3**. As clearly presented in **Eq. 6**, with larger Young's modulus at medium speed as listed in **Table 1**, the calculated ERR was bigger with same incision length. However, the difference of speed-dependence Young's modulus was small compared to corresponding speed-dependent G_c, so the critical $2a_c$ reaches first at fast speed which had largest G_c, and further at medium and lastly at slow speeds. The pattern was valid for these two injectors and also for all injection system, as presented in **Table 2**, listing quantitative results for all six injectors. It is also be observed from **Table 2** that the larger the injector size, the bigger the required safe incision length. The intersection of G and G_c lines gave the allowed minimal incision length, below this length, the pre-existing incision became unstable and torn. In particular, at fast incision speed, it was energetically stationary with a tear length $2a \geq 1.537$ mm for injector U delivery and $2a \geq 2.436$ mm for injector CT delivery. At medium incision speed, the incision was safe with a tear length $2a \geq 1.976$ mm and $2a \geq 3.133$ mm for U and CT advancement, respectively. The critical minimal tear length were 2.391 and 3.790 mm at slow speed.

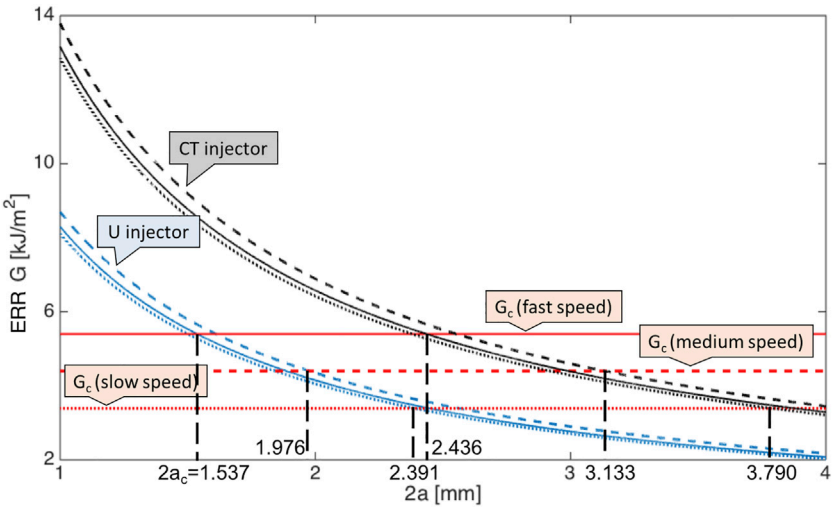

FIGURE 3 | Energy release rates for an isotropic large plate plotted against the incision length $2a$ at three incision speeds given CT (black lines) and U injection systems (blue lines). Results at fast speed are in solid lines, medium speed in dashed lines and slow speed in dotted lines. The corresponding critical energy release rates G_c (red lines) are also given for reference. The six junctions points between same type of lines represent the critical lengths $2a_c$.

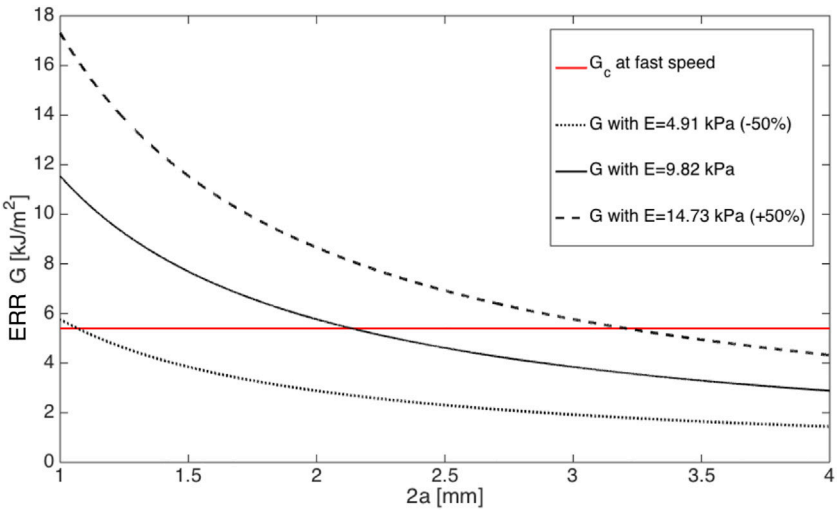

FIGURE 4 | ERRs plotted against the incision length $2a$ in ±50% moduli at fast incision speed. Note that G_c is plotted as a reference.

Among all the given injectors (Nanavaty and Kubrak-Kisza, 2017), the minimum incision length was 1.537 mm for U system at fast incision speed, this value is below the recommended value of 2.2 mm (Nanavaty and Kubrak-Kisza, 2017; Kim et al., 2014), which indicates the operation can be conducted with no further damage. However, many other choices required larger pre-existing incision, and were highly dependent on the injection speed.

Taken an average injector size of d = 1.730 mm amongst the six mentioned systems, the modulus of cornea tissue was shifted by ± 50%, then the critical incision length at fast speed changed according to **Figure 4**, which clearly revealed that ERR with softer material first joined critical ERR and resulted in a smaller minimal incision length.

3.2 Numerical Results

We then compared our analytical results with numerical simulations. A typical FE result is shown in **Figure 5**, where the incision length was $2a$ = 2.2 mm, injector size was the average value of six mentioned systems d = 1.730 mm and E = 9.82 MPa at fast speed, the crack opened subjected to the applied loading, and maximal principal stress was concentrated at the crack tip. For each contour near the crack tip, one corresponding ERR could be output in Abaqus and depicted in **Figure 5B**. The first three contour integrals are commonly neglected, because the crack tip is so close and can lead to unwanted effects. Therefore, contour integrals 4–10, were used for evaluation and they well

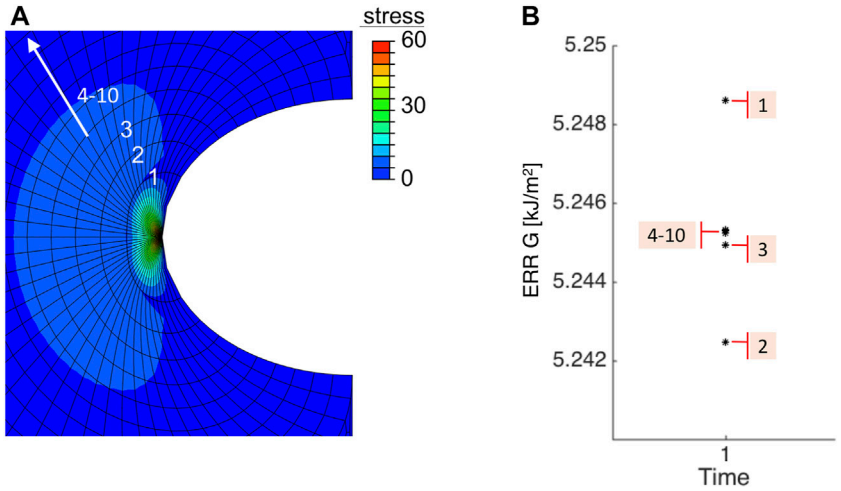

FIGURE 5 | Numerical result of **(A)** the maximal principal in-plane stress and **(B)** values of ERR under 10 contours near the crack tip. Note that the first three contour integrals were neglected.

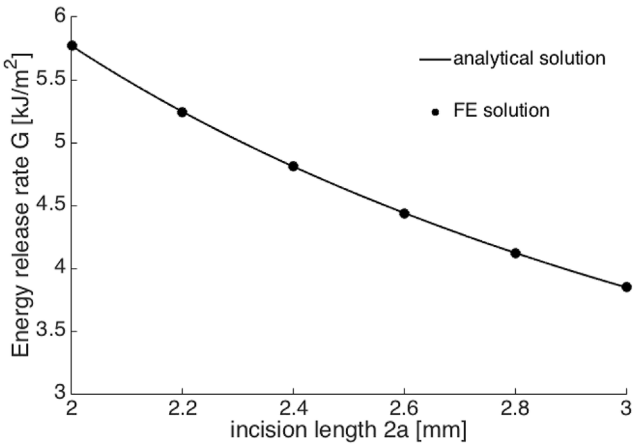

FIGURE 6 | The comparison between FE numerical solutions (black dots) and analytical solutions (black line).

converged to a single value of 5.244 kJ/m^2, which agreed with the analytical result 5.246 kJ/m^2 calculated from **Eq. 6**. Regardless of inducing further damage, ERRs could be calculated within linear theory, however, the tear further propagation, if exists, was not presented in FE simulations.

This FE model was then saved as a *Python* script to create new Abaqus jobs. Linux commands were used to edit the incision length $2a$ from 2.0 to 3.0 mm in an increment of 0.2 mm in script. With each $2a$, corresponding applied stress σ_0 that results in $b/2$ displacement at the middle of crack surface was found by walking around the analytical solutions from **Supplementary Equation S8** (the detailed derivation could be found in **Supplementary Material**). Once matched, the corresponding ERR could be output, which is illustrated in **Figure 6**. The agreement between the FE simulation and analytical solutions indicated that more realistic scenarios, for example, a circular shape and/or anisotropic corneal material could be further considered and implemented in numerical simulations.

4 DISCUSSION

In this study, both the analytical and numerical methods revealed the potential of suggesting there exists a safe and effective surgery incision length for IOL delivery. Taken six commercially available IOL injection systems as examples, the recommended 2.2 mm incision can not be treated as a universal standard.

4.1 Effect of Injector Size

The critical incision length is dependent on many factors, a typical one is the size of injector, a larger injector results in a larger required critical pre-existing length. It is also recommended to twist the injector so that the major axis keeps align with the tear during surgery, i.e., the tear opening can be maintained in its smallest magnitude. Studies have shown that stretching this incision or wound enlargement is affected by the type of injector cartridge or insertion method used (Ouchi, 2012). Whereas creating smaller diameter injector nozzles would hamper the ease of IOL insertion. Reducing the thickness of the nozzle material or designing a slit in the nozzle to buffer the stretch force (as seen in a few of IOL designs) would be a good compromise (Nanavaty and Kubrak-Kisza, 2017).

4.2 Effect of Insertion Speed

Due to the critical ERR difference in the effect of speeds of IOL insertion on the clear corneal wound structure, fast insertion was better than slow insersion since smaller safe tear length was needed. Other experimental studies also found that slow IOL insertion may affect clear corneal wound structure more than fast IOL insertion, and this appeared to be due to vertical stretching of

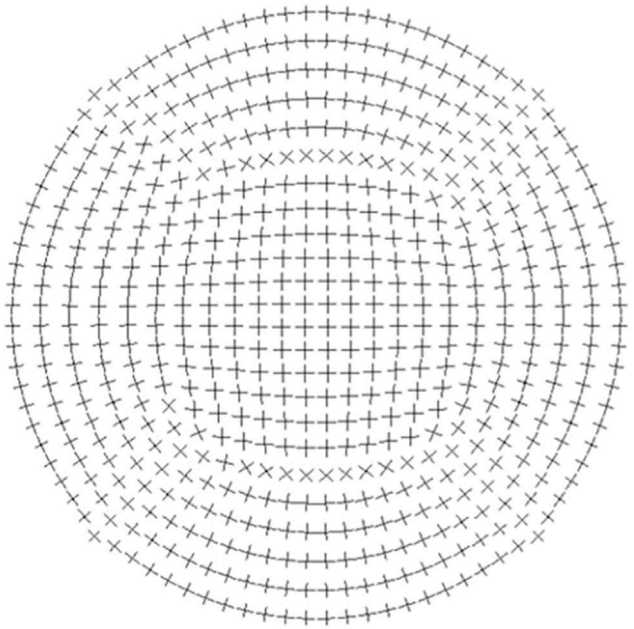

FIGURE 7 | Sketch of fibril orientation adopted from (Pandolfi, 2020). The cornea is composed of bundles of collagen fibrils oriented in orthotropic manner.

the insertion cartridge by the IOL (Ouchi, 2012; El Massry et al., 2016). In their experiment, 80 randomized eyes underwent clear corneal phacoemulsification to either fast IOL insertion (one revolution per second) or slow IOL insertion (one-quarter revolution per second). A screw plunger-type injector was used in both groups. The change in wound size after IOL insertion was significantly larger in the slow group. More eyes in the slow group required corneal hydration, and wound structure changes on optical coherence tomography were more prominent.

4.3 Effect of Energy Release Rate

The key work in FE simulations was to work out the value of ERR. There are many numerical methods existing for calculating G (Zehnder, 2012), and most rely, not on evaluating the singular stress field at the tips, but rather on the global energy and work, so an accurate value for G can be obtained with modest mesh refinement.

The evaluated G_c gave a floor barrier for safe delivery. We noted that the value of G_c was patient-specific, and in practice could be higher or lower than the values we used here, especially when cornea is in infection or under drugs. If G_c is increased, then the required length is decreased according to **Eq. 6**, the less likely the tissue is torn.

4.4 Effect of Cornea Geometry

The cornea geometry was considered as an infinite 2D plate compared to its central tear. However, in ductile bio-materials like cornea, the energy that rupturing the chemical bonds along the crack plane plays a relatively small role in resisting crack growth, with a large part of fracture energy being associated with plastic flow near the crack tip. This "plastic zone" size should not be so large as to interact with the specimen's free boundaries or to destroy the basic nature of the singular stress distribution. Hence, due to the finite dimension of cornea, the value of G_c should be modified by a ratio β which depends on the geometry of the cornea tissue and location of the pre-existing tear. For example, in a square specimen with a central tear, $\beta = 1.12$ (Murakami, 1987). The natural curvature and varying thickness of a three-dimensional cornea (Pandolfi, 2020) will need to be carefully treated in further studies.

4.5 Effect of Material Property

Figure 4 indicated that having a softer material was optimal to avoid further tissue damage to secure a more successful IOL delivery. However, the quantitative effect of this action on critical ERR is unknown and needs to be further studied.

The numerical model also allowed us to study a more realistic cornea material. According to X-ray scattering measurements, the layer-wise cornea is characterized by a strong fibril orientation, about 66% of the fibrils are oriented in the 45° sectors along the vertical and the horizontal direction. At the center of the cornea collagen is organized in an orthogonal configuration, and at the limbus it runs circumferentially, as seen in **Figure 7**. The tissue shows a typical organization of a material with symmetries (Pandolfi and Manganiello, 2006). In this context, it is worth investigating the effect of material organization on ERR. Hence a transversely isotropic material was assigned in the numerical simulations, typically with moduli $E_x/E_y = \eta$ and $\eta = 0.25, 0.5, 1, 2, 4$, respectively, where E_x is the modulus along the tear length and E_y is the one that perpendicular to E_x. **Table 4** clearly illustrates that E_y is the dominate factor that has effects on ERR, indicating that the incision is preferably along the direction with larger modulus. In practice, it is recommended to conduct a circumferential cut near the limbus.

However, the organization of the corneal tissue is far complex than linearity, presenting a clear anisotropic behaviour due to a hierarchically organized collagen, the level of anisotropy is highly location dependent (Bryant and McDonnell, 1996; Daxer and Fratzl, 1997). Several nonlinear constitutive models based on hyperelastic material assumptions have been proposed and developed to represent in various numerical applications, for example, in refractive surgery, tonometer indentation test and air puff test (Simonini and Pandolfi, 2015; Montanino et al., 2018; Pandolfi, 2020). For clinical applications, patient-specific

TABLE 4 | ERR against the material orthotropy ratio η.

η	E_x (MPa)	E_y (MPa)	ERR (kJ/m^2)
2	19.64	9.82	5.301
1.5	14.73	9.82	5.267
1	9.82	9.82	5.244
0.75	9.82	14.73	6.740
0.5	9.82	19.64	8.029

geometrical and material features are required in future FE models.

4.6 Limitations

All our estimations were based on model assumptions and the parameters estimated from pigs. This could only serve as a guideline as a more accurate estimation was not possible unless we have access to the material properties of each individual patient.

The elastic modulus of human corneas (Bryant and McDonnell, 1996) of average value of 0.79–0.83 MPa is at least one order smaller compared to the porcine parameters of around 10 MPa used herein. This may explain the reason why the recommended critical incision lengths for different injectors were mostly larger than expected. The trend and the affecting factors listed in **Table 2** can serve as a useful guidance for human operations.

5 CONCLUSION

In this work, based on the Griffith's critical ERR criterion, analytical and numerical solutions were both provided to answer the clinical question, i.e., if the critical incision length is enough for a safe injection in a cataract surgery. Several important factors were examined (e.g., the size of nozzle inserted into the wound, corneal tissue properties and injection speed) quantitatively, indicating that a smaller injection size, a faster insertion speed and a softer material, a larger ERR would guarantee a safer operation.

Our study suggested that the current recommended incision depth of 2.2 mm in IOL delivery was, in most circumstances, not large enough to avoid tearing and tissue damage, as observed in clinical practice. Setting a universal length aiming at all type of injectors was not appropriate and the suggested minimum incision length for different injector diameter is listed in **Table 2**. Our results supported and explained many clinical findings, suggesting that a surgeon could insert the IOL quickly to lessen wound damage. However, caution must be used with the quick-insertion method because rapid insertion might induce tissue injury, especially with a wound-assisted method. It was also recommended to advance IOL injector *via* its minor axis, and the tear was preferably along the circumferential direction due to tissue orthotropy.

DATA AVAILABILITY STATEMENT

The original contributions presented in the study are included in the article/**Supplementary Material**, further inquiries can be directed to the corresponding author.

AUTHOR CONTRIBUTIONS

NQ: Conceptualization, methodology, investigation, visualization, formal analysis, writing-original draft; DL: Conceptualization, investigation, writing—review and editing; LW: Investigation, methodology, review and editing; KR: Investigation, review and editing; XL: conceptualization, methodology, review and editing.

ACKNOWLEDGMENTS

We gratefully acknowledge the financial support from the National Natural Science Foundation of China (No. 11902181), the National Natural Science Foundation of Shandong Province (No. ZR2019QA014), and the United Kingdom EPSRC grants (EP/S030875/1 and EP/S020950/1).

SUPPLEMENTARY MATERIAL

The Supplementary Material for this article can be found online at: https://www.frontiersin.org/articles/10.3389/fphys.2022.834214/full#supplementary-material

REFERENCES

Al Mahmood, A. M., Al-Swailem, S. A., and Behrens, A. (2014). Clear Corneal Incision in Cataract Surgery. *Middle East. Afr. J. Ophthalmol.* 21, 25–31. doi:10.4103/0974-9233.124084

Bernhisel, A., and Pettey, J. (2020). Manual Small Incision Cataract Surgery. *Curr. Opin. Ophthalmol.* 31, 74–79. doi:10.1097/icu.0000000000000624

Bryant, M. R., and McDonnell, P. J. (1996). Constitutive Laws for Biomechanical Modeling of Refractive Surgery. *J. Biomechanical Eng.* 118, 473–481. doi:10.1115/1.2796033

Daxer, A., and Fratzl, P. (1997). Collagen Fibril Orientation in the Human Corneal Stroma and its Implication in Keratoconus. *Invest. Ophthalmol. Vis. Sci.* 38, 121–129.

El Massry, A. A., Shama, A., Goweida, M. B., and El Zawawi, R. A., (2016). Effect of Intraocular Lens Insertion Speed on Surgical Wound Structure during Phacoemulsification. *Delta J. Ophthalmol.* 17, 137.

Griffith, A. A. (1921). Vi. The Phenomena of Rupture and Flow in Solids. *Philosophical Trans. R. Soc. Lond. Ser. A, containing Pap. a Math. or Phys. character* 221, 163–198.

He, Q., Huang, J., He, X., Yu, W., Yap, M., and Han, W. (2021). Effect of Corneal Incision Features on Anterior and Posterior Corneal Astigmatism and Higher-Order Aberrations after Cataract Surgery. *Acta Ophthalmol.* 99, e1027–e1040. doi:10.1111/aos.14778

Irwin, G. R., and Wells, A. A. (1965). A Continuum-Mechanics View of Crack Propagation. *Metallurgical Rev.* 10, 223–270. doi:10.1179/mtlr.1965.10.1.223

Kim, Y.-K., Kim, Y. W., Woo, S. J., and Park, K. H. (2014). Comparison of Surgically-Induced Astigmatism after Combined Phacoemulsification and 23-gauge Vitrectomy: 2.2-mm vs. 2.75-mm Cataract Surgery. *Korean J. Ophthalmol.* 28, 130–137. doi:10.3341/kjo.2014.28.2.130

Matossian, C., Makari, S., and Potvin, R. (2015). Cataract Surgery and Methods of Wound Closure: a Review. *Clin. Ophthalmol.* 9, 921–928. doi:10.2147/OPTH.S83552

Montanino, A., Angelillo, M., and Pandolfi, A. (2018). Modelling with a Meshfree Approach the Cornea-Aqueous Humor Interaction during the Air Puff Test. *J. Mech. Behav. Biomed. Mater.* 77, 205–216. doi:10.1016/j.jmbbm.2017.05.042

Murakami, Y. (1987). *Stress Intensity Factors Handbook*, Vol. II. Oxford): Pergamon Press.

Nanavaty, M. A., and Kubrak-Kisza, M. (2017). Evaluation of Preloaded Intraocular Lens Injection Systems: *Ex Vivo* Study. *J. Cataract Refractive Surg.* 43, 558–563. doi:10.1016/j.jcrs.2017.02.019

Oshika, T., and Wolfe, P. (2019). *In Vitro* comparison of Delivery Performance of 4 Preloaded Intraocular Lens Injector Systems for Corneal and Sclerocorneal Incisions. *J. Cataract Refractive Surg.* 45, 840–846. doi:10.1016/j.jcrs.2018.10.050

Ouchi, M. (2012). Effect of Intraocular Lens Insertion Speed on Surgical Wound Structure. *J. Cataract Refractive Surg.* 38, 1771–1776. doi:10.1016/j.jcrs.2012.06.031

Pandolfi, A. (2020). Cornea Modelling. *Eye Vis.* 7, 2. doi:10.1186/s40662-019-0166-x

Pandolfi, A., and Manganiello, F. (2006). A Model for the Human Cornea: Constitutive Formulation and Numerical Analysis. *Biomech. Model. Mechanobiol* 5, 237–246. doi:10.1007/s10237-005-0014-x

Randleman, J. B., and Lockwood, J. C. (2016). *Intraocular Lens Designs and Materials (Thieme)*.

Shepherd, J. R. (1989). Induced Astigmatism in Small Incision Cataract Surgery. *J. Cataract Refractive Surg.* 15, 85–88. doi:10.1016/s0886-3350(89)80145-2

Simonini, I., and Pandolfi, A. (2015). Customized Finite Element Modelling of the Human Cornea. *PLOS One* 10, e0130426. doi:10.1371/journal.pone.0130426

Sun, C. T., Jin, Z. H., and Sun, C. T. (2012). *Fracture Mechanics*. Boston: Academic Press.

Tonsomboon, K., Koh, C. T., and Oyen, M. L. (2014). Time-dependent Fracture Toughness of Cornea. *J. Mech. Behav. Biomed. Mater.* 34, 116–123. doi:10.1016/j.jmbbm.2014.01.015

Westergaard, H. M. (1933). Stresses at a Crack, Size of the Crack, and the Bending of Reinforced concrete. *J. Proceedings*.

Zehnder, A. T. (2012). *Fracture Mechanics*. Springer.

Zhang, L., Schickhardt, S., Fang, H., Auerbach, F., Cagampang, P., Merz, P. R., et al. (2022). Comparison of a New Iol Injector System against 3 Standard Iol Injector Systems with Different Incision Sizes: Miyake-Apple View Experimental Laboratory Study. *J. Cataract Refract Surg.* 48, 230–237. doi:10.1097/j.jcrs.0000000000000736

Conflict of Interest: The authors declare that the research was conducted in the absence of any commercial or financial relationships that could be construed as a potential conflict of interest.

Publisher's Note: All claims expressed in this article are solely those of the authors and do not necessarily represent those of their affiliated organizations, or those of the publisher, the editors and the reviewers. Any product that may be evaluated in this article, or claim that may be made by its manufacturer, is not guaranteed or endorsed by the publisher.

Copyright © 2022 Qi, Lockington, Wang, Ramaesh and Luo. This is an open-access article distributed under the terms of the Creative Commons Attribution License (CC BY). The use, distribution or reproduction in other forums is permitted, provided the original author(s) and the copyright owner(s) are credited and that the original publication in this journal is cited, in accordance with accepted academic practice. No use, distribution or reproduction is permitted which does not comply with these terms.

frontiers | Frontiers in Physiology

ORIGINAL RESEARCH
published: 13 May 2022
doi: 10.3389/fphys.2022.850707

Measuring the Reliability of Postural Sway Measurements for a Static Standing Task: The Effect of Age

Pei-Yi Lo[1], *Bo-Lin Su*[2], *Yu-Lin You*[1], *Chen-Wen Yen*[2], *Shih-Ting Wang*[1] and *Lan-Yuen Guo*[1,3,4,5,6]*

[1]Department of Sports Medicine, College of Medicine, Kaohsiung Medical University, Kaohsiung, Taiwan, [2]Department of Mechanical and Electro-mechanical Engineering, National Sun Yat-Sen University, Kaohsiung, Taiwan, [3]College of Medicine, Kaohsiung Medical University, Kaohsiung, Taiwan, [4]Department of Medical Research, Kaohsiung Medical University Hospital, Kaohsiung, Taiwan, [5]College of Health Sciences, Kaohsiung Medical University, Kaohsiung, Taiwan, [6]College of Humanities and Social Sciences, National Pingtung University of Science and Technology, Pintung, Taiwan

Background: A force plate is used to determine the ability to balance ability. However, only some medical centers or laboratories are equipped with force plates because they are costly so a low-cost force plate is required for home care or health care institutes. Few studies compare the reliability of postural sway measurements in terms of age. This study proposes a low-cost force plate to select reliable parameters to evaluate postural sway.

Objectives: To determine the intra-rater reliability of a novel force plate and the effect of age difference on the intra-rater test-retest reliability for the center of pressure (COP).

Methods: Forty participants were enrolled for this study: 20 youths and 20 older adults. Participants stood on a custom-made and low-cost force plate with eyes opened and eyes closed to measure COP-related parameters. The within-day test-retest reliability was measured at two sessions on the same day and the between-days reliability was measured on two different days. The COP-related parameters include the average velocity of COP, the average velocity in the antero-posterior and medio-lateral directions, the mean distance of COP and the mean distance in the antero-posterior and medio-lateral directions. An intra-class correlation coefficient test with one-way random model was performed to determine the reliability of different variables within-days and between-days. The results were presented in single measurement of intraclass correlation coefficient (ICC), the standard error of measurements, and the minimal detectable changes of each COP-related parameters.

Results: The novel low-cost force plate demonstrates excellent reliability in terms of the COP velocity related parameters for within- and between-day measurements. The ICC of COP distance related parameters were good to excellent reliability for between-day measurements (range: 0.43–0.84). Older adults demonstrated excellent reliability in terms of the mean distance for antero-posterior and the results were better than those for younger participants for the eyes-opened and eyes-closed conditions. The reliability in terms of the mean distance for medio-lateral was poor to good for older adults (range: 0.38–0.55), and excellent for younger participants.

OPEN ACCESS

Edited by:
Christina Maria Pabelick, Mayo Clinic, United States

Reviewed by:
Arthur Sá Ferreira, University Center Augusto Motta, Brazil
Marco Arkesteijn, Aberystwyth University, United Kingdom

***Correspondence:**
Lan-Yuen Guo
yuen@kmu.edu.tw

Specialty section:
This article was submitted to Clinical and Translational Physiology, a section of the journal Frontiers in Physiology

Received: *08 January 2022*
Accepted: *25 April 2022*
Published: *13 May 2022*

Citation:
Lo P-Y, Su B-L, You Y-L, Yen C-W, Wang S-T and Guo L-Y (2022) Measuring the Reliability of Postural Sway Measurements for a Static Standing Task: The Effect of Age. Front. Physiol. 13:850707. doi: 10.3389/fphys.2022.850707

Conclusion: The novel and low-cost force plate reliably measured balance and age affects the reliability of different COP variables, so the results of this study were pertinent to the selection of COP measures.

Keywords: age effect, balance ability, reliability, force plate, center of pressure

1 INTRODUCTION

Falling and the related problems afflict the older adults (Corriveau et al., 2001). For normal activities, posture control involves adjusting body's direction and balance when standing (Lafond et al., 2004). Many reasons for falling have been proposed (Tinetti 1987). One of the most common causes is reduced ability to balance. Balance is the ability to control body coordination when moving or maintaining a loading posture (Sheldon 1963; Wolfson et al., 1986; Woollacott et al., 1986; Tracey et al., 2012; Huang and Yang 2019; Liu 2021).

Balance involves coordinating the transfer of the center of mass and the center of pressure (COP). For different postures and movements, the central nervous system uses inputs from vision, vestibular sense and proprioception to maintain balance. The deterioration of balance in the older adults can cause falls (Lord and Dayhew 2001). the ability to balance decreases with age because sensory inputs are changed and older adults who exhibit poor postural control demonstrate greater muscle co-activation to compensate for a decline in proprioception (Manchester et al., 1989; Nagai et al., 2011). The deterioration of proprioception can increase reliance on feedforward during dynamic tasks (Piirainen et al., 2013). Balance intervention is used to improve proprioception and postural control (Ross and Guskiewicz 2006; Wortmann and Docherty 2013; Nam et al., 2018). The ability to control posture is measured by measuring the center of pressure while standing on a force plate. Balance can be measured subjectively and objectively. Subjective methods involve a questionnaire assessment, that is, limited to a specific age or personal recognition disorder. Objective methods measure the COP excursion, the postural sway and the distribution of loading (Berg et al., 1989; Prieto et al., 1993; Kairy et al., 2003; Anker et al., 2008; Blum and Korner-Bitensky 2008; Mercer et al., 2009). A force plate is used to evaluate the balance ability by calculating COP-related parameters, such as the excursion velocity or the displacement, to give information about posture control (Palmieri et al., 2002). Force plates are expensive because the force sensors must measure the three-dimensional orientation of the force. They are too expensive for home care or community care settings so this study used a custom-made novel and low-cost force plate that uses four force sensors, but simplifies the measurement to a one-dimensional orientation force, so it is significantly cheaper than current options (Su et al., 2015; Hong et al., 2016; Hong et al., 2017).

Balance ability can be evaluated by observing the COP excursion and COP-related parameters, such as excursion velocity. However, the COP-related parameters that are obtained from the force plate must be reliable. To reliably measure the ability to balance, the reliability of the proposed force plate must be determined prior to its use to measure the ability to balance. Reliability is a measurement of the ability to achieve similar results for different measurement times for stable individuals (Guyatt et al., 1992). A reliable force plate is an essential element of any system to measure the ability to balance and reliable parameters must be used to prevent clinical failures. The measurement of the effectiveness of any method of balance intervention requires reliable parameters (Corriveau et al., 2001). The use of the force plate to measure COP is a validated and reliable method to evaluate balance performance (Li et al., 2016). The reliability of COP measures has been investigated in the previous studies (Carpenter et al., 2001; Bauer et al., 2008; Swanenburg et al., 2008; Pinsault and Vuillerme 2009; Moghadam et al., 2011; Da Silva et al., 2013; Li et al., 2016; Levy et al., 2018). The reliabilities of average COP velocity while quiet standing on the rigid and foam surface with eyes open and eyes close were ranged from 0.82 to 0.93 (Moghadam et al., 2011). In addition, older adults who sustained at least one fall within 1 year demonstrated lower reliabilities of COP-related parameters, such as, sway distance in anteroposterior (AP) and mediolateral (ML) direction than older adults who did not have fall experience within one year (Swanenburg et al., 2008). In previous study, older adults demonstrated greater reliability of average COP velocity in AP and ML direction compared to young adults (Lin et al., 2008). In addition, the reliability studies used intra-class correlation coefficient (ICC) to present relative reliability or absolute reliability, such as standard error of measurement (SEM) to test the reproducibility (Weir 2005). The COP velocity related parameters demonstrated good to excellent test retest reliability, and, the sway path distance exhibited good reliability in both eyes open and eye close conditions (Golriz et al., 2012; Hébert-Losier and Murray 2020). Hence the COP velocity and COP path distance related parameters are appropriate variables to evaluate balance ability.

Some studies showed that the mean distance of COP for older adults was greater than the value for young subjects for a balance test (Prieto et al., 1996; Slobounov et al., 2006). Many studies also identified significantly greater postural sway in the older population than in younger cohorts (Prieto et al., 1996; Slobounov et al., 2006). The effect of age on the reliability of postural sway measurements determines the variables that are used to evaluate postural sway and the effectiveness of any intervention. However, very few studies measure the reliability of COP-related parameters to determine which variables can be used to measure the ability to balance for different age groups.

This study determines the reliability of the novel and low-cost force plate for young participants and then for an older adult group to determine whether there are differences in reliability for different age groups. This study hypothesized that the novel and low-cost force plate exhibits sufficient within- and between-day

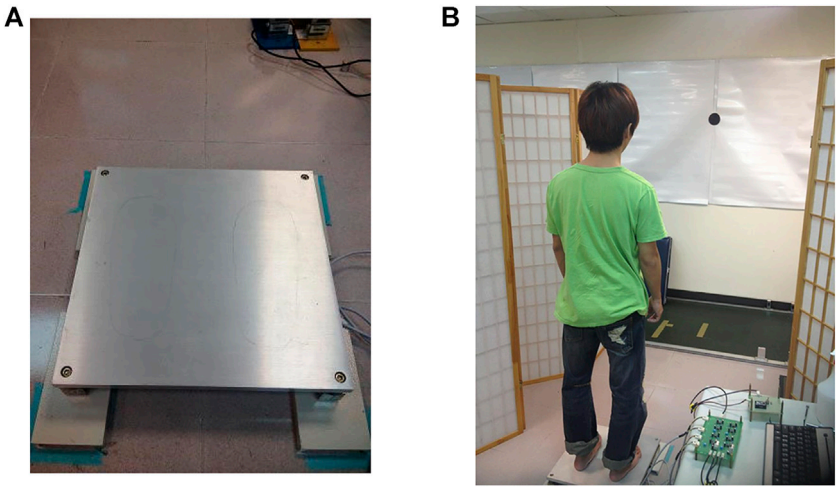

FIGURE 1 | (A) The proposed low-cost force plate and **(B)** The experimental evironment.

reliability for use to evaluate the ability to balance by measuring COP-related parameters. It is also hypothesized that age affects the reliability of COP measurements.

2 MATERIALS AND METHODS

2.1 Participants

A G*Power 3.1.9.7 program was used to calculate the sample size of the present study. The sample size was calculated according to the study design and the previous study (Fleiss 1986; Fritz et al., 2012). At least 28 participants were needed to achieve 80% statistical power with an alpha level of 0.05 for repeated measurement study design. The correlation among measurements were set at 0.80 (high reliability) with a moderate effect size (Cohen's d equals to 0.5) (Fritz et al., 2012).

The sampling methods of this study was convenient sampling. Forty subjects (20 youths, average age: 20.1 ± 1.3 years, and 20 older adults, average age: 68.7 ± 2.9 years) participated in this study. The basic profiles are shown below. Subjects were 18–25 years old or 65–75 years old. Subjects with lower limb neuromuscular injuries (e.g.: polio, stroke), musculoskeletal injuries (e.g.: fractures) or pain in the lower limbs were excluded. This study is approved by the Institutional Review Board of Kaohsiung Medical University Hospital [Approval number: KMUHIRB-2012-08-07(I)].

2.2 Procedures

This study included one investigator (rater) who had 2 years experiences in biomechanics investigation perform COP measures for all participants. Participants' characteristics were determined before the test and questions were asked about medical records. Subjects then stood on a custom-made force plate (**Figure 1A**) to measure the height of their eyes from the ground. A mark was made 2 m from this height and the subject looked directly at the for the test. The mark was a circle with a diameter of 10 cm. In order to control across groups, participants were requested to stand on the center of force plate where there were feet-like marker. A previous study, the average step width of 18 healthy young (aged 27.7 years) participants was found to be 9.5 cm with 1.8 cm standard deviation (SD) and the average step width of 12 older adults was 10.4 cm with 3.4 cm SD (Owings and Grabiner 2004). Hence, the stance width of the present study was about 12 cm, which was measured by the distance of the heel between feet and the distance of the first metatarsal between feet.

A custom-made force plate contained 4 force sensors on the corner of the force plate same as the commercial force plate. However, the 4 force sensors installed in this custom-made force plate are single-axis. The experimental system used the graphical programming environment NI LabVIEW (National Instrument, Austin, TX, United States) for performing system control, signal processing, and graphical user interface (GUI) functions. Similar to a commercially available force platform, the force platform used in this work is a rectangular plate with force transducers located at its four corners. The size of the platform is 40 cm by 40 cm. Our previous work have carefully compared this force platform and a commercial force platform (Kistler 9286AA) to verify comparable repeatability and accuracy (Hong et al., 2016). After amplification, analog voltage signals obtained by the load cells of the force platform are converted to digital signals 24-bit DAQ (data acquisition) card (NI 9234). The digitized force signals were sent to a PC using a USB chassis (NI cDAQ-9174). The sampling frequency was set to 512 Hz.

The single-axis force sensor can be used to measure the balance performance while quiet standing because of that the vertical ground reaction force (GRF) is much larger than the anteroposterior (AP) and mediolateral (ML) GRFs. Hence, those GRFs can be considered negligible in computing the center of pressure while quiet standing task (Duarte and Freitas 2010; Huang et al., 2013; Bartlett et al., 2014). That's why the balance board of Nintendo Wii can be a valid and reliable tool for evaluating the standing balance ability (Park and Lee 2014). The calculation of the COP in AP and ML with single-axis force sensor can be referred to the our previous study (Hong

et al., 2016). Concluded above, the single axis force plate can be used to evaluate the balance performance while quiet standing.

A rater who had 2 years experiences in biomechanics investigation conducted the reliability evaluations. The protocol involved standing on two legs with eyes opened and closed three times for 40 s, with 1 min rest between each measurement session. During the examination, participants looked directly at the 2 m mark and stood on the marked spot on the force plate, with both arms naturally placed beside the thighs. Subjects refrained from deep breathing to minimize body sway and sound from outside the test environment was minimized (**Figure 1B**).

The reliability of the custom-made force plate was tested using within-day test-retests and between-day test-retests. Participants underwent the COP measures in the same laboratory environment, by the same investigator. The within day reliability test-retest were performed for two sessions on the same day by a break of 5 min and the between days reliability test-retest were performed for four different sessions on two different days. Participants underwent the same procedures and protocols on next day.

2.3 Data Analysis

The calculation of the COP in AP and ML with single-axis force sensor can be referred to the our previous study (Hong et al., 2016). This study used the data for 40 s and the first 5 s and the last 5 s of data were removed. The remaining 30 s was analyzed in terms of average velocity (V), medio-lateral average velocity (V-ML), antero-posterior average velocity (V-AP), mean distance (MD), medio-lateral mean distance (MD-ML) and antero-posterior mean distance (MD-AP).

There are 4 steps to calculate the mean distance including the mean COP in anteroposterior (AP) and in mediolateral (ML) directions, the AP and ML time series relative to the mean COP, the resultant distance time series and the mean distance (Prieto et al., 1996; Quijoux et al., 2021). First of all, the mean COP can be calculated as the averaged COP trajectory in AP and ML directions. The COP trajectory in AP and ML directions were noted as AP_0 and ML_0, then, the mean COP in AP and ML directions would be:

$$\begin{aligned}\text{The mean COP}_{\text{AP}} &= \frac{1}{\text{N}}\sum_{n=1}^{N}\text{AP}_0,\ \text{n} = 1, 2, 3, \ldots \text{N}.\\ \text{The mean COP}_{\text{ML}} &= \frac{1}{\text{N}}\sum_{n=1}^{N}\text{ML}_0,\ \text{n} = 1, 2, 3, \ldots \text{N}.\end{aligned} \tag{1}$$

After that, the AP and ML time series were referenced to the mean COP can be calculated as following equations:

$$\begin{aligned}\text{AP}(\text{n}) &= \sum_{n=1}^{N}\text{AP}_0(\text{n}) - \text{COP}_{\text{AP}}\\ \text{ML}(\text{n}) &= \sum_{n=1}^{N}\text{ML}_0(\text{n}) - \text{COP}_{\text{ML}}\end{aligned} \tag{2}$$

Resultant distance (RD) time series represented a distance between the mean COP and the COP in AP_0 and ML_0 time series as follows:

$$\text{RD}(\text{n}) = \sum_{n=1}^{N}\left[\text{AP}(\text{n})^2 + \text{ML}(\text{n})^2\right]^{\frac{1}{2}} \tag{3}$$

Finally, the mean distance is the mean of the RD time series and that can be calculated as **Eq. 4**.

$$\text{The mean distance}(\text{mm}) = \frac{1}{\text{N}}\sum_{n=1}^{N}\text{RD}(\text{n}) \tag{4}$$

The mean velocity was calculated by averaging the total excursion over time (Prieto et al., 1996; Quijoux et al., 2021).

$$\begin{aligned}&\text{The total excursion}(\text{mm})\\ &= \sum_{n=1}^{N}\left\{[\text{AP}(\text{n}+1) - \text{AP}(\text{n})]^2 + [\text{ML}(\text{n}+1) - \text{ML}(\text{n})]^2\right\}^{\frac{1}{2}}\end{aligned} \tag{5}$$

$$\text{The mean velocity}(\text{mm/s}) = \frac{\textit{Total excursion}}{\text{Total time}} \tag{6}$$

2.4 Statistical Analysis

SPSS software version 20.0 (SPSS Inc. Chicago, IL) was used for statistical analysis. An intra-class correlation coefficient (ICC) with one-way random model was performed to determine the reliability of different variables within-days and between-days. The results were presented in single measurement of ICC, SEM and minimal detectable changes of COP-related parameters. An ICC value of greater than 0.75 represents excellent reliability, a value of between 0.4 and 0.75 represents fair or good reliability and a value of less than 0.4 represents poor reliability (Fleiss 1986). A 95% confidence interval (CI) is used to measure the precision of the estimate for each ICC value. The α level is 0.05. The SEM represented the variance extent between measurements, and, the smaller SEM, the greater reproducibility, the calculation of SEM of COP-related parameters was as follows: the standard deviation * (1-ICC coefficient)$^{1/2}$, in addition, the minimal detectable changes of the COP-related parameters were also calculated.

3 RESULTS

3.1 The Reliability of the Novel Force Plate

In terms of the within-day reliability measurement, the results for V (ICC: 0.91 and 0.84 for eyes open and eyes close conditions, respectively), V-ML (ICC: 0.87 and 0.87 for eyes open and eyes close conditions, respectively), V-AP (ICC: 0.97 and 0.84 for eyes open and eyes close conditions, respectively), MD (ICC: 0.56 and 0.75 for eyes open and eyes close conditions, respectively), and, MD-ML (ICC: 0.57 and 0.72 for eyes open and eyes close conditions, respectively) demonstrated good to excellent reliability for eyes-opened and eyes-closed tests (**Table 1**). The results for MD-AP showed poor reliability (ICC: 0.37 with SEM 0.91 and 0.60 with SEM 0.84 for eyes open and eyes close conditions, respectively) (**Table 1**).

In terms of between-days reliability, the results for V, V-ML, and V-AP for the COP while standing with eyes-opened and eyes-closed demonstrated excellent reliability (ICCs for the eyes-opened test, with respective values of: 0.90, 0.89, and 0.89. ICC values for the eyes-closed are 0.91, 0.92, and 0.85, respectively. The MD, MD-ML, and MD-AP results demonstrate good to excellent reliability for the eyes-opened and eyes-closed tests (**Table 2**).

TABLE 1 | Within-day reliability for different COP variables in young participants.

		Session 1	Session 2	SEM	MDC	ICC (95%CI)
		Mean ± SD	Mean ± SD			
Average velocity (mm/s)	EO	9.96 ± 3.26	9.92 ± 2.85	0.81	2.25	0.93* (0.84,0.97)
	EC	12.01 ± 4.00	11.19 ± 3.62	1.53	4.23	0.84* (0.65,0.93)
Medio-lateral average velocity (mm/s)	EO	7.63 ± 3.02	7.22 ± 2.56	1.01	2.80	0.87* (0.70,0.95)
	EC	7.32 ± 3.02	6.76 ± 2.51	1.00	2.78	0.87* (0.70,0.94)
Antero-posterior average velocity (mm/s)	EO	11.78 ± 3.79	12.03 ± 3.69	0.65	1.80	0.97* (0.93,0.99)
	EC	15.00 ± 4.86	14.08 ± 4.81	1.93	5.36	0.84* (0.65,0.93)
Mean distance (mm)	EO	7.06 ± 1.68	7.48 ± 1.90	1.19	3.30	0.56 (0.17,0.80)
	EC	7.10 ± 2.13	7.09 ± 2.04	1.04	2.89	0.75* (0.48,0.90)
Medio-lateral mean distance (mm)	EO	3.51 ± 1.28	3.56 ± 1.51	1.11	3.08	0.57 (0.19,0.80)
	EC	2.91 ± 1.36	3.04 ± 1.37	0.86	2.39	0.72 (0.52,0.90)
Antero-posterior mean distance (mm)	EO	5.41 ± 1.28	5.77 ± 1.49	0.91	2.52	0.37 (–0.07,0.69)
	EC	5.85 ± 1.68	5.78 ± 1.48	0.84	2.32	0.60 (0.23,0.82)

**ICC, value > 0.75: excellent reliability.*
EO, Eyes opened; EC, Eyes closed; ICC, Intraclass coefficient.

TABLE 2 | Between-days reliability for different COP variables in young participants.

Between days		Day 1	Day 2	SEM	MDC	ICCs (95%CI)
		Mean ± SD	Mean ± SD			
Average velocity (V) (mm/s)	EO	9.94 ± 3.01	9.83 ± 2.23	0.42	1.18	0.90* (0.74,0.96)
	EC	11.60 ± 3.68	11.15 ± 2.96	0.68	1.88	0.91* (0.76,0.96)
Medio-lateral average velocity (mm/s)	EO	7.42 ± 2.71	7.53 ± 2.20	0.35	0.97	0.89* (0.73,0.96)
	EC	7.07 ± 2.71	7.12 ± 2.15	0.67	1.86	0.92* (0.79,0.97)
Antero-posterior average velocity (mm/s)	EO	11.93 ± 3.69	11.67 ± 2.66	0.32	0.89	0.89* (0.71,0.96)
	EC	14.54 ± 4.66	13.93 ± 3.74	0.45	1.24	0.85* (0.62,0.94)
Mean distance (mm)	EO	7.27 ± 1.59	7.15 ± 1.75	0.75	2.07	0.71 (0.26,0.89)
	EC	7.10 ± 1.94	7.42 ± 2.21	1.40	3.89	0.64 (0.10,0.86)
Medio-lateral mean distance (mm)	EO	3.54 ± 1.23	3.54 ± 1.31	0.48	1.32	0.61 (0.02,0.85)
	EC	2.98 ± 1.28	3.10 ± 1.25	0.80	2.22	0.50 (-0.26,0.80)
Antero-posterior mean distance (mm)	EO	5.59 ± 1.15	5.44 ± 1.30	0.63	1.74	0.81* (0.52,0.93)
	EC	5.82 ± 1.41	6.09 ± 1.74	1.15	3.20	0.80* (0.50,0.92)

**ICC, value > 0.75: excellent reliability.*
EO, Eyes opened; EC, Eyes closed; ICC, Intraclass correlation coefficient; CI, Confidence interval.

3.2 The Reliability of Balance Ability Measurements for the Young and Older Adults

The reliability of the results for COP velocity, the V-AP and the V-ML for young participants and the older adults group demonstrate excellent reliability for the eyes-opened and eyes-closed test (**Table 3**). The reliability of the results for MD, MD-ML, and MD-AP for young participants demonstrated good to excellent reliability for the eyes-opened and eyes-closed tests.

For older adults, the results for MD and MD-AP demonstrated excellent reliability, which was higher than the results for young participants for the eyes-opened and eyes-closed tests. The reliability of the results for MD-ML for older adults was poor (for the eyes-opened tests) to good (for the eyes-closed tests), but younger participants demonstrated excellent reliability in terms of this parameter (**Table 3**). In the comparisons of the COP measures between age groups. Younger participants demonstrated smaller SEM in average velocity in AP direction and average distance in ML direction than that in the older adult group (**Table 3**). However, the older adult group demonstrated smaller SEM in the remaining parameters than that in the younger participant group (**Table 3**). The MDC values of COP-related parameters in younger participant group ranged from 0.67 to 1.36 for eyes-opened test, while, the MDC values in older adult group ranged from 0.51 to 1.36 for eyes-opened test. Besides, for eyes-closed test, the MDC values in younger participant group ranged from 0.78 to 1.88, and, values in older adult group ranged from 0.59 to 1.36 (**Table 3**).

4 DISCUSSION

The proposed low-cost force plate can be used in clinics, for home care and in health care institutes because it is cheaper than a commercial force plate and is reliable equipment to measure the ability to balance. This is the first study to determine the test-retest reliability for a low-cost force plate for a protocol to measure the ability to balance and the first to determine the test-retest reliability of parameters to measure the ability to balance for different age groups, in order to determine the

TABLE 3 | Between-days reliability for different COP variables for younger and older participants.

Tests	Youth		Older adults	
Parameters	**EO**	**EC**	**EO**	**EC**
Average velocity				
ICC	0.90*	0.91*	0.95*	0.98*
95%CI	0.74–0.96	0.76–0.96	0.88–0.98	0.95–0.99
SEM	0.42	0.68	0.49	0.49
MDC	1.18	1.88	1.36	1.36
Average velocity in AP				
ICC	0.89*	0.92*	0.96*	0.98*
95%CI	0.73–0.96	0.79–0.97	0.89–0.98	0.96–0.99
SEM	0.32	0.45	0.40	0.48
MDC	0.89	1.24	1.10	1.33
Average velocity in ML				
ICC	0.89*	0.85*	0.92*	0.94*
95%CI	0.71–0.96	0.62–0.94	0.80–0.97	0.84–0.98
SEM	0.35	0.67	0.23	0.21
MDC	0.97	1.86	0.65	0.59
Mean distance				
ICC	0.71	0.64	0.83*	0.91*
95%CI	0.26–0.89	0.10–0.86	0.58–0.93	0.77–0.96
SEM	0.75	1.40	0.94	1.08
MDC	2.07	3.89	2.59	2.99
Mean distance in AP				
ICC	0.61	0.50	0.93*	0.92*
95%CI	0.02–0.85	–0.26–0.80	0.83–0.97	0.80–0.97
SEM	0.63	1.15	0.54	0.99
MDC	1.74	3.20	1.51	2.75
Mean distance in ML				
ICC	0.81*	0.80*	0.38	0.55
95%CI	0.52–0.93	0.50–0.92	–0.56–0.76	–0.13–0.82
SEM	0.48	0.80	0.67	0.60
MDC	1.32	2.22	1.86	1.66

**ICC, value > 0.75: excellent reliability.*

EO, Eyes opened; EC, Eyes closed; ICC, Intraclass correlation coefficient; CI, Confidence interval

variables, measure the ability to balance for different age groups using this low-cost force plate.

Most of the results for within-day test-retest reliability in terms of COP-related parameters that were measured using the proposed low-cost force plate indicated good to excellent reliability and the between-day test-retest results demonstrated good to excellent reliability. Age affects the reliability of the MD-AP and MD-ML parameters. These results support the hypotheses for this study.

4.1 The Reliability of the Novel and Low-Cost Force Plate

In the current study, most of the COP-related parameters that were measured for static standing on two legs demonstrated good to excellent reliability for all except the MD-AP parameter for the within-day test-retest measurements. All of the COP-related parameters that are measured for this study demonstrate good to excellent between-day reliability.

The results for velocity for eyes-opened and eyes-closed tests demonstrated excellent between-day reliability, which was similar to the results of previous studies (Swanenburg et al., 2008; Moghadam et al., 2011). The between-day reliability for average velocity, V-AP and MD-AP for eyes-opened and eyes-closed test for older adults in the present study were excellent. The ICCs values were also higher than those for a previous study involving a balance evaluation protocol using a commercial force plate (AMTI, Watertown, MA, United States) for older adults (Swanenburg et al., 2008). In Lin et al. study, the SEM of mean velocity in AP and ML directions for between-day reliability measurement while performing quiet standing with eyes-closed were 1.2 and 2.1 (mm/s) in younger participants and 2.4 and 2.9 (mm/s) in older adults (Lin et al., 2008), which were greater than the present study at the same task condition (0.45 and 0.67 mm/s for mean velocity in AP and ML directions, respectively, in younger participants and 0.48 and 0.21 mm/s in AP and ML directions,

respectively, in older adults). These results indicated that reproducibility of COP measures in those parameters were better by using the custom-made force plate than using commercial force plate (Lin et al., 2008). The SEM of average velocity in AP direction while young adults performing standing still for 10 repeated trials measured by the commercial force plate (Equi+, model PF01, Aix les Bains, France) in the previous study (Pinsault and Vuillerme 2009) was greater than the present study, moreover, the average velocity of older adults while performing quiet standing with eye-closed in the present study were smaller than that in the previous study (Swanenburg et al., 2008), which measured the balance protocol for 4 trials in one session while standing quietly with or without vision by using a commercial force plate with 50 Hz sampling rate (AMTI, United States) in older adults (Swanenburg et al., 2008). The MDC values of average velocity in AP and ML directions in both young (MDC for average velocity in AP: 1.24; ML: 1.86 mm/s) and older adults (MDC for average velocity in AP: 1.33; ML: 0.59 mm/s) of the present study were smaller than that in previous studies which used commercial force plate to measure COP of young (MDC for average velocity in AP: 3.33; ML: 5.82 mm/s) and older (MDC for average velocity in AP: 6.65; ML: 8.04 mm/s) adults (Lin et al., 2008).

The ICC results also demonstrated good reliability (ICCs: 0.71 for eyes-opened and 0.73 for eyes-closed tests) for healthy participants who did not have fall experience (Swanenburg et al., 2008). The ICC values for MD-ML were higher than the ICC values for MD-AP for within- and between-days for this study. Previous studies reported that the MD-ML can be used to determine whether the subject experiences falling (Bergland and Wyller 2004). These results showed that the proposed low-cost force plate demonstrates sufficient within- and between-day reliability (good to excellent) to be used to measure the ability to balance by measuring COP-related parameters. Some factors might influence the results of reliability measurements were reported (Hébert-Losier and Murray 2020). In the present study, we requested participants to look at a 10 cm diameter which was 2 m mark away from force plate, this might result in a more stable and constant measurement condition while performing eyes-opened test, because of that the head movement might affect the magnitude of sway. However, in the previous studies, they did not report whether participants have target to look at or not (Bauer et al., 2008; Lin et al., 2008; Swanenburg et al., 2008; Pinsault and Vuillerme 2009; Li et al., 2016).

4.2 The Effect of Age on the Reliability of Measurements of the Ability to Balance

Both groups for this study demonstrated excellent between-day reliability in terms of average COP velocity, V-AP and V-ML for the eyes-opened and eyes-closed test. The ICC values for V-AP, V-ML, and MD for the older adult group were higher than those for the younger group for this study. These findings were similar to those of a previous study, which also demonstrated excellent reliability for V-AP and V-ML and higher reliability in terms of these parameters for the older adults group than the younger group while performing upright and quiet standing with eyes-closed condition for three trials in each condition, as measured using a commercial force plate with 100 Hz sampling rate (AMTI OR6-7 series, Watertown, MA, United States) (Lin et al., 2008).

In the present study, for the eyes-opened and eyes-closed tests, only the older adult group demonstrated excellent reliability for the MD and MD-AP. The younger group demonstrated good reliability in terms of these parameters. Young participants demonstrated excellent reliability for MD-ML but the older adults group demonstrated poor to good reliability. This may be because movement for control in the AP direction is more accurate relative to the ML direction (Amoud et al., 2007), so there was a greater in the inter-session variation, which increases the ICC value. older adults who have a high risk of falling demonstrate a lower MD-AP value than young individuals and older adults who have a low risk of falling (Norris et al., 2005). Besides, older adults in this study demonstrated higher reliability for MD-AP than MD-ML. The decrease in the ability to balance with aging occurs primarily in the mediolateral direction (Day et al., 1993), so older adults may rely on vision to compensate for a decrease in balance in terms of lateral stability. Without vision, the variability increases between trials and the ICC values decreased, especially in the mediolateral direction (Day et al., 1993).

There were age-related differences in COP-measurements and that can be detected by the proposed low-cost force plate and the results are similar trends to those of previous studies that use commercial force plates. The older adults demonstrated better ICCs in average velocity in ML direction, and mean distance in AP direction with smaller SEM compared to younger participants. These results provided suggestions to choose reliable COP-related parameters to evaluate balance ability in older adults.

4.3 Study Limitations

Participants in the current study were healthy because the reliability evaluation must use stable individuals (Guyatt et al., 1992) to determine the reliability of equipment and the reliability of parameters to determine the effect of age. Other populations, such as individuals with experience of falling, must be studied to identify the aging effects on the reliability of parameters.

To measure the ability to balance, the present study requested participant to stand on two legs because standing on a single leg is dangerous for the older adults. Standing on one leg can also cause instability so there is greater variability in the studies. To determine the effect of age on COP-related parameters to measure the ability to balance, this study required participants to stand on two legs. However, a problem with balance may cause older adults to fall while walking or when obstacles are encountered (Chou et al., 2001), so these functional movements must be studied further.

5 CONCLUSION

The results for within- and between-day reliability indicate that the proposed low-cost force plate is a reliable tool for COP

measurements for a static standing task with both eyes closed and both eyes opened, to determine the ability to balance.

Older adults demonstrated excellent test-retest reliability for MD-AP but young subjects demonstrate excellent reliability for MD-ML. This study provided suggestions for the selection of reliable COP-related parameters for a static standing task to measure the ability to balance for different age groups.

DATA AVAILABILITY STATEMENT

The original contributions presented in the study are included in the article/**Supplementary Material**, further inquiries can be directed to the corresponding author.

ETHICS STATEMENT

The studies involving human participants were reviewed and approved by this study was approved by Institutional Review Board of Kaohsiung Medical University Hospital. The patients/participants provided their written informed consent to participate in this study.

AUTHOR CONTRIBUTIONS

Conceptualization, L-YG and P-YL; methodology, P-YL and S-TW; software, C-WY and B-LS; validation, B-LS and C-WY; data analysis, P-YL, S-TW, and Y-LY; writing—original draft preparation, P-YL; writing—review and editing, L-YG and Y-LY; funding acquisition, L-YG and C-WY, All authors have read and agree to the published version of the manuscript.

FUNDING

This work is supported by NSYSU-KMU joint research project (NSYSUKMU101-017). This study is also financially supported by the Ministry of Science and Technology, Taiwan (MOST110-2221-E-037-001 and MOST110-2622-E-037-001).

SUPPLEMENTARY MATERIAL

The Supplementary Material for this article can be found online at: https://www.frontiersin.org/articles/10.3389/fphys.2022.850707/full#supplementary-material

REFERENCES

Amoud, H., Abadi, M., Hewson, D. J., Michel-Pellegrino, V., Doussot, M., and Duchêne, J. (2007). Fractal Time Series Analysis of Postural Stability in Elderly and Control Subjects. *J. Neuroeng Rehabil.* 4 (1), 12. doi:10.1186/1743-0003-4-12

Anker, L. C., Weerdesteyn, V., van Nes, I. J. W., Nienhuis, B., Straatman, H., and Geurts, A. C. H. (2008). The Relation between Postural Stability and Weight Distribution in Healthy Subjects. *Gait Posture* 27 (3), 471–477. doi:10.1016/j.gaitpost.2007.06.002

Bartlett, H. L., Ting, L. H., and Bingham, J. T. (2014). Accuracy of Force and Center of Pressure Measures of the Wii Balance Board. *Gait posture* 39 (1), 224–228. doi:10.1016/j.gaitpost.2013.07.010

Bauer, C., Gröger, I., Rupprecht, R., and Gaßmann, K. G. (2008). Intrasession Reliability of Force Platform Parameters in Community-Dwelling Older Adults. *Archives Phys. Med. rehabilitation* 89 (10), 1977–1982. doi:10.1016/j.apmr.2008.02.033

Berg, K., Williams, J. I., and Gayton, D. (1989). Measuring Balance in the Elderly: Preliminary Development of an Instrument. *Physiother. Can.* 41, 304–311. doi:10.3138/ptc.41.6.304

Bergland, A., and Wyller, T. B. (2004). Risk Factors for Serious Fall Related Injury in Elderly Women Living at Home. *Inj. Prev.* 10 (5), 308–313. doi:10.1136/ip.2003.004721

Blum, L., and Korner-Bitensky, N. (2008). Usefulness of the Berg Balance Scale in Stroke Rehabilitation: a Systematic Review. *Phys. Ther.* 88 (5), 559–566. doi:10.2522/ptj.20070205

Carpenter, M. G., Frank, J. S., Winter, D. A., and Peysar, G. W. (2001). Sampling Duration Effects on Centre of Pressure Summary Measures. *Gait posture* 13 (1), 35–40. doi:10.1016/s0966-6362(00)00093-x

Chou, L.-S., Kaufman, K. R., Brey, R. H., and Draganich, L. F. (2001). Motion of the Whole Body's Center of Mass when Stepping over Obstacles of Different Heights. *Gait posture* 13 (1), 17–26. doi:10.1016/s0966-6362(00)00087-4

Corriveau, H., Hébert, R., Prince, F., and Raîche, M. (2001). Postural Control in the Elderly: an Analysis of Test-Retest and Interrater Reliability of the COP-COM Variable. *Archives Phys. Med. Rehabilitation* 82 (1), 80–85. doi:10.1053/apmr.2001.18678

Da Silva, R. A., Bilodeau, M., Parreira, R. B., Teixeira, D. C., and Amorim, C. F. (2013). Age-related Differences in Time-Limit Performance and Force Platform-Based Balance Measures during One-Leg Stance. *J. Electromyogr. Kinesiol.* 23 (3), 634–639. doi:10.1016/j.jelekin.2013.01.008

Day, B. L., Steiger, M. J., Thompson, P. D., and Marsden, C. D. (1993). Effect of Vision and Stance Width on Human Body Motion when Standing: Implications for Afferent Control of Lateral Sway. *J. physiology* 469 (1), 479–499. doi:10.1113/jphysiol.1993.sp019824

Duarte, M., and Freitas, S. M. S. F. (2010). Revisão sobre posturografia baseada em plataforma de força para avaliação Do equilíbrio. *Rev. Bras. Fisioter.* 14 (3), 183–192. doi:10.1590/s1413-35552010000300003

Fleiss, J. L. (1986). *The Design and Analysis of Clinical Experiments*. New York, NY: Willey.

Fritz, C. O., Morris, P. E., and Richler, J. J. (2012). Effect Size Estimates: Current Use, Calculations, and Interpretation. *J. Exp. Psychol. General.* 141 (1), 2–18. doi:10.1037/a0024338

Golriz, S., Hebert, J. J., Foreman, K. B., and Walker, B. F. (2012). The Reliability of a Portable Clinical Force Plate Used for the Assessment of Static Postural Control: Repeated Measures Reliability Study. *Chiropr. Man. Ther.* 20 (1), 14–16. doi:10.1186/2045-709X-20-14

Guyatt, G. H., Kirshner, B., and Jaeschke, R. (1992). Measuring Health Status: what Are the Necessary Measurement Properties? *J. Clin. Epidemiol.* 45 (12), 1341–1345. doi:10.1016/0895-4356(92)90194-r

Hébert-Losier, K., and Murray, L. (2020). Reliability of Centre of Pressure, Plantar Pressure, and Plantar-Flexion Isometric Strength Measures: a Systematic Review. *Gait posture* 75, 46–62. doi:10.1016/j.gaitpost.2019.09.027

Hong, C. Y., Guo, L. Y., Song, R., Nagurka, M. L., Sung, J. L., and Yen, C. W. (2016). Assessing Postural Stability via the Correlation Patterns of Vertical Ground Reaction Force Components. *Biomed. Eng. Online* 15 (1), 90–18. doi:10.1186/s12938-016-0212-z

Hong, C. Y., Guo, L. Y., Song, R., Nagurka, M. L., Sung, J. L., and Yen, C. W. (2017). Developing a Low-Cost Force Treadmill via Dynamic Modeling. *J. Healthc. Eng.* 2017, 9. doi:10.1155/2017/9875471

Huang, C.-W., Sue, P.-D., Abbod, M., Jiang, B., and Shieh, J.-S. (2013). Measuring Center of Pressure Signals to Quantify Human Balance Using Multivariate Multiscale Entropy by Designing a Force Platform. *Sensors* 13 (8), 10151–10166. doi:10.3390/s130810151

Huang, C. C., and Yang, C. M. (2019). Motion Sickness and Postural Control while Performing Visual Search Task in Moving Environments. *Phys. Educ. J.* 52 (1), 39–54. doi:10.1177/0031512516651437

Kairy, D., Paquet, N., and Fung, J. (2003). A Postural Adaptation Test for Stroke Patients. *Disabil. Rehabilitation* 25 (3), 127–135. doi:10.1080/0963828021000024924

Lafond, D., Corriveau, H., and Prince, F. (2004). Postural Control Mechanisms during Quiet Standing in Patients with Diabetic Sensory Neuropathy. *Diabetes Care* 27 (1), 173–178. doi:10.2337/diacare.27.1.173

Levy, S. S., Thralls, K. J., and Kviatkovsky, S. A. (2018). Validity and Reliability of a Portable Balance Tracking System, BTrackS, in Older Adults. *J. geriatric Phys. Ther.* 41 (2), 102–107. doi:10.1519/jpt.0000000000000111

Li, Z., Liang, Y.-Y., Wang, L., Sheng, J., and Ma, S.-J. (2016). Reliability and Validity of Center of Pressure Measures for Balance Assessment in Older Adults. *J. Phys. Ther. Sci.* 28 (4), 1364–1367. doi:10.1589/jpts.28.1364

Lin, D., Seol, H., Nussbaum, M. A., and Madigan, M. L. (2008). Reliability of COP-Based Postural Sway Measures and Age-Related Differences. *Gait posture* 28 (2), 337–342. doi:10.1016/j.gaitpost.2008.01.005

Liu, Y. C. (2021). Effects of 12 Weeks of Dynamic Visual Acuity Training Onyoung-Elderly and Old-Elderly's Visual Ability and Balance. *Phys. Educ. J.* 54 (1), 13–21. doi:10.6222/pej.202103_54(1).0002

Lord, S. R., and Dayhew, J. (2001). Visual Risk Factors for Falls in Older People. *J. Am. Geriatrics Soc.* 49 (5), 508–515. doi:10.1046/j.1532-5415.2001.49107.x

Manchester, D., Woollacott, M., Zederbauer-Hylton, N., and Marin, O. (1989). Visual, Vestibular and Somatosensory Contributions to Balance Control in the Older Adult. *J. gerontology* 44 (4), M118–M127. doi:10.1093/geronj/44.4.m118

Mercer, V. S., Hankins, C. C., Spinks, A. J., and Tedder, D. D. (2009). Reliability and Validity of a Clinical Test of Reaction Time in Older Adults. *J. Geriatric Phys. Ther.* 32 (3), 103–110. doi:10.1519/00139143-200932030-00004

Moghadam, M., Ashayeri, H., Salavati, M., Sarafzadeh, J., Taghipoor, K. D., Saeedi, A., et al. (2011). Reliability of Center of Pressure Measures of Postural Stability in Healthy Older Adults: Effects of Postural Task Difficulty and Cognitive Load. *Gait Posture* 33 (4), 651–655. doi:10.1016/j.gaitpost.2011.02.016

Nagai, K., Yamada, M., Uemura, K., Yamada, Y., Ichihashi, N., and Tsuboyama, T. (2011). Differences in Muscle Coactivation during Postural Control between Healthy Older and Young Adults. *Archives gerontology geriatrics* 53 (3), 338–343. doi:10.1016/j.archger.2011.01.003

Nam, S.-m., Kim, K., and Lee, D. Y. (2018). Effects of Visual Feedback Balance Training on the Balance and Ankle Instability in Adult Men with Functional Ankle Instability. *J. Phys. Ther. Sci.* 30 (1), 113–115. doi:10.1589/jpts.30.113

Norris, J. A., Marsh, A. P., Smith, I. J., Kohut, R. I., and Miller, M. E. (2005). Ability of Static and Statistical Mechanics Posturographic Measures to Distinguish between Age and Fall Risk. *J. biomechanics* 38 (6), 1263–1272. doi:10.1016/j.jbiomech.2004.06.014

Owings, T. M., and Grabiner, M. D. (2004). Variability of Step Kinematics in Young and Older Adults. *Gait posture* 20 (1), 26–29. doi:10.1016/s0966-6362(03)00088-2

Palmieri, R. M., Ingersoll, C. D., Stone, M. B., and Krause, B. A. (2002). Center-of-pressure Parameters Used in the Assessment of Postural Control. *J. Sport Rehabil.* 11, 51–66. doi:10.1123/jsr.11.1.51

Park, D. S., and Lee, G. (2014). Validity and Reliability of Balance Assessment Software Using the Nintendo Wii Balance Board: Usability and Validation. *J. Neuroeng Rehabil.* 11 (1), 99–108. doi:10.1186/1743-0003-11-99

Piirainen, J. M., Linnamo, V., Cronin, N. J., and Avela, J. (2013). Age-related Neuromuscular Function and Dynamic Balance Control during Slow and Fast Balance Perturbations. *J. Neurophysiology* 110 (11), 2557–2562. doi:10.1152/jn.00476.2013

Pinsault, N., and Vuillerme, N. (2009). Test-retest Reliability of Centre of Foot Pressure Measures to Assess Postural Control during Unperturbed Stance. *Med. Eng. Phys.* 31 (2), 276–286. doi:10.1016/j.medengphy.2008.08.003

Prieto, T. E., Myklebust, J. B., Hoffmann, R. G., Lovett, E. G., and Myklebust, B. M. (1996). Measures of Postural Steadiness: Differences between Healthy Young and Elderly Adults. *IEEE Trans. Biomed. Eng.* 43 (9), 956–966. doi:10.1109/10.532130

Prieto, T. E., Myklebust, J. B., and Myklebust, B. M. (1993). Characterization and Modeling of Postural Steadiness in the Elderly: a Review. *IEEE Trans. Rehab. Eng.* 1, 26–34. doi:10.1109/86.242405

Quijoux, F., Nicolaï, A., Chairi, I., Bargiotas, I., Ricard, D., Yelnik, A., et al. (2021). A Review of Center of Pressure (COP) Variables to Quantify Standing Balance in Elderly People: Algorithms and Open-access Code. *Physiol. Rep.* 9 (22), e15067. doi:10.14814/phy2.15067

Ross, S. E., and Guskiewicz, K. M. (2006). Effect of Coordination Training with and without Stochastic Resonance Stimulation on Dynamic Postural Stability of Subjects with Functional Ankle Instability and Subjects with Stable Ankles. *Clin. J. Sport Med.* 16 (4), 323–328. doi:10.1097/00042752-200607000-00007

Sheldon, J. H. (1963). The Effect of Age on the Control of Sway. *Gerontol. Clin. (Basel)* 5, 129–138. doi:10.1159/000244784

Slobounov, S., Haibach, P., and Newell, K. (2006). Aging-related Temporal Constraints to Stability and Instability in Postural Control. *Eur. Rev. Aging Phys. Activity* 3 (2), 55–62. doi:10.1007/s11556-006-0012-8

Su, B. L., Song, R., Guo, L. Y., and Yen, C. W. (2015). Characterizing Gait Asymmetry via Frequency Sub-band Components of the Ground Reaction Force. *Biomed. Signal Process. Control* 18 (0), 56–60. doi:10.1016/j.bspc.2014.11.008

Swanenburg, J., de Bruin, E. D., Favero, K., Uebelhart, D., and Mulder, T. (2008). The Reliability of Postural Balance Measures in Single and Dual Tasking in Elderly Fallers and Non-fallers. *BMC Musculoskelet. Disord.* 9, 162. doi:10.1186/1471-2474-9-162

Tinetti, M. E. (1987). Factors Associated with Serious Injury during Falls by Ambulatory Nursing Home Residents. *J. Am. Geriatr. Soc.* 35 (7), 644–648. doi:10.1111/j.1532-5415.1987.tb04341.x

Tracey, S.-Y., Anderson, D. I., Hamel, K. A., Gorelick, M. L., Wallace, S. A., and Sidaway, B. (2012). Kicking Performance in Relation to Balance Ability over the Support Leg. *Hum. Mov. Sci.* 31 (6), 1615–1623. doi:10.1016/j.humov.2012.07.001

Weir, J. P. (2005). Quantifying Test-Retest Reliability Using the Intraclass Correlation Coefficient and the SEM. *J. Strength & Cond. Res.* 19 (1), 231–240. doi:10.1519/00124278-200502000-00038

Wolfson, L. I., Whipple, R., Amerman, P., and Kleinberg, A. (1986). Stressing the Postural Response. A Quantitative Method for Testing Balance. *J. Am. Geriatr. Soc.* 34 (12), 845–850. doi:10.1111/j.1532-5415.1986.tb07256.x

Woollacott, M. H., Shumway-Cook, A., and Nashner, L. M. (1986). Aging and Posture Control: Changes in Sensory Organization and Muscular Coordination. *Int. J. Aging Hum. Dev.* 23 (2), 97–114. doi:10.2190/vxn3-n3rt-54jb-x16x

Wortmann, M. A., and Docherty, C. L. (2013). Effect of Balance Training on Postural Stability in Subjects with Chronic Ankle Instability. *J. Sport Rehabil.* 22 (2), 143–149. doi:10.1123/jsr.22.2.143

Conflict of Interest: The authors declare that the research was conducted in the absence of any commercial or financial relationships that could be construed as a potential conflict of interest.

Publisher's Note: All claims expressed in this article are solely those of the authors and do not necessarily represent those of their affiliated organizations, or those of the publisher, the editors and the reviewers. Any product that may be evaluated in this article, or claim that may be made by its manufacturer, is not guaranteed or endorsed by the publisher.

Copyright © 2022 Lo, Su, You, Yen, Wang and Guo. This is an open-access article distributed under the terms of the Creative Commons Attribution License (CC BY). The use, distribution or reproduction in other forums is permitted, provided the original author(s) and the copyright owner(s) are credited and that the original publication in this journal is cited, in accordance with accepted academic practice. No use, distribution or reproduction is permitted which does not comply with these terms.

frontiers | Frontiers in Physiology

ORIGINAL RESEARCH
published: 23 May 2022
doi: 10.3389/fphys.2022.911072

Sex Modulates Cardiovascular Effects of Icodextrin-Based Peritoneal Dialysis Solutions

Ramón Paniagua[1], Elvia García-López[2], Marcela Ávila-Díaz[1]*, María-de-Jesús Ventura[1], Oscar Orihuela[3], María-del-Carmen Prado-Uribe[1], Juan-Manuel Gallardo-Montoya[1] and Bengt Lindholm[2]*

[1]Centro Médico Nacional Siglo XXI, Unidad de Investigación Médica en Enfermedades Nefrológicas, Hospital de Especialidades, Instituto Mexicano del Seguro Social, México, Mexico, [2]Karolinska Institut, Stockholm, Sweden, [3]Centro Médico Nacional Siglo XXI, Departamento de Cardiología, Hospital de Especialidades, Instituto Mexicano del Seguro Social, México, Mexico

OPEN ACCESS

Edited by:
Claudio de Lucia,
Scientific Clinical Institute Maugeri (ICS Maugeri), Italy

Reviewed by:
Raymond Theodorus Krediet,
Academic Medical Center, Netherlands
Pasqual Barretti,
Sao Paulo State University, Brazil
Simon J. Davies,
Keele University, United Kingdom
Christian Verger,
RDPLF, France

***Correspondence:**
Ramón Paniagua
jrpaniaguas@gmail.com
Marcela Ávila-Díaz
cramav@gmail.com

Specialty section:
This article was submitted to Clinical and Translational Physiology, a section of the journal Frontiers in Physiology

Received: 01 April 2022
Accepted: 27 April 2022
Published: 23 May 2022

Citation:
Paniagua R, García-López E, Ávila-Díaz M, Ventura M-d-J, Orihuela O, Prado-Uribe M-d-C, Gallardo-Montoya J-M and Lindholm B (2022) Sex Modulates Cardiovascular Effects of Icodextrin-Based Peritoneal Dialysis Solutions. Front. Physiol. 13:911072. doi: 10.3389/fphys.2022.911072

Background/Aims: Some previous observations have noted that after six months of peritoneal dialysis (PD) treatment with icodextrin solutions, blood pressure (BP) and NT-proBNP tend to return to baseline values. This may be due to accumulation of icodextrin products that exert a colloid osmotic effect, which drives water into the bloodstream, causing the rise in blood pressure. Since icodextrin is metabolized by α-Amylase and its gene copies are lower in females than in males, we hypothesized icodextrin metabolites reach higher concentrations in females and that cardiovascular effects of icodextrin are influenced by sex.

Methods: Secondary analysis of a RCT comparing factors influencing fluid balance control in diabetic PD patients with high or high average peritoneal transport receiving icodextrin (n = 30) or glucose (n = 29) PD solutions. Serum icodextrin metabolites, osmolality, body composition and Inferior Vena Cava (IVC) diameter were measured at baseline, and at 6 and 12 months of follow-up.

Results: After six months of treatment, icodextrin metabolites showed higher levels in females than in males, particularly G5-7 and >G7, serum osmolality was lower in females. In spite of reduction in total and extracellular body water, ultrafiltration (UF) was lower and IVC diameter and BP increased in females, suggesting increment of blood volume.

Conclusion: Females undergoing PD present with higher levels of icodextrin metabolites in serum that may exert an increased colloid-osmotic pressure followed by less UF volumes and increment in blood volume and blood pressure. Whether this could be due to the lesser number of α-Amylase gene copies described in diabetic females deserves further investigation.

Keywords: peritoneal dialysis, icodextrin, diabetes, α-amylase, blood volume, sex

INTRODUCTION

Icodextrin is a specific fraction of dextrin (a starch-derived water-soluble glucose polymer) that has been successfully used as a D-glucose substitute as colloid osmotic agent in peritoneal dialysis (PD) solutions. It does not easily diffuse through the peritoneal membrane which allows longer permanence in the peritoneal cavity exerting a sustained and more efficient peritoneal ultrafiltration (UF) (Ho-Dac-Pannekeet, et al., 1996; Krediet and Mujais, 2002). Since 1990s, icodextrin solution has been used to increase UF for a better management of patients with fluid overload reducing total body water (TBW), extracellular water (ECW) and improving blood pressure (Mistry, et al., 1994; Davies, et al., 2003). All these benefits have been consistently reproduced without compromising residual renal function or urine output (Htay, et al., 2018). Icodextrin solutions have additional advantages; they reduce peritoneal glucose exposure and absorption which in turn prolongs patient and PD technique survival (Han, et al., 2012), and facilitates metabolic control in diabetic patients (Szeto and Johnson, 2017; Wang, et al., 2015). These combined effects are particularly useful in diabetic patients with high/fast peritoneal solute transport rate among whom icodextrin increases UF without metabolic risk (Cueto-Manzano and Correa-Rotter, 2000).

In spite of its notably advantages, some less favorable changes were noted in patients treated with icodextrin solutions. Over six months of continuous use, patients show trend of blood pressure back to baseline levels, as well as increments in the circulating levels of atrial and brain natriuretic peptides, markers of expansion of blood volume and myocardial damage (Davies, et al., 2008; Bouchi, et al., 2006). Furthermore, in a randomized controlled trial comparing glucose PD solutions against icodextrin solutions, focusing on the glucose sparing effects of icodextrin, a higher rate of cardiovascular adverse events was noted (Li, et al., 2013). In some papers, authors have suggested accumulation of icodextrin metabolites as a plausible cause of this phenomenon; however, this has not been addressed (Bouchi, et al., 2006).

Icodextrin leaves peritoneal cavity and reaches blood stream via the lymphatic circulation, this account from 20 to 40% for the longer dwell of 8–16 h. In the circulation, icodextrin is hydrolyzed by circulating α-Amylase, yielding oligosaccharides (also called icodextrin metabolites) such as maltose (G2), maltotriose (G3), maltotetraose (G4) and maltopentaose (G5) and these molecules may accumulate over the long term (Davies, 1994; García-Lopez, et al., 2005; Garcia-Lopez et al., 2008). Based on this known mechanism, it can be assumed that production and accumulation of icodextrin metabolites in blood with potential capacity to exert colloid osmotic effect and increase blood volume depends of α-Amylase activity. Interestingly, the number of serum amylase gene copies has recently found associated with the risk of develop obesity and diabetes. The number of this gene and enzyme activity are reduced in diabetics and even more reduced in females (Viljakainen, et al., 2015; Nakajima, 2016; Al-Akl et al., 2021).

In this study, we address the hypothesis that icodextrin metabolites reach higher concentrations in female than in male diabetic patients undergoing Continuous Ambulatory Peritoneal Dialysis (CAPD) and those cardiovascular effects of icodextrin are influenced by sex.

MATERIALS AND METHODS

Design

A secondary analysis was performed with data from a prospective, multicenter, randomized controlled trial of diabetic patients undergoing CAPD with high and high average peritoneal transport type in whom icodextrin-based solutions were compared with glucose-based solutions as regards ability to control hypertension and edema as signs of fluid overload and metabolic control (Paniagua, et al., 2009). Briefly, after randomization, all patients received three 2-L exchanges of 1.5% dextrose (Dianeal, Baxter) for the daytime dwells. For the long dwell, patients in the control group ($n = 29$) received at least one bag of 2.5% dextrose (Dianeal, Baxter) and patients in the icodextrin group ($n = 30$) received 7.5% icodextrin (Extraneal, Baxter). Liberal use of 2.5% or 4.25% dextrose solutions was allowed in both groups in order to reach the treatment goal. The study protocol was approved by the Local Research Committees of all the participating hospitals, and the National Commission for Scientific Research of the Instituto Mexicano del Seguro Social (IMSS).

Patient Population

Patients were included if they had end stage renal disease secondary to diabetic nephropathy, if they had high or high average peritoneal transport type, and signed a written informed consent. Patients were excluded when seropositive for hepatitis B or HIV, if they had malignancies, or were receiving immunosuppressive medication. Patients who had had a peritonitis episode 1 month or less before being screened were also excluded. There was no selection by age, gender, residual renal function or time on dialysis. Patients were followed-up for 12 months (Paniagua, et al., 2009).

Data Collection

Clinical and demographic data were collected at baseline from medical records. In-office blood pressure was measured every month; 24-h ambulatory blood pressure; body composition by electrical bioimpedance (Biodynamics, Seattle, WA, USA) and echocardiogram with Doppler (Toshiba Sonolayer ultrasound system. Toshiba Corporation, Tochigi-Ken, Japan) were taken at baseline, at 6 and 12 months, and inferior vena cava diameter calculated (Vicente-Martinez et al., 2004). Biochemical parameters including serum α-Amylase activity, as well as inflammation and cardiovascular biochemical variables were also recorded in the same periods. For the secondary analysis, additional biochemical measurements were made, among them icodextrin metabolites and osmolality of serum.

Plasma α-Amylase activity was measured using an adapted routine method using p -nitrophenol maltoheptaoside as a substrate (Anderstam, et al., 2003). Plasma icodextrin metabolites, G2-G7 were measured using gel filtration high-

TABLE 1 | Demography, clinical and biochemical characteristics of patients at baseline.

Parameter	Glucose	Icodextrin	*p* Value
N	29	30	
Age (years)	60.5 ± 9.3	58.9 ± 7.9	0.47
Gender (n) (female/male)	13f/16 m	18f/12 m	0.30
Weight (kg)	61.5 ± 12.3	62.1 ± 10.4	0.85
Height (cm)	159.0 ± 13.7	156.6 ± 7.4	0.41
BMI (kg/m2)	24.10 ± 3.41	25.18 ± 3.74	0.70
Systolic BP (mmHg)	139.8 ± 29.4	148.9 ± 24.1	0.20
Diastolic BP (mmHg)	80.2 ± 16.4	84.9 ± 15.0	0.27
Total body water (% body weight)	59.49 ± 7.77	59.42 ± 7.44	0.90
Extracellular body fluid volume (% body weight)	26.95 ± 2.99	26.86 ± 3.02	0.70
Comorbidity			
Acute myocardial infarct	2	4	0.31
Stroke	2	2	0.68
Allergy	2	6	0.42
Serum albumin (g/dl)	2.71 ± 0.40	2.67 ± 0.48	0.70
Hemoglobin (g/dl)	10.6 ± 2.4	10.8 ± 2.2	0.71
Hematocrit (%)	31.6 ± 7.0	30.9 ± 6.5	0.72
Insulin use (n)	17	17	0.81
Serum glucose (mg/dl)	172 ± 152	164 ± 88	0.81
HbA1c (%)	7.59 ± 2.80	8.01 ± 2.80	0.57
Serum Sodium (mEq/L)	132.8 ± 3.68	133.04 ± 3.71	0.78
Time on PD (months)	19.6 ± 16.6	17.6 ± 14.1	0.61
D/P Cr PET 4 h	0.79 ± 0.09	0.81 ± 0.08	0.74
pCrCl (L/week)	54.1 ± 10.3	54.1 ± 11.2	0.99
rCrCl (L/week)[a]	0.90 | 2.73	0.70 | 5.70	0.14
Total CrCl (L/week)	55.73 ± 10.35	57.30 ± 9.94	0.63
pKt/V 6	1.90 ± 0.3	1.80 ± 0.40	0.22
rKt/V (L/week)[a]	0.12 | 0.40	0.14 | 0.08	0.17
Total Kt/V	1.92 ± 0.35	1.82 ± 0.38	0.30
r(CrCl + ureaCl)/2 (ml/minute)[a]	0.63 | 0.20	0.61 | 0.37	0.14
Urine volume (mL/24 h)	149 ± 255	253 ± 300	0.16
Peritoneal ultrafiltration (mL/24 h)	1414 ± 703	1271 ± 745	0.45

BMI, body mass index; BP , blood pressure, HbA1c = Glycated hemoglobin
[a]*= median|IQR.*

performance liquid chromatography as described elsewhere (García-Lopez, et al., 2005). The concentrations of G8 to G10 (if present) were estimated as they eluted successively at predictable elution times since no commercial standards are available (Garcia-Lopez et al., 2008). Serum osmolality was assessed by osmometer (Wescor 5520, USA), and serum sodium by ion selective electrode (ILyte $Na^+K^+Cl^-$ system, Lexinton, MS, USA).

Statistics

Data are expressed as percentages or mean ± SD according characteristics of variables. For statistical analysis, patients of each group were divided by gender and differences were analyzed by repeated comparisons over time. Pearson´s correlations were done between biochemical indices and cardiovascular variables. All statistical analysis was done with SPSSw v24.

RESULTS

A complete description of data at baseline is in the original paper (Paniagua, et al., 2009). **Table 1** shows a summary of that data. There were no significant differences between glucose and icodextrin groups at baseline. Patients had a much-reduced residual renal function, but values of total and peritoneal Kt/V as well as peritoneal ultrafiltration were considered appropriate for dialysis adequacy.

Table 2 shows body fluid compartments, biochemical, renal, and cardiovascular data for the 30 patients in the icodextrin group at baseline by sex, 18 females and 12 males. As expected, body size parameters and body fluid composition were different between sexes, and icodextrin dose by BSA 10% higher in females. In both sexes, residual renal function was very low. **Figure 1** shows selected biochemical variables. In panel A are values of serum α-Amylase activity showing that females had lower values in comparison with males. Panel B shows changes in icodextrin metabolites observed in the total number of patients: the highest concentrations were reached in the 2-4 glucose molecules fragment and the lowest in >7 molecules fragment. Considered as a whole group, the concentration of icodextrin fragments remained constant. Panels C to E show concentrations of different fragments divided by sex. Significantly higher concentrations in fragments G5-G7 and >G7 were noted in females after six months of treatment. Panel F shows changes in serum osmolality where female patients had lower values, which is opposite to increments in icodextrin fragments. **Table 3**

TABLE 2 | Cardiovascular vaiables by sex at baseline.

Sex	Female	Male	Total	p
n	18	12	30	—
Age (year)	59.39 ± 8.66	58.08 ± 6.88	58.87 ± 7.90	0.665
Weight (kg)	59.72 ± 11.27	65.69 ± 8.00	62.11 ± 10.37	0.124
Height (cm)	152.19 ± 5.12	163.17 ± 5.13	156.58 ± 7.43	0.000
Body mass index (kg/m^2)	25.61 ± 4.42	24.54 ± 2.44	25.18 ± 3.74	0.405
Body surface area (m^2)	1.556 ± 0.146	1.708 ± 0.117	1.617 ± 0.153	0.010
Systolic blood pressure (mmHg)	153.56 ± 34.32	157.50 ± 23.01	155.13 ± 29.92	0.730
Diastolic blood pressure (mmHg)	85.50 ± 15.81	91.50 ± 14.32	87.90 ± 15.27	0.300
Serum glucose (mg/dl)	157.45 ± 73.31	179.32 ± 161.62	167.83 ± 122.72	0.515
Serum urea (mg/dl)	105.77 ± 26.73	119.54 ± 32.86	112.31 ± 30.34	0.082
Serum creatinine (mg/dl)	7.93 ± 2.16	10.45 ± 3.04	9.12 ± 2.89	0.005
Serum sodium (mEq/L)	134.47 ± 2.84	135.02 ± 2.94	134.70 ± 2.85	0.620
Serum osmolality (mOsm/kg)	296.59 ± 16.24	294.92 ± 27.66	295.90 ± 21.26	0.839
Protein intake (g/kg/day)	1.24 ± 0.37	1.14 ± 0.30	1.20 ± 0.35	0.450
r(CrCl + ureaCl)/2 (mL/min/1.73 m^2)[a]	0.16 ± 0.26	0.41 ± 0.49	0.30 ± 0.40	0.056
Total body water (% of BW)	57.05 ± 7.89	62.98 ± 5.19	59.42 ± 7.44	0.019
Extracellular water (% of BW)	26.60 ± 3.45	27.26 ± 2.31	26.86 ± 3.02	0.568
Peritoneal ultrafiltration (mL/24 h)	1173.89 ± 485.23	1417.00 ± 1029.27	1271.13 ± 744.67	0.390
Left ventricle mass index (g/m^2)	265.83 ± 92.89	298.46 ± 64.13	278.89 ± 82.96	0.299
Inferior Vena Cava diameter (mm)	12.14 ± 4.57	16.56 ± 5.29	14.48 ± 5.32	0.087
NT-proBNP (ng/ml)	4.87 ± 1.68	4.73 ± 2.40	4.82 ± 1.96	0.849
Icodextrin dose (g/m^2)	97.25 ± 9.58	88.20 — 6.10	93.63 — 9.40	0.010

[a]= *Residual renal function.*

contains data of changes of serum glucose, urea, and serum sodium concentrations, as well as, osmolality, and total icodextrin fragments from baseline to 12 months. The average throughout the follow-up of total icodextrin fragments concentration is also shown. Urea increased in men and decreased in women while sodium decreased more significantly in women.

Figure 2 shows changes observed in cardiovascular parameters. Changes in systolic and diastolic blood pressure are in panels A and B. Diastolic blood pressure showed a sustained reduction in both sexes, but the change was more marked but not statistically significant in males. Systolic blood pressure showed trend back towards baseline values after six months without differences by sex. Ultrafiltration had different trends by sex, in males ultrafiltration increased and in females it had small decrements. The most important changes were seen in inferior vena cava diameter (panel D) with clear increments in females and reduction in males. Changes in Left ventricle mass index had the same pattern than systolic blood pressure, reduction at six months and trend back to baseline values after that. NT-proBNP levels had significant decrements along time without differences among sexes.

DISCUSSION

Data herein presented show measurable quantities of icodextrin metabolites in blood of diabetic patients treated with icodextrin PD solutions. Concentrations of icodextrin metabolites are higher in female than in male patients and were related with increments in the inferior vena cava diameter, a marker of blood volume. Changes in diameter of vena cava were in parallel with a trend back to baseline of systolic blood pressure after six months of treatment but were not followed by increments in LVMI or NT-proBNP values. These data suggest that icodextrin dose used may be excessive for women size, may be insufficiently metabolized by diabetic women, perhaps reflecting a smaller number of α-Amylase gene copies in this population (Viljakainen, et al., 2015; Nakajima, 2016), and/or decreased of α-Amylase activity (Al-Akl et al., 2021).

Icodextrin PD solutions have been successfully used since the 1990s. The colloid osmotic properties of icodextrin allows a sustained peritoneal ultrafiltration rate without the risk of excessive exposition to high glucose concentration in patients with fluid overload, a condition often seen in diabetic patients with high/fast peritoneal solute transport rate (Cho et al., 2013; Silver et al., 2014; Htay et al., 2018; Goossen et al., 2020).

In spite of its clinical value, some unexpected findings have been reported in patients treated with icodextrin solutions, among them increments in atrial natriuretic peptide, a cardiac hormone related with volume overload, and brain natriuretic peptide, another cardiac hormone related with volume and stretch overload as well as abnormal myocardial remodeling. Increments in LVM have also been reported. A plausible explanation for these findings is the accumulation of icodextrin metabolites in blood, which might exert a colloid osmotic effect and promotes expansion of blood volume (Bouchi et al., 2006; Davies et al., 2008).

Data from this secondary analysis are in line with the proposed explanation, icodextrin metabolites concentration increases along time. Small but significant increments were seen in all the measured size fragments. It is important to mention that only concentration and not the whole pool were measured since increments in blood volume was estimated indirectly. Early

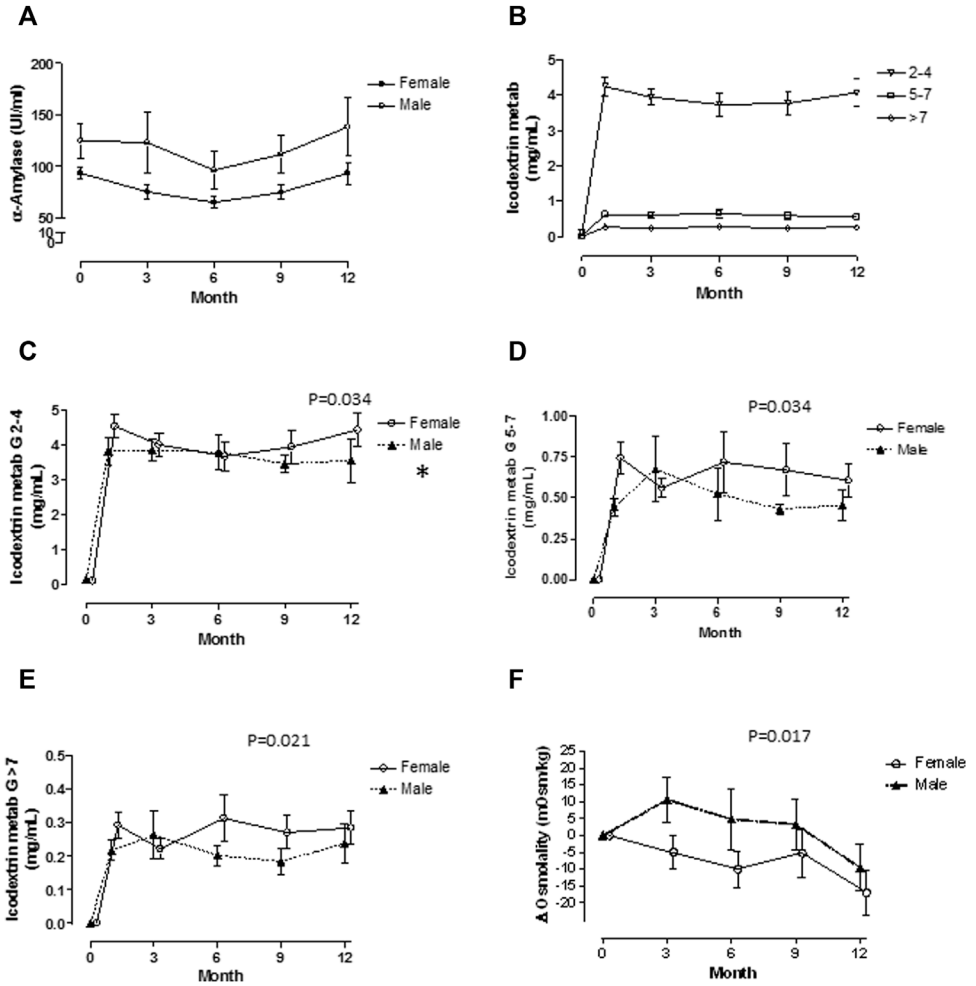

FIGURE 1 | Biochemical variables are shown by sex. α-Amylase activity **(A)** was significantly lower in females. Plasma levels of Icodextrin metabolites were inversely related with its molecular size **(B)**. Plasma levels of G2-G4 were not different by sex **(C)**, but significant increments in G5-G7 **(D)** and >G7 **(E)**, were found in females over males after 6 months of treatment. Plasma osmolality was lower in females **(F)**.

TABLE 3 | Changes from baseline values of selected biochemical variables.

Variable	Change	Female	Male	p
Serum Glucose (mg/dl)	Δ 0 to 12 Months	−22.96 ± 21.78	−3.43 ± 40.58	0.674
BUN (mg/dl)	Δ 0 to 12 Months	−6.27 ± 6.89	24.81 ± 6.57	0.002
Serum Albumin (g/dl)	Δ 0 to 12 Months	−0.22 ± 0.17	−0.06 ± 0.13	0.442
Serum Sodium (mEq/L)	Δ 0 to 6 Months	−4.192 ± 1.08	−1.08 ± 0.826	0.035
Serum Osmolality (mOsm/L)	Δ 0 to 12 Months	−6.00 ± 2.73	−2.39 ± 1.83	0.287
ICO fragments (Total)	Δ 0 to 12 Months	5.343 ± 0.58	4.681 ± 0.41	0.366

increments in icodextrin metabolites could be masked by increment in blood volume and be detectable until they accumulate along time and reach threshold of the technique used for the analysis. However, the decline observed in osmolality is an indirect support of the increment of icodextrin products, this mean displacement of other active molecules and ions accounting for osmolality (Mistry et al., 1994; Wolfson et al., 2002).

Explanations for the higher increments of icodextrin metabolites in women are not clear. Icodextrin pharmacokinetics follows a simple, single-compartment model that can be approximated by zero-order absorption and first-order elimination (Moberly et al., 2002), this means the main factors affecting its blood concentration are administered dose and hydrolysis or elimination. A standard volume of 2.0 L/Bag

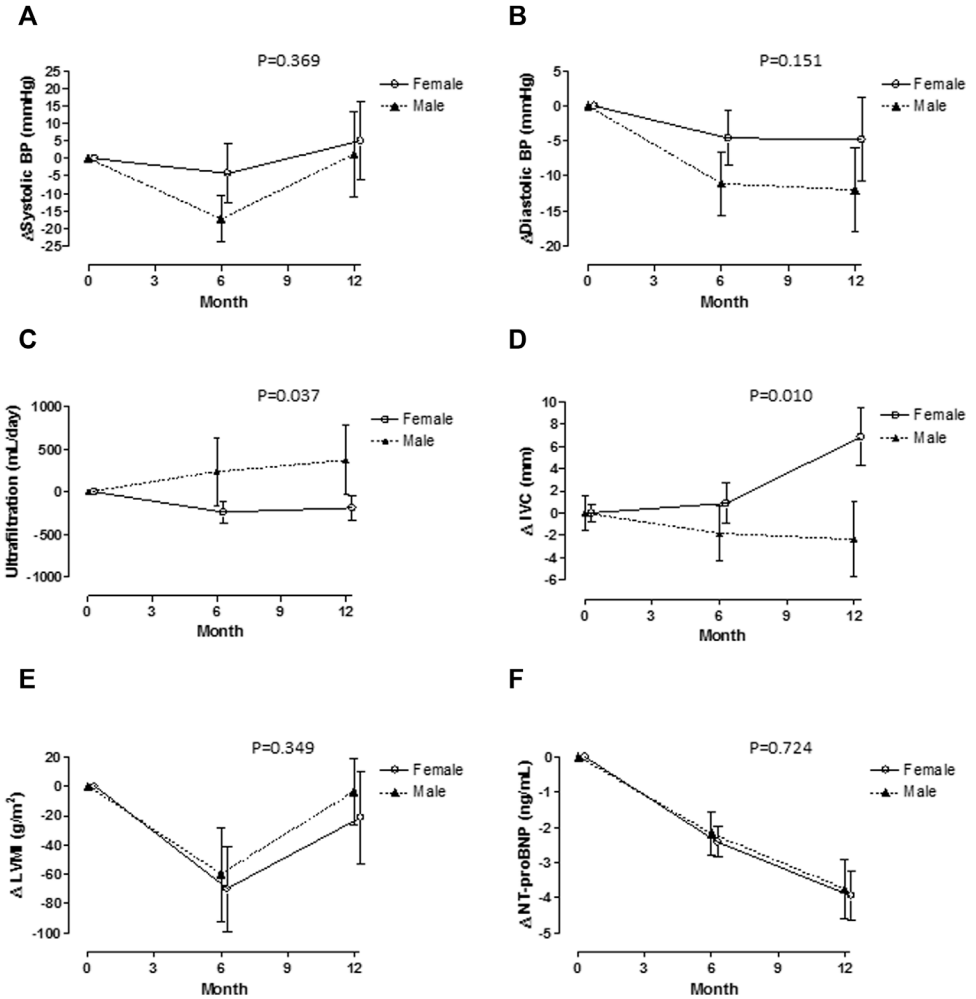

FIGURE 2 | Cardiovascular variables are shown by sex. Systolic blood pressure **(A)** decreased at six months, but move back to baseline values there were no differences by sex. Diastolic blood pressure decreased after six months with a more significant change in females **(B)**. Changes in ultrafiltration were different, in males increased and in females had small decrements **(C)**. Inferior Vena Cava varied in opposite way, increased in females and decreased in males **(D)**. Left ventricle mass index and NT-proBNP changes are shown in **(E,F)**, there were no significant differences by sex.

was used in all patients; this means the amount of icodextrin by body surface area was higher in females. On the other hand, net UF was lower among females; this picture might be secondary to increased intraperitoneal pressure which promotes more lymphatic absorption of peritoneal fluid and the icodextrin it contains. Intraperitoneal pressure was not measured; however, high fluid volume/body surface area ratio promotes more pressure and less UF (Paniagua, et al., 2004; Ventura, et al., 2000; Krediet, et al., 1988).

Another explanation derives from the efforts to find prognostic markers for the future development of obesity and diabetes. Biochemical and genetic research suggest that small number of genes copies encoding salivary and pancreatic α-Amylases confers higher susceptibility for this disease. Less number of α-Amylases genes copies is present in obese and diabetic patients compared with normal subjects. Furthermore, the number is even small in women than in men, which match with epidemiological studies showing higher prevalence of obesity and diabetes in women than in men (Nakajima, 2016; Viljakainen, et al., 2015). Differences in genetic pattern have not been found in some studies; however, lower serum α-Amylase activity is significantly associated with diabetes in women (Al-Akl, et al., 2021). Icodextrin comes into blood stream via lymphatic vessels, then it is metabolized by α-Amylase in small fragments, this means Icodextrin fragments depend on α-Amylase amount and activity (Olszowska, et al., 2019). Data from the present study are congruent with aforementioned findings. All patients were diabetic and differences in icodextrin metabolites higher in females, and α-Amylase activity was lower in females, the group which is expected to have a smaller number of α-Amylase gene copies.

And additional but not proved explanation is related enzyme activity. Macroamylase is an enzymatically active circulating complex of amylase bound noncovalently to immunoglobulins

or to polysaccharides which is cleared from circulation by the kidney. Its size, interferes the bound of large substrates and consequently total activity decreases (Rosenblum et al., 1992). Contribution of Macroamylase to total α-Amylase activity in end stage renal disease patients is unknown. However, the presence of icodextrin could interfere its activity in hydrolyzing icodextrin itself and other small oligosaccharides. Icodextrin also exerts a competitive inhibition on normal α-Amylase. It is important to mention that in PD patients with regular use of icodextrin solutions, the plasma enzyme activity may decrease until 90% (Schoenicke et al., 2002). This means, the amount of available enzyme units is insufficient for icodextrin metabolism, which may be even more important in diabetic women who have low copies of α-Amylase genes and activity.

We do not know whether the observed concentrations of icodextrin metabolites completely explain increments in blood volume represented by increased inferior vena cava diameters. Calculations of the colloid osmotic pressure generated by icodextrin fragments indicates that 76% of pressure is generated by fragments larger than 8.5 kDa and small fragments of 2.1 kDa generates only 3% (Nishimura, et al., 2008). As was previously mentioned, blood volume was not measured and the pool of each fragment cannot be calculated.

Changes in blood pressure and Left ventricle mass index move according to concentrations of icodextrin metabolites; however, differences between sexes were not clear. Small sample size may explain the lack of statistical difference.

The study has some limitations including a small sample size. In spite of that, significant differences were seen in the most important findings. Other refers to indirect measurements of blood volume; inferior vena cava diameter has significant correlation with measurements with dilution methods and repeated measurements in the same patients reduce variability. Measurement of number of α-Amylase gene copies was not done; this evaluation requires complex technologies since the number of copies should be accompanied with evaluation of gene expression and the kinetic characteristics of the enzyme, particularly with its susceptibility of inhibition by icodextrin.

In summary, these data suggest that females are more susceptible to accumulation of icodextrin metabolites during long term PD treatment with standardized PD solution volumes, and that this might cause blood volume expansion, and return of blood pressure and Left ventricle mass index to baseline values. Further studies are necessary for the adequate evaluation of genetic and biochemical characteristics of α-Amylase as a possible determinant of icodextrin metabolites. Adjustments of icodextrin prescription on basis of diabetes, gender, and body size need also be analyzed.

DATA AVAILABILITY STATEMENT

The original contributions presented in the study are included in the article/Supplementary materials, further inquiries can be directed to the corresponding authors.

ETHICS STATEMENT

The studies involving human participants were reviewed and approved by Comité Nacional de Investigación Científica, IMSS. The patients/participants provided provided their written informed consent to participate in this study.

AUTHOR CONTRIBUTIONS

RP: Study design, conduction, and analysis. EG-L: Study conduction and icodextrin metabolite assay. MA-D: Biochemical analysis adviser and results analysis. MV: Study organization and conduction. OO: Cardiology assesments and results analysis. MP-U: Biochemical analysis. BL: Paper organization and review.

ACKNOWLEDGMENTS

Authors want to thank Mr. Alejandro Hinojosa-Rojas for his assistance in data management, and Ms. Susan Drier for her help in manuscript preparation.

REFERENCES

Al-Akl, N. S., Thompson, R. I., and Arredouani, A. (2021). Reduced Odds of Diabetes Associated with High Plasma Salivary α-amylase Activity in Qatari Women: a Cross-Sectional Study. *Sci. Rep.* 11 (1), 11495. doi:10.1038/s41598-021-90977-y

Anderstam, B., García–López, E., Heimbürger, O., and Lindholm, B. (2003). Determination of α-Amylase Activity in Serum and Dialysate from Patients Using Icodextrin-Based Peritoneal Dialysis Fluid. *Perit. Dial. Int.* 23, 146–150. doi:10.1177/089686080302300209

Bouchi, R., Babazono, T., Inoue, A., Tanaka, M., Tanaka, N., Hase, M., et al. (2006). Icodextrin Increases Natriuretic Peptides in Diabetic Patients Undergoing CAPD. *Perit. Dial. Int.* 26, 604–607. doi:10.1177/089686080602600517

Cho, Y., Johnson, D. W., Badve, S., Craig, J. C., Strippoli, G. F. K., and Wiggins, K. J. (2013). Impact of Icodextrin on Clinical Outcomes in Peritoneal Dialysis: a Systematic Review of Randomized Controlled Trials. *Nephrol. Dial. Transpl.* 28, 1899–1907. doi:10.1093/ndt/gft050

Cueto-Manzano, A. M., and Correa-Rotter, R. (2000). Is High Peritoneal Transport Rate an Independent Risk Factor for CAPD Mortality? *Kidney Int.* 57, 314–320. doi:10.1046/j.1523-1755.2000.00817.x

Davies, D. S. (1994). Kinetics of Icodextrin. *Perit. Dial. Int.* 14, 45–51. doi:10.1177/089686089401402S07

Davies, S. J., Lopez, E. G., Woodrow, G., Donovan, K., Plum, J., Williams, P., et al. (2008). Longitudinal Relationships between Fluid Status, Inflammation, Urine Volume and Plasma Metabolites of Icodextrin in Patients Randomized to Glucose or Icodextrin for the Long Exchange. *Nephrol. Dial. Transplant.* 23, 2982–2988. doi:10.1093/ndt/gfn176

Davies, S. J., Woodrow, G., Donovan, K., Plum, J., Williams, P., Johansson, A. C., et al. (2003). Icodextrin Improves the Fluid Status of Peritoneal Dialysis Patients: Results of a Double-Blind Randomized Controlled Trial. *Jasn* 14, 2338–2344. doi:10.1097/01.asn.0000083904.12234.27

De Jesús Ventura, M., Amato, D., Correa–Rotter, R., and Paniagua, R. (2000). Relationship between Fill Volume, Intraperitoneal Pressure, Body Size, and Subjective Discomfort Perception in CAPD Patients. *Perit. Dial. Int.* 20, 188–193. doi:10.1177/089686080002000205

García-López, E., Anderstam, B., Heimbürger, O., Amici, G., Werynski, A., and Lindholm, B. (2005). Determination of High and Low Molecular Weight Molecules of Icodextrin in Plasma and Dialysate, Using Gel Filtration Chromatography, in Peritoneal Dialysis Patients. *Perit. Dial. Int.* 25, 181–191. doi:10.1177/089686080502500213

García-López, E., Werynski, A., Heimbürger, O., Filho, J. C., Lindholm, B., and Anderstam, B. (2008). Rate of Synthetic Oligosaccharide Degradation as a Novel Measure of Amylase Activity in Peritoneal Dialysis Patients. *Perit. Dial. Int.* 28, 296–304. doi:10.1177/089686080802800317

Goossen, K., Becker, M., Marshall, M. R., Bühn, S., Breuing, J., Firanek, C. A., et al. (2020). Icodextrin versus Glucose Solutions for the Once-Daily Long Dwell in Peritoneal Dialysis: An Enriched Systematic Review and Meta-Analysis of Randomized Controlled Trials. *Am. J. Kidney Dis.* 75, 830–846. doi:10.1053/j.ajkd.2019.10.004

Han, S. H., Ahn, S. V., Yun, J. Y., Tranaeus, A., and Han, D.-S. (2012). Effects of Icodextrin on Patient Survival and Technique Success in Patients Undergoing Peritoneal Dialysis. *Nephrol. Dial. Transplant.* 27, 2044–2050. doi:10.1093/ndt/gfr580

Ho-Dac-Pannekeet, M. M., Schouten, N., Langendijk, M. J., Hiralall, J. K., de Waart, D. R., Struijk, D. G., et al. (1996). Peritoneal Transport Characteristics with Glucose Polymer Based Dialysate. *Kidney Int.* 50, 979–986. doi:10.1038/ki.1996.399

Htay, H., Johnson, D. W., Wiggins, K. J., Badve, S. V., Craig, J. C., Strippoli, G. F., et al. (2018). Biocompatible Dialysis Fluids for Peritoneal Dialysis. *Cochrane Database Syst. Rev.* 10 (10), CD007554. doi:10.1002/14651858.CD007554.pub3

Krediet, R., and Mujais, S. (2002). Use of Icodextrin in High Transport Ultrafiltration Failure. *Kidney Int.* 62, S53–S61. doi:10.1046/j.1523-1755.62.s81.8.x

Krediet, R. T., Boeschoten, E. W., Struijk, D. G., and Arisz, L. (1988). Differences in the Peritoneal Transport of Water, Solutes and Proteins between Dialysis with Two- and with Three-Litre Exchanges. *Nephrol. Dial. Transpl.* 3, 198–204.

Li, P. K. T., Culleton, B. F., Ariza, A., Do, J.-Y., Johnson, D. W., Sanabria, M., et al. (2013). Randomized, Controlled Trial of Glucose-Sparing Peritoneal Dialysis in Diabetic Patients. *Jasn* 24, 1889–1900. doi:10.1681/ASN.2012100987

Mistry, C. D., Gokal, R., Peers, E., Brown, C. B., Smith, S., Edwards, D. L., et al. (1994). A Randomized Multicenter Clinical Trial Comparing Isosmolar Icodextrin with Hyperosmolar Glucose Solutions in CAPD. *Kidney Int.* 46, 496–503. doi:10.1038/ki.1994.300

Moberly, J. B., Mujais, S., Gehr, T., Hamburger, R., Sprague, S., Kucharski, A., et al. (2002). Pharmacokinetics of Icodextrin in Peritoneal Dialysis Patients. *Kidney Int.* 62 (81), S23–S33. doi:10.1046/j.1523-1755.62.s81.5.x

Nakajima, K. (2016). Low Serum Amylase and Obesity, Diabetes and Metabolic Syndrome: A Novel Interpretation. *Wjd* 7, 112–121. doi:10.4239/wjd.v7.i6.112

Nishimura, K., Kamiya, Y., Miyamoto, K., Nomura, S., and Horiuchi, T. (2008). Molecular Weight of Polydisperse Icodextrin Effects its Oncotic Contribution to Water Transport. *J. Artif. Organs.* 11, 165–169. doi:10.1007/s10047-008-0423-6

Olszowska, A., Waniewski, J., Stachowska-Pietka, J., Garcia-Lopez, E., Lindholm, B., and Wańkowicz, Z. (2019). Long Peritoneal Dialysis Dwells with Icodextrin: Kinetics of Transperitoneal Fluid and Polyglucose Transport. *Front. Physiol.* 10, 1326. doi:10.3389/fphys.2019.01326

Paniagua, R., de Jesús Ventura, M., Rodríguez, E., Sil, J., Galindo, T., Hurtado, M. E., et al. (2004). Impact of Fill Volume on Peritoneal Clearances and Cytokine Appearance in Peritoneal Dialysis. *Perit. Dial. Int.* 24, 156–162. doi:10.1177/089686080402400206

Paniagua, R., Ventura, M.-d. -J., Ávila-Díaz, M., Cisneros, A., Vicenté–Martínez, M., Furlong, M.-d. -C., et al. (2009). Icodextrin Improves Metabolic and Fluid Management in High and High-Average Transport Diabetic Patients. *Perit. Dial. Int.* 29, 422–432. doi:10.1177/089686080902900409

Rosenblum, J. L., Hortin, G. L., Smith, C. H., Pashos, G. E., and Landt, M. (1992). Macroamylases: Differences in Activity against Various-Size Substrates. *Clin. Chem.* 38, 1454–1458. doi:10.1093/clinchem/38.8.1454

Schoenicke, G., Grabensee, B., and Plum, J. (2002). Dialysis with Icodextrin Interferes with Measurement of Serum Alpha-Amylase Activity. *Nephrol. Dial. Transpl.* 17, 1988–1992. doi:10.1093/ndt/17.11.1988

Silver, S. A., Harel, Z., and Perl, J. (2014). Practical Considerations when Prescribing Icodextrin: a Narrative Review. *Am. J. Nephrol.* 39, 515–527. doi:10.1159/000363417

Szeto, C. C., and Johnson, D. W. (2017). Low GDP Solution and Glucose-Sparing Strategies for Peritoneal Dialysis. *Seminars Nephrol.* 37, 30–42. doi:10.1016/j.semnephrol.2016.10.005

Vicenté-Martı´nez, M., Martı´nez-Ramı´rez, L., Muñoz, R., Avila, M., Ventura, M.-d. -J., Rodrı´guez, E., et al. (2004). Inflammation in Patients on Peritoneal Dialysis Is Associated with Increased Extracellular Fluid Volume. *Archives Med. Res.* 35, 220–224. doi:10.1016/j.arcmed.2004.01.003

Viljakainen, H., Andersson-Assarsson, J. C., Armenio, M., Pekkinen, M., Pettersson, M., Valta, H., et al. (2015). Low Copy Number of the AMY1 Locus Is Associated with Early-Onset Female Obesity in Finland. *PLoS One* 10 (7), e0131883. doi:10.1371/journal.pone.0131883

Wang, I.-K., Li, Y.-F., Chen, J.-H., Liang, C.-C., Liu, Y.-L., Lin, H.-H., et al. (2015). Icodextrin Decreases Technique Failure and Improves Patient Survival in Peritoneal Dialysis Patients. *Nephrology* 20, 161–167. doi:10.1111/nep.12375

Wolfson, M., Piraino, B., Hamburger, R. J., and Morton, A. R. (2002). A Randomized Controlled Trial to Evaluate the Efficacy and Safety of Icodextrin in Peritoneal Dialysis. *Am. J. Kidney Dis.* 40, 1055–1065. doi:10.1053/ajkd.2002.36344

Conflict of Interest: The authors declare that the research was conducted in the absence of any commercial or financial relationships that could be construed as a potential conflict of interest.

Publisher's Note: All claims expressed in this article are solely those of the authors and do not necessarily represent those of their affiliated organizations, or those of the publisher, the editors and the reviewers. Any product that may be evaluated in this article, or claim that may be made by its manufacturer, is not guaranteed or endorsed by the publisher.

Copyright © 2022 Paniagua, García-López, Ávila-Díaz, Ventura, Orihuela, Prado-Uribe, Gallardo-Montoya and Lindholm. This is an open-access article distributed under the terms of the Creative Commons Attribution License (CC BY). The use, distribution or reproduction in other forums is permitted, provided the original author(s) and the copyright owner(s) are credited and that the original publication in this journal is cited, in accordance with accepted academic practice. No use, distribution or reproduction is permitted which does not comply with these terms.

frontiers | Frontiers in Physiology

SYSTEMATIC REVIEW
published: 07 June 2022
doi: 10.3389/fphys.2022.906597

The Effectiveness of Duloxetine for Knee Osteoarthritis: An Overview of Systematic Reviews

*Qinxin Zhou[1,2†], Jixin Chen[1,2†], Weijie Yu[1,2], Kun Yang[1,2], Tianci Guo[1,2], Puyu Niu[1,2], Yuntian Ye[1,2] and Aifeng Liu[1,2]**

[1]Department of Orthopaedic Surgery, First Teaching Hospital of Tianjin University of Traditional Chinese Medicine, Tianjin, China, [2]National Clinical Research Center for Chinese Medicine Acupuncture and Moxibustion, Tianjin, China

Background: Knee osteoarthritis (KOA) has become a public health problem. Several systematic reviews (SRs) have reported that duloxetine may be an effective treatment for improving pain and depressive symptoms in patients with KOA.

Aim: To evaluate the available results and provide scientific evidence for the efficacy and safety of duloxetine for KOA.

Methods: A comprehensive search strategy was conducted across eight databases from inception to 31 December 2021. Two researchers independently selected eligible studies, collected data and evaluated those included SRs' quality. For assessing methodological quality, the Assessing the Methodological Quality of Systematic Reviews 2 (AMSTAR 2) was employed. Risk of Bias in Systematic Reviews (ROBIS) was used to assess the risk of bias. Preferred Reporting Items for Systematic Review and Meta-analyses (PRISMA) was utilized for assessing reporting quality. In addition, the Grading of Recommendations Assessment, Development, and Evaluation (GRADE) was used to determine primary outcome indicators' evidence quality.

Results: Totally 6 SRs were contained in this overview. After assessment based on AMSTAR 2, ROBIS, and PRISMA, unsatisfactory results in terms of methodological quality, risk of bias as well as reporting quality, were obtained. Limitations included a search of grey literature, the reasons for selecting the study type, an excluded study list and the specific reasons, reporting bias assessment, and reporting of potential sources of conflict of interest. According to the GRADE results, the evidence quality was high in 0, moderate in 5, low in 19, and very low in 36. Limitations were the most commonly downgraded factor, followed by publication bias and inconsistency.

Conclusion: Duloxetine may be an effective treatment for improving pain and depressive symptoms in KOA patients with acceptable adverse events. However, due to the low quality of the available evidence, the original study design and the quality of evidence from SRs should be further improved, so as to provide strong scientific evidence for definitive conclusions.

Systematic Review Registration: PROSPERO; (http://www.crd.york.ac.uk/PROSPERO/), identifier (CRD42021289823).

Keywords: duloxetine, knee osteoarthritis, depression, overview, systematic review, methodological quality

OPEN ACCESS

Edited by:
Christina Maria Pabelick, Mayo Clinic, United States

Reviewed by:
Guoju Hong, University of Alberta, Canada
Mohamed Mortada, Zagazig University, Egypt

****Correspondence:***
Aifeng Liu
draifeng@163.com

†These authors have contributed equally to this work

Specialty section:
This article was submitted to Clinical and Translational Physiology, a section of the journal Frontiers in Physiology

Received: *28 March 2022*
Accepted: *16 May 2022*
Published: *07 June 2022*

Citation:
Zhou Q, Chen J, Yu W, Yang K, Guo T, Niu P, Ye Y and Liu A (2022) The Effectiveness of Duloxetine for Knee Osteoarthritis: An Overview of Systematic Reviews. Front. Physiol. 13:906597. doi: 10.3389/fphys.2022.906597

1 INTRODUCTION

Knee osteoarthritis (KOA) refers to one of the most frequent joint diseases, characterized by progressive cartilage loss, subchondral bone remodeling and synovial inflammation, causing symptoms such as chronic pain, joint stiffness as well as physical and psychological disturbances (Pigeolet et al., 2021; Sharma, 2021). Over the past 20 years, around 250 million people across the world have been diagnosed with KOA, and the global prevalence has increased significantly (GBD 2015 Disease and Injury Incidence and Prevalence Collaborators, 2015). In addition to chronic pain and disability, nearly 21% of adults undergoing KOA suffer from depression, and the relative risk of depression in people with KOA compared to those without KOA is 1.17 (Kessler et al., 2003; Stubbs et al., 2016). In patients suffering from KOA, including depression, the depressive or anxious mood is associated with higher levels of pain (Axford et al., 2010). They were reported to have higher healthcare utilization costs and more frequent use of pain medication due to low awareness of depression (Gleicher et al., 2011). In addition, this group of patients were also less probably to fully comply with the recommended treatment regimens than KOA patients with undiagnosed depression, thereby increasing the burden of illness and the difficulty of management (Sale et al., 2008). Current guidelines have evaluated over 50 treatments for osteoarthritis of the knee (Bannuru et al., 2019; Kolasinski et al., 2020). Oral medications contain acetaminophen, NSAIDs, and strong and weak opioids. The guidelines recommend paracetamol as a first-line drug and NSAIDs and opioids as second and third-line drugs. However, there are still reservations in association with the long-term safety and efficacy of NSAIDs and opioids (Bruyère et al., 2019; Arden et al., 2021).

Duloxetine refers to a 5-hydroxytryptamine and noradrenaline reuptake inhibitor that treats pain using the downstream pain modulation system (Ferreira et al., 2021). Guidelines for osteoarthritis, such as the Osteoarthritis Research Society International (OARSI) and the American College of Rheumatology, recommend the application of duloxetine for pain management (Bannuru et al., 2019; Kolasinski et al., 2020). Chronic pains associated with osteoarthritis involve dysfunction of central pain pathways in line with researches about the pathophysiology of KOA pain (Malfait and Schnitzer, 2013; Miller et al., 2014). Studies have demonstrated that imbalances in the 5-hydroxytryptamine and norepinephrine systems within the central pain pathway exert a vital function in the onset of pain sensitization (Miller et al., 2017; Bannuru et al., 2019). Therefore, duloxetine may be a better treatment. In animal models of central sensitization to KOA, duloxetine is effective in relieving persistent pain (Havelin et al., 2016). Duloxetine is currently being clinically applied for the treatment of KOA and has exhibited good symptom relief (Wang et al., 2017; Uchio et al., 2018; Koh et al., 2019). The number of clinical studies and SRs reporting the efficacy of duloxetine for the treatment of KOA is increasing. As a top element of the evidence pyramid, SRs are often considered to aid in identifying, evaluating, and synthesizing study-based evidence in order to assist with clinical decision-making (Siddaway et al., 2019). Nevertheless, the conclusions of these SRs are controversial due to the irregular reporting, methodological flaws, and low-quality evidence. Meanwhile, their clinical guidance needs to be further validated. Only high-quality evidence-based medical evidence is reliable, while low-quality evidence can instead generate mislead clinicians. An overview of SRs is a comprehensive approach to evaluating studies across multiple SRs and synthesizing evidence (Thomson et al., 2010; Smith et al., 2011; Baker et al., 2014; Huang et al., 2021).

To our knowledge, this overview of SRs is the first attempt with the purpose of assessing the efficacy and safety of duloxetine SRs objectively and comprehensively in enhancing pain and depressive symptoms in patients undergoing KOA. We aim to provide a scientific basis for clinicians, decision-makers and patients with KOA as well as a basis for guidance for future SR producers.

TABLE 1 | Search strategy for PubMed database.

Query	Search item
# 1	Osteoarthritis, Knee (Mesh)
# 2	Osteoarthritis, Knee (Title/Abstract)
# 3	Knee osteoarthritis (Title/Abstract)
# 4	Knee osteoarthritides (Title/Abstract)
# 5	Knee pain (Title/Abstract)
# 6	Knee joint osteoarthritis (Title/Abstract)
# 7	Knee arthritis (Title/Abstract)
# 8	Osteoarthritis of knee (Title/Abstract)
# 9	KOA (Title/Abstract)
# 10	Gonarthrosis (Title/Abstract)
# 11	Osteoarthrosis (Title/Abstract)
# 12	# 1 OR # 2–11
# 13	Duloxetine hydrochloride (MeSH)
# 14	Duloxetine (Title/Abstract)
# 15	Cymbalta (Title/Abstract)
# 16	# 13 OR # 14–15
# 17	Meta-analysis (Publication Type)
# 18	Meta-analysis (MeSH)
# 19	Systematic evaluation (Title/Abstract)
# 20	Systematic review (Title/Abstract)
# 21	Meta analysis (Title/Abstract)
# 22	Meta analyses (Title/Abstract)
# 23	# 17 OR # 18–22
# 24	# 12 AND # 16 AND # 23

2 METHODS

2.1 Protocols and Registration

A predetermined written protocol of the current overview was registered in the PROSPERO database with the registration number: CRD42021289823.

2.2 Search Strategy

Two independent researchers conducted electronic literature searches in four international electronic databases (PubMed,

EMBASE, Cochrane Library, and Web of Science) and four Chinese electronic databases (Chinese National Knowledge Infrastructure, Chinese Biological Medicine, WanFang and Chongqing VIP database) from the inception to 31 December 2021. In addition, the research registry, relevant grey literature and consultation with experts in the relevant fields were further searched manually. No language restriction was applied. This study utilized the following search terms, including ("osteoarthritis of the knee" OR "knee osteoarthritis" OR "koa" OR "gonarthritis" OR "knee pain") AND ("duloxetine" OR "duloxetine hydrochloride" OR "Cymbalta") AND ("systematic review" OR "systematic evaluation" OR "meta-analyses" OR "meta-analysis"). Apart from that, the search strategy was illustrated by PubMed (**Table 1**).

2.3 Inclusion Criteria

This study included SRs matched with the following criteria: 1) Study design: SRs of RCTs reporting the effects of duloxetine on KOA. To be eligible for this overview, several restrictions were applied on SRs. Besides, a comprehensive search strategy was conducted using 5 or more databases. RCTs in the included SRs should conduct at least 2-weeks duloxetine interventions with >10 patients in each group. SRs were reported according to the PRISMA statement guidelines, with quantitative synthesis (meta-analysis) and language restricted to Chinese and English. 2) Study participants met the KOA diagnostic criteria of the American College of Rheumatology, regardless of gender, age, race, nationality, or disease duration. 3) Study intervention: the treatment group adopted duloxetine as the main drug, while the control group used standard drug treatment without duloxetine, placebo, or no treatment. 4) Study outcome measures included Brief Pain Inventory-Severity (BPI-S), Patient Global Improvement-Inventory (PGI-I), Western Ontario and McMaster Universities score total score (WOMAC), WOMAC pain score, WOMAC physical function score, WOMAC stiffness score, 30% reduction and 50% reduction.

2.4 Exclusion Criteria

Repeated publications; non-SRs; the control group using duloxetine as the treatment; conference abstracts.

2.5 Literature Screening and Data Extraction

In accordance with the search strategy, two researchers imported the retrieved titles into Endnote software. After the removal of duplicates, titles and abstracts of articles detected in the search are screened independently by two members and categorized as included, unclear or exclude. The full reports of all articles that categorized as included or unclear are examined regarding the compliance of reviews with eligibility criteria. If there was any dispute, they discussed and agreed, or the third member decided whether to include it or not. Based on the data extracted from SRs by two independent members, the following could be summarized including first author's initials, publication year, number of included RCTs, sample size, interventions in the treatment and control groups, a tool for assessing quality, adverse events, outcomes as well as main conclusions of the included SRs.

2.6 Review Quality Assessment

The quality evaluation of this overview mainly followed the Cochrane Handbook and the methods of relevant high systematic evaluation re-evaluation studies. The quality evaluation mainly contained four aspects of evaluation, respectively, methodological quality, report quality, evidence quality and risk of bias and was performed by two investigators independently. If differences were encountered, the consensus was achieved through negotiation, and a third party ruled if necessary.

2.6.1 Methodological Quality Evaluation

Evaluation of the methodology quality of the included SRs was done based on the AMSTAR 2 tool, which is a comprehensive critical appraisal instrument to evaluate SRs of randomized trials (Shea et al., 2017). The contained studies were rated as high quality according to the criteria of "no or only 1 non-critical entry non-conformity," "more than 1 non-critical entry non-conformity" and "moderate quality". The included studies were rated as high, medium, low, and very low quality in line with the criteria of "no or one non-critical entry non-conformity," "more than one non-critical entry non-conformity," "one non-critical entry non-conformity," "one non-critical entry non-conformity," "one non-critical entry non-conformity," "low quality," and "very low quality". In addition, totally16 entries were evaluated, including seven key entries, namely, entries 2, 4, 7, 9, 11, 13, and 15.

2.6.2 Risk of Bias Evaluation

The risk of bias evaluation of the included SRs was performed using 24 entries in the ROBIS tool, which is the first rigorously developed tool designed particularly in order to evaluate the risk of bias in SRs (Whiting et al., 2016). The instrument is finished in 3 phases, which can assist in judging the risk of bias during the process of review, results as well as conclusions. Each entry was described by the authors, and responses to all questions were indicated by "yes," "probably yes," "could be," "no," and "no information". Finally, the risk of bias in the field was judged as "low," "high," or "uncertain". The risk of bias in this area is "low" if all the landmark questions are answered as "yes" or "probably yes". If any of the landmark questions are answered by "maybe" or "could be," the risk of bias in this area is "low". If the answers to any of the landmark questions were "may or may not" or "no", the risk of bias was "high". If the offered information was inadequate to make a judgment, the risk of bias was "uncertain". In addition, the risk of bias was "uncertain" if the information provided was not sufficient.

2.6.3 Report Quality Evaluation

The PRISMA statement is a reporting guidance that reflects advances in methods with the purpose of identifying, selecting, appraising, and synthesizing studies and can be adopted for evaluating the reporting quality in the contained SRs (28). The

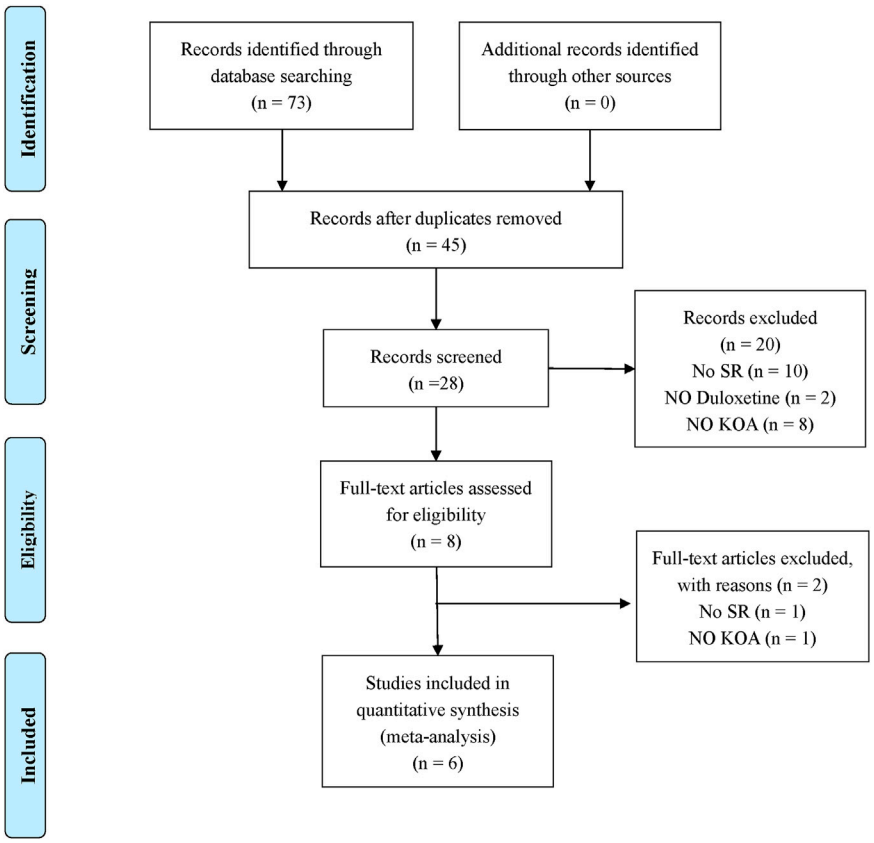

FIGURE 1 | Literature selection procedure.

PRISMA statement list is consisted of 27 entries, including seven perspectives of SRs, respectively, title, abstract, introduction, methods, results, discussion, and funding (Page et al., 2021). The answer options for each item contain "yes," "no," and "partial yes". The completion of each project is denoted as a ratio. In addition, the PRISMA statement claims that reports with completeness of less than 50% of each entry are considered to have a deficiency in the reported information.

2.6.4 GRADE Evidence Quality Evaluation

The quality of evidence for each outcome indicator involved in the SRs was assessed by the GRADE tool, with limitations, inconsistency, non-directness, imprecision as well as publication bias as downgrading factors (Guyatt et al., 2008). Apart from that, the quality of evidence was regarded to have high quality with no downgrading, moderate quality with 1 downgrade, low quality with 2 downgrades as well as very low quality with 3 downgrades and above. The current work carried out a descriptive analysis of extracting findings from the contained researches concerning the effectiveness and safety of duloxetine in treating KOA.

2.7 Data Synthesis and Presentation

A narrative synthesis was applied in the current overview. In addition, the features and results of each SR as well as the findings of AMSTAR 2, ROBIS, GRADE, and PRISMA were shown in tables and figures.

3 RESULTS

3.1 Literature Search

According to the search strategy, 73 original titles were initially examined, including 12 from Chinese National Knowledge Infrastructure, 3 from WanFang database, 1 for Chongqing VIP database, 0 from Chinese Biological Medicine, 16 from PubMed, 17 from EMBASE, 0 from The Cochrane Library, and 24 from Web of Science. In addition, the title list was imported into Endnote software. After the duplicates were screened out, eight articles were left. After referring to the full text, six papers were finally included (Wang et al., 2015; Chen et al., 2019; Gao et al., 2019; Osani and Bannuru, 2019; Qu et al., 2020; Chen et al., 2021). The literature screening process is detailed in **Figure 1**.

3.2 Basic Features of Included Literature

Totally 6 SRs were included in this study, all of which have been published between 2015–2021, with 3 published in 2019. The number of RCTs in the SRs ranged from 3 to 6. Among them, five were published in English (Wang et al., 2015; Chen et al., 2019;

TABLE 2 | Characteristics of the included SRs.

Author (year)	Country	Number of RCT (Total population)	Intervention		Outcome measures	Quality assessment tool	Overall conclusion
			Treatment group	Control group			
Wang (2015)	China	3 (*n* = 1001)	Duloxetine 60/120 mg, Qd	Placebo	BPI-S, 30% pain reduction rate, 50% pain reduction rate, PGI-I, WOMAC physical function score, AEs, TFAEs, SAEs, TDR	Jadad score	This analysis suggests duloxetine [60/120 mg, quaque die (Qd)], compared with placebo control, resulted in a greater reduction in pain, improved function and patient-rated impression of improvement, and acceptable adverse effects for the treatment of OAK pain after approximately 10–13 weeks of treatment.
Chen (2019)	China	6 (*n* = 2059)	Duloxetine 60/120 mg, Qd	Placebo	BPI-S, weekly 24-h average pain score, 30% pain reduction rate, 50% pain reduction rate, WOMAC stiffness score, WOMAC physical function score, TFAEs, SAEs, TDR	Cochrane risk of bias tool	Duloxetine is effective in the management of chronic pain and loss of physical function in knee OA with acceptable adverse events despite having no advantage in treating joint stiffness. Future trials should focus on determining the optimal treatment regimen.
Gao (2019)	China	5 (*n* = 1774)	Duloxetine 60/120 mg, Qd	Placebo	BPI-S, 30% pain reduction rate, 50% pain reduction rate, PGI-I, WOMAC total score, WOMAC pain score, WOMAC stiffness score, WOMAC physical function score, TFAEs, SAEs, TDR	Cochrane risk of bias tool	Duloxetine was an effective and safe choice to improve pain and functional outcome in OA patients. However, further studies are still needed to find out the optimal dosage for OA and examine its long-term efficacy and safety.
Osani (2019)	America	5 (*n* = 1713)	Duloxetine 60/120 mg, Qd	Placebo	WOMAC pain score, WOMAC physical function score, TFAEs, SAEs, TDR, Gastrointestinal adverse event, Quality of life improvement, Improvement of depressive symptoms	Cochrane risk of bias tool	Duloxetine may be an effective treatment option for individuals with knee OA, but use of the drug is associated with a significantly higher risk of adverse events
Qu (2020)	China	6 (*n* = 2059)	Duloxetine 60/120 mg, Qd	Placebo	BPI-S, WOMAC total score, WOMAC pain score, WOMAC stiffness score, WOMAC physical function score, Dry mouth, Drowsiness, Nausea	Cochrane risk of bias tool	Duloxetine can relieve pain and improve knee function in PATIENTS with KOA, but it is necessary to pay attention to the occurrence of adverse reactions
Chen (2021)	China	6 (*n* = 2059)	Duloxetine 60/120 mg, Qd	Placebo	BPI-S, BPI-I, 30% pain reduction rate, 50% pain reduction rate, Pain reduction average rate, PGI-I, CGI-I, WOMAC pain score, WOMAC stiffness score, WOMAC physical function score, TFAEs, SAEs, SF-36 physical functional subscale, SF-36 bodily pain subscale, SF-36 role physical subscale	Cochrane risk of bias tool	Duloxetine may be an effective treatment option for knee OA patients but further rigorously designed and well-controlled randomized trials are warranted.

Abbreviations: AEs, adverse events; BPI-I, Brief Pain Inventory-Interference; BPI-S, Brief Pain Inventory-Severity; CGI-S, Clinical Global Impressions of Severity; PGI-I, Patient's Global Impression of Improvement; SAEs, Serious adverse events; SF-36, 36-Item Short-Form Health Status Survey; TDR, Treatment discontinuation rate; TEAEs, treatment-emergent adverse events; WOMAC, Western Ontario and McMaster Universities Osteoarthritis Index.

Gao et al., 2019; Osani and Bannuru, 2019; Chen et al., 2021) and one in Chinese (Qu et al., 2020). Among the risk of bias assessment tools for RCTs, one paper chose the Jadad score (Wang et al., 2015) and five papers selected the Cochrane Handbook recommended risk of bias assessment tools (Chen et al., 2019; Gao et al., 2019; Osani and Bannuru, 2019; Qu et al., 2020; Chen et al., 2021). In addition, six papers decided on duloxetine 60/120 mg, with Qd as the intervention group and placebo as the control group, finding that duloxetine improved pain and function in KOA patients while attention is required to be paid to the occurrence of adverse events. **Table 2** presents the basic characteristics of the included studies.

3.3 Results of Review Quality Assessment

3.3.1 Methodological Quality

Table 3 showed the findings of methodological quality assessed by AMSTAR 2 tool. All SRs were rated to be the critical low quality. For the critical items, 3 SRs (Wang et al., 2015; Osani and Bannuru, 2019; Qu et al., 2020) reported either predefined protocol (item 2). No SR reported the comprehensive search strategy (item 4), offered the list of excluded studies and provided the reasons for exclusion (item 7) completely. When it came to the evaluation of risk of bias, 5 SRs considered random sequence allocation as well as the selection of the outcome report (item 9). In terms of statistical combination, 6 SRs (100%) integrated the

TABLE 3 | Results of the AMSTAR 2 assessments.

Author (year)	AMSTAR 2																Overall quality
	Q1	Q2	Q3	Q4	Q5	Q6	Q7	Q8	Q9	Q10	Q11	Q12	Q13	Q14	Q15	Q16	
Wang (2015)	Y	N	N	PY	N	Y	N	PY	PY	Y	Y	N	Y	Y	Y	N	Critically low
Chen (2019)	Y	Y	N	PY	N	Y	N	PY	Y	Y	Y	N	Y	Y	N	N	Critically low
Gao (2019)	Y	Y	N	PY	N	Y	N	PY	Y	Y	Y	N	Y	Y	N	N	Critically low
Osani (2019)	Y	N	N	PY	N	Y	N	PY	Y	N	Y	N	Y	Y	Y	N	Critically low
Qu (2020)	Y	N	N	PY	N	Y	N	PY	Y	Y	Y	N	Y	Y	N	N	Critically low
Chen (2021)	Y	Y	N	PY	N	Y	N	PY	Y	Y	Y	N	Y	Y	N	N	Critically low
Number of Y (%)	6 (100)	3 (50)	0 (0)	0 (0)	0 (0)	6 (100)	0 (0)	0 (0)	5 (83.3)	5 (83.3)	6 (100)	0 (0)	6 (100)	6 (100)	2 (33.3)	0 (0)	

Abbreviations: Y, Yes; PY, Partial Yes; N, No.

Q1: Did the research questions and inclusion criteria for the review include the components of PICO?

Q2: Did the report of the review contain an explicit statement that the review methods were established prior to the conduct of the review and did the report justify any significant deviations from the protocol?

Q3: Did the review authors explain their selection of the study designs for inclusion in the review?

Q4: Did the review authors use a comprehensive literature search strategy?

Q5: Did the review authors perform study selection in duplicate?

Q6: Did the review authors perform data extraction in duplicate?

Q7: Did the review authors provide a list of excluded studies and justify the exclusions?

Q8: Did the review authors describe the included studies in adequate detail?

Q9: Did the review authors use a satisfactory technique for assessing the risk of bias (RoB) in individual studies that were included in the review?

Q10: Did the review authors report on the sources of funding for the studies included in the review?

Q11: If meta-analysis was performed did the review authors use appropriate methods for statistical combination of results?

Q12: If meta-analysis was performed, did the review authors assess the potential impact of RoB in individual studies on the results of the meta-analysis or other evidence synthesis?

Q13: Did the review authors account for RoB in individual studies when interpreting/discussing the results of the review?

Q14: Did the review authors provide a satisfactory explanation for, and discussion of, any heterogeneity observed in the results of the review?

Q15: If they performed quantitative synthesis did the review authors carry out an adequate investigation of publication bias (small study bias) and discuss its likely impact on the results of the review?

Q16: Did the review authors report any potential sources of conflict of interest, including any funding they received for conducting the review?

result with suitable methods (item 11) and explained RoB in individual studies while exploring the results (item 13). The last critical item (item 15) was associated with publication bias and 2 SRs (Wang et al., 2015; Osani and Bannuru, 2019) reported it fully. Items 3, 5, 12, and 16 were rated especially low quality. In addition, all SRs had chosen RCT, without accounting for the causes of selection. No SR reported the potential sources of conflicts of interest containing the funding sources for the studies.

3.4 Risk of Bias of Included SRs

The results of the risk of bias evaluated by ROBIS tool demonstrated that all SRs were rated as low risk in Domain 1 of Phase 2 (study eligibility criteria). In terms of Domain 2, by evaluating the identification and selection of studies, 6 (100%) SRs were rated to be low-risk. 1 SR (Wang et al., 2015) was rated as high risk in Domain 3 (data collection and study appraisal) with 3 SRs (Chen et al., 2019; Gao et al., 2019; Qu et al., 2020) being rated as high risk in Domain 4 (synthesis and findings). Finally, 2 SRs (Chen et al., 2019; Gao et al., 2019) were rated to be low-risk in Phase 3 (risk of bias in the review). **Table 4** and **Figure 2** show the detailed results.

3.5 Reporting Quality of Included SRs

The results of reporting quality assessed by PRISMA checklists were shown in **Table 5**. The reporting of the titles, introductions, and discussions of the SRs included is complete (100%). However, some entries were reported to be deficient (<50%) such as item 2 (abstract), item 6 (Information sources), item 7 (Search strategy), item 10 (Data items), item 14 (Reporting bias assessment), item 15 (Certainty assessment), item 16 (Study election), item 20 (Results of syntheses), and item 27 (Availability of data, code and other materials).

3.6 Evidence Quality Grading

The findings of evidence quality rated by GRADE were presented in **Table 6**. The included SRs had a total of 60 outcome indicators. 6 SRs were initially graded as high in evidence because they included RCTs, and were rated for five downgrading factors, respectively, limitations (n = 60, 100%), publication bias (n = 43, 71.7%), inconsistency (n = 32, 53.3%), imprecision (n = 28, 46.7%), and indirectness (n = 0, 0%). The final results revealed that none was high quality, 5 (8.3%) were moderate quality, 19 (31.7%) were low quality, and 36 (60%) were critically low quality.

3.7 Observation Index and Efficacy Evaluation

We summarize the information contained in the SRs, as reported in **Table 7**.

TABLE 4 | Results of the ROBIS tool.

Review	Phase 2				Phase 3
	1.Study eligibility criteria	2.Identification and selection of studies	3.Data collection and study appraisal	4.Synthesis and findings	Risk of bias in the review
Wang (2015)	☺	☹	☹	☺	☺
Chen (2019)	☺	☹	☺	☹	☹
Gao (2019)	☺	☹	☺	☹	☹
Osani (2019)	☺	☹	☺	?	☺
Qu (2020)	☺	☹	☺	☹	☺
Chen (2021)	☺	☹	☺	☺	☺

Abbreviations ☺ = low risk of bias; ☹ = high risk of bias; ? = unclear.

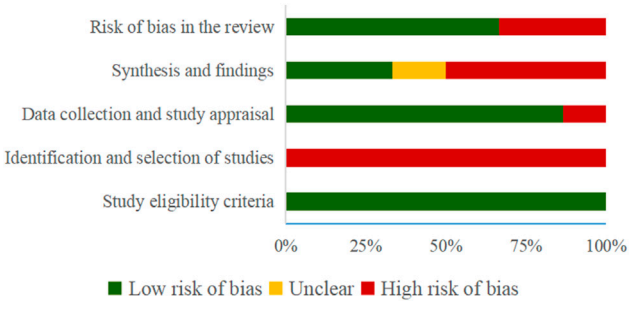

FIGURE 2 | Risk of bias of the included SRs with ROBIS tool.

3.7.1 Pain Reductions

Five SRs (Wang et al., 2015; Chen et al., 2019; Gao et al., 2019; Qu et al., 2020; Chen et al., 2021) reported BPI-S to describe that duloxetine could reduce pain in KOA Patients. All SRs showed that duloxetine was superior to the control group in reducing pain in KOA patients. The largest sample size (Chen et al., 2021) included 5 RCTs with a total of 1,695 patients (MD −0.74, 95% CI, −0.92; −0.57, $p < 0.00001$). The results were statistically and clinically significant.

3.7.2 Improvements in Pain

Four SRs (Wang et al., 2015; Chen et al., 2019; Gao et al., 2019; Chen et al., 2021) reported 30% pain reduction rate and 50% pain reduction rate, which were denoted as moderate and substantial improvements separately. With nearly 30% pain reduction rate, the largest sample size (Chen et al., 2021) included 5 RCTs with a total of 1,696 patients (MD −0.54, 95% CI −0.71; −0.37, $p < 0.00001$). With about 50% pain reduction rate, the largest sample size (Chen et al., 2021) included 5 RCTs with a total of 1,696 patients (MD −0.87, 95% CI −1.07; −0.66, $p < 0.00001$). All SRs demonstrated that duloxetine was superior to the control group in the improvement of pain in KOA patients.

Four SRs (Gao et al., 2019; Osani and Bannuru, 2019; Qu et al., 2020; Chen et al., 2021) reported WOMAC pain score. The largest sample size included 4 RCTs with a total of 1,628 patients (MD −0.81, 95% CI −0.92; −0.69, $p < 0.00001$). 2 SRs (Gao et al., 2019; Qu et al., 2020) reported WOMAC total scores. 6 SRs reported WOMAC physical function score. The largest sample size (Chen et al., 2021) included 6 RCTs with a total of 1986 patients (MD −4.22, 95% CI −5.14; −3.30, $p < 0.00001$). 4 SRs (Chen et al., 2019; Gao et al., 2019; Qu et al., 2020; Chen et al., 2021) reported WOMAC stiffness score. The largest sample size (Chen et al., 2021) included 6 RCTs with a total of 2002 patients (MD −0.47, 95% CI −0.60; −0.34, $p < 0.00001$). These SRs' consensuses were that the duloxetine group was more effective. The SR published in 2019 reported that duloxetine is efficient in managing chronic pain and loss of physical function but has no advantage in the treatment of joint stiffness. Meanwhile, statistically obvious differences in the variable between duloxetine and placebo were also demonstrated.

3.7.3 Patient's Global Impression

Three SRs (Wang et al., 2015; Gao et al., 2019; Chen et al., 2021) reported PGI-I. The largest sample size (Chen et al., 2021) included 5 RCTs with a total of 1741 patients (MD −0.48, 95% CI −0.58; −0.37, $p < 0.00001$). Besides, one SR (Chen et al., 2021) reported that the global impression of the patient measured by CCG-I was significantly improved with duloxetine (MD −0.34, 95% CI −0.44; −0.24, $p < 0.00001$).

3.7.4 Quality of Life and Depressive Symptoms

One SR (Osani and Bannuru, 2019) reported duloxetine showed no significant effects on depression symptoms (SMD −0.09, 95% CI −0.26; 0.07, P: no report) whereas results on quality of life were statistically significant (SMD 0.40, 95% CI 0.26; 0.53, P: no report). In one SR (Chen et al., 2021), involving 3 RCTs and 826 patients, duloxetine was found to negatively influence the reduction of bodily pain (MD = 1.22; 95% CI 0.08; 2.35, $p = 0.04$) and physical functioning subscales (MD 1.62, 95% CI 0.12; 3.13, $p = 0.03$) of the SF-36. The SF-36 physical subscale also showed no indication of improvement (MD = 1.04, 95% CI −0.10; 2.18, $p = 0.07$).

3.7.5 Safety

The main causes of TEAES in the duloxetine therapy group included constipation, nausea, sweating, cough, myalgia, joint pain, palpitations and dry mouth. The results of SRs revealed that duloxetine was associated with a high incidence of TEAES. The largest sample size (Chen et al., 2021) included 5 RCTs with a total of 1,762 patients (RR 1.31, 95% CI, 1.20; 1.43, $p < 0.00001$). Furthermore, all SRs agreed that there existed no obvious difference in the incidence of serious adverse events between the duloxetine and placebo groups. The largest sample size (Chen

TABLE 5 | Results of the PRISMA assessments.

Section/topic	Items	Wang (2015)	Chen (2019)	Gao (2019)	Osani (2019)	Qu (2020)	Chen (2021)	Compliance (%)
Title								
	1.Title	Y	Y	Y	Y	Y	Y	100
Abstract								
	2.Abstract	PY	PY	PY	PY	PY	PY	0
Introduction								
	3.Rationale	Y	Y	Y	Y	Y	Y	100
	4.Objectives	Y	Y	Y	Y	Y	Y	100
Methods								
	5.Eligibility criteria	Y	Y	Y	Y	Y	Y	100
	6.Information sources	PY	PY	PY	PY	PY	PY	0
	7.Search strategy	N	N	N	N	N	N	0
	8. Selection process	Y	Y	Y	Y	Y	Y	100
	9.Data collection process	Y	Y	Y	Y	Y	Y	100
	10.Data items	PY	PY	PY	PY	PY	PY	0
	11.Study risk of bias assessment	Y	Y	Y	Y	Y	Y	100
	12.Effect measures	Y	Y	Y	Y	Y	Y	100
	13.Synthesis methods	PY	PY	PY	PY	PY	PY	0
	14.Reporting bias assessment	Y	N	N	Y	N	N	66.7
	15.Certainty assessment	N	N	Y	N	N	N	16.7
Results								
	16.Study election	PY	PY	PY	PY	PY	PY	0
	17.Study characteristics	Y	Y	Y	Y	Y	Y	100
	18.Risk of bias within studies	N	Y	Y	Y	Y	Y	83.3
	19.Results of individual studies	Y	Y	Y	N	Y	Y	83.3
	20.Results of syntheses	PY	PY	PY	Y	PY	PY	16.7%
	21.Reporting biases	N	Y	Y	Y	N	N	50%
	22.Certainty of evidence	Y	Y	Y	Y	Y	Y	100%
Discussion								
	23.Discussion	Y	Y	Y	Y	Y	Y	100%
Other information								
	24.Registration and protocol	N	Y	Y	N	N	Y	50%
	25.Support	Y	Y	Y	N	Y	Y	83.3%
	26.Competing interests	Y	Y	Y	Y	N	Y	83.3%
	27.Availability of data, code and other materials	PY	PY	PY	PY	PY	PY	0%

Abbreviations: Y, yes (a complete report); PY, partially yes (a partially compliant report); N, no (no report).

et al., 2021) included 5 RCTs with a total of 1,762 patients (RR 0.92, 95% CI, 0.40; 2.11, $p = 0.84$). 4 SRs (Wang et al., 2015; Chen et al., 2019; Gao et al., 2019; Osani and Bannuru, 2019) reported that duloxetine is significantly associated with treatment discontinuation rate. The largest sample size (Chen et al., 2019) included 5 RCTs with totally 1,762 patients (RR 2.26, 95% CI 1.63; 3.12, $p < 0.00001$).

4 DISCUSSION

4.1 Summary of the Main Results

Admittedly, this is the first review of SRs exploring the efficacy and safety of duloxetine for the treatment of KOA. We critically evaluated the published SRs by adopting AMSTAR 2, ROBIS, PRISMA, and GRADE. In addition, the reporting quality according to the PRISMA checklist was relatively good, with a relatively complete manuscript structure and 4 SRs (Chen et al., 2019; Gao et al., 2019; Osani and Bannuru, 2019; Chen et al., 2021) being adequately reported by over 70%. However, in the grading results, the quality of evidence was poor, with all SRs assessed by AMSTAR 2 which had over one critical flaw. Thus, all SRs were rated very low. By adopting the ROBIS tool, the ratings for the two SRs (Chen et al., 2019; Gao et al., 2019) were unsatisfactory, suggesting that the conclusions based on the contained SRs may have difference from the true picture. GRADE results have revealed that duloxetine reduces pain in patients with KOA and improves joint function in those patients. Although all SRs appear to show the benefits of duloxetine, the results of the comprehensive review are not ideal. No definitive conclusions can be drawn. According to the published results, caution is required when recommending duloxetine as the treatment for patients with KOA.

4.2 Implications for Further Studies

The current overview introduces several challenges for producers of SRs that should be taken into consideration. The results of AMSTAR 2 tool and PRISMA checklist suggest that the methodological quality of SRs requires to be enhanced in the following areas. SRs should be registered in advance in the international preregistration database (PROSPERO) and should also detail the reasons for the type of study design, contributing to lower risk of bias in SRs. SRs should provide a comprehensive search strategy and focus on the search for grey

TABLE 6 | GRADE quality grading of included SRs.

Author (year)	Outcomes (n)	Limitations	Inconsistency	Indirectness	Imprecision	Publication bias	Quality of evidence
Wang (2015)	WOMAC physical function score (3)	−1①	0	0	−1③	0	L
	PGI-I scores (3)	−1①	−1②	0	0	0	L
	30% pain reduction rate (3)	−1①	0	0	0	0	M
	50% pain reduction rate (3)	−1①	−2②	0	−1③	0	CL
	BPI-S score (3)	−1①	0	0	0	0	M
	Adverse events (3)	−1①	0	0	−1③	0	L
	Serious adverse events (3)	−1①	0	0	−1③	0	L
	Treatment emergent adverse events (3)	−1①	0	0	−1③	0	L
	Treatment discontinuation rate (3)	−1①	−1②	0	−1③	0	CL
Chen (2019)	WOMAC stiffness score (6)	−1①	0	0	−1③	−1④	CL
	WOMAC physical function score (6)	−1①	−1②	0	−1③	−1④	CL
	BPI-S score (5)	−1①	0	0	0	−1④	L
	30% pain reduction rate (4)	−1①	0	0	0	−1④	L
	50% pain reduction rate (4)	−1①	−1②	0	0	−1④	CL
	Weekly 24-h average pain score (3)	−1①	0	0	0	−1④	L
	Treatment emergent adverse events (5)	−1①	0	0	−1③	−1④	CL
	Serious adverse events (5)	−1①	0	0	−1③	−1④	CL
	Treatment discontinuation rate (5)	−1①	0	0	−1③	−1④	CL
Gao (2019)	WOMAC total score (5)	−1①	−1②	0	−1③	−1④	CL
	WOMAC pain score (4)	−1①	−2②	0	−1③	−1④	CL
	WOMAC stiffness score (4)	−1①	−2②	0	−1③	−1④	CL
	WOMAC physical function score (4)	−1①	−2②	0	−1③	−1④	CL
	PGI-I scores (5)	−1①	−1②	0	0	−1④	CL
	BPI-S score (5)	−1①	−1②	0	0	−1④	CL
	30% pain reduction rate (5)	−1①	0	0	0	−1④	L
	50% pain reduction rate (4)	−1①	−2②	0	0	−1④	CL
	Treatment emergent adverse events (5)	−1①	0	0	0	−1④	L
	Serious adverse events (5)	−1①	0	0	−1③	−1④	CL
	Treatment discontinuation rate (3)	−1①	−1②	0	−1③	−1④	CL
Osani (2019)	WOMAC pain score (5)	−1①	−1②	0	0	0	L
	WOMAC physical function score (5)	−1①	−1②	0	0	0	L
	Treatment emergent adverse events (5)	−1①	−2②	0	0	0	CL
	Serious adverse events (5)	−1①	0	0	0	0	M
	Treatment discontinuation rate (5)	−1①	0	0	0	0	M
	Gastrointestinal adverse event (5)	−1①	−1②	0	0	0	L
	Quality of life improvement (3)	−1①	0	0	0	0	M
	Improvement of depressive symptoms (2)	−1①	0	0	−1③	0	L
Qu (2020)	WOMAC total score (2)	−1①	−1②	0	−1③	−1④	CL
	WOMAC pain score (3)	−1①	0	0	0	−1④	L
	WOMAC stiffness score (3)	−1①	−1②	0	−1③	−1④	CL
	WOMAC physical function score (3)	−1①	−2②	0	0	−1④	CL
	BPI-S score (5)	−1①	0	0	0	−1④	L
	Dry mouth (2)	−1①	−1②	0	0	−1④	CL
	Drowsiness (2)	−1①	0	0	0	−1④	L
	Nausea (2)	−1①	−1②	0	0	−1④	CL
Chen (2021)	30% pain reduction rate (5)	−1①	0	0	−1③	−1④	CL
	50% pain reduction rate (5)	−1①	0	0	0	−1④	L
	Pain reduction average rate (5)	−1①	0	0	−1③	−1④	CL
	WOMAC pain score (4)	−1①	−2②	0	0	−1④	CL
	WOMAC stiffness score (6)	−1①	−1②	0	−1③	−1④	CL
	WOMAC physical function score (6)	−1①	−1②	0	0	−1④	CL
	SF-36 physical functional subscale (2)	−1①	−2②	0	−1③	−1④	CL
	SF-36 bodily pain subscale (2)	−1①	−2②	0	0	−1④	CL
	SF-36 role physical subscale (3)	−1①	−2②	0	−1③	−1④	CL
	PGI-I scores (5)	−1①	−1②	0	0	−1④	CL
	CGI-S scores (4)	−1①	−2②	0	−1③	−1④	CL
	Treatment emergent adverse events (5)	−1①	−2②	0	−1③	−1④	CL
	Serious adverse events (5)	−1①	0	0	−1③	−1④	CL
	BPI-I score (3)	−1①	−1②	0	−1③	−1④	CL
	BPI-S score (5)	−1①	0	0	0	−1④	L

Abbreviations: CL, critically low; L, low; M: moderate; H, high; ①, The design of the experiment with a large bias in random, distributive hiding or blind; ②, The confidence interval overlaps less, the heterogeneity test P is Critically small, and the I^2 is larger; ③, Confidence interval is not narrow enough; ④, Fewer studies are included and there may be greater publication bias.

literature and offer a detailed search strategy for at least one major database in order to the transparency of systematic evaluation. Literature exclusion lists and reasons should be provided to facilitate quality judgment and screening of selected literature. SRs should detail the fundamental features of the included studies, which is beneficial for understanding the comparability of study baselines. SRs should employ reasonable tools with the purpose of evaluating the inclusion risk of bias in the involved studies. Studies should completely describe issues such as funding information and conflicts of interest. In addition, researchers should conduct descriptions of other analytical methods like the sensitivity analysis and subgroup analysis as well as report evidence summaries in the GREAD summary of results form. While many items in AMSTAR 2 tool and PRISMA checklist are repeatable, the different purposes of each tool make them complementary, causing more comprehensive assessments. The ROBIS tool makes up for the lack by evaluating the risk of bias in SRs. Perry et al., 2021.

It could be discovered that the risk of bias was comparatively high in domains 2 and 4 of phase 2 when we adopted the ROBIS tool. In domain 2, we concentrated on identifying and selecting studies. In order to evaluate SR effectively, researchers must focus on whether they search a proper range of databases and electronic sources. As an alternative to searching databases, conference reports and clinical trial registration platforms need to be used to find relevant reports. In domain 4, there was a high risk of bias in the synthesis of findings. Although all data was synthesized, we were not capable of determining whether the necessary methods of data analysis and synthesis were followed before the SRs. As a result, some studies may not have been included in the synthesis. Moreover, it is essential to carry out a funnel plot or sensitivity analysis to assess the robustness of the findings as well as to minimize or address biases in primary studies in the synthesis.

As a result of the GRADE Tool, most indicators were rated as very low-quality evidence, implying variations in the findings. The main factors for downgrading included limitations and publication bias, followed by inconsistency. The downgraded limitations suggested that all studies were unclear or had large limitations in terms of randomization, allocation concealment, and blinding. In addition, future clinical trials should concentrate on a top-level design. It is most apparent from the low number of negative results and asymmetry of funnel plots that publication bias was present. The inconsistency was caused by the high heterogeneity of the included studies and the large I^2 values after the merger, indicating that other analysis methods, like sensitivity analysis and subgroup analysis, should be performed to account for the heterogeneity.

4.3 Selection of Knee Osteoarthritis Outcome Indicators

The current study adopted the BPI scale for describing changes in pain scores. The BPI is primarily employed to assess pain in the past 24 h or the past 1 week. The main components of the assessment contain the level of pain, the type of pain, and the influence of pain on daily function. Based on our knowledge, the visual analogue scale (VAS) is the most commonly used scale to evaluate pain in KOA patients and features the highest reliability (Myles et al., 2017). In comparison with the VAS, the BPI measures pain intensity while testing the impact of pain on psychology, mood, and sleep, providing a more comprehensive assessment of pain (Poquet and Lin, 2016; Alizadeh-Khoei et al., 2017; Chiarotto et al., 2019). As a result, BPI is more suitable for use in KOA patients undergoing depression. The WOMAC, PGI-I, CGI-I, BPI, and SF-36 scales are comprehensive scales that each has its own focus. The WOMAC scale is categorized into three categories, respectively, pain, stiffness, and physical function. It is highly reliable and can effectively evaluate the course of disease and treatment effect in patients suffering from KOA. PGI-I is a global index that can be applied to assess a condition's response to therapy (Viktrup et al., 2012; Bjelic-Radisic et al., 2018). PGI-I has only been tested on women undergoing stress incontinence. Apart from that, it has not been demonstrated that it applies to KOA patients. The Clinical Global Impressions scale is one of the most extensively applied scales in clinical trials in psychopharmacology (Mohebbi et al., 2018). The SF-36, a brief health questionnaire, provides a comprehensive overview of the respondents' quality of life in eight areas (Brazier et al., 1992; Ware and Sherbourne, 1992). The result was reported by 1 SR, showing that duloxetine exerted a negative effect on improving the SF-36 physical function subscale and the physical pain subscale, without any statistically significant difference in the SF-36 role physical scale (Apolone and Mosconi, 1998; Lins and Carvalho, 2016). One SR (Osani and Bannuru, 2019) reported improvement in depressive symptoms, exhibiting no improvement in depressive symptoms in KOA patients with duloxetine. The result may be resulted from the small sample size and inaccurate conclusions due to the explicit exclusion of patients with depression in four studies and the exclusion of participants who were taking any other antidepressants in one study. In addition, we recommend adopting the Hamilton Rating Scale for Depression for describing the improvement in depressive symptoms in future studies (Hamilton, 1960; Zimmerman et al., 2013). Whether SF-36, PGI-I, and CGI-I can be used as indicators in order to assess the quality of life of KOA patients still needs to be further investigated. Inconsistent diagnostic criteria of SRs may generate inconsistent effectiveness evaluation criteria and ultimately influence the reliability of the results.

Despite some deficiencies in the 6 SRs, duloxetine may help to improve pain and depressive symptoms in KOA patients. Till present, numerous studies have shown that KOA patients with depressive symptoms, increased pain intensity, and functional limitations exhibit depressive symptoms in the context of musculoskeletal disorders. Duloxetine, a 5-hydroxytryptamine and norepinephrine reuptake inhibitor, may enhance the efficacy of depression and pain in KOA patients by providing pharmacological management of pain and depression as well as promoting bidirectional physical and psychological improvement. Besides, it is also recommended that future studies examine the effects of duloxetine in these populations

TABLE 7 | Results of included SRs.

Author	Comparisons	Outcomes (n)	Total patient number in Intervention group/total patient number in control group or total participants in both groups, study number
Wang	Duloxetine 60–120 mg QD vs. Placebo	BPI-S score (3)	MD −0.88, 95% CI −1.11; −0.65, $p < 0.00001$ (490/502, $n = 3$)
		30% pain reduction rate (3)	RR 1.49, 95% CI 1.31; 1.70, $p < 0.00001$ (488/501, $n = 3$)
		50% pain reduction rate (3)	RR 1.69, 95% CI 1.27; 2.25, $p = 0.0004$ (488/501, $n = 3$)
		PGI-I scores (3)	MD −0.47, 95% CI −0.63; −0.30, $p < 0.00001$ (481/495, $n = 3$)
		WOMAC physical function score (3)	MD −4.25, 95% CI −5.82; −2.68, $p < 0.00001$ (480/497, $n = 3$)
		Adverse events (3)	RR 2.15, 95% CI 1.48; 3.11, $p < 0.00001$ (503/508, $n = 3$)
		Serious adverse events (3)	RR 1.30, 95% CI 0.48; 3.47, $p = 0.61$ (503/508, $n = 3$)
		Treatment emergent adverse events (3)	RR 1.32, 95% CI 1.16; 1.49, $p < 0.00001$ (503/508, $n = 3$)
		Treatment discontinuation rate (3)	RR 1.43, 95% CI 1.14; 1.78, $p = 0.002$ (503/508, $n = 3$)
Chen	Duloxetine 60–120 mg QD vs. Placebo	BPI-S score (5)	WMD −0.74, 95% CI −0.92; −0.57, $p < 0.00001$ (842/853, $n = 5$)
		Weekly 24-h average pain score (3)	WMD −0.76, 95% CI −0.96; −0.56, $p < 0.00001$ (564/559, $n = 3$)
		30% pain reduction rate (4)	RR 1.43, 95% CI 1.29; 1.59, $p < 0.00001$ (672/678, $n = 4$)
		50% pain reduction rate (4)	RR 1.71, 95% CI 1.46; 1.99, $p < 0.00001$ (672/678, $n = 4$)
		WOMAC stiffness score (6)	WMD −0.47, 95% CI −0.60; −0.34, $p < 0.00001$ (993/1003, $n = 6$)
		WOMAC physical function score (6)	WMD −4.44, 95% CI −5.24; −3.64, $p < 0.00001$ (995/1001, $n = 6$)
		Treatment emergent adverse events (5)	RR 1.31, 95% CI 1.20; 1.44, $p < 0.00001$ (880/882, $n = 5$)
		Serious adverse events (5)	RR 0.92, 95% CI 0.40; 2.11, $p = 0.84$ (880/882, $n = 5$)
		Treatment discontinuation rate (5)	RR 2.26, 95% CI 1.63; 3.12, $p < 0.00001$ (880/882, $n = 5$)
Gao	Duloxetine 60–120 mg QD vs. Placebo	BPI-S score (5)	MD −0.77, 95% CI −0.95; −0.59, $p < 0.00001$ (842/853, $n = 5$)
		30% pain reduction rate (5)	RR 1.42, 95% CI 1.30; 1.56, $p < 0.00001$ (844/855, $n = 5$)
		50% pain reduction rate (4)	RR 1.62, 95% CI 1.30; 2.02, $p < 0.0001$ (716/727, $n = 4$)
		PGI-I scores (5)	MD −0.48, 95% CI −0.59; −0.37, $p < 0.00001$ (835/849, $n = 5$)
		WOMAC total score (5)	MD −5.43, 95% CI −6.87; −3.99, $p < 0.00001$ (740/739, $n = 5$)
		WOMAC pain score (4)	MD −1.63, 95% CI −2.63; −0.63, $p = 0.001$ (726/731, $n = 4$)
		WOMAC stiffness score (4)	MD −0.58, 95% CI −0.75; −0.41, $p < 0.00001$ (726/732, $n = 4$)
		WOMAC physical function score (4)	MD −4.22, 95% CI −6.17; −2.28, $p < 0.0001$ (740/739, $n = 4$)
		Treatment emergent adverse events (5)	RR 1.32, 95% CI 1.20; 1.44, $p < 0.0001$ (879/882, $n = 5$)
		Serious adverse events (5)	RR 0.84, 95% CI 0.37; 1.90, $p = 0.68$ (879/882, $n = 5$)
		Treatment discontinuation rate (3)	RR 1.88, 95% CI 1.29; 2.75, $p = 0.001$ (487/494, $n = 3$)
Osani	Duloxetine 60–120 mg QD vs. Placebo	WOMAC pain score (5)	SMD −0.38, 95% CI −0.48; −0.28, P: no report
		WOMAC physical function score (5)	SMD −0.35, 95% CI −0.46; −0.24, P: no report
		Treatment emergent adverse events (5)	RR 1.53, 95% CI 1.21; 1.92, P: no report
		Serious adverse events (5)	RR 1.03, 95% CI 0.42; 2.54, P: no report
		Treatment discontinuation rate (5)	RR 2.17, 95% CI 1.57; 3.01, P: no report
		Gastrointestinal adverse event (5)	RR 4.43, 95% CI 3.45; 5.69, P: no report
		Quality of life improvement (3)	SMD 0.40, 95% CI 0.26; 0.53, P: no report
		Improvement of depressive symptoms (2)	SMD −0.09, 95% CI −0.26; 0.07, P: no report
Qu	Duloxetine 60–120 mg QD vs. Placebo	WOMAC total score (2)	MD −0.34, 95% CI −0.48; −0.20, $p < 0.05$ (392/388, $n = 2$)
		WOMAC pain score (3)	MD −0.41, 95% CI −0.54;−0.29, $p < 0.05$ (519/524, $n = 3$)
		WOMAC stiffness score (3)	MD −0.24, 95% CI −0.37;−0.12, $p < 0.05$ (519/524, $n = 3$)
		WOMAC physical function score (3)	MD −0.43, 95% CI −0.55;−0.31, $p < 0.05$ (536/532, $n = 3$)
		BPI-S score (5)	MD −0.38, 95% CI −0.48;−0.28, $p < 0.05$ (842/853, $n = 5$)
		Dry mouth (2)	RR 3.55, 95% CI 2.00; 6.29, $p < 0.05$ (382/378, $n = 2$)
		Drowsiness (2)	RR 3.23, 95% CI 1.88; 5.54, $p < 0.05$ (382/378, $n = 2$)
		Nausea (2)	RR 6.95, 95% CI 2.99; 16.15, $p < 0.05$ (382/378, $n = 2$)
Chen	Duloxetine 60–120 mg QD vs. Placebo	30% pain reduction rate (5)	MD −0.54, 95% CI −0.71; −0.37, $p < 0.00001$ (842/854, $n = 5$)
		50% pain reduction rate (5)	MD −0.87, 95% CI −1.07; −0.66, $p < 0.00001$ (842/854, $n = 5$)
		Pain reduction average rate (5)	MD −0.68, 95% CI −0.87; −0.48, $p < 0.00001$ (842/854, $n = 5$)
		WOMAC pain score (4)	MD −0.81, 95% CI −0.92; −0.69, $p < 0.00001$ (813/815, $n = 4$)
		WOMAC stiffness score (6)	MD −0.47, 95% CI −0.60; −0.34, $p < 0.00001$ (998/1004, $n = 6$)
		WOMAC physical function score (6)	MD −4.22, 95% CI −5.14; −3.30, $p < 0.00001$ (988/998, $n = 6$)
		SF-36 physical functional subscale (3)	MD 1.62, 95% CI 0.12; 3.13, $p = 0.03$ (409/417, $n = 3$)
		SF-36 bodily pain subscale (3)	MD 1.22, 95% CI 0.08; 2.35, $p = 0.04$ (409/417, $n = 3$)
		SF-36 role physical subscale (3)	MD 1.04, 95% CI −0.10; 2.18, $p = 0.07$ (409/417, $n = 3$)
		PGI-I score (5)	MD −0.48, 95% CI −0.58; −0.37, $p < 0.00001$ (867/874, $n = 5$)
		CGI-S score (4)	MD −0.34, 95% CI −0.44; −0.24, $p < 0.00001$ (717/731, $n = 4$)
		Treatment emergent adverse events (5)	RR 1.31, 95% CI, 1.20; 1.43, $p < 0.00001$ (880/882, $n = 5$)
		Serious adverse events (5)	RR 0.92, 95% CI, 0.40; 2.11, $p = 0.84$ (880/882, $n = 5$)
		BPI-I score (3)	MD −0.76, 95% CI,−0.96; −0.56, $p < 0.00001$ (453/471, $n = 3$)
		BPI-S score (5)	MD −0.74, 95% CI,−0.92; −0.57, $p < 0.00001$ (842/853, $n = 5$)

with KOA and depression concomitantly. Moreover, large and well-controlled RCTs are still required with the purpose of assessing the long-term safety of duloxetine and its use as an alternative to conventional therapy.

4.4 Strengths and Limitations

First, this review is the first attempt to comprehensively review the methodology and quality of reporting of SRs on duloxetine for pain management in KOA patients with depressive symptoms. Secondly, we conducted the overview based on a predesigned protocol, lowering the probability of bias. However, there exist several limitations. There may have been studies in other languages missed because the study only employed computerized searches of English and Chinese publications. We only included SRs of RCTs. Moreover, some studies may generate negative results and not been published (Ioannidis, 2016; Heathers et al., 2019). Therefore, the number of included literatures was small, which may have generated the bias due to literature omission. In the evaluation using AMSTAR 2, PRISMA, ROBIS, and GRADE, although different researchers performed the evaluation and cross-checking, there may exist evaluation differences due to subjective differences in the scale entries. As a result, the results may not have been as accurate as they could have been since we were not capable of synthesizing all the evidence.

5 CONCLUSION

To conclude, duloxetine may become an effective therapy for improving pain and depressive symptoms in patients with KOA. However, this finding must be treated with caution given the generally low methodological and evidentiary quality of the involved researches. Future studies should concentrate on RCTs in patients undergoing concomitant OA and depression with the purpose of assessing the certain benefits of duloxetine in these populations. In addition, investigators need to improve the methodological quality, risk of bias as well as reporting quality of SRs to provide better quality evidence for evidence-based medicine.

DATA AVAILABILITY STATEMENT

The original contributions presented in the study are included in the article/Supplementary Material, further inquiries can be directed to the corresponding author.

AUTHOR CONTRIBUTIONS

Conception and design: QZ, JC, and AL. Provision of study materials: WY, TG, and YY. Collection and assembly of data: PN, QZ, and AL. Data analysis and interpretation: KY, JC, and AL. Manuscript writing: QZ, JC, and AL. Final approval of manuscript: QZ, JC, and AL. Accountable for all aspects of the work: QZ, JC, and AL. All authors read critically reviewed and approved the final manuscript as submitted.

FUNDING

This research was supported by the Science and Technology Project of Tianjin, China (No. 21KPXMRC00050) and the National Natural Science Foundation of China (No. 81873316).

REFERENCES

Alizadeh-Khoei, M., Sharifi, F., Akbari, M. E., Fadayevatan, R., and Haghi, M. (2017). Iranian Brief Pain Inventory: Validation and Application in Elderly People with Cancer Pain. *J. Pain Symptom Manage* 54 (4), 563–569. doi:10.1016/j.jpainsymman.2017.07.015

Apolone, G., and Mosconi, P. (1998). The Italian SF-36 Health Survey: Translation, Validation and Norming. *J. Clin. Epidemiol.* 51 (11), 1025–1036. doi:10.1016/s0895-4356(98)00094-8

Arden, N. K., Perry, T. A., Bannuru, R. R., Bruyère, O., Cooper, C., Haugen, I. K., et al. (2021). Non-surgical Management of Knee Osteoarthritis: Comparison of ESCEO and OARSI 2019 Guidelines. *Nat. Rev. Rheumatol.* 17 (1), 59–66. doi:10.1038/s41584-020-00523-9

Axford, J., Butt, A., Heron, C., Hammond, J., Morgan, J., Alavi, A., et al. (2010). Prevalence of Anxiety and Depression in Osteoarthritis: Use of the Hospital Anxiety and Depression Scale as a Screening Tool. *Clin. Rheumatol.* 29 (11), 1277–1283. doi:10.1007/s10067-010-1547-7

Baker, P. R., Costello, J. T., Dobbins, M., and Waters, E. B. (2014). The Benefits and Challenges of Conducting an Overview of Systematic Reviews in Public Health: a Focus on Physical Activity. *J. public health (Oxford, Engl.* 36 (3), 517–521. doi:10.1093/pubmed/fdu050

Bannuru, R. R., Osani, M. C., Vaysbrot, E. E., Arden, N. K., Bennell, K., Bierma-Zeinstra, S. M. A., et al. (2019). OARSI Guidelines for the Non-surgical Management of Knee, Hip, and Polyarticular Osteoarthritis. *Osteoarthr. Cartil.* 27 (11), 1578–1589. doi:10.1016/j.joca.2019.06.011

Bjelic-Radisic, V., Ulrich, D., Hinterholzer, S., Reinstadler, E., Geiss, I., Aigmueller, T., et al. (2018). Psychometric Properties and Validation of Two Global Impression Questionnaires (PGI-S, PGI-I) for Stress Incontinence in a German-speaking Female Population. *Neurourol. Urodyn.* 37 (4), 1365–1371. doi:10.1002/nau.23447

Brazier, J. E., Harper, R., Jones, N. M., O'Cathain, A., Thomas, K. J., Usherwood, T., et al. (1992). Validating the SF-36 Health Survey Questionnaire: New Outcome Measure for Primary Care. *Bmj* 305 (6846), 160–164. doi:10.1136/bmj.305.6846.160

Bruyère, O., Honvo, G., Veronese, N., Arden, N. K., Branco, J., Curtis, E. M., et al. (2019). An Updated Algorithm Recommendation for the Management of Knee Osteoarthritis from the European Society for Clinical and Economic Aspects of Osteoporosis, Osteoarthritis and Musculoskeletal Diseases (ESCEO). *Seminars Arthritis Rheumatism* 49 (3), 337–350. doi:10.1016/j.semarthrit.2019.04.008

Chen, B., Duan, J., Wen, S., Pang, J., Zhang, M., Zhan, H., et al. (2021). An Updated Systematic Review and Meta-Analysis of Duloxetine for Knee Osteoarthritis Pain. *Clin. J. Pain* 37 (11), 852–862. doi:10.1097/ajp.0000000000000975

Chen, L., Gong, M., Liu, G., Xing, F., Liu, J., and Xiang, Z. (2019). Efficacy and Tolerability of Duloxetine in Patients with Knee Osteoarthritis: a Meta-Analysis of Randomised Controlled Trials. *Intern Med. J.* 49 (12), 1514–1523. doi:10.1111/imj.14327

Chiarotto, A., Maxwell, L. J., Ostelo, R. W., Boers, M., Tugwell, P., and Terwee, C. B. (2019). Measurement Properties of Visual Analogue Scale, Numeric Rating Scale, and Pain Severity Subscale of the Brief Pain Inventory in Patients with

Low Back Pain: A Systematic Review. *J. Pain* 20 (3), 245–263. doi:10.1016/j.jpain.2018.07.009

Ferreira, G. E., McLachlan, A. J., Lin, C.-W. C., Zadro, J. R., Abdel-Shaheed, C., O'Keeffe, M., et al. (2021). Efficacy and Safety of Antidepressants for the Treatment of Back Pain and Osteoarthritis: Systematic Review and Meta-Analysis. *Bmj* 372, m4825. doi:10.1136/bmj.m4825

Gao, S. H., Huo, J. B., Pan, Q. M., Li, X. W., Chen, H. Y., and Huang, J. H. (2019). The Short-Term Effect and Safety of Duloxetine in Osteoarthritis: A Systematic Review and Meta-Analysis. *Med. Baltim.* 98 (44), e17541. doi:10.1097/md.0000000000017541

GBD Disease and Injury Incidence and Prevalence Collaborators (2015). Global, Regional, and National Incidence, Prevalence, and Years Lived with Disability for 301 Acute and Chronic Diseases and Injuries in 188 Countries, 1990-2013: a Systematic Analysis for the Global Burden of Disease Study 2013. *Lancet* 386 (9995), 743–800. doi:10.1016/S0140-6736(15)60692-4

Gleicher, Y., Croxford, R., Hochman, J., and Hawker, G. (2011). A Prospective Study of Mental Health Care for Comorbid Depressed Mood in Older Adults with Painful Osteoarthritis. *BMC Psychiatry* 11, 147. doi:10.1186/1471-244x-11-147

Guyatt, G. H., Oxman, A. D., Vist, G. E., Kunz, R., Falck-Ytter, Y., Alonso-Coello, P., et al. (2008). GRADE: an Emerging Consensus on Rating Quality of Evidence and Strength of Recommendations. *Bmj* 336 (7650), 924–926. doi:10.1136/bmj.39489.470347.ad

Hamilton, M. (1960). A Rating Scale for Depression. *J. Neurol. Neurosurg. Psychiatry* 23 (1), 56–62. doi:10.1136/jnnp.23.1.56

Havelin, J., Imbert, I., Cormier, J., Allen, J., Porreca, F., and King, T. (2016). Central Sensitization and Neuropathic Features of Ongoing Pain in a Rat Model of Advanced Osteoarthritis. *J. Pain* 17 (3), 374–382. doi:10.1016/j.jpain.2015.12.001

Heathers, J. A., Nagata, J. M., and Murray, S. B. (2019). Publication Bias in Trials with and without Null Findings-Reply. *Jama* 322 (12), 1214. doi:10.1001/jama.2019.11144

Huang, J., Liu, H., Chen, J., Cai, X., and Huang, Y. (2021). The Effectiveness of Tai Chi in Patients with Breast Cancer: An Overview of Systematic Reviews and Meta-Analyses. *J. Pain Symptom Manage* 61 (5), 1052–1059. doi:10.1016/j.jpainsymman.2020.10.007

Ioannidis, J. P. (2016). The Mass Production of Redundant, Misleading, and Conflicted Systematic Reviews and Meta-Analyses. *Milbank Q.* 94 (3), 485–514. doi:10.1111/1468-0009.12210

Kessler, R. C., Berglund, P., Demler, O., Jin, R., Koretz, D., Merikangas, K. R., et al. (2003). The Epidemiology of Major Depressive Disorder. *Jama* 289 (23), 3095–3105. doi:10.1001/jama.289.23.3095

Koh, I. J., Kim, M. S., Sohn, S., Song, K. Y., and Choi, N. Y. (2019). Duloxetine Reduces Pain and Improves Quality of Recovery Following Total Knee Arthroplasty in Centrally Sensitized Patients: A Prospective, Randomized Controlled Study. *J. Bone Jt. Surg. Am.* 101 (1), 64–73. doi:10.2106/jbjs.18.00347

Kolasinski, S. L., Neogi, T., Hochberg, M. C., Oatis, C., Guyatt, G., Block, J., et al. (2020). 2019 American College of Rheumatology/Arthritis Foundation Guideline for the Management of Osteoarthritis of the Hand, Hip, and Knee. *Arthritis Care Res. Hob.* 72 (2), 149–162. doi:10.1002/acr.24131

Lins, L., and Carvalho, F. M. (2016). SF-36 Total Score as a Single Measure of Health-Related Quality of Life: Scoping Review. *SAGE Open Med.* 4, 2050312116671725. doi:10.1177/2050312116671725

Malfait, A.-M., and Schnitzer, T. J. (2013). Towards a Mechanism-Based Approach to Pain Management in Osteoarthritis. *Nat. Rev. Rheumatol.* 9 (11), 654–664. doi:10.1038/nrrheum.2013.138

Miller, R. E., Malfait, A. M., and Block, J. A. (2017). Current Status of Nerve Growth Factor Antibodies for the Treatment of Osteoarthritis Pain. *Clin. Exp. Rheumatol.* 35 (5), 85–87.

Miller, R. E., Miller, R. J., and Malfait, A.-M. (2014). Osteoarthritis Joint Pain: the Cytokine Connection. *Cytokine* 70 (2), 185–193. doi:10.1016/j.cyto.2014.06.019

Mohebbi, M., Dodd, S., Dean, O. M., and Berk, M. (2018). Patient Centric Measures for a Patient Centric Era: Agreement and Convergent between Ratings on the Patient Global Impression of Improvement (PGI-I) Scale and the Clinical Global Impressions - Improvement (CGI-S) Scale in Bipolar and Major Depressive Disorder. *Eur. Psychiatry* 53, 17–22. doi:10.1016/j.eurpsy.2018.05.006

Myles, P. S., Myles, D. B., Galagher, W., Boyd, D., Chew, C., MacDonald, N., et al. (2017). Measuring Acute Postoperative Pain Using the Visual Analog Scale: the Minimal Clinically Important Difference and Patient Acceptable Symptom State. *Br. J. Anaesth.* 118 (3), 424–429. doi:10.1093/bja/aew466

Osani, M. C., and Bannuru, R. R. (2019). Efficacy and Safety of Duloxetine in Osteoarthritis: a Systematic Review and Meta-Analysis. *Korean J. Intern Med.* 34 (5), 966–973. doi:10.3904/kjim.2018.460

Page, M. J., McKenzie, J. E., Bossuyt, P. M., Boutron, I., Hoffmann, T. C., Mulrow, C. D., et al. (2021). The PRISMA 2020 Statement: an Updated Guideline for Reporting Systematic Reviews. *Bmj* 372, n71. doi:10.1136/bmj.n71

Perry, R., Whitmarsh, A., Leach, V., and Davies, P. (2021). A Comparison of Two Assessment Tools Used in Overviews of Systematic Reviews: ROBIS versus AMSTAR-2. *Syst. Rev.* 10 (1), 273. doi:10.1186/s13643-021-01819-x

Pigeolet, M., Jayaram, A., Park, K. B., and Meara, J. G. (2021). Osteoarthritis in 2020 and beyond. *Lancet* 397 (10279), 1059–1060. doi:10.1016/s0140-6736(21)00208-7

Poquet, N., and Lin, C. (2016). The Brief Pain Inventory (BPI). *J. Physiother.* 62 (1), 52. doi:10.1016/j.jphys.2015.07.001

Qu, G. X., Li, H. C., Cui, H. W., and Fu, K. (2020). Efficacy and Safety of Duloxetine in the Improvement of Pain Symptoms of Knee OsteoarthritisA Meta-Analysis. *China Pharm.* 31 (11), 1372–1376.

Sale, J. E., Gignac, M., and Hawker, G. (2008). The Relationship between Disease Symptoms, Life Events, Coping and Treatment, and Depression Among Older Adults with Osteoarthritis. *J. Rheumatol.* 35 (2), 335–342.

Sharma, L. (2021). Osteoarthritis of the Knee. *N. Engl. J. Med.* 384 (1), 51–59. doi:10.1056/nejmcp1903768

Shea, B. J., Reeves, B. C., Wells, G., Thuku, M., Hamel, C., Moran, J., et al. (2017). AMSTAR 2: a Critical Appraisal Tool for Systematic Reviews that Include Randomised or Non-randomised Studies of Healthcare Interventions, or Both. *Bmj* 358, j4008. doi:10.1136/bmj.j4008

Siddaway, A. P., Wood, A. M., and Hedges, L. V. (2019). How to Do a Systematic Review: A Best Practice Guide for Conducting and Reporting Narrative Reviews, Meta-Analyses, and Meta-Syntheses. *Annu. Rev. Psychol.* 70, 747–770. doi:10.1146/annurev-psych-010418-102803

Smith, V., Devane, D., Begley, C. M., and Clarke, M. (2011). Methodology in Conducting a Systematic Review of Systematic Reviews of Healthcare Interventions. *BMC Med. Res. Methodol.* 11 (1), 15. doi:10.1186/1471-2288-11-15

Stubbs, B., Aluko, Y., Myint, P. K., and Smith, T. O. (2016). Prevalence of Depressive Symptoms and Anxiety in Osteoarthritis: a Systematic Review and Meta-Analysis. *Age Ageing* 45 (2), 228–235. doi:10.1093/ageing/afw001

Thomson, D., Russell, K., Becker, L., Klassen, T., and Hartling, L. (2010). The Evolution of a New Publication Type: Steps and Challenges of Producing Overviews of Reviews. *Res. synthesis methods* 1 (3-4), 198–211. doi:10.1002/jrsm.30

Uchio, Y., Enomoto, H., Alev, L., Kato, Y., Ishihara, H., Tsuji, T., et al. (2018). A Randomized, Double-Blind, Placebo-Controlled Phase III Trial of Duloxetine in Japanese Patients with Knee Pain Due to Osteoarthritis. *J. Pain Res.* 11, 809–821. doi:10.2147/jpr.s164128

Viktrup, L., Hayes, R. P., Wang, P., and Shen, W. (2012). Construct Validation of Patient Global Impression of Severity (PGI-S) and Improvement (PGI-I) Questionnaires in the Treatment of Men with Lower Urinary Tract Symptoms Secondary to Benign Prostatic Hyperplasia. *BMC Urol.* 12, 30. doi:10.1186/1471-2490-12-30

Wang, G., Bi, L., Li, X., Li, Z., Zhao, D., Chen, J., et al. (2017). Efficacy and Safety of Duloxetine in Chinese Patients with Chronic Pain Due to Osteoarthritis: a Randomized, Double-Blind, Placebo-Controlled Study. *Osteoarthr. Cartil.* 25 (6), 832–838. doi:10.1016/j.joca.2016.12.025

Wang, Z. Y., Shi, S. Y., Li, S. J., Chen, F., Chen, H., Lin, H. Z., et al. (2015). Efficacy and Safety of Duloxetine on Osteoarthritis Knee Pain: A Meta-Analysis of Randomized Controlled Trials. *Pain Med.* 16 (7), 1373–1385. doi:10.1111/pme.12800

Ware, J. E., Jr., and Sherbourne, C. D. (1992). The MOS 36-item Short-form Health Survey (SF-36). I. Conceptual Framework and Item Selection. *Med. Care* 30 (6), 473–483. doi:10.1097/00005650-199206000-00002

Whiting, P., Savović, J., Higgins, J. P., Caldwell, D. M., Reeves, B. C., Shea, B., et al. (2016). ROBIS: A New Tool to Assess Risk of Bias in Systematic Reviews Was Developed. *J. Clin. Epidemiol.* 69, 225–234. doi:10.1016/j.jclinepi.2015.06.005

Zimmerman, M., Martinez, J. H., Young, D., Chelminski, I., and Dalrymple, K. (2013). Severity Classification on the Hamilton Depression Rating Scale. *J. Affect Disord.* 150 (2), 384–388. doi:10.1016/j.jad.2013.04.028

Conflict of Interest: The authors declare that the research was conducted in the absence of any commercial or financial relationships that could be construed as a potential conflict of interest.

Publisher's Note: All claims expressed in this article are solely those of the authors and do not necessarily represent those of their affiliated organizations, or those of the publisher, the editors and the reviewers. Any product that may be evaluated in this article, or claim that may be made by its manufacturer, is not guaranteed or endorsed by the publisher.

Copyright © 2022 Zhou, Chen, Yu, Yang, Guo, Niu, Ye and Liu. This is an open-access article distributed under the terms of the Creative Commons Attribution License (CC BY). The use, distribution or reproduction in other forums is permitted, provided the original author(s) and the copyright owner(s) are credited and that the original publication in this journal is cited, in accordance with accepted academic practice. No use, distribution or reproduction is permitted which does not comply with these terms.

frontiers | Frontiers in Physiology

ORIGINAL RESEARCH
published: 23 June 2022
doi: 10.3389/fphys.2022.915563

Comparison of Retinal Changes Following Silicone Oil and Perfluoropropane Gas Tamponade for Proliferative Diabetic Retinopathy Patients

Tan Wang[1,2†], *Erqian Wang*[1,2†], *Huan Chen*[1,2], *Ningning Li*[3] *and Hanyi Min*[1,2*]

[1]*Department of Ophthalmology, Peking Union Medical College Hospital, Chinese Academy of Medical Sciences and Peking Union Medical College, Beijing, China,* [2]*Key Laboratory of Ocular Fundus Diseases, Chinese Academy of Medical Sciences and Peking Union Medical College, Beijing, China,* [3]*Operating Room, Peking Union Medical College Hospital, Chinese Academy of Medical Sciences and Peking Union Medical College, Beijing, China*

OPEN ACCESS

Edited by:
Gaetano Santulli,
Albert Einstein College of Medicine, United States

Reviewed by:
Antonio Longo,
University of Catania, Italy
Alexander E Berezin,
Zaporizhia State Medical University, Ukraine

***Correspondence:**
Hanyi Min
minhy@pumch.cn

[†]*These authors have contributed equally to this work and share first authorship*

Specialty section:
This article was submitted to Clinical and Translational Physiology, a section of the journal Frontiers in Physiology

Received: *15 April 2022*
Accepted: *08 June 2022*
Published: *23 June 2022*

Citation:
Wang T, Wang E, Chen H, Li N and Min H (2022) Comparison of Retinal Changes Following Silicone Oil and Perfluoropropane Gas Tamponade for Proliferative Diabetic Retinopathy Patients. Front. Physiol. 13:915563. doi: 10.3389/fphys.2022.915563

Purpose: To investigate the different tamponade effects of intravitreal silicone oil (SO) and perfluoropropane gas on the retinal structure and vasculature in proliferative diabetic retinopathy (PDR) patients.

Methods: Thirty-eight eligible patients (47 eyes) with PDR requiring pars plana vitrectomy (PPV) were enrolled in the prospective observational study. Subjects were divided into two groups after PPV: SO group subjects underwent SO tamponade, whereas Gas group subjects underwent perfluoropropane gas tamponade. The primary outcomes of this study were longitudinal changes in retinal structure and vasculature between 10 and 90 days after the operation. Secondary outcomes were longitudinal changes in peripapillary retinal nerve fiber layer (pRNFL) thickness between 10 and 90 days after the operation in each sector.

Results: Thirty-six eyes of 27 patients with a median age of 56.6 ± 9.8 years completed follow-up and were statistically analyzed. No significant difference in demographics or clinical characteristics was found between the two groups. Eyes in the SO group had a statistically significant decrease in pRNFL thickness at 90 days after PPV ($p < 0.001$), and there was a significant intergroup difference compared with the Gas group ($p = 0.001$), except for the temporal sector. Eyes in the Gas group had a statistically significant increase in parafoveal vessel density (VD) of the superficial vascular complex (SVC) at 90 days after PPV ($p = 0.023$), although there was no significant intergroup difference. The type of tamponade, changes in full retina thickness, and parafoveal SVC VD showed a significant correlation with changes in pRNFL thickness (all $p < 0.05$).

Conclusion: SO tamponade resulted in a significantly greater decrease in pRNFL over 90 days than gas tamponade in patients with PDR. In addition, the change in the pRNFL was significantly correlated with changes in full retina thickness and SVC VD after the operation.

Keywords: proliferative diabetic retinopathy, pars plana vitrectomy, retinal nerve fiber layer, silicone oil, perfluoropropane, optical coherence tomography, angiography

INTRODUCTION

Severe vision loss occurs commonly in patients with proliferative diabetic retinopathy (PDR) as a result of neovascularization and fibrovascular proliferation (Moss et al., 1998). Pars plana vitrectomy (PPV) is an indicated treatment for patients with PDR when nonclearing vitreous hemorrhage (VH), tractional retinal detachment (TRD), or macula-threatening retinal detachment occur. However, when patients with PDR undergo PPV with higher grades of vitreoretinal (VR) adhesion, VR adhesion removal during PPV is challenging and may result in posterior and/or peripheral retinal holes (Michels and De Bustros, 1988; Gupta et al., 2012). Vitreous substitutes of SO and long-acting gas have been reported to be useful during PPV in cases with advanced diabetic complications, complex rhegmatogenous retinal detachment, and proliferative vitreoretinopathy (Schwartz et al., 2014).

Although SO and long-acting gas tamponade are currently in wide use for patients with PDR and high-grade VR adhesion undergoing PPV, few studies have compared the effects of different tamponades on the postoperative retinal thickness and perfusion function of the individual retina in patients with PDR.

Advances in optical coherence tomography (OCT) technology enable the detection of macular architectural changes, while OCT angiography (OCTA) is able to precisely detect perfusion function, such as vessel density (VD) of the superficial vascular complex (SVC), deep vascular complex (DVC) on the macula, and radial peripapillary capillaries (RPC) (Spaide et al., 2018;Christou et al., 2021).

In this study, we evaluated such longitudinal changes in postoperative retinal thickness and perfusion function in patients with PDR who had undergone PPV treatments by comparing the differences in cohorts administered long-acting gas versus SO tamponades.

METHODS

This prospective, observational study was conducted at the Department of Ophthalmology, Peking Union Medical College Hospital (PUMCH). This study adhered to the tenets of the Declaration of Helsinki. The Institutional Review Board of PUMCH approved and authorized the patient consent forms and the study protocol in May 2018. Signed informed consent was obtained from all patients after they had been informed of the nature and possible consequences of the study procedures.

Research Participants

Patients with PDR requiring single PPV following intravitreal SO or sterilized air (gas) tamponade between June 2018 and February 2019 were enrolled in the study. The study was not blinded to surgeons or patients or randomized to groups but was blinded to data analysts.

The inclusion criteria were as follows: 1) type I or II DM was diagnosed and medically managed; 2) patient aged over 18 years; 3) PDR with indications for PPV, including macula-threatening retinal detachment, TRD, and nonclearing VH; Snellen best-corrected visual acuity ranged from 20/40 to light perception with projection in the subject's study eye.

The exclusion criteria were as follows: 1) high intraocular pressure (IOP) prior to PPV or high IOP for more than 1 week after PPV (>22 mmHg) under medicine; 2) a history of glaucoma, ischemic optic neuropathy, uveitis, or other retinal or optic nerve diseases; 3) a history of intraocular surgery except for refractive and cataract surgery; 4) a high myopia of over—6.00 diopters or axial length (AL) >26.50 mm; 5) opacity of the lens or cornea or opaque refractive media at any follow-up visit; and 6) medically uncontrolled systemic hypertension during the follow-up period (systolic. 200 mmHg or diastolic. 120 mmHg); 7) recurrent retinal detachment within 90 days after PPV, which required a secondary surgical repair; 8) SO removal was performed less than 90 days after PPV; 9) failure to complete follow-up or failure to follow-up on time; or 10) poor image quality: OCT/OCTA signal strength index < 6.

Subjects enrolled in the study were allocated to one of the following treatment cohorts: SO group participants underwent vitreous substitution with 1,000 centistoke SO during PPV, whereas the Gas group participants underwent vitreous substitution with 12% C3F8 gas during PPV. SO was chosen for patients who were traveling by airplane, had poor vision in their fellow eye, could not maintain a face-down position, or needed early good postoperative vision. SO was also chosen in some patients with inferior retinal detachment or avulsion.

Evaluations and Surgical Techniques

Visual acuity (VA) with a Snellen chart, IOP measurement, biomicroscopy of the anterior and posterior segments, axial length, HbA1c and SD-OCT were measured or performed before PPV and 10 and 90 days after PPV. We also collected the following clinical characteristics: phakic eyes/pseudophakic eyes, duration of diabetes and type of diabetes, location and number of retinal breaks, whether hypertension was complicated and duration of hypertension.

Informed consent was obtained preoperatively. Before surgery, adequate doctor–patient communication was carried out with each of our patients. One surgeon (H.M.) performed procedures.

First, 0.05 mg of ranibizumab for pretreatment (Lucentis; Novartis) was injected into the vitreous cavity under topical anesthesia. One week later, a single PPV plus SO or 12% C3F8 gas tamponade was performed under retrobulbar anesthesia using the Constellation Vision System (Alcon Laboratories, Inc., Texas, United States) and a 25G trocar cannula system. The vitreous cavity was cleaned, and the peripheral vitreous was trimmed with an indentation. The proliferated membrane was peeled completely and/or separated into pieces until the retina could be attached completely. After fluid-gas exchange, PRP was performed.

SO (Oxane 5700, Bausch & Lomb, Rochester, N.Y., United States) or 12% C3F8 gas was injected fully until normal IOP was attained. While all sclerotomies were sutured in SO tamponade cases, only the leaking sclerotomies were sutured in gas tamponade cases. Following surgeries, patients used topical antibiotics, corticosteroids, and IOP-lowering medications as needed. The prone position or head-down

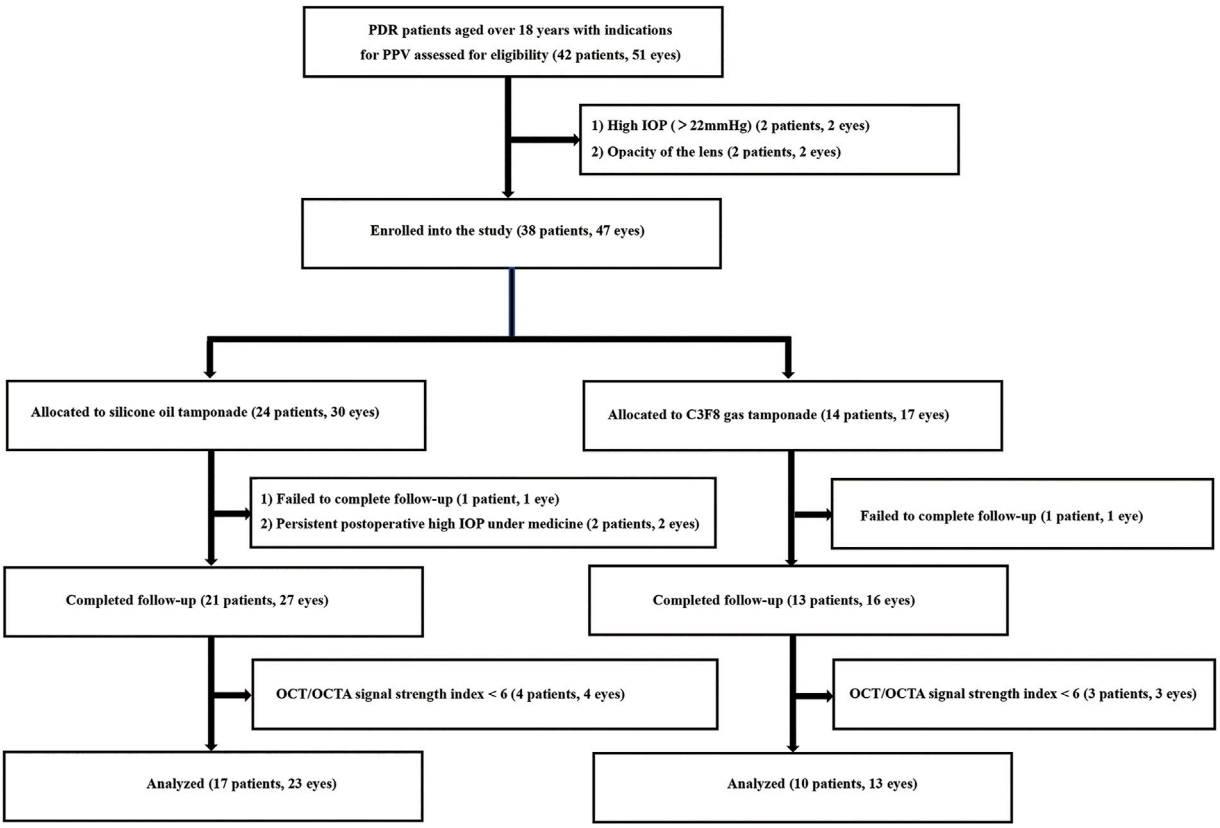

FIGURE 1 | Study flowchart. PDR, proliferative diabetic retinopathy; PPV, pars plana vitrectomy; OCT, optical coherence tomography; OCTA, optical coherence tomography angiography; IOP, intraocular pressure; SO, silicone oil.

position was adopted within 2 weeks in the two groups. IOP-lowering medications would be used only in cases of need.

No patient underwent combined cataract surgery during the procedure. The three follow-up visit times for all participants occurred at 10, 30, and 90 days after PPV. SO removal was performed approximately 3 months after SO tamponade surgery.

OCT Imaging and Processing

Optic disk and macula evaluation were performed using the spectral domain OCT device RTVue XR Avanti (Optovue, Inc., Fremont, CA, United States). This device uses a light source of 840 nm and operates at a scan speed of 70,000 A-scans per second. Images on a 3 mm × 3 mm macula and a 4.5 mm × 4.5 mm optic disc scan were captured *via* dilated pupil capture after pupillary dilation using 1% tropicamide drops.

For quantitative assessment of the parafoveal VD of SVC, DVC, and RPC, we used the built-in software AngioVue AngioAnalytics (Version 2017.1, Optovue Inc., Fremont, CA, United States). This software utilizes a split-spectrum amplitude decorrelation angiography algorithm with a three-dimensional projection artifact removal technique. All image acquisitions were made by one investigator (E.W.). The OCT/OCTA signal strength index (from 1 to 10) was also provided by the software.

Outcome Measures

The primary outcome measures of this study were longitudinal changes in retinal thickness and perfusion function between 10 and 90 days after PPV, including pRNFL thickness, RPC VD, inner limiting membrane to inner plexiform layer thickness, full retinal thickness, SVC VD, and DVC VD. Secondary outcome measures were longitudinal changes in pRNFL thickness between 10 and 90 days after PPV in each sector.

Sample Size Calculation and Statistical Analysis

The longitudinal change in pRNFL thickness between 10 and 90 days after PPV in the SO group and Gas group was found to be −22.5 μm and −4.0 μm, respectively, by sampling. Assuming a study power of 90%, an alpha of 0.05, and equal group allocation, 12 subjects per cohort was determined to be the minimum sample size needed. Once 12 subjects per cohort completed a 90 day follow-up, enrollment ended, and the remaining subjects who were already enrolled were allowed to complete follow-up. Statistical analysis was performed using SPSS software (version 22.0; SPSS Inc., Chicago, IL). The normal distribution of all variables was verified by the Kolmogorov–Smirnov method. Baseline clinical characteristics were compared between the two groups (SO vs. Gas) using an independent Student's *t* test, Mann–Whitney U test, and Fisher's

TABLE 1 | Baseline characteristics of subjects included in the analysis[a]

Variables	SO group (n = 23)	Gas group (n = 13)	$p^{\dagger}$
Age, y	56.0 ± 15.0	58.6 ± 7.0	0.478
Male gender (%)	9 (39.1)	6 (46.2)	0.736
Right Eye (number [%])	8(34.8)	6 (65.2)	0.723
Phakic eyes/pseudophakic eyes	17/3	13/0	0.261
Visual acuity (LogMAR)	2.0 ± 1.4	1.6 ± 0.9	0.102
Axial length (mm)	23.1 ± 0.6	23.0 ± 0.9	0.967
IOP (mmHg)	14.7 ± 3.0	15.2 ± 2.6	0.589
HbA1c (%)	7.6 ± 3.4	8.0 ± 1.4	0.619
Duration of diabetes (years)	7.5 ± 13.4	15.4 ± 7.4	0.061
Type 2 diabetes (number [%])	21 (91.3)	13 (100.0)	0.525
Hypertension (number [%])	12 (52.2)	8 (61.5)	0.731
Duration of hypertension (years)	2.0 ± 5.0	1.0 ± 11.0	0.733

[a]*Quantitative data and qualitative data are expressed as the mean ± SD, or median ± IQR, and number of people (%), respectively.*

[†]p *values refer to independent Student's t test, Mann–Whitney U test and Fisher's exact test were used to explore the differences in characteristics between two groups.*

IOP, intraocular pressure.

exact test. The paired *t* test or Wilcoxon signed rank test was used to compare the parameters between the two follow-up visits. The intergroup differences in longitudinal changes in evaluation indicators between 10 and 90 days after PPV were tested using an independent Student's *t* test or Mann–Whitney U test. Correlations between the change in pRNFL thickness and other variables were evaluated using Spearman's correlation analysis. A *p* value of less than 0.05 was considered statistically significant.

RESULTS

Basic Information

A total of 38 eligible patients (47 eyes) with PDR were enrolled and underwent a baseline examination and PPV. Among these, 11 patients (11 eyes) were excluded for the following reasons: failure to complete follow-up (2 patients, 2 eyes), postoperative persistent high IOP under medicine (2 patients, 2 eyes), and poor image quality (7 patients, 7 eyes; **Figure 1**). A total of 27 patients (36 eyes, 15 females and 12 males) completed all follow-up visits and were statistically analyzed. The median age of the patients was 56.6 ± 9.8 years. The mean time of DM was 11.9 ± 10.0 years. The mean axial length was 23.1 ± 0.8 mm. The median logMAR VA was 2.0 ± 1.7 (Snellen equivalent 20/2000) before the operation and 1.5 ± 1.0 (Snellen equivalent 20/632) 90 days after the operation ($p = 0.125$). The mean IOP was 14.8 ± 2.9 mmHg before the operation and 16.5 ± 5.1 mmHg 90 days after the operation ($p = 0.066$). Three eyes in the SO group and one eye in the gas group had elevated IOP not exceeding 30 mmHg in the first postoperative week and were controlled with medical therapy. As shown in **Table 1**, no significant difference in demographics or clinical characteristics was found between the two groups. The SO was kept well in the vitreous cavity in all patients in the SO group and never escaped to the anterior chamber during follow-up.

Longitudinal Changes in the Two Groups

Longitudinal changes in all evaluation indicators between 10 and 90 days after PPV in the two groups are presented in **Table 2**. Eyes in the SO group had a statistically significant decrease in pRNFL thickness at 90 days after PPV (10 days after PPV: 148.2 ± 56.3, 90 days after PPV: 102.6 ± 50.8 μm, $p < 0.001$). Eyes in the Gas group had a statistically significant increase in parafoveal SVC VD at 90 days after PPV (10 days after PPV: 34.4 ± 3.8%, 90 days after PPV: 36.6 ± 7.0%, $p = 0.023$).

Different Tamponade Effects Between the Two Groups and Analysis of the Related Factors

Intergroup comparisons of all evaluation indicators for the longitudinal changes between 10 and 90 days after PPV are shown in **Table 3**. Compared to the Gas group, the SO group exhibited a greater decrease in pRNFL thickness, which led to a significant difference (SO: −26.3 ± 31.3 μm, Gas: −5.2 ± 17.3 μm, $p = 0.001$). No significant results were observed in other indicators of retinal thickness and capillary plexus flow density changes during follow-up.

Table 4 shows the correlation between changes in pRNFL thickness and other variables. The type of tamponade, changes in full retina thickness and parafoveal SVC VD showed a significant correlation with changes in pRNFL thickness ($p < 0.001$, $p = 0.024$, and $p = 0.042$, respectively).

Changes in pRNFL Thickness in Each Sector

As shown in **Table 5** and **Figure 2**, Superior ($p = 0.001$), Nasal ($p < 0.001$), and Inferior $p < 0.001$) pRNFL thicknesses at 90 days after PPV significantly decreased compared with those at 10 days after PPV in the SO group. In addition, the decreases in pRNFL thickness in the superior ($p = 0.024$), nasal ($p = 0.003$), and inferior ($p = 0.011$) sectors in the SO group were significantly greater than those in the Gas group.

DISCUSSION

SO is frequently used as a vitreous substitute during PPV surgery in patients with PDR (Castellarin et al., 2003; Altan et al., 2008). It

TABLE 2 | Longitudinal changes in evaluation indicators in the SO group and Gas group[a]

Groups	Measurements	10 days after PPV	90 days after PPV	$p^{\dagger}$
SO Group	pRNFL thickness (μm)	147.0 ± 61.1	106.1 ± 49.8	<**0.001**
	RPC VD (%)	42.3 ± 6.1	42.2 ± 5.0	0.420
	ILM_IPL thickness (μm)	119.8 ± 50.7	125.4 ± 43.9	0.415
	Full retinal thickness (μm)	414.6 ± 99.1	379.5 ± 123.0	0.062
	SVC VD (%)	36.8 ± 5.2	35.2 ± 8.9	0.940
	DVC VD (%)	40.9 ± 6.4	40.0 ± 6.3	0.528
Gas Group	pRNFL thickness (μm)	111.2 ± 19.4	104.8 ± 15.7	0.235
	RPC VD (%)	42.8 ± 6.5	42.6 ± 2.9	0.311
	ILM_IPL thickness (μm)	112.0 ± 21.7	111.3 ± 22.4	0.972
	Full retinal thickness (μm)	377.2 ± 55.3	371.3 ± 64.1	0.531
	SVC VD (%)	34.4 ± 3.8	36.6 ± 7.0	**0.023**
	DVC VD (%)	41.7 ± 3.9	40.1 ± 4.8	0.321

Bold values indicate statistically significant differences.

[a]*Quantitative data are expressed as the mean ± standard deviation or median ± interquartile range.*

[†]*p values refer to the paired t test or Wilcoxon signed rank test exploring the differences in evaluation indicators between 10 and 90 days after PPV.*

PPV, pars plana vitrectomy; SO, silicone oil; pRNFL, peripapillary retinal nerve fiber layer; RPC, radial peripapillary capillaries; VD, vessel density; ILM, inner limiting membrane; IPL, inner plexiform layer; SVC, superficial vascular complex; DVC, deep vascular complex.

TABLE 3 | Intergroup differences in longitudinal changes in evaluation indicators[a].

Measurements	Changes between 10 and 90 days after PPV		
	SO group	Gas group	$p^{\dagger}$
pRNFL thickness (μm)	−21.9 ± 31.8	−5.1 ± 12.6	**0.002**
RPC VD (%)	0.5 ± 3.7	1.1 ± 3.2	0.895
ILM_IPL thickness (μm)	−5.7 ± 33.2	−0.7 ± 16.4	0.510
Full retinal thickness (μm)	−39.0 ± 95.2	−5.9 ± 33.0	0.141
SVC VD (%)	−0.1 ± 5.6	1.9 ± 2.9	0.164
DVC VD (%)	−0.9 ± 6.5	−1.5 ± 5.3	0.758

Bold values indicate statistically significant differences.

[a]*Quantitative data are expressed as the mean ± standard deviation or median ± interquartile range.*

[†]*p values refer to independent Student's t test or the Mann–Whitney U test exploring the intergroup differences in longitudinal changes in evaluation indicators between 10 and 90 days after PPV.*

PPV, pars plana vitrectomy; SO, silicone oil; pRNFL, peripapillary retinal nerve fiber layer; RPC, radial peripapillary capillaries; VD, vessel density; ILM, inner limiting membrane; IPL, inner plexiform layer; SVC, superficial vascular complex; DVC, deep vascular complex.

TABLE 4 | Correlations between changes in pRNFL thickness and other variables.

Measurements	Changes of pRNFL thickness	
	Correlation coefficient	p^{*}
Changes of RPC VD	0.166	0.334
Changes of ILM_IPL thickness	0.327	0.052
Changes of full retina thickness	0.375	**0.024**
Changes of SVC VD	0.341	**0.042**
Changes of DVC VD	0.017	0.921
Type of tamponade	0.523	**0.001**

Bold values indicate statistically significant differences.

[*]*p values refer to Spearman's correlation analysis exploring the correlations between the changes in pRNFL, thickness and other variables.*

pRNFL, peripapillary retinal nerve fiber layer; RPC, radial peripapillary capillaries; VD, vessel density; ILM, inner limiting membrane; IPL, inner plexiform layer; SVC, superficial vascular complex; DVC, deep vascular complex.

is able to reduce the incidence of NVG, act as a barrier to angiogenic factors, and allow further photocoagulation in the early postoperative period when endolaser uptake is inadequate (McLeod, 1986; Pearson et al., 1993; Castellarin et al., 2003; Morphis et al., 2012). However, SO tamponade has difficulty acquiring a complete oil fill during PPV and requires a second surgery for extraction from the eye. Many surgeons prefer using C3F8 gas as a vitreous substitute in PDR patients due to its characteristics of higher surface tension, buoyant force, and spontaneous reabsorption compared with that of SO (Castellarin et al., 2003;Schwartz et al., 2014).

VR surgeons frequently confront a dilemma when determining which vitreous substitute to select during PPV in advanced indications of PDR, such as TRD or extensive fibrous proliferation, especially when iatrogenic retinal breaks occur. To avoid postoperative problems such as proliferative vitreoretinopathy, retinal detachment, or VH, surgeons must take precautions before performing the procedure.

Vitreous substitution of BSS, air, gas, and SO tamponade has been compared by several retrospective studies without reporting a difference in postoperative outcomes (Yorston et al., 2008;Ostri et al., 2014;Dikopf et al., 2015;Jackson et al., 2016). A randomized clinical trial (RCT) that compared gas and SO tamponade in eyes with diabetic retinopathy showed that the postoperative BCVA was poorer in SO tamponade eyes than in gas tamponade eyes at

TABLE 5 | Intergroup differences in longitudinal changes in peripapillary retinal nerve fiber layer thickness in each sector[a].

Measurements	SO group at 10 days after PPV	SO group at 90 days after PPV	$p^{\dagger}$	Gas group at 10 days after PPV	Gas group at 90 days after PPV	$p^{\dagger}$	Changes (between10 days and 90 days after PPV in SO group)	Changes (between10 days and 90 days after PPV in gas group)	$p^{\ddagger}$ (intergroup difference of changes between 10 and 90 days after PPV)
Superior	147.3 ± 76.5	122.1 ± 79.2	**0.001**	132.3 ± 19.3	123.7 ± 21.7	0.067	−25.5 ± 27.5	−8.6 ± 15.4	**0.024**
Nasal	108.5 ± 79.7	79.8 ± 27.5	<**0.001**	88.0 ± 25.7	74.7 ± 16.7	0.055	−36.2 ± 43.9	−8.5 ± 21.2	**0.003**
Inferior	178.0 ± 76.2	145.5 ± 59.6	<**0.001**	136.9 ± 24.0	129.1 ± 26.4	0.198	−26.7 ± 31.1	−4.3 ± 13.8	**0.011**
Temporal	122.7 ± 80.3	130.2 ± 68.6	0.563	103.7 ± 37.6	100.1 ± 34.8	0.701	−1.57 ± 37.2	−1.3 ± 22.1	0.974

Bold values indicate statistically significant differences.

[a]*Quantitative data are expressed as the mean ± standard deviation or median ± interquartile range;*

[†]p *values referring to the paired* t *test or Wilcoxon signed rank test were used to compare the parameters between the two follow-up visits;*

[‡]p *values referring to independent Student's t test or Mann–Whitney U test were used to explore the intergroup differences in longitudinal changes in evaluation indicators between 10 and 90 days after PPV.*

PPV, pars plana vitrectomy; SO, silicone oil.

6 months (Rush et al., 2021). In addition, some studies have observed a decline in VA following SO tamponade in patients undergoing PPV surgery for diabetic TRD, and SO has been hypothesized to be harmful to the retina (Yorston et al., 2008;Jackson et al., 2016). Pallor of the optic nerve was more prevalent following SO tamponade, implying that long-term SO tamponade may contribute to optic nerve injury (Shroff et al., 2018).

There is a paucity of studies investigating detailed changes in the retina following SO or gas tamponade in PDR patients undergoing PPV surgery. However, some studies reported changes in eyes with rhegmatogenous retinal detachment (RRD). Zhou et al. (2020) reported that compared to gas, SO could have more negative tamponade effects on both fundus vasculature and structure. A retrospective study completed by Inan et al. (2020) found thinning in the layers of the ganglion cell layer, outer plexiform layer, and outer nuclear layer in the SO group. Moreover, Liu et al. (2021) reported that the parafoveal vessel densities in the SVC and the corresponding inner retinal thickness were significantly reduced in the affected eyes compared to the contralateral eyes in the SO group but similar between the affected eyes and the contralateral eyes in the Gas group. These studies suggest that the use of SO tamponade affects retinal layer thickness more significantly than perfluoropropane gas tamponade in eyes with RRD.

In this study, we investigated the effects of SO and gas on the retina in eyes with PDR by comparing changes in postoperative retinal thickness and VD using SD-OCT *in vivo*. We found that SO tamponade had a significant effect on the postoperative decrease in pRNFL thickness, and there was a significant intergroup difference in the changes between 10 and 90 days after PPV surgery. To further explore the factors associated with changes in the pRNFL after PPV, we found that the type of tamponade (SO or C3F8 Gas) had a strong correlation with changes in pRNFL thickness in patients with PDR. These findings strongly support the appearance of optic nerve pallor observed in an earlier study (Shroff et al., 2018). Zhou et al. (2020) also reported that compared to gas tamponade, SO tamponade resulted in a more pronounced decrease in nerve fiber layer thickness, although the study was carried out in eyes with RRD.

However, the exact mechanism by which SO significantly reduces the thickness of pRNFLs remains uncertain. First, SO-induced mechanical stress in the fovea can result in the subsequent early loss of ONL cell bodies (Dooley et al., 2015). Although mechanical stress may be related to increased IOP, in our study, eyes with IOP elevation could immediately be controlled with IOP-lowering agents, and none of the eyes showed IOP elevation greater than 30 mmHg. Severe optic neuropathy could result from SO tamponade through subretinal migration of SO (Knecht et al., 2007;Majid et al., 2008). Migration of phagocytosed emulsified oil bubbles by macrophages might be a mechanism for subretinal migration of SO (Budde et al., 2001). However, subretinal migration of SO was not found in our study. Another possible mechanism of retinal thinning is SO-related idiopathic reactions or retinal ionic environmental changes (Winter et al., 2000). Local changes in concentrations of potassium due to the failure of potassium siphoning by Müller cells and apoptosis and subsequent neuronal degeneration changes could be indirect mechanisms (Winter et al., 2000; Newsom et al., 2004). It was reported that the micromolecule in SO might diffuse from the oil and penetrate into retinal tissue, inducing inflammation and retinal toxicity (Gonvers et al., 1986; Gabel et al., 1987). This seems to be consistent with our analysis, which showed that changes in full retinal thickness and SVC VD in the macula had a strong correlation with changes in pRNFL thickness.

It is somewhat surprising that no significant intergroup differences were found in the temporal sector. A possible explanation for this might be that the temporal side is closer to the macula and has a relatively good blood supply. The significant correlation observed in the correlation analysis in this study between changes in pRNFL thickness and SVC VD in the macula might be an explanation.

Furthermore, changes in perfusion function between 10 and 90 days after PPV surgery were also investigated after PPV. It

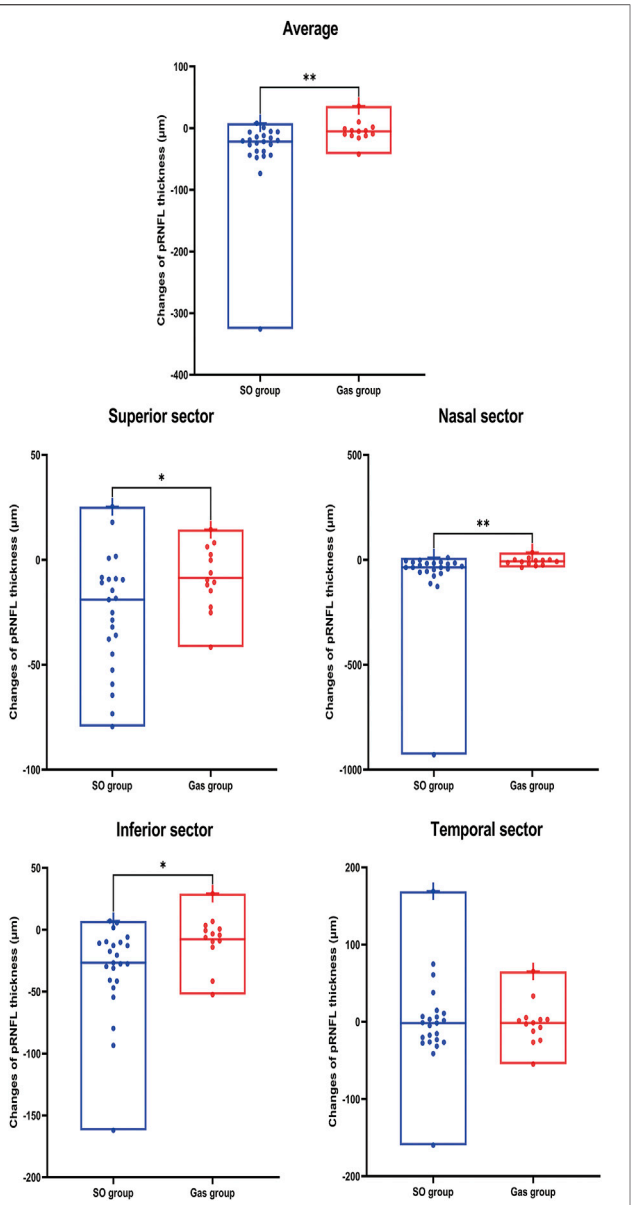

FIGURE 2 | Changes in pRNFL thickness on average and in each sector were compared between the two groups. SO, silicone oil. *p* value: *, < 0.05; **, < 0.01; ***, < 0.001; ****, < 0.0001.

was interesting that gas tamponade had a significant effect on the postoperative increase in parafoveal SVC VD, while SO tamponade had a mild effect on the postoperative decrease in parafoveal SVC VD. However, there was not a significant intergroup difference. This result was similar to that found in a study conducted in patients with primary RRD (Zhou et al., 2020).

Regarding the effects on full retinal thickness and thickness between the inner limiting membrane and inner plexiform layer, SO had more negative tamponade effects than Gas, with no statistically significant intergroup differences. These trends were almost consistent with previous studies in RRD eyes (Inan et al., 2020; Zhou et al., 2020; Liu et al., 2021), although the etiology and mechanisms of RRD and PDR were quite different.

This study has some limitations. First, the two vitreous substitution groups in this prospective, observational study were not randomized but rather based on patient need or ocular condition because randomization would raise some ethical issues. Second, on account of the tamponade choice and timely SO removal in clinical practice in our ophthalmic center, the observation time was relatively short, and only comparisons between gas and SO tamponade were analyzed. Extended SO tamponade, on the other hand, may be followed by more adverse effects, such as glaucoma, cataract formation, and peri-SO reproliferation (Tsui et al., 2020). Furthermore, the sample size of our study was relatively small. In the future, large-scale clinical trials with other vitreous substitution groups, such as BSS, air, or short-acting gas, are needed.

In conclusion, SO tamponade had a significantly greater decrease in pRNFL over 90 days than perfluoropropane gas tamponade, whereas no significant intergroup difference was observed in the temporal sector in patients with PDR. The changes in the pRNFL were correlated with changes in full retina thickness and parafoveal SVC VD after the operation. Therefore, surgeons should be aware of the reduction of pRNFL thickness in patients with SO tamponade to manage them appropriately regarding any changes in retina.

DATA AVAILABILITY STATEMENT

The raw data supporting the conclusion of this article will be made available by the authors, without undue reservation.

ETHICS STATEMENT

The studies involving human participants were reviewed and approved by the Institutional Review Board of PUMCH. The patients/participants provided their written informed consent to participate in this study.

AUTHOR CONTRIBUTIONS

HM designed the research. TW, EW, and NL conducted the research and analyzed the data. HM, TW, EW and HC wrote the article. HM had primary responsibility for the final content. All authors read and approved the final manuscript.

FUNDING

This research did not receive any specific grant from funding agencies in the public, commercial, or not-for-profit sectors.

REFERENCES

Altan, T., Acar, N., Kapran, Z., Unver, Y. B., and Ozdogan, S. (2008). Transconjunctival 25-gauge Sutureless Vitrectomy and Silicone Oil Injection in Diabetic Tractional Retinal Detachment. *Retina* 28, 1201–1206. doi:10.1097/iae.0b013e3181853d3c

Budde, M., Cursiefen, C., Holbach, L. M., and Naumann, G. O. H. (2001). Silicone Oil-Associated Optic Nerve Degeneration. *Am. J. Ophthalmol.* 131, 392–394. doi:10.1016/s0002-9394(00)00800-x

Castellarin, A., Grigorian, R., Bhagat, N., Del Priore, L., and Zarbin, M. A. (2003). Vitrectomy with Silicone Oil Infusion in Severe Diabetic Retinopathy. *Br. J. Ophthalmol.* 87, 318–321. doi:10.1136/bjo.87.3.318

Christou, E. E., Stavrakas, P., Batsos, G., Christodoulou, E., and Stefaniotou, M. (2021). Association of OCT-A Characteristics with Postoperative Visual Acuity after Rhegmatogenous Retinal Detachment Surgery: a Review of the Literature. *Int. Ophthalmol.* 41, 2283–2292. doi:10.1007/s10792-021-01777-2

Dikopf, M. S., Patel, K. H., Setlur, V. J., and Lim, J. I. (2015). Surgical Outcomes of 25-gauge Pars Plana Vitrectomy for Diabetic Tractional Retinal Detachment. *Eye* 29, 1213–1219. doi:10.1038/eye.2015.126

Dooley, I., Treacy, M., O'Rourke, M., Khaild, I., and Kilmartin, D. (2015). Serial Spectral Domain Ocular Coherence Tomography Measurement of Outer Nuclear Layer Thickness in Rhegmatogenous Retinal Detachment Repair. *Curr. Eye Res.* 40, 1073–1076. doi:10.3109/02713683.2014.971936

Gabel, V.-P., Kampik, A., and Burkhardt, J. (1987). Analysis of Intraocularly Applied Silicone Oils of Various Origins. *Graefe's Arch. Clin. Exp. Ophthalmol.* 225, 160–162. doi:10.1007/bf02175441

Gonvers, M., Hornung, J. P., and De Courten, C. (1986). The Effect of Liquid Silicone on the Rabbit Retina. *Arch. Ophthalmol.* 104, 1057–1062. doi:10.1001/archopht.1986.01050190115049

Gupta, B., Wong, R., Sivaprasad, S., and Williamson, T. H. (2012). Surgical and Visual Outcome Following 20-gauge Vitrectomy in Proliferative Diabetic Retinopathy over a 10-year Period, Evidence for Change in Practice. *Eye* 26, 576–582. doi:10.1038/eye.2011.348

Inan, S., Polat, O., Ozcan, S., and Inan, U. U. (2020). Comparison of Long-Term Automated Retinal Layer Segmentation Analysis of the Macula between Silicone Oil and Gas Tamponade after Vitrectomy for Rhegmatogenous Retinal Detachment. *Ophthalmic Res.* 63, 524–532. doi:10.1159/000506382

Jackson, T. L., Johnston, R. L., Donachie, P. H. J., Williamson, T. H., Sparrow, J. M., and Steel, D. H. W. (2016). The Royal College of Ophthalmologists' National Ophthalmology Database Study of Vitreoretinal Surgery. *JAMA Ophthalmol.* 134, 79–85. quiz 120. doi:10.1001/jamaophthalmol.2015.4587

Knecht, P., Groscurth, P., Ziegler, U., Laeng, H. R., Jaggi, G. P., and Killer, H. E. (2007). Is Silicone Oil Optic Neuropathy Caused by High Intraocular Pressure Alone? A Semi-biological Model. *Br. J. Ophthalmol.* 91, 1293–1295. doi:10.1136/bjo.2007.117390

Liu, Y., Lei, B., Jiang, R., Huang, X., Zhou, M., and Xu, G. (2021). Changes of Macular Vessel Density and Thickness in Gas and Silicone Oil Tamponades after Vitrectomy for Macula-On Rhegmatogenous Retinal Detachment. *BMC Ophthalmol.* 21, 392. doi:10.1186/s12886-021-02160-6

Majid, M. A., Hussin, H. M., Biswas, S., Haynes, R. J., Mayer, E. J., and Dick, A. D. (2008). Emulsification of Densiron-68 Used in Inferior Retinal Detachment Surgery. *Eye* 22, 152–157. doi:10.1038/sj.eye.6702784

Mcleod, D. (1986). Silicone-oil Injection during Closed Microsurgery for Diabetic Retinal Detachment. *Graefe's Arch. Clin. Exp. Ophthalmol.* 224, 55–59. doi:10.1007/bf02144135

Michels, R. G., and De Bustros, S. (1988). Vitrectomy for Complications of Proliferative Diabetic Retinopathy. *J. Diabet. Complicat.* 2, 62–67. doi:10.1016/0891-6632(88)90004-9

Morphis, G., Irigoyen, C., Eleuteri, A., Stappler, T., Pearce, I., and Heimann, H. (2012). Retrospective Review of 50 Eyes with Long-Term Silicone Oil Tamponade for More Than 12 Months. *Graefes Arch. Clin. Exp. Ophthalmol.* 250, 645–652. doi:10.1007/s00417-011-1873-8

Moss, S., Klein, R., and Klein, B. E. (1998). The 14-year Incidence of Visual Loss in a Diabetic Population,. *Ophthalmology* 105, 998–1003. doi:10.1016/s0161-6420(98)96025-0

Newsom, R. S. B., Johnston, R., Sullivan, P. M., Aylward, G. B., Holder, G. E., and Gregor, Z. J. (2004). Sudden Visual Loss after Removal of Silicone Oil. *Retina* 24, 871–877. doi:10.1097/00006982-200412000-00005

Ostri, C., Lux, A., Lund-Andersen, H., and La Cour, M. (2014). Long-term Results, Prognostic Factors and Cataract Surgery after Diabetic Vitrectomy: a 10-year Follow-Up Study. *Acta Ophthalmol.* 92, 571–576. doi:10.1111/aos.12325

Pearson, R. V., Mcleod, D., and Gregor, Z. J. (1993). Removal of Silicone Oil Following Diabetic Vitrectomy. *Br. J. Ophthalmol.* 77, 204–207. doi:10.1136/bjo.77.4.204

Rush, R. B., Del Valle Penella, A., Reinauer, R. M., Rush, S. W., and Bastar, P. G. (2021). Silicone Oil versus Perfluoropropane Gas Tamponade during Vitrectomy for Tractional Retinal Detachment or Fibrous Proliferation. *Retina* 41, 1407–1415. doi:10.1097/iae.0000000000003052

Schwartz, S. G., Flynn, H. W., Jr., Lee, W. H., and Wang, X. (2014). Tamponade in Surgery for Retinal Detachment Associated with Proliferative Vitreoretinopathy. *Cochrane Database Syst. Rev.* 2, CD006126. doi:10.1002/14651858.CD006126.pub3

Shroff, C. M., Gupta, C., Shroff, D., Atri, N., Gupta, P., and Dutta, R. (2018). BIMANUAL MICROINCISION VITREOUS SURGERY FOR SEVERE PROLIFERATIVE DIABETIC RETINOPATHY: OUTCOME IN MORE Than 300 EYES. *Retina* 38 (Suppl. 1), S134–S145. doi:10.1097/IAE.0000000000002093

Spaide, R. F., Fujimoto, J. G., Waheed, N. K., Sadda, S. R., and Staurenghi, G. (2018). Optical Coherence Tomography Angiography. *Prog. Retin. Eye Res.* 64, 1–55. doi:10.1016/j.preteyeres.2017.11.003

Tsui, M. C., Hsieh, Y. T., and Yang, C. M. (2020). Silicone Oil Removal after Extended Tamponade in Proliferative Diabetic Retinopathy-A Long Range of Follow-Up. *Eye (Lond)* 34, 2307–2314. doi:10.1038/s41433-020-0815-2

Winter, M., Eberhardt, W., Scholz, C., and Reichenbach, A. (2000). Failure of Potassium Siphoning by Müller Cells: a New Hypothesis of Perfluorocarbon Liquid-Induced Retinopathy. *Invest. Ophthalmol. Vis. Sci.* 41, 256–261.

Yorston, D., Wickham, L., Benson, S., Bunce, C., Sheard, R., and Charteris, D. (2008). Predictive Clinical Features and Outcomes of Vitrectomy for Proliferative Diabetic Retinopathy. *Br. J. Ophthalmol.* 92, 365–368. doi:10.1136/bjo.2007.124495

Zhou, Y., Zhang, S., Zhou, H., Gao, M., Liu, H., and Sun, X. (2020). Comparison of Fundus Changes Following Silicone Oil and Sterilized Air Tamponade for Macular-On Retinal Detachment Patients. *BMC Ophthalmol.* 20, 249. doi:10.1186/s12886-020-01523-9

Conflict of Interest: The authors declare that the research was conducted in the absence of any commercial or financial relationships that could be construed as a potential conflict of interest.

Publisher's Note: All claims expressed in this article are solely those of the authors and do not necessarily represent those of their affiliated organizations, or those of the publisher, the editors and the reviewers. Any product that may be evaluated in this article, or claim that may be made by its manufacturer, is not guaranteed or endorsed by the publisher.

Copyright © 2022 Wang, Wang, Chen, Li and Min. This is an open-access article distributed under the terms of the Creative Commons Attribution License (CC BY). The use, distribution or reproduction in other forums is permitted, provided the original author(s) and the copyright owner(s) are credited and that the original publication in this journal is cited, in accordance with accepted academic practice. No use, distribution or reproduction is permitted which does not comply with these terms.

frontiers | Frontiers in Physiology

ORIGINAL RESEARCH
published: 15 July 2022
doi: 10.3389/fphys.2022.862732

Study on Proteomics-Based Aortic Dissection Molecular Markers Using iTRAQ Combined With Label Free Techniques

*Ting Deng[1,2,3,4†], Yongguang Liu[5†], Akindavyi Gael[2,3,4,6], Xiaohua Fu[7], Xiaofang Deng[8], Yunfeng Liu[2,3,4], Yizhang Wu[2,3,4], Yingzhi Wu[2,3,4], Huimin Wang[2,3,4], Yuying Deng[2,3,4], Jun Lai[2,3,4] and Qiang Fu[2,3,4,6]**

[1]Department of Cardiovascular Disease, First Affiliated Hospital of Guangzhou University of Chinese Medicine, Guangzhou, China, [2]Department of Cardiology, Laboratory of Heart Center, Heart Center, Zhujiang Hospital, Southern Medical University, Guangzhou, China, [3]Guangdong Provincial Biomedical Engineering Technology, Research Center for Cardiovascular Disease, Guangdong, China, [4]Sino-Japanese Cooperation Platform for Translational Research in the Heart Failure, Guangzhou, China, [5]Department of Organ Transplantation, Zhujiang Hospital, Southern Medical University, Guangzhou, China, [6]Department of Cardiology, Shenzhen Hospital, Southern Medical University, Shenzhen, China, [7]Department of Invasive Technology, Zhujiang Hospital, Southern Medical University, Guangzhou, China, [8]Department of Neonatology, Guangdong Provincial People's Hospital, Guangzhou, China

OPEN ACCESS

Edited by:
Yih-Kuen Jan,
The University of Illinois at Urbana-Champaign, United States

Reviewed by:
Yang-Yang Qu,
Southeast University, China
Alexander E. Berezin,
Zaporizhia State Medical University, Ukraine

***Correspondence:**
Qiang Fu
fuqiang671866@163.com

†These authors have contributed equally to this work

Specialty section:
This article was submitted to Clinical and Translational Physiology, a section of the journal Frontiers in Physiology

Received: *26 January 2022*
Accepted: *23 May 2022*
Published: *15 July 2022*

Citation:
Deng T, Liu Y, Gael A, Fu X, Deng X, Liu Y, Wu Y, Wu Y, Wang H, Deng Y, Lai J and Fu Q (2022) Study on Proteomics-Based Aortic Dissection Molecular Markers Using iTRAQ Combined With Label Free Techniques. Front. Physiol. 13:862732. doi: 10.3389/fphys.2022.862732

Background: Aortic dissection refers to the separation of aortic media and extension along the long axis to form the true and false chambers of the aortic wall. 65–70% of the patients died of cardiac tamponade, arrhythmia, dissection rupture, etc. At present, echocardiography, computed tomography angiography (CTA), etc. are the main diagnosis tools for aortic dissection. To date, there is no rapid serum molecular marker that can be used for differential diagnosis and risk assessment.

Objectives: To screen serum molecular markers systematically amid aortic dissection and acute coronary syndrome and to preliminarily identify the pathogenesis of acute aortic dissection.

Methods: Related disputes cases of all hospitals were statistically analyzed for the AAD medical disputes ratio, early death ratio and misdiagnosis ratio from the database of Guangdong Province Medical Disputes Coordination Committee from 2013 to 2017. Serum and Aortic tissues samples were respectively quantified by iTRAQ and label-free analysis, further validated by ELISA and protein verified by immunofluorescence and Western blot from AAD and control patients enrolled from the Zhujiang Hospital of Southern Medical University and Guangdong Province people's Hospital from 2016 to 2018.

Results: AAD cases ratio accounted for 15.29% in all 150 cardiovascular disputes, 59.26% in all cardiovascular death less than 24 h, and 88.89% in the patients who remained undiagnosed at the time of death, 84 proteins (66 and 18 upregulated and downregulated, respectively) were identified by iTRAQ and 16 proteins (9 and 7 upregulated and downregulated, respectively) by Label-free. Nine proteins (Lumican, FGL1, PI16, MMP9, FBN1, MMP2, VWF, MMRN1, and PF4) related to the

pathogenesis of aortic dissection were identified by David /Ease and String techniques as candidate biomarkers for verification test. Four proteins (Lumican, FGL1, PI16, and MMP9) were found to be statistically different after ELISA verification. The expression of FGL1, PI16, and MMP9 proteins was pathologically significantly increased except for Lumican. Histologically, TGF-β1, α-SMA, and Collagen1 were also significantly higher in the aortic group.

Conclusion: Lumican, FGL1, PI16, and MMP9 may be potential biomarkers in AAD patients, and the Lumican-mediated TGF-β1 pathway is likely to be involved in the pathogenesis of aortic dissection.

Keywords: aortic dissection, proteomic, iTRAQ, label-free, Lumican

1 INTRODUCTION

Acute aortic dissection (AAD) is a major vascular disease with high mortality and poor prognosis. As a life-threatening cardiovascular disease, the related untreated mortality rate is about 1–2% per hour after the onset of symptoms (Hagan et al., 2000). Early diagnosis is crucial and can even save lives (Klompas, 2002). One of the main challenges in establishing the diagnosis is to differentiate AAD from other sudden severe chest pain diseases, especially acute myocardial infarction (AMI) and pulmonary embolism (PE), because patients suffering from these diseases present similar symptoms but require different treatments. Misdiagnosis of AAD often leads to catastrophic bleeding or AAD deterioration, especially when thrombolytic drugs are used improperly (Wilcox et al., 1988; Butler et al., 1990).

According to 2014 ESC guidelines for the diagnosis and treatment of aortic dissection, imaging remained the main method of diagnosis and differential diagnosis (Suzuki et al., 2008). However, CTA, transthoracic or transesophageal ultrasound, and other imaging methods are time-consuming and present various risks in the process of examination. The detection of serological markers is more objective, and blood marker testing can reduce patient movement. Unfortunately, there are currently no widely available AAD biomarkers with high sensitivity and specificity. At present, research on aortic dissection markers are mainly based on the pathophysiological development process of the disease, which mainly includes smooth muscle protein, matrix metalloprotease, elastic protein fragment, D-dimer, and some other proteins. However, these molecules cannot be clinically widely used because of the lack of specificity and sensitivity.

The combination of isobaric Tags for Relative and Absolute Quantitation (iTRAQ) and label-free methods can be used to identify biomarkers of various diseases (Wen et al., 2009). Combining these two methods, we proceeded to determine the serum biomarkers released after aortic dissection, which can provide a wider range of proteomics for AAD diagnosis. Discovery of new molecular markers, the diagnosis of aortic dissection can be more sensitive and specific, reduce the dependence on imaging equipment and physicians' experience, provide reliable and economical tools for lower-level hospitals that lack the support of relevant conditions, thereby reducing misdiagnosis and delays, and achieve the purpose of optimal diagnosis and treatment.

2 MATERIALS AND METHODS

2.1 Ethical Approval of the Study Protocol

Written informed consent was obtained from all the participants before enrollment. The protocol of this study was carried out according to the principles of the Declaration of Helsinki and approved by the Medical Ethics Committee in Zhujiang Hospital (Case No: 2018-XXGNK-001). The protocol is available at www.clinicaltrials.gov (ChiCTR1800015743). This trial was conducted and monitored according to the guidelines for Good Clinical Practice. The design of this study is shown in **Figure 1**.

2.2 Analysis of Cardiovascular Disputes Cases

We collected cardiovascular dispute cases registered in the database of the Guangdong Province Medical Disputes Coordination Committee in all hospitals in the Guangdong Province from January 2013 to December 2017. Patients were divided into two groups (AAD group and non-AAD group). The overall mortality rate, 24 h mortality rate, and undiagnosed mortality rate were separately calculated according to different levels of hospitals (**Figure 2**).

2.3 Analysis of Clinical Sera and Tissues Samples

2.3.1 Materials Collection

Seventy-seven AAD patients (AAD group) with sudden chest pain within 72 h and 73 patients with non-AAD chest pain were enrolled from the Zhujiang Hospital of Southern Medical University and Guangdong Province people's Hospital for serum analysis from January 2016 to December 2018. Nine AAD patients and nine organ donors' aortic tissues were

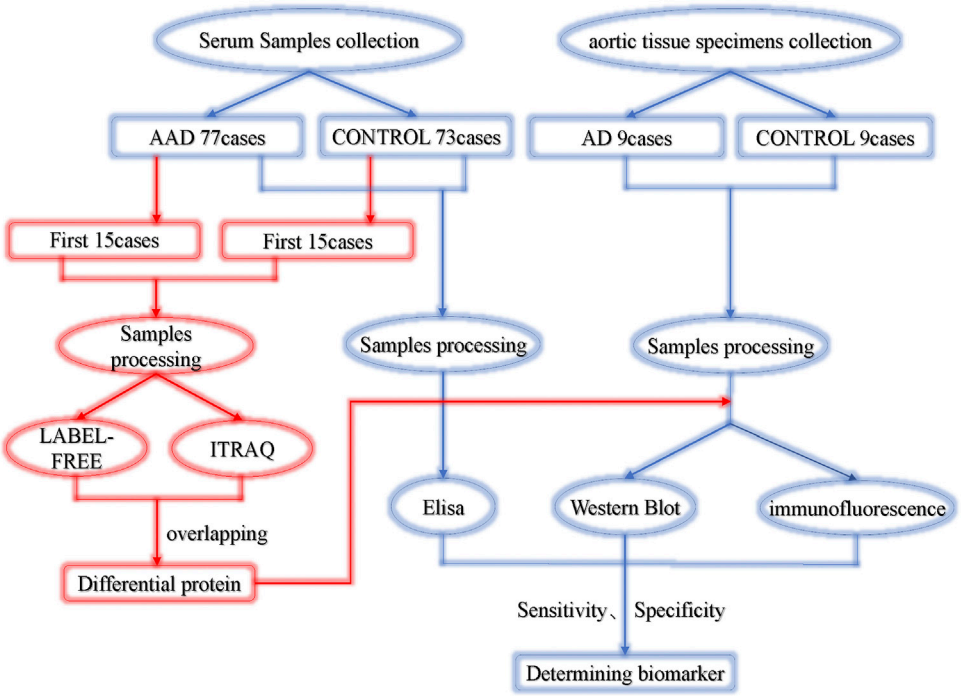

FIGURE 1 | Experimental design. AAD, acute aortic dissection; ACS, acute coronary syndrome.

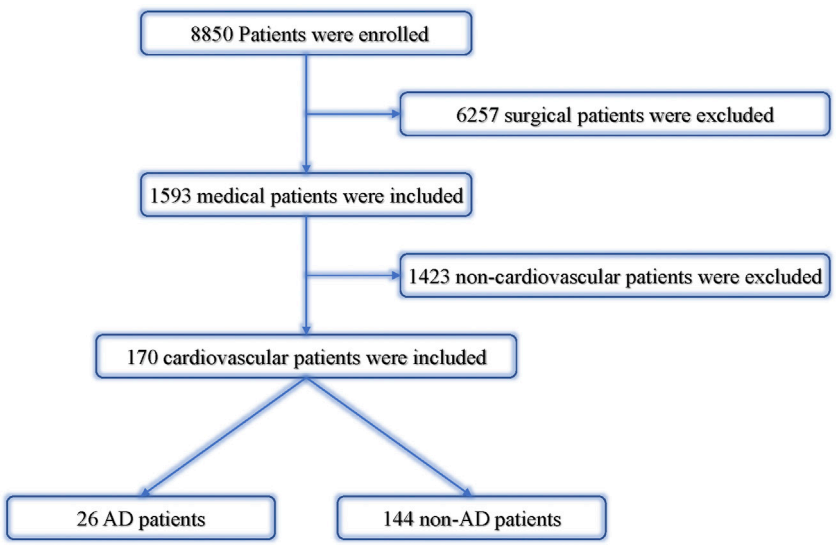

FIGURE 2 | Analysis of cardiovascular dispute cases. AD, aortic dissection; non-AD, without aortic dissection.

collected from the same institutions. Serum samples were collected immediately after admission and kept at a temperature of 4°C for 1 h and centrifuged at 3,000 rpm for 15 min. After obtaining informed consent, the aortic tissue specimens were retrieved, rinsed with PBS, labeled, aliquoted, and quickly put into liquid nitrogen for rapid freezing. Both serum and tissue specimens were stored at −80°C until further analysis.

2.3.1.1 Serum Collection

The inclusion criteria were as follows: 1) age: ≥18 years old; 2) no gender restrictions; 3) patients with chest pain within 72 h; 4)

TABLE 1 | Clinical features of the iTRAQ, label-free analysis subjects.

	AAD	Control	P value
N	15	15	/
Age (mean±SD)	56.93 ± 13.24	63.87 ± 12.39	0.150[a]
Gender (male/female, n)	14/1	13/2	1.000[b]
Hypertension (N)	14	8	0.035[b]
Smoke (N)	10	6	0.272[b]
Diabetes	1	4	0.330[b]
Weight	73.83 ± 11.16	60.37 ± 8.40	0.001[a]
Height (N)	1.69 ± 0.04	1.68 ± 0.07	0.701[a]
BMI	25.73 ± 3.38	21.3 ± 2.22	<0.001[a]
HGB	137.4 ± 18.5	128.7 ± 15.0	0.171[a]
PLT	196.4 ± 95.1	267.4 ± 94.4	0.050[a]
RBC	4.44 ± 0.70	4.43 ±1.01	0.962[a]
WBC	12.33 ± 5.08	9.15 ± 2.40	0.037[a]
ALT	19.5 (13.3, 27.5)	36.5 (27.0, 59.0)	0.007[C]
AST	19.0 (16.0,32.0)	76.0 (27.8, 218.5)	0.004[C]
CK	95.0 (69.0, 209.0)	177.0 (99.8, 2307.1)	0.081[C]
CKMB	8.7 (6.3, 16.4)	25.6 (15.5, 182.3)	0.001[C]
Creatinine	110.3 (91.7, 163.8)	120.0 (93.0, 146.0)	0.727[c]
INR	1.07 ± 0.07	1.11 ± 0.20	0.449[a]
APTT	37.6 (34.3, 40.0)	37.7 (33.5, 42.3)	0.852[c]
FIB	3.75 (2.01, 6.04)	3.71 (3.29, 4.06)	0.868[c]

[a]*t-test.*

[b]*Chi-square test.*

[C]*Mann-Whitney U test. BMI, Body Mass Index; HGB, hemoglobin; PLT, platelets; RBC, red blood cell; WBC, white blood cell; ALT, alanine transaminase; AST, aspartate aminotransferase; CK, creatine kinase; CKMB, creatine kinase-MB; INR, International normalized ratio; APTT, activated partial thromboplastin time; FIB, fibrinogen.*

TABLE 2 | Clinical features of the validation analysis subjects.

	AAD	Control	P value
N	77	73	/
Age (mean±SD)	57.88 ± 12.33	59.34 ± 10.12	0.431[a]
Gender (male/female, n)	60/17	58/15	0.819[b]
Hypertension (N)	69	51	0.003[b]
Smoke (N)	48	46	0.620[b]
Diabetes	20	18	0.853[b]
Weight T	68.72 ± 12.36	63.22 ± 10.02	0.003[a]
Height HP (N)	1.66 ± 0.07	1.65 ± 0.08	0.498[a]
BMI	24.99 ± 3.60	23.23 ± 2.90	0.001[a]
HB	132.0 ± 17.2	130.3 ± 30.0	0.670[a]
PLT	208.6 ± 102.2	234.7 ± 85.2	0.092[a]
RBC	4.46 (4.15,4.88)	4.53 (4.09,5.33)	0.319[c]
WBC	11.87 ± 4.29	9.76 ± 3.80	0.002[a]
ALT	19.5 (15.0,29.3)	28.0 (19.5,40.0)	0.006[c]
AST	21.0 (18.0,30.0)	19.0 (26.0,70.0)	0.039[c]
CK	99.9 (65.3,179.5)	139.4 (77.4,666.8)	0.005[c]
CKMB	9.85 (7.93,14.15)	18.85 (12.50,57.05)	<0.001[c]
SCR	9.85 (7.93,14.15)	84.6 (69.0,106.2)	0.092[c]
INR	1.12 (1.05,1.22)	1.03 (0.95,1.12)	<0.001[c]
APTT	39.1 (35.6,42.9)	38.1 (34.7,42.4)	0.543[c]
FIB	4.10 (3.04,6.23)	3.42 (2.95,24.14)	0.024[c]

[a]*t-test.*

[b]*Chi-square test.*

[C]*Mann-Whitney U test. BMI, Body Mass Index; HGB, hemoglobin; PLT, platelets; RBC, red blood cell; WBC, white blood cell; ALT, alanine transaminase; AST, aspartate aminotransferase; CK, creatine kinase; CKMB, creatine kinase-MB; INR, International normalized ratio; APTT, activated partial thromboplastin time; FIB, fibrinogen.*

patients with acute aortic dissection confirmed by aortic CTA or angiography. The exclusion criteria were as follows: 1) pregnant or lactating women; 2) history of cardiopulmonary resuscitation (CPR) and cardiac interventional therapy or surgery in 1 week; 3) severe hepatorenal insufficiency; 4) patients in shock requiring vasoactive drugs on admission. The first 15 patients in the AAD group and control group were analyzed by iTRAQ and label-free. All enrolled patients' serum was tested for ELISA. The clinical features of the two groups were summarized (**Table 1**). The average age of AAD and ACS patients was 56.93 ± 13.24 years and 63.87 ± 12.39 years, respectively. ELISA was used to verify the clinical features of 77 AAD and 73 non-AAD patients as summarized (**Table 2**). The mean age of AAD patients was 57.88 ± 12.33 years. The average age of ACS patients was 59.34 ± 10.12 years. There was no significant difference in age distribution between the two groups ($p > 0.05$).

TABLE 3 | Clinical features of Western blot, immunofluorescence analysis subjects.

	AD	CONTROL	P
N	9	9	/
Age (mean±SD)	49.33±6.61	50.11±7.51	0.819[a]
Gender (male/female, n)	8/1	8/1	1.000[b]
Hypertension (N)	7	5	0.620[b]
Smoke (N)	6	5	1.000[b]
Diabetes	0	0	1.000[b]
HB	130.8 ± 19.6	107.6 ± 38.9	0.136[a]
PLT	220.0 (164.5,283.0)	125.0 (82.5,264.0)	0.401[c]
RBC	4.28 ± 0.66	3.53 ± 1.10	0.097[a]
WBC	9.43 (7.57,15.76)	11.30 (6.68,17.70)	0.895[c]
ALT	21.0 (11.5,40.0)	21.0 (18.0,63.5)	0.331[c]
AST	20.0 (18.0,25.5)	53.0 (25.5,126.5)	0.007[c]
CK	95.0 (40.0,136.5)	299.8 (79.5,1862.7)	0.102[c]
CKMB	14.5 (10.5,22.8)	40.1 (19.2,44.5)	0.019[c]
CR	87.6 (68.7,105.5)	146.0 (96.3,210.6)	0.024[c]
DDI	2080 (1275,14695)	7580 (2865,10000)	0.400[c]
INR	1.18 ± 0.12	1.44 ± 0.40	0.095[a]
APTT	46.4 ± 9.0	40.8 ± 12.0	0.279[a]
FIB	4.61 ± 2.04	7.00 ± 2.14	0.027[a]

[a]*t-test.*

[b]*Chi-square test.*

[C]*Mann-Whitney U test. BMI, Body Mass Index; HGB, hemoglobin; PLT, platelets; RBC, red blood cell; WBC, white blood cell; ALT, alanine transaminase; AST, aspartate aminotransferase; CK, creatine kinase; CKMB, creatine kinase-MB; INR, International normalized ratio; APTT, activated partial thromboplastin time; FIB, fibrinogen.*

2.3.1.2 Tissues Samples Collection

The inclusion criteria were as follows: 1) age: ≥18 years old; 2) no gender restrictions; 3) patients with acute aortic dissection confirmed by aortic CTA or angiography; 4) aortic valve replacement is required in patients with AAD**.** The exclusion criteria were as follows: 1) pregnant or lactating women; 2) history of CPR and cardiac interventional therapy or surgery in 1 week; 3) severe hepatorenal insufficiency; 4) patients in shock requiring vasoactive drugs on admission; 5) hereditary aortic dissection patients. The average age of AAD patients was 49.3 ± 6.61 years old. The average age of organ donors was 50.1 ± 7.51 years old (**Table 3**).

2.3.2 Biomarker Verification Method

2.3.2.1 iTRAQ Multiplex Labeling and Chromatography

The 14 most abundant proteins were retrieved from each group of serum samples using Agilent multiple affinity removal liquid chromatography column-Human 14 (Agilent Technologies,

Santa Clara, United States). Each sample was dissolved, reduced, and alkylated, then digested overnight with trypsin [w (trypsin): w (protein) = 1:20] at 37°C. ITRAQ reagent labeling was carried out in accordance with AB SCIEX's iTRAQ labeling kit specification (Zhang et al., 2016). ITRAQ 118 119 121 was used in the control group and iTRAQ 113 114 117 was used in the AAD group. The marked peptides of each group were mixed and graded by the Agilent 1260 Infinity II HPLC system (Zhai et al., 2013).

2.3.2.2 Label-Free Sample Preparation and MS Analysis for Experiments

Agilent multiple affinity removal LC column-human 14 of the corresponding samples was used to remove the high abundance protein, and the low abundance component solution was obtained. Mass spectrometry was performed after FASP digestion, and each sample was separated by a nanoliter flow rate Easy nLC system. Buffer A solution was 0.1% formic acid aqueous solution and B solution was 0.1% formic acid acetonitrile aqueous solution (acetonitrile is 80%). The chromatographic column was equilibrated with 100% liquid A, and the samples were separated from the automatic sampler to the analytical column (Thermo scientific, Acclaim PepMap RSLC 50 μm × 15 cm, nano viper, P/N164943) at a flow rate of 300 nl/min. After chromatographic separation was carried out, samples were analyzed by a Q-Exactive Plus spectrometer. The analysis time was 60 min (Zhang et al., 2016).

2.3.2.3 Bioinformatics Analysis

For the analysis of iTRAQ and label-free markers, the ProteinPilot search engine (AB Sciex) was used for protein identification by searching for human species in the UniProtKB/Swiss-Prot database. For the bioinformatics analysis of differentially expressed proteins, GeneGO MetaCoreTM soft (https://portal.genego.com/) was used. After comparing proteins in label-free and iTRAQ, common target-related proteins were found to appear in both lists. In addition, the possible signal network of BF may be predicted by the automatic expansion of common target-related proteins; this emphasizes the most unique approach in the network, including the pathways that include the most protein nodes, it also shows the subcellular location of proteins in the network. Finally, we used GO seq for the GO enrichment analysis, pathway enrichment analysis was assessed by hypergeometric test, protein interaction prediction was confirmed by protein interaction database String, and the Cytoscape software was used for interaction network display.

2.3.3 ELISA Analysis

We used Lumican (abcam, United States), PF4 (abcam, United States), VWF (abcam, United States), MMP9 (R&D Systems Company, United States), MMP2 (R&D Systems Company, United States), MMRN1 (Biomatik, United States), FGL1 (Biomatik, United States), FBN1 (Biomatik, United States), and PI16 (abbexa, United Kingdom) to detect the aforementioned proteins by the enzyme-linked immunosorbent assay, ELISA. The procedure was carried out in strict accordance with the manufacturer's instructions, the samples were diluted 20–100 times differently, the original standard provided by the kit was gradually diluted, and the standard curve was used to calculate the biomarker concentration in the sample.

2.3.4 Immunofluorescence Staining

The formalin-fixed, paraffin-embedded aortic sections were deparaffinized, dehydrated, antigen-repaired, and blocked with 5% BSA for 40 min at room temperature, followed by PI16 (1:200, NVUS, United States), FGL1 (1:200, NOVUS, United States), MMP9 (1:100, Abcam, United States), and LUM (1:100, Abcam, United States) at 4°C overnight. The sections were washed with PBS and then incubated with a secondary antibody conjugated to Alexa Fluor dye (1:500) for 2 h at room temperature. The nuclei were stained with DIPA for 5 min at room temperature. Images were captured using the Image-Pro Plus V4.5 software. Fluorescence was detected by using a Leica SP5 confocal microscope (Leica Microsystems Inc., Wetzlar, Germany). The magnification was 200 folds and the average signal intensity normalized to the aortic region between the groups was compared.

2.3.5 Western Blot Analysis

Western blot was utilized on aortic tissue samples from nine patients with aortic dissection and nine normal organs donor to verify the results of four proteins (Lumican, FGL1, PI16, and MMP9). Briefly, 20 μg of protein were separated by 10% SDS-PAGE gel and transferred to the nitrocellulose membrane. The membrane was blocked with 5% skim milk overnight, then incubated at 4°C with PI16 (1:500, NOVUS, United States), FGL1 (1:500, NOVUS, United States), MMP9 (1:1,000, Abcam, United States), Lumican (1:1,000, Abcam, United States) overnight, and GAPDH (1:10,000, Bioworld, United States) antibodies and was then incubated with anti-rabbit or anti-mouse secondary antibodies (Boster, China) at a dilution of 1:8,000. Signals were detected using an enhanced chemiluminescence reagent (Pierce). Band density was quantified using the Image-Pro Plus software, and fold changes in Lumican, PI16, MMP9, and FGL1 densities were normalized to positive control and GAPDH levels.

3 STATISTICAL ANALYSIS

All statistical analyses were performed using SPSS 20.0 (SPSS, Chicago, USA) and GraphPad Prism 5 (GraphPad Inc. La Jolla, CA). Data are expressed as the mean ± SD and medians (interquartile range or n (%)). All continuous variables were tested for the normal distribution of data with the Shapiro-Wilk test. Comparisons of continuous variables between two groups were conducted with the independent-samples T-test or the Mann-Whitney U test. The chi-square test was performed to

TABLE 4 | Clinical features of the medical dispute analysis subjects.

	AD	nonAD	P
N	26	144	/
Age (mean±SD)	47.31 ± 13.55	55.65 ± 16.35	0.015[a]
Gender (male/female, n)	20/6	103/41	0.571[b]
Rate of mortality (diagnosis is not clear)	88.89%	66.40%	0.025[b]
Mortality ratio	—	—	0.784[b]
First-class hospital	5	25	—
Second-class hospital	9	42	—
Third-class hospital	12	77	—

[a]*t-test.*

[b]*Chi-square test. AD,Aortic dissection*

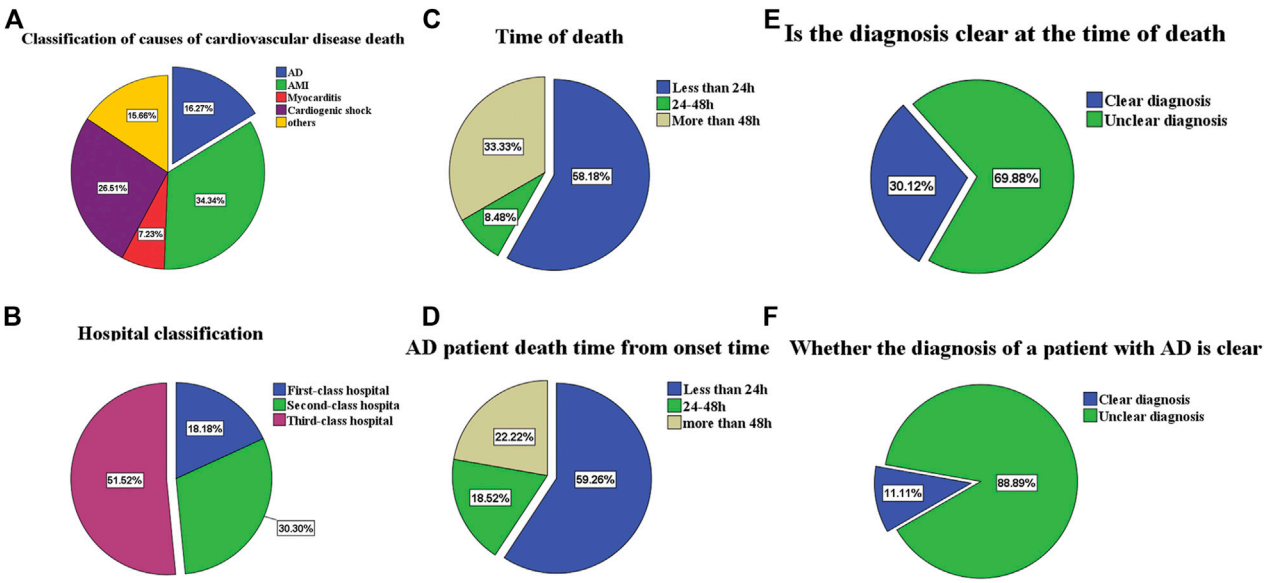

FIGURE 3 | (A) is the proportion of deaths from cardiovascular patients. **(B)** is classification of hospitals for the patients. **(C)** is the proportion of different death times of cardiovascular patients. **(D)** is AD patients death time from onset time. **(E)** is the proportion of unexplained death at death. **(F)** is the proportion of unexplained death at death for AD patients.

compare qualitative parameters between two groups. Independent and joint detection of candidate biomarkers were amalyzed by receiver operator characteristic (ROC) curve and logical regression modeling. $p < 0.05$ was considered statistically significant.

4 RESULTS

4.1 AAD Distribution Within Cardiovascular Disputes Cases

In the past 5 years, the AAD cases ratio accounted for 16.27% in all cardiovascular disputes, 84.6% in all cardiovascular death less than 48 h, and 88.89% in the patients who remained undiagnosed at the time of death. Overall mortality rate, 24 h mortality rate, and undiagnosed mortality rate were separately calculated according to different levels of hospitals (**Table 4**; **Figure 3**).

4.2 Identification and Functional Classification of Serum Proteome

A total of 725 proteins were identified by iTRAQ and 84 were differentially expressed proteins, of which 66 were up-regulated (A/B > 1.2) and 18 were down-regulated (A/B < 1.2). Label-free identified 490 proteins of which 16 were differentially expressed. 9 were up-regulated (A/B > 1.2) and 7 were down-regulated (A/B < 1.2). The cluster analysis of differentially expressed proteins showed that the protein expression in the AAD group was significantly higher than that in the control group (**Figure 4A**).

According to Gene Ontology (GO), the differential proteins and temptation-free proteins obtained by the two methods were classified according to "molecular function," "biological process," and "cell composition," and sorted according to the number of proteins. The GO analysis showed that the differential protein of the AAD group was concentrated in the extracellular matrix compared with the control group, and the extracellular component was the main component (**Figure 4B**).

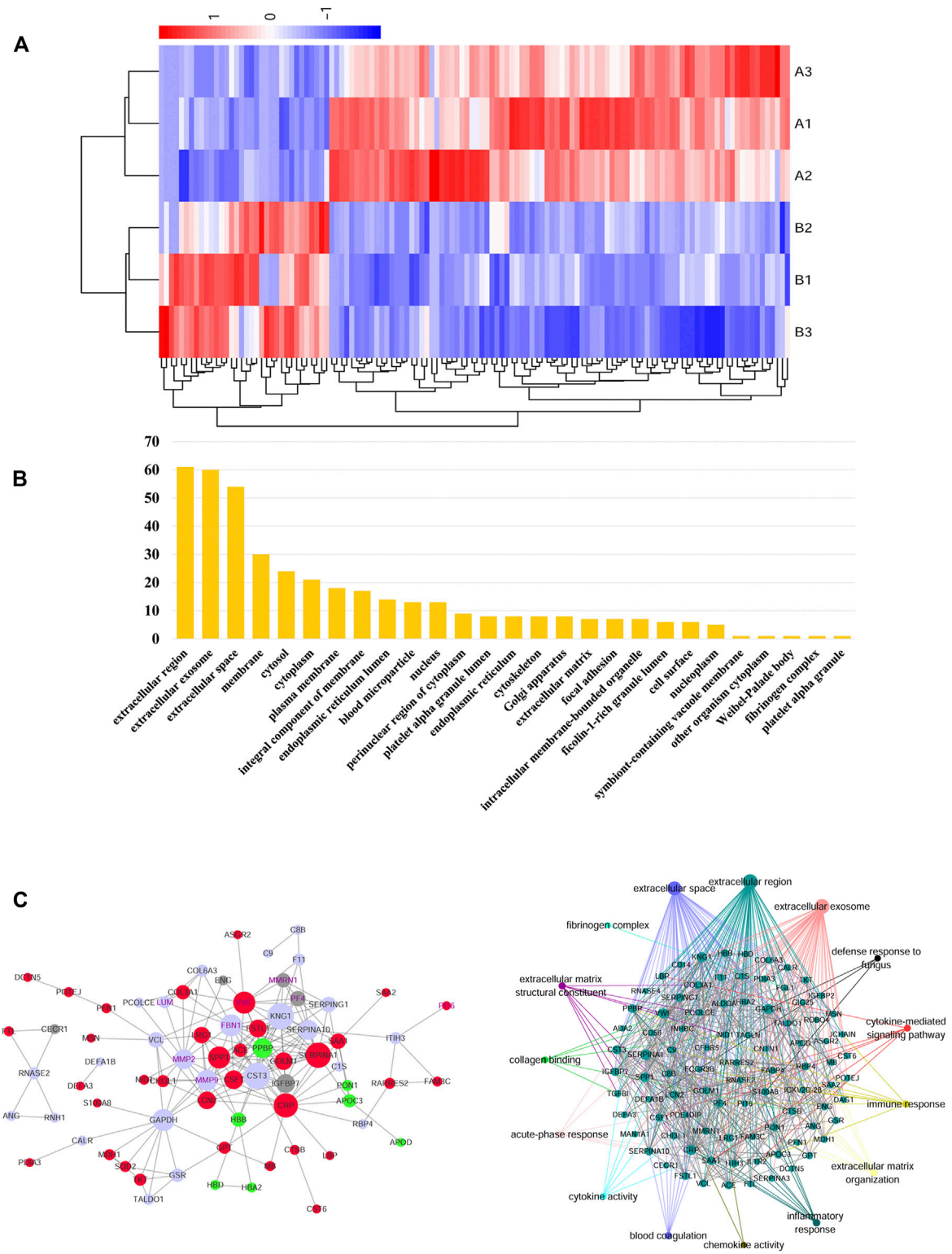

FIGURE 4 | (A) In the heat map of the 127 differential metabolites in AAD and ACS, the colors changing from blue to red indicate more metabolites. In the correlation network of metabolites with $|r| > 1$, red plots indicate upregulated metabolites and blue plots indicate downregulated metabolites in the two groups. **(B)** Bioinformatics analysis for the differentially expressed proteins in the AAD and ACS group. Diagram showing the biological process (BP) and cellular component (CC) of differentially expressed proteins of the two groups using the DAVID analysis. **(C)** Network of AAD VS. ACS clustered by the Ingenuity Pathway Analysis. Protein–protein interaction was generated by Cytoscape between the AAD vs. ACS group.

TABLE 5 | Subset of differentially expressed proteins between the AAD and control groups.

Accession	Name	Biological process	Protein class	AAD:CON	Up/down
P02741	CRP	Acute-phase response	—	11.38	Up
P05109	S100A8	DNA replication	Signaling molecule	3.65	Up
D3DQX7	SAA1	Cellular component movement	Transporter	35.08	Up
Q08830	FGL1	Cell adhesion	Signaling molecule	2.26	Up
P0DJI8	SAA1	Cellular component movement	Defense protein	2.003	Up
Q6UXB8	PI16	—	Immunity protein	1.223	Up
P0DJI8	SAA1	Cellular component movement	Transporter	2.19	Up
P04275	VWF	Cell adhesion	Protease inhibitor	1.536	Up
P14780	MMP9	—	Metalloprotease	1.518	Up
P35555	FBN1	Anatomical structure morphogenesis	Cell adhesion molecule	1.415	Up
P08253	MMP2	—	Metalloprotease	1.099	Down
Q14126	DSG2	Cellular process	Cadherin	1.092	Down
P51884	LUM	Cell growth	—	1.038	Down
O75882	ATRN	Cellular process	Extracellular matrix	1.033	Down
P23142	FBLN1	—	—	0.999	Down

This table lists the highest Unused ProtScores from the upregulated and downregulated proteins. AAD, acute aortic dissection; CON, normal controls.

TABLE 6 | Label-free with or without protein results.

Protein IDs	Protein IDs	Biological process	Protein class	AAD/Control
P02776	PF4	—	Chemokine	Control
Q5T9B9	ENG	—	—	Control
A0A024RDA6	IGFBP7	Regulation of cell growth	—	AAD
P07737	PFN1	Cellular process	—	AAD
Q08830	FGL1	Cell adhesion	Signaling molecule	AAD
Q13201	MMRN	—	Extracellular matrix glycoprotein	AAD

This table lists all or nothing from the upregulated proteins and downregulated proteins. AAD, acute aortic dissection.

For the biological function analysis, the map was drawn based on the proteins with the highest scores in the IPA and PPI analysis. Exploring the global PPI that may use Cytoscape, we found that FGL1, PI16, MMP9, and Lumican were involved in platelet aggregation, blood coagulation, and many other processes. At the same time, FGL1 improved TGF-β1-induced fibrosis by regulating hemostasis, platelet aggregation, coagulation, and many other processes (**Figure 4C**).

For screening biomarkers, the study selected upregulated secretory proteins (proteins that could not be downregulated by ELISA). Considering that the most abundant protein albumin in the serum may be affected by liver function, infection, nutrition, and many other factors, it was excluded from the verification list. Therefore, four proteins were provided for verification: FGL1, PI16, MMP9, and Lumican.

4.3.1 Verification of Candidate Molecular Markers

Based on iTRAQ and label-free proteomics findings, Lumican, MMP9, PI16, FGL1, FBN1, PF4, MMP2, VWF, and MMRN1 were selected as potential biomarkers for verification targets. Different expressions of individual proteins in AAD (N = 77) and non-AAD (N = 73) groups (**Tables 5**, **6**) were analyzed. Excluding the proteins with no significant difference between the two groups, four proteins (Lumican, PI16, FGL1, and MMP9) with statistical difference were selected as the final molecular markers. Their expression in aortic dissection group was significantly higher than that in the control group ($p < 0.05$) (**Figure 5**).

4.3.2 ROC Curve Analysis of the Diagnostic Value of Lumican, PI16, MMP9, and FGL1

The ROC curve was selected for AAD diagnosis by Lumican, MMP9, PI16, and FGL1, and the cutoff value of the maximum Youden index was selected to obtain appropriate sensitivity and specificity. Lumican AUC (0.636), sensitivity 70.1%, specificity 57.5%; PI16 AUC (0.739), sensitivity 55.8%, specificity 78.1%; FGL1 AUC (0.607), sensitivity 90.9%, specificity 43.8%. The AUC (0.641) of MMP9 had a sensitivity of 84.4% and a specificity of 43.8%. PI16 + FGL1 AUC (0.769), sensitivity of 71.4%, specificity of 71.2%; Lumican + PI16 AUC (0.742), sensitivity 90.9%, specificity 43.8%; Lumican + FGL1 AUC (0.653), sensitivity 59.7%, specificity 71.2%. PI16 + FGL1 + Lumican combined with AUC (0.780), sensitivity 67.5%, specificity 76.7% (**Table 7**; **Figure 6**). Among all these results, Lumican + PI16 displayed the highest sensitivity and the combination of 3 proteins displayed the highest specificity.

Logical regression analysis of biomarkers in the diagnosis of AAD: the combined prediction model was established using Lumican test results and PI16 and FGL1 as independent variables and dependent variables: logarithm (p)= −4.861 + 0.561 * Lumican + 1.783 * PI16+0.983 * FGL1. Then variables and statistics were substituted into the model (**Table 8**).

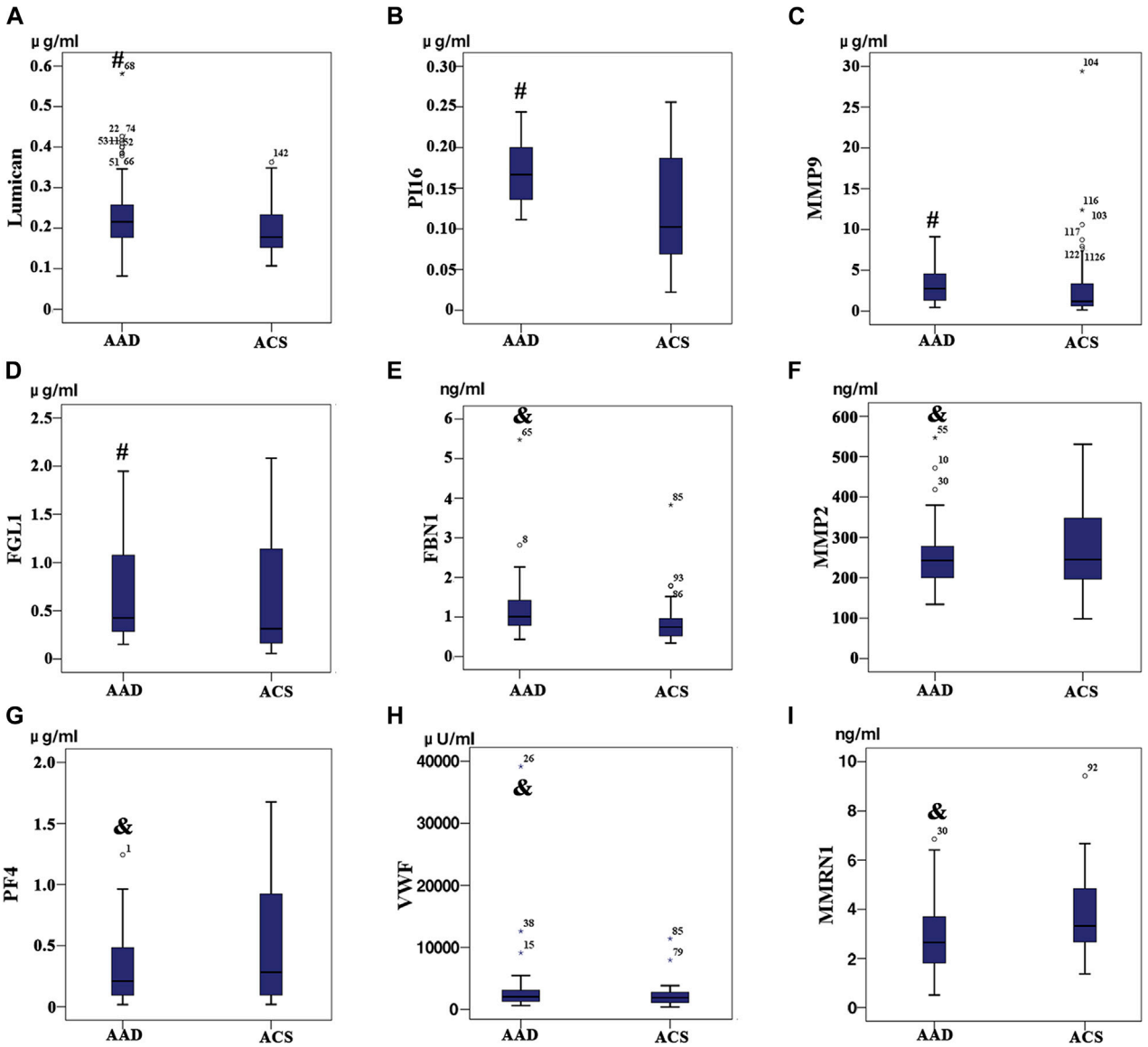

FIGURE 5 | Among the patients with acute aortic dissection (AAD) and Acute coronary syndrome (ACS), **(A)** Lumican, **(B)** Peptidase inhibitor 16, **(C)** Fibrinogen-like protein 1 and **(D)** Matrix metalloproteinase-9 expression level exhibit significant differences between the two group ($p < 0.05$); **(E)** Profibrin 1 antigen (FBN1), **(F)** platelet factor 4 (PF4), **(G)** the Von Willebrand factor (VWF), **(H)** matrix metalloproteinase-2 (MMP-2), **(I)** MMRN1 ($p > 0.05$) expression level did not exhibit any significant differences between the two groups ($p > 0.05$).

TABLE 7 | The diagnostic efficiency analysis of four AAD biomarkers.

	AUC	*p*-value	95% CI	Sensitivity (%)	Specificity (%)	Cutoff (ng/dl)	Youden index
LUMICAN	0.636	0.004	0.547–0.725	70.1	57.5	1.865	0.276
PI16	0.739	0.000	0.661–0.816	55.8	78.1	1.973	0.339
FGL1	0.607	0.024	0.512–0.702	90.9	43.8	0.223	0.347
MMP9	0.641	0.003	0.552–0.731	84.4	43.8	0.99	0.282
PI16 + LUM	0.742	0.000	0.665–0.819	90.9	43.8	0.33	0.347
PI16 + FGL1	0.769	0.000	0.693–0.845	71.4	71.2	0.515	0.426
LUMICAN + FGL1	0.653	0.001	0.565–0.741	59.7	71.2	0.517	0.309
LUMICAN + FGL1 + PI16	0.780	0.000	0.707–0.852	67.5	76.7	0.675	0.442

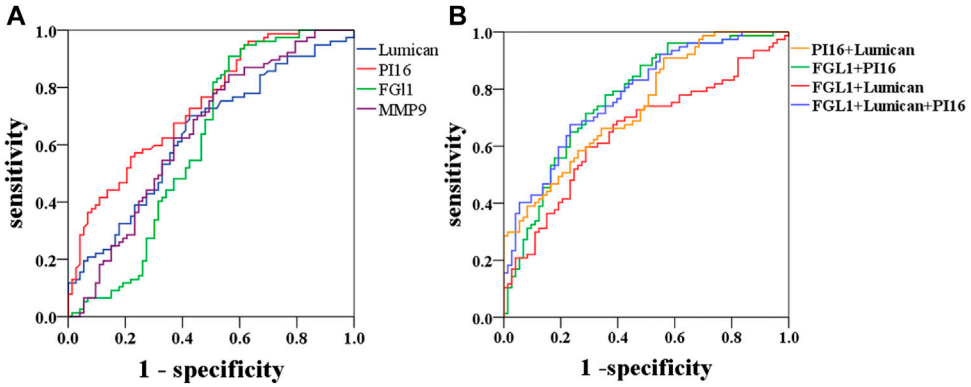

FIGURE 6 | Diagnostic outcomes in the discovery phase are shown via the receiver operating characteristic curve (ROC) curves for PI16, MMP9, and FGL1 to discriminate AAD from controls, $p < 0.05$. PI16 indicates peptidase inhibitor 16, FGL1 indicates fibrinogen-like protein 1, and MMP9 indicates matrix metalloproteinase-9.

TABLE 8 | Logistic regression analysis results of AAD diagnosis with Lumican, PI16, and FGL1.

	B	SE	WALD	*p*	OR	95% CI
LUMICAN	0.561	0.278	4.062	0.044	1.752	1.016–3.022
PI16	1.783	0.37	23.189	0.000	5.945	2.878–12.28
FGL1	0.983	0.397	6.126	0.013	2.673	1.227–5.824
CONSANT	−4.861	0.975	24.848	0.000	0.008	

4.4 Identification of TGF-β1-Mediated Signaling Pathway Relative Proteins in Aortic Tissues Samples

In order to verify the relative proteins involved in the TGF-β1-mediated signaling pathway, immunofluorescence staining and Western blot analyses were performed on the ascending aortic artery samples from the deceased AAD patients and organ donors groups. Fibrosis-related α-sma and collagen 1 were significantly higher in the AAD patients group. PI16, MMP9, FGL1, and TGF-β1 were significantly higher in the aortic wall of AAD patients ($p < 0.001$). Lumican was significantly higher in the serum of AAD patients but no significant difference in the Western blot of human tissue specimens (**Figures 7**, **8**).

5 DISCUSSION

AAD is a life-threatening emergency cardiovascular event with a 1–2% increase in mortality every hour after onset. The AAD misdiagnosis rate in the emergency room accounts for 38% (Song et al., 2013). Delayed diagnosis significantly increases the risk of death. Many patients die of aortic rupture or serious complications before a definite diagnosis is established, and a considerable proportion of cases of undiagnosed eventually end up in medical disputes.

Over the past few decades, the number of cases involving medical disputes in some developed countries has increased dramatically, such as the United Kingdom (Goldenberg et al., 2012), the United States (Quraishi et al., 2012), Australia (Jena et al., 2011), New Zealand (Blake, 2010), and Japan (Hiyama et al., 2009). According to a national survey in China, there were 9,831 disputes with 5,519 injured medical personnel in 2006. In 2007, 73.3% of mainland Chinese hospitals reported violent incidents. Because of the sudden occurrence and rapid development of some diseases, some studies have found that patients who die within 48 h are more prone to class I diagnostic errors. A report by the American Institute of Medical Research found that diagnostic errors resulted in about 10% of patients death and as many as 17% of hospital adverse events (McCarthy, 2015). Some studies also found cardiovascular disease were the most common diagnosis in emergency department, and aortic dissection and myocardial infarction caused more death and missed grade I diagnosis (80% and 66.7% per group) (Liu et al., 2017). In this study, we used data from the Guangdong Medical Coordination Committee during 2013–2017. Over the past 5 years, there were a total of 170 cases of medical disputes in cardiovascular patients. Whether different hospitals' level or physicians' experience, the AAD medical disputes ratio, early death ratio, and misdiagnosis ratio remain high. The delay in the diagnosis of AAD is a recognized problem (patient transfer risks, imaging time-consuming, and physicians' misunderstanding) that needs to be improved because the mortality rate is as high as 1%/h before diagnosis (Harris et al., 2011). Contributing to the diagnosis of diseases and benefit patients and caregivers, it is urgent to identify fast, noninvasive, economical, and effective biomarkers.

Cardiac biomarkers, such as for myocardial necrosis (cardiac troponin) and heart failure (natriuretic peptide), have been shown to be successful (Nienaber and Eagle, 2003; Hochholzer et al., 2010; van Kimmenade and Januzzi, 2011). Cardiac troponin is a single biomarker with sufficient sensitivity and specificity, in addition to its favorable release time process, it covers the time window necessary for unambiguity in the clinical environment. According to guidelines, cardiac troponin (cTnT) can furthermore classify ACS and is used as prognosis for MI outcome. Based on a long history of understanding MI mechanism, cTnT has been gradually selected as biomarker for myocardial injury (Cullen et al., 2014). Moreover, current

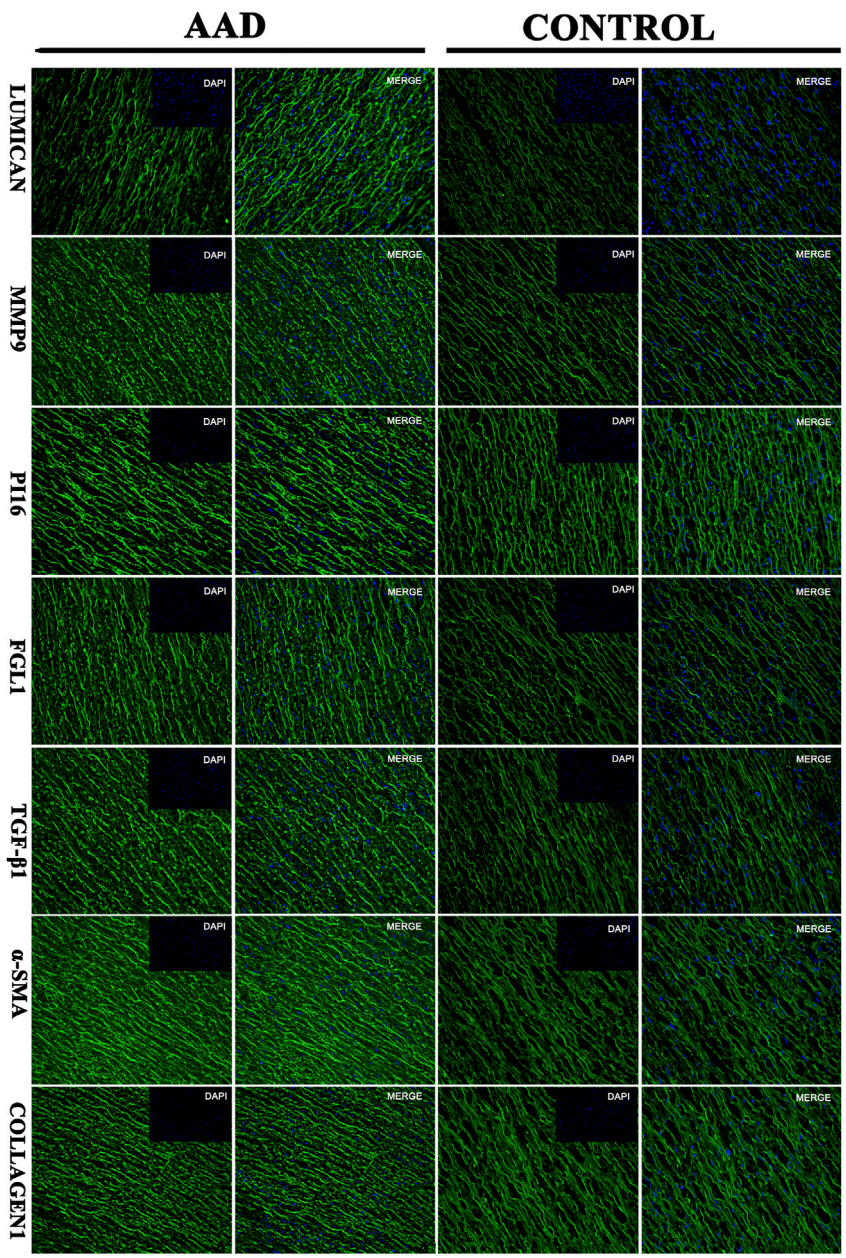

FIGURE 7 | Immunofluorescence: the target protein of the aortic dissection group and the control group (Lumican, matrix metalloproteinase-9 (MMP9), peptidase inhibitor 16 (PI16, peptidase inhibitor 16), fibrinogen-like protein 1 (FGL1, fibrinogen-like protein 1).

studies are mainly trying to investigate hotspots for AAD markers focused on the pathophysiological development of the disease. Protein markers studies mainly include smooth muscle protein, matrix metalloproteinases, elastin fragments, D-dimer, sST2, and some other proteins, relatively due to various courses of the disease, such as aortic wall degradation, vascular smooth muscle injury, cell necrosis, inflammation, coagulation activation, and extracellular matrix remodeling (Shao et al., 2014). Soluble ST2 has been validated as a biomarker for acute aortic dissection (Wang et al., 2018). The changes of these serum proteins in aortic dissection have been relatively clearly studied, but none of them have good clinical diagnostic value. There is still a long way to determine for AAD pathophysiological mechanism and its biomarkers study. Furthermore discovery and screening researches are still of great value.

Furthermore, with the continuous development and innovation of related technologies proteomics have been clinically used as a marker finding for a long time in the absence of mechanism key points (Arab et al., 2006; Pontillo et al., 2015; de Franciscis et al., 2016; Mesaros and Blair, 2016). Lumican had been reported as a diagnostic marker with sensitivity and specificity of 73.33% and 98.33%,

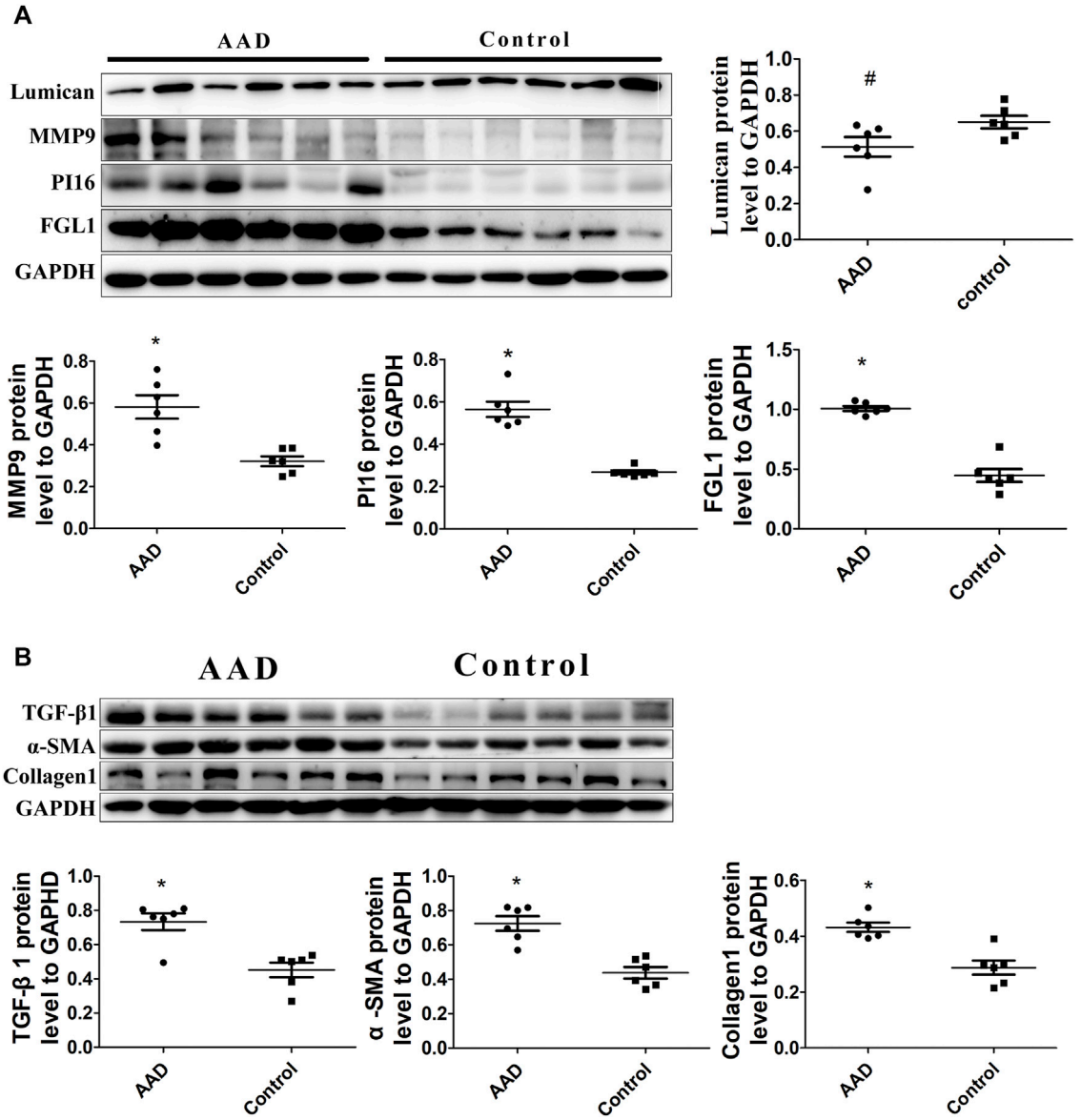

FIGURE 8 | (A) Western blot analysis showed increased levels of PI16, FGL1, and MMP9 in aortic dissection ($p < 0.001$), but Lumican is decreased ($p > 0.05$). **(B)** Western blot analysis also showed increased levels of TGF-β1, α-sma, and collagen1 in aortic dissection ($p < 0.001$).

respectively, while it was, respectively, 93.33% and 68.33% for D-dimer (Xiao et al., 2016). Moreover, fibrillin-1, emilin-1, decorin, protein DJ-1, and histone H4 were confirmed as diagnostic markers via Western blot signs of the expression of transforming growth factor-β1 (TGF-β1) signal increase and damaged aortic wall remodeling (Zhang et al., 2015). Withal, fibronectin, and Lumican were selected as differential proteins between the aortic dissection and control group (Gu et al., 2011) and it was found that the expression of extracellular superoxide dismutase SOD was lower than that of the control group ($p < 0.001$) (Liao et al., 2008). In principle, more beneficial quantification with combined high-throughput genomics or proteomics biomolecular data sets methods can acquire greater proteomic coverage than traditional research methods (Kell and Oliver, 2004; Garland et al., 2012; Feala et al., 2013). In this study, iTRAQ and label-free techniques were used to identify serum samples from AAD and ACS patients. The most relevant proteins were selected after a wide range of two overlaps. In this study, a total of nine proteins were found to most likely be tested for serum ELISA in a large number of patients. Three related markers: PI16, Lumican and FGL1 were found, and the ROC curve was drawn to reflect the sensitivity and specificity. The area under the PI16 curve alone was 0.739, the sensitivity was 55.8%, and the specificity was 78.1%, while the area under the PI16 combined with Lumican ROC curve

was 0.742, the sensitivity was 90.9%, and the specificity was 43.8%. The area under the ROC curve of the three proteins was 0.78, the sensitivity was 67.5%, and the specificity was 76.7%. The optimal sensitivity and specificity of PI16, Lumican and FGL1 could improve the diagnostic accuracy of AAD. At present, our main diagnosis method still relies on CTA, but CTA takes a long time [18]. Misdiagnosis and delayed diagnosis will lead to medical disputes, and therefore, other simple and inexpensive biomarkers for ADD diagnosis is important in clinical practice.

Based on KEGG (https://www.genome.jp/kegg/pathway.html), Lumican is an important ECM component of the aortic wall that is synthesized in the smooth muscle cells (Qin et al., 2001) of the aortic wall (Naito, 2005). It supports the differentiation of aortic smooth muscle cells and related elastic fiber arrangement and growth, and plays an important role in cell proliferation, migration, and tissue repair (Saika et al., 2003). Jin et al. (2019) found that the knockdown of FGL1 inhibited the production of TGF-β1. In response to profibrotic TGF-β1 signaling, Lumican enhances and accelerates the formation of collagen fibrils, so Lumican expression is positively correlated with profibrotic cytokines (Krishnan et al., 2012). Lumican and FGL1 may be involved in the TGF-β1 signaling pathway-related protein synthesis. The TGF-β1 signaling pathway inducing fibrosis synthesis may play a key role in aortic wall injury and repair. In general, TGF-β1 induced fibrosis participates widely in AAD mechanism such as endothelial malfunction, intima weakening, vascular wall injury and repair, therefore we came up with a hypothesis: the pathogenesis of aortic dissection maybe related to the Lumican-mediated TGF-β1 pathway. Based on immunofluorescence and Western blot of aortic wall specimen of the AAD and organ donors groups, fibrosis-related α-sma and collagen 1 were significantly higher. PI16, MMP9, FGL1, and TGF-β1 were significantly higher in the aortic wall of AAD patients than those of organ donors. These results prove that TGF-β1 mediated fibrosis plays key role in AAD injury and repair process. As for Lumican, previous study showed that Lumican levels was higher in AAD patients than healthy volunteers [42]. Lumican expression was detected in the intima and media of the ascending aorta in patients with AAD [43]. From a clinical point of view, we speculated that the reason for the different expression trends of Lumican in serum and tissue is that Lumican was produced and released into the blood when the aortic dissection tissue re-ruptured, and therefore this protein was highly expressed in the blood compared to that in the tissue. Hence, a hypothesis was put forward: Lumican can be used as an early diagnostic marker for aortic dissection. Lumican activation maybe initially involved as a trigger to the TGF-β1-mediated fibrosis pathway, but further studies still need to be verified through an animal model.

As mentioned above, aortic dissection is a high-risk disease with extremely high mortality. The current pathogenesis is unclear and lacks diagnostic markers of high-specificity and sensitivity. In this study, four effective diagnostic markers were found by combined proteomics methods. Through Elisa verification of a large number of clinical specimens and western-blot verification of aortic tissue specimens, we concluded that: Lumican, PI16, MMP9, and FGL1 protein may be a potential biomarker in patients with aortic dissection, and the pathogenesis of aortic dissection may be related to lumican mediated TGF-β1 pathway. However, there are still some limitations in our study. As a single-center study, our findings should be validated by a multicenter study with a larger population to confirm the diagnostic efficacy and accuracy of this novel assay. In particular, our validation population should include normal people without disease. Future validation studies evaluating Lumican, FGL1, and PI16, and comparing them with other biomarkers, such as NT-proBNP, cardiac troponins and DDI, are thus needed. Finally, further medical image-based confirmatory diagnoses are still essential in clinical practice.

DATA AVAILABILITY STATEMENT

The datasets presented in this study can be found in online repositories. The name of the repository and accession number can be found below: ProteomeXchange, http://www.proteomexchange.org/, PXD032857.

ETHICS STATEMENT

The protocol of this study was carried out according to the principles of the Declaration of Helsinki and approved by the Medical Ethics Committee in Zhujiang Hospital (Case No: 2018-XXGNK-001). The protocol is available at www.clinicaltrials.gov (ChiCTR1800015743). The patients/participants provided their written informed consent to participate in this study. Written informed consent was obtained from the individual(s) for the publication of any potentially identifiable images or data included in this article.

AUTHOR CONTRIBUTIONS

All authors listed have made a substantial, direct, and intellectual contribution to the work and approved it for publication.

FUNDING

This work was supported by the Nature Science Foundation of China (No. 81573732), Guangdong Provincial Administration of Traditional Chinese Medicine (No. 20221143) and Guangdong Natural Science Foundation (No. 2015A030313304).

SUPPLEMENTARY MATERIAL

The Supplementary Material for this article can be found online at: https://www.frontiersin.org/articles/10.3389/fphys.2022.862732/full#supplementary-material

Supplementary Figure S1 | Nomogram for predicting AAD probability.

REFERENCES

Arab, S., Gramolini, A. O., Ping, P., Kislinger, T., Stanley, B., van Eyk, J., et al. (2006). Cardiovascular Proteomics. *J. Am. Coll. Cardiol.* 48, 1733–1741. doi:10.1016/j.jacc.2006.06.063

Blake, P. (2010). Medical Mishap: No Fault Compensation as an Alternative to Civil Litigation - a Review of 30 years' Experience with the New Zealand Accident Compensation Corporation System. *Med. Leg. J.* 78, 126–137. doi:10.1258/mlj.2010.010027

Butler, J., Davies, A. H., and Westaby, S. (1990). Streptokinase in Acute Aortic Dissection. *BMJ* 300, 517–519. doi:10.1136/bmj.300.6723.517

de Franciscis, S., Metzinger, L., and Serra, R. (2016). The Discovery of Novel Genomic, Transcriptomic, and Proteomic Biomarkers in Cardiovascular and Peripheral Vascular Disease: The State of the Art. *BioMed Res. Int.* 2016, 1–10. doi:10.1155/2016/7829174

Feala, J. D., Abdulhameed, M. D. M., Yu, C., Dutta, B., Yu, X., Schmid, K., et al. (2013). Systems Biology Approaches for Discovering Biomarkers for Traumatic Brain Injury. *J. Neurotrauma* 30, 1101–1116. doi:10.1089/neu.2012.2631

Garland, P., Broom, L. J., Quraishe, S., Dalton, P. D., Skipp, P., Newman, T. A., et al. (2012). Soluble Axoplasm Enriched from Injured CNS Axons Reveals the Early Modulation of the Actin Cytoskeleton. *Plos One* 7, e47552. doi:10.1371/journal.pone.0047552

Goldenberg, S. D., Volpé, H., and French, G. L. (2012). Clinical Negligence, Litigation and Healthcare-Associated Infections. *J. Hosp. Infect.* 81, 156–162. doi:10.1016/j.jhin.2012.04.020

Gu, G., Cheng, W., Yao, C., Yin, J., Tong, C., Rao, A., et al. (2011). Quantitative Proteomics Analysis by Isobaric Tags for Relative and Absolute Quantitation Identified Lumican as a Potential Marker for Acute Aortic Dissection. *J. Biomed. Biotechnol.* 2011, 1–10. doi:10.1155/2011/920763

Hagan, P. G., Nienaber, C. A., Isselbacher, E. M., Bruckman, D., Karavite, D. J., Russman, P. L., et al. (2000). The International Registry of Acute Aortic Dissection (IRAD). *JAMA* 283, 897–903. doi:10.1001/jama.283.7.897

Harris, K. M., Strauss, C. E., Eagle, K. A., Hirsch, A. T., Isselbacher, E. M., Tsai, T. T., et al. (2011). Correlates of Delayed Recognition and Treatment of Acute Type A Aortic Dissection. *Circulation* 124, 1911–1918. doi:10.1161/circulationaha.110.006320

Hiyama, T., Yoshihara, M., Tanaka, S., and Chayama, K. (2009). Trend in Japanese Malpractice Litigation Involving Gastrointestinal Endoscopy. *Am. J. Gastroenterol.* 104, 251–252. doi:10.1038/ajg.2008.20

Hochholzer, W., Morrow, D. A., and Giugliano, R. P. (2010). Novel Biomarkers in Cardiovascular Disease: Update 2010. *Am. Heart J.* 160, 583–594. doi:10.1016/j.ahj.2010.06.010

Jena, A. B., Seabury, S., Lakdawalla, D., and Chandra, A. (2011). Malpractice Risk According to Physician Specialty. *N. Engl. J. Med.* 365, 629–636. doi:10.1056/nejmsa1012370

Jin, H., Kang, G.-Y., Jeon, S., Kim, J.-M., Park, Y. N., Cho, J., et al. (2019). Identification of Molecular Signatures Involved in Radiation-Induced Lung Fibrosis. *J. Mol. Med.* 97, 37–47. doi:10.1007/s00109-018-1715-9

Kell, D. B., and Oliver, S. G. (2004). Here Is the Evidence, Now what Is the Hypothesis? the Complementary Roles of Inductive and Hypothesis-Driven Science in the Post-genomic Era. *Bioessays* 26, 99–105. doi:10.1002/bies.10385

Klompas, M. (2002). Does This Patient Have an Acute Thoracic Aortic Dissection? *JAMA* 287, 2262–2272. doi:10.1001/jama.287.17.2262

Krishnan, A., Li, X., Kao, W.-Y., Viker, K., Butters, K., Masuoka, H., et al. (2012). Lumican, an Extracellular Matrix Proteoglycan, Is a Novel Requisite for Hepatic Fibrosis. *Lab. Invest.* 92, 1712–1725. doi:10.1038/labinvest.2012.121

Cullen, L., Than, M., and Peacock, W. F. (2014). Undetectable Hs-cTnT in the Emergency Department and Risk of Myocardial Infarction. *J. Am. Coll. Cardiol.* 64, 632–633.

Liao, M., Liu, Z., Bao, J., Zhao, Z., Hu, J., Feng, X., et al. (2008). A Proteomic Study of the Aortic Media in Human Thoracic Aortic Dissection: Implication for Oxidative Stress. *J. Thorac. Cardiovasc. Surg.* 136, 65–72. doi:10.1016/j.jtcvs.2007.11.017

Liu, D., Gan, R., Zhang, W., Wang, W., Saiyin, H., Zeng, W., et al. (2017). Autopsy Interrogation of Emergency Medicine Dispute Cases: How Often Are Clinical Diagnoses Incorrect? *J. Clin. Pathol.* 71, 67–71. doi:10.1136/jclinpath-2017-204484

McCarthy, M. (2015). Diagnostic Error Remains a Pervasive, Underappreciated Problem, US Report Says. *BMJ* 351, h5064. doi:10.1136/bmj.h5064

Mesaros, C., and Blair, I. A. (2016). Mass Spectrometry-Based Approaches to Targeted Quantitative Proteomics in Cardiovascular Disease. *Clin. Proteomics* 13, 20. doi:10.1186/s12014-016-9121-1

Naito, Z. (2005). The Role of Small Leucine-Rich Proteoglycan (SLRP) Family in Pathological Lesions and Cancer Cell Growth. *J. Nippon. Med. Sch.* 72, 137–145. doi:10.1272/jnms.72.137

Nienaber, C. A., and Eagle, K. A. (2003). Aortic Dissection: New Frontiers in Diagnosis and Management. *Circulation* 108, 628–635. doi:10.1161/01.cir.0000087009.16755.e4

Pontillo, C., Filip, S., Borràs, D. M., Mullen, W., Vlahou, A., and Mischak, H. (2015). CE-MS-based Proteomics in Biomarker Discovery and Clinical Application. *Prot. Clin. Appl.* 9, 322–334. doi:10.1002/prca.201400115

Qin, H., Ishiwata, T., and Asano, G. (2001). Effects of the Extracellular Matrix on Lumican Expression in Rat Aortic Smooth Muscle Cellsin Vitro. *J. Pathol.* 195, 604–608. doi:10.1002/path.994

Quraishi, N. A., Hammett, T. C., Todd, D. B., Bhutta, M. A., and Kapoor, V. (2012). Malpractice Litigation and the Spine: the NHS Perspective on 235 Successful Claims in England. *Eur. Spine J.* 21, 196–199. doi:10.1007/s00586-012-2203-5

Saika, S., Miyamoto, T., Tanaka, S.-i., Tanaka, T., Ishida, I., Ohnishi, Y., et al. (2003). Response of Lens Epithelial Cells to Injury: Role of Lumican in Epithelial-Mesenchymal Transition. *Invest. Ophthalmol. Vis. Sci.* 44, 2094–2102. doi:10.1167/iovs.02-1059

Shao, N., Xia, S., Wang, J., Zhou, X., Huang, Z., Zhu, W., et al. (2014). The Role of D-Dimers in the Diagnosis of Acute Aortic Dissection. *Mol. Biol. Rep.* 41, 6397–6403. doi:10.1007/s11033-014-3520-z

Song, Y., Xie, Y., Liu, F., Zhao, C., Yu, R., Ban, S., et al. (2013). Expression of Matrix Metalloproteinase-12 in Aortic Dissection. *BMC Cardiovasc Disord.* 13, 34. doi:10.1186/1471-2261-13-34

Suzuki, T., Distante, A., Zizza, A., Trimarchi, S., Villani, M., Salerno Uriarte, J. A., et al. (2008). Preliminary Experience with the Smooth Muscle Troponin-like Protein, Calponin, as a Novel Biomarker for Diagnosing Acute Aortic Dissection. *Eur. Heart J.* 29, 1439–1445. doi:10.1093/eurheartj/ehn162

van Kimmenade, R. R. J., and Januzzi, J. L. (2011). Emerging Biomarkers in Heart Failure. *Clin. Chem.* 58, 127–138.

Wang, Y., Tan, X., Gao, H., Yuan, H., Hu, R., Jia, L., et al. (2018). Magnitude of Soluble ST2 as a Novel Biomarker for Acute Aortic Dissection. *Circulation* 137, 259–269. doi:10.1161/circulationaha.117.030469

Wen, T., Liu, L., and Xiong, G.-Z. (2009). Matrix Metalloproteinase Levels in Acute Aortic Dissection, Acute Pancreatitis and Other Abdominal Pain. *Emerg. Med. J.* 26, 715–718. doi:10.1136/emj.2008.067645

Wilcox, R. G., Olsson, C. G., Skene, A. M., Von Der Lippe, G., Jensen, G., Hampton, J. R., et al. (1988). Trial of Tissue Plasminogen Activator for Mortality Reduction in Acute Myocardial Infarction. *Lancet* 332, 525–530. doi:10.1016/s0140-6736(88)92656-6

Xiao, Z., Xue, Y., Yao, C., Gu, G., Zhang, Y., Zhang, J., et al. (2016). Acute Aortic Dissection Biomarkers Identified Using Isobaric Tags for Relative and Absolute Quantitation. *BioMed Res. Int.* 2016, 1–7. doi:10.1155/2016/6421451

Zhai, L., Chang, C., Li, N., Duong, D. M., Chen, H., Deng, Z., et al. (2013). Systematic Research on the Pretreatment of Peptides for Quantitative Proteomics Using a C18 Microcolumn. *Proteomics* 13, 2229–2237. doi:10.1002/pmic.201200591

Zhang, D.-M., Feng, L.-X., Liu, M., Jin, W.-H., Luo, J., Nie, A.-Y., et al. (2016). Possible Target-Related Proteins and Signal Network of Bufalin in A549 Cells Suggested by Both iTRAQ-Based and Label-free Proteomic Analysis. *Proteomics* 16, 935–945. doi:10.1002/pmic.201500418

Zhang, K., Pan, X., Zheng, J., Xu, D., Zhang, J., and Sun, L. (2015). Comparative Tissue Proteomics Analysis of Thoracic Aortic Dissection with Hypertension

Using the iTRAQ Technique. *Eur. J. Cardio-Thorac* 47, 431–438. doi:10.1093/ejcts/ezu171

Conflict of Interest: The authors declare that the research was conducted in the absence of any commercial or financial relationships that could be construed as a potential conflict of interest.

Publisher's Note: All claims expressed in this article are solely those of the authors and do not necessarily represent those of their affiliated organizations, or those of the publisher, the editors, and the reviewers. Any product that may be evaluated in this article, or claim that may be made by its manufacturer, is not guaranteed or endorsed by the publisher.

Copyright © 2022 Deng, Liu, Gael, Fu, Deng, Liu, Wu, Wu, Wang, Deng, Lai and Fu. This is an open-access article distributed under the terms of the Creative Commons Attribution License (CC BY). The use, distribution or reproduction in other forums is permitted, provided the original author(s) and the copyright owner(s) are credited and that the original publication in this journal is cited, in accordance with accepted academic practice. No use, distribution or reproduction is permitted which does not comply with these terms.

Frontiers in Physiology

Understanding how an organism's components work together to maintain a healthy state

The second most-cited physiology journal, promoting a multidisciplinary approach to the physiology of living systems - from the subcellular and molecular domains to the intact organism and its interaction with the environment.

Discover the latest Research Topics

See more →

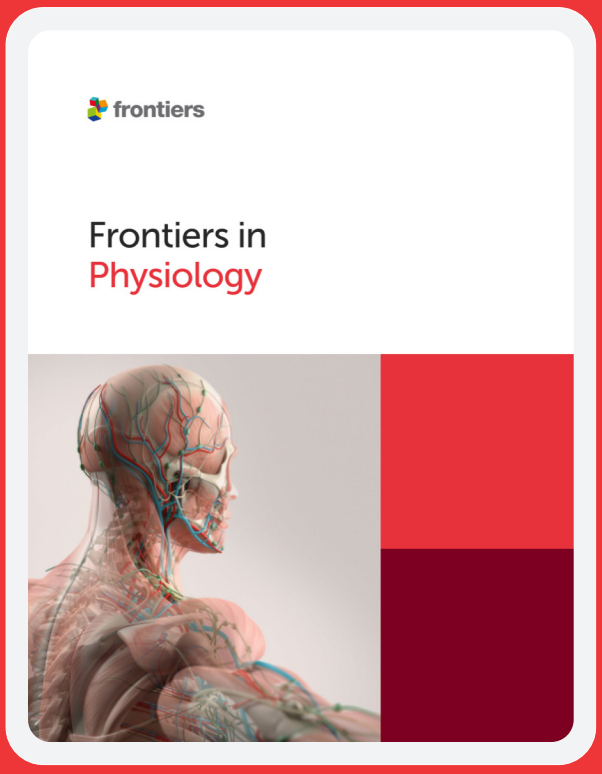

Frontiers

Avenue du Tribunal-Fédéral 34
1005 Lausanne, Switzerland
frontiersin.org

Contact us

+41 (0)21 510 17 00
frontiersin.org/about/contact